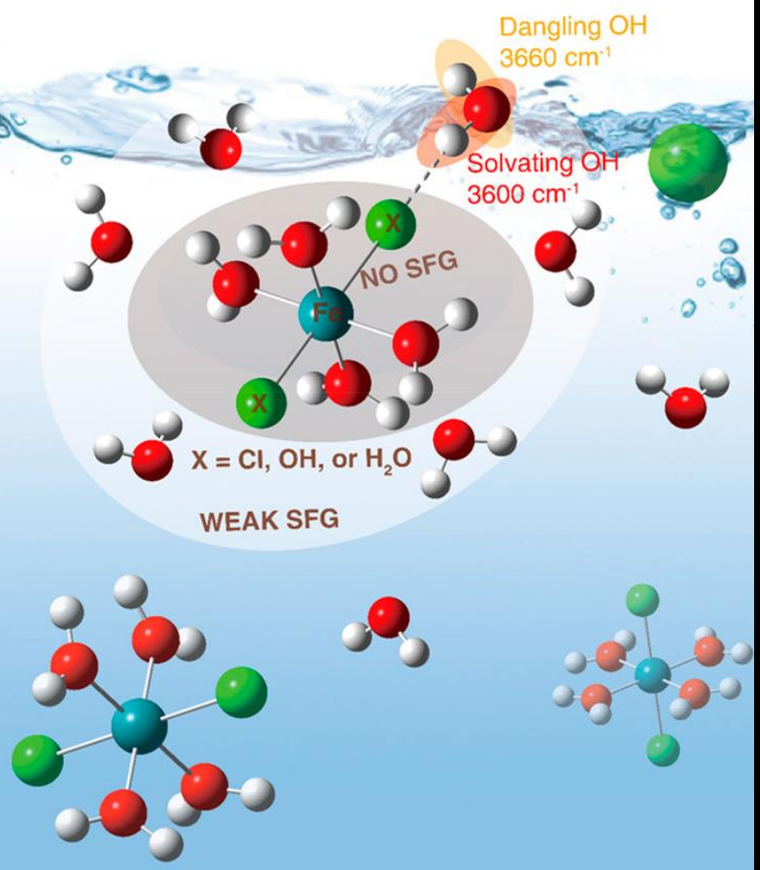

CPIMS 15

Fifteenth Condensed Phase and Interfacial Molecular Science (CPIMS) Research Meeting

Gaithersburg Marriot
Washingtonian Center
Gaithersburg, MD
November 4-6, 2019

U.S. DEPARTMENT OF ENERGY | Office of Science

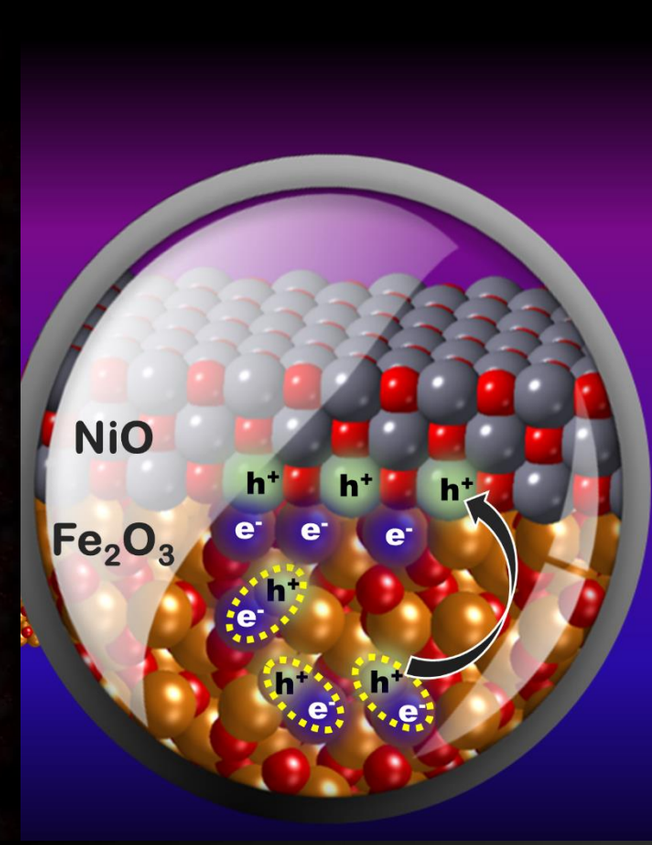

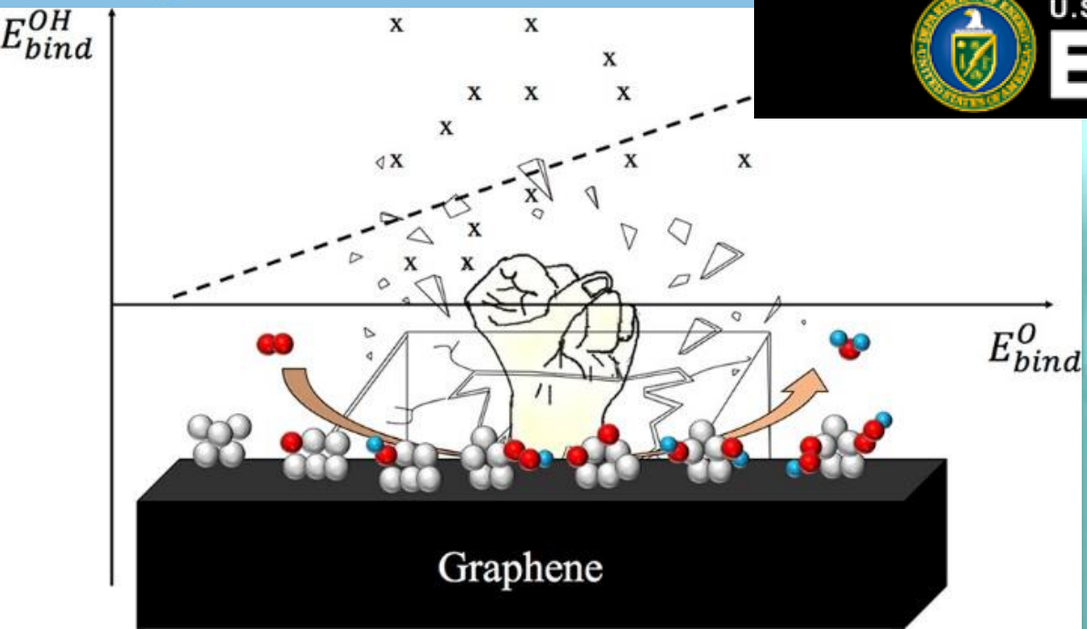

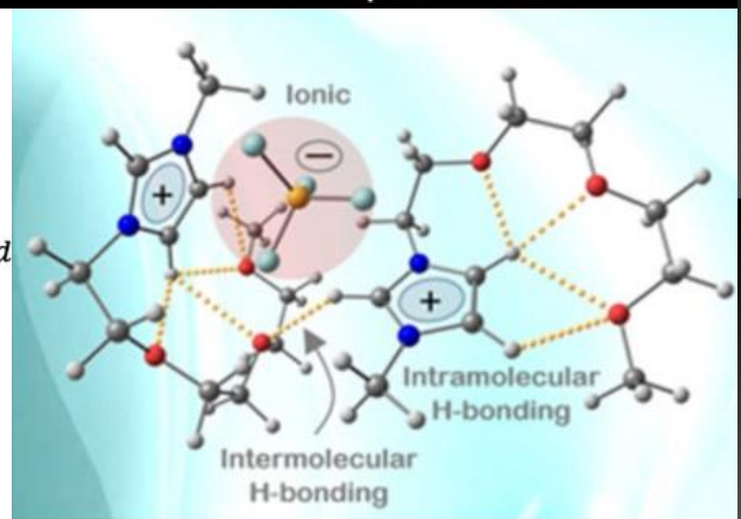

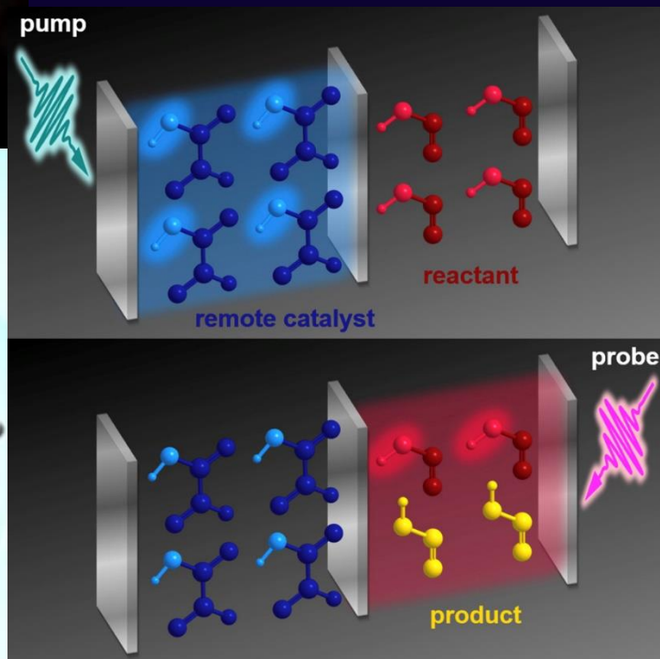

CPIMS 15

ABOUT THE COVER GRAPHICS

Submitted by L. Robert Baker, and Heather Allen (Ohio State University)

For more information, see L. Lin, J. Husek, S. Biswas, S. M. Baumler, T. Adel, K. Ng, L. R. Baker, and H. C. Allen, “Iron(III) Speciation Observed at Aqueous and Glycerol Surfaces: Vibrational Sum Frequency and X-ray,” *Journal of the American Chemical Society* **141**, 13525 (2019). DOI: 10.1021/jacs.9b05231

Abstract begins on page 9

Submitted by Ismaila Dabo and Susan B. Sinnott (Pennsylvania State University)

For more information, see abstract, which begins on page 34

Submitted by L. Robert Baker (Ohio State University)

For more information, see S. Biswas, J. Husek, S. Londo, E. A. Fugate and L. R. Baker, "Identifying the Acceptor State in NiO Hole Collection Layers: Direct Observation of Exciton Dissociation and Interfacial Hole Transfer Across a Fe_2O_3/NiO Heterojunction", *Physical Chemistry Chemical Physics* **20**, 24545 (2018). DOI: 10.1039/c8cp04502j

Abstract begins on page 18

Submitted by Anastassia N. Alexandrova (University of California, Los Angeles)

For more information, see B. Zandkarimi and A. N. Alexandrova, “Dynamics of Subnanometer Pt Clusters Can Break the Scaling Relationships in Catalysis”, *Journal of Physical Chemistry Letters* **10**, 460 (2019). DOI: 10.1021/acs.jpclett.8b03680

Abstract begins on page 5

Submitted by James F. Wishart (Brookhaven National Laboratory) and Mark A. Johnson (Yale University)

For more information, see H. J. Zeng, M. A. Johnson, J. D. Ramdihal, R. A. Sumner, C. Rodriguez, S. I. Lall-Ramnarine, and J. F. Wishart “Spectroscopic Assessment of Intra- and Intermolecular Hydrogen Bonding in Ether-Functionalized Imidazolium Ionic Liquids”, *Journal of Physical Chemistry A* **123**, 8370 (2019). DOI: 10.1021/acs.jpca.9b04345

Abstract begins on page 69

Submitted by Joel Yuen-Zhou (University of California, San Diego)

For more information, see M. Du, R. F. Ribeiro, and J. Yuen-Zhou, “Remote Control of Chemistry in Optical Cavities” *Chem* **5**, 1 (2019). DOI: 10.1016/j.chempr.2019.02.009

Abstract begins on page 170

Program and Abstracts for

CPIMS 15

Fifteenth Research Meeting of the Condensed Phase and Interfacial Molecular Science (CPIMS) Program

Gaithersburg Marriott Washingtonian Center
Gaithersburg, Maryland
November 4-6, 2017

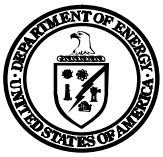

U.S. DEPARTMENT OF ENERGY | Office of Science

Office of Basic Energy Sciences
Chemical Sciences, Geosciences & Biosciences Division

The research grants and contracts described in this document are supported by the U.S. DOE Office of Science, Office of Basic Energy Sciences, Chemical Sciences, Geosciences and Biosciences Division.

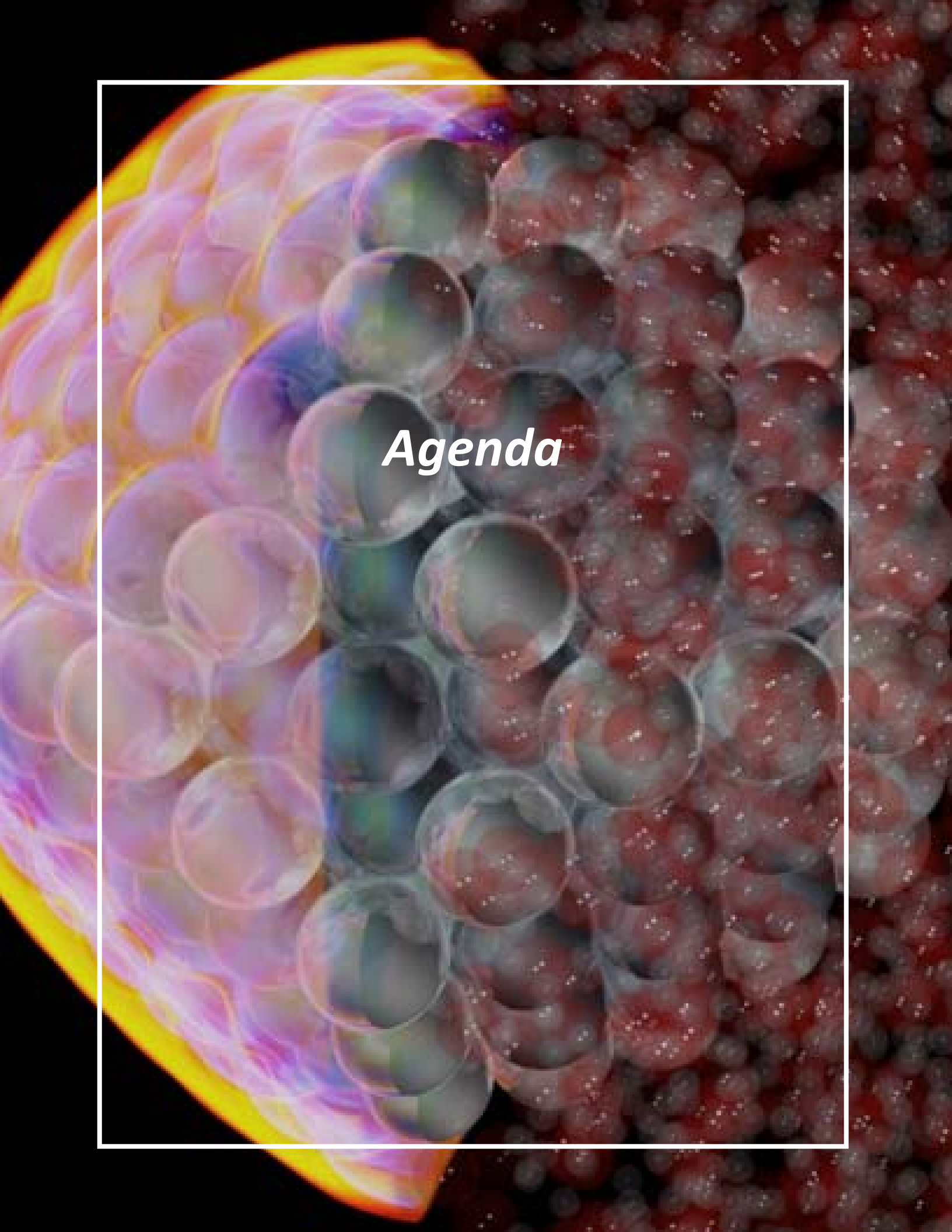
Agenda

CPIMS 15

U.S. DEPARTMENT OF ENERGY | Office of Science

Office of Basic Energy Sciences
Chemical Sciences, Geosciences & Biosciences Division

Fifteenth Condensed Phase and Interfacial Molecular Science (CPIMS) Research Meeting
Gaithersburg Marriott Washingtonian Center, Gaithersburg, Maryland

---

Monday, November 4

7:30 am **** Continental Breakfast (Salons A-E) ****

All Presentations Held in Salons A-E

Session I Chair: **James Rustad**, DOE BES/Chemical Sciences, Geosciences, and Biosciences Division

8:30 am *Update from BES Chemical Sciences, Geosciences, and Biosciences Division*
Bruce Garrett, DOE BES/Chemical Sciences, Geosciences, and Biosciences Division

9:30 am *Aqueous Iron Salt Solutions and Interfaces: Understanding Hydration through Electric Field and Spectroscopy Measurement*
Heather Allen, Ohio State University

10:00 am *Size Dependence of Liquid-Liquid Phase Separation in Aerosol Particles*
Miriam Freedman, Pennsylvania State University

10:30 am *Probing the Structure and Dynamics of Water under Heterogeneous Nanoconfinement Through Ultrafast Vibrational Spectro/microscopy and Many-Body Molecular Dynamics*
Francesco Paesani and Wei Xiong, University of California, San Diego

11:10 am **** Break ****

Session II Chair: **Aaron Holder**, DOE BES/Chemical Sciences, Geosciences, and Biosciences Division

11:30 am *Chemical Stability and Dynamical Evolution of Nanostructured Alloys under Voltage*
Ismaila Dabo and Susan Sinnott, Pennsylvania State University

Noon *The Water-Anatase TiO_2 Interface*
Annabella Selloni, Princeton University

12:30 pm **** Working Lunch (Salons A-E) ****

Lunch Presentation: *Updates from the CPIMS Program*, **Gregory Fiechtner**, DOE BES/Chemical Sciences, Geosciences, and Biosciences Division

1:30 pm–2:00 pm Free/Discussion Time

Session III Chair: **Wei Xiong,** University of California, San Diego

2:00 pm *Polariton Chemistry: Molecules in Cavities*
Joel Yuen-Zhou, University of California, San Diego

2:30 pm *Fundamental Mechanisms of Oxide Evolution on Semiconductor Surfaces*
Sylwia Ptasinska, University of Notre Dame

3:00 pm *XUV Spectroscopy of Surfaces: From Semiconductors to Solvated Ions*
Robert Baker, Ohio State University

3:30 pm **** Break ****

Session IV: Overview of New Projects

Chair: **Ethan Crumlin,** Lawrence Berkeley National Laboratory

3:45 pm *Metastable Nature of Active Sites at Cluster Catalysts*
Philippe Sautet, University of California, Los Angeles

4:00 pm *Size-Selected Sub-Nano Electrocatalysis*
Scott Anderson, University of Utah

4:15 pm **** Break ****

4:30 pm *Probing Electrochemical Reactivity under Nanoconfinement Using Molecularly Pillared Two Dimensional Materials*
Veronica Augustyn, North Carolina State University

4:45 pm *Divalent-to-Monovalent Redox Potentials of Transition Metal Ions in Aqueous Solution*
Aliaksandra Lisouskaya, University of Notre Dame

5:00 pm **** Break ****

5:30 pm *Modeling Potential Fluctuations at the Electrode-Electrolyte Interface*
Adam Willard, Massachusetts Institute of Technology

6:00 pm **** Reception (No Host, Lobby Lounge) ****

6:30 pm **** Dinner (on your own) ****

Tuesday, November 5

7:30 am **** Continental Breakfast (Salons A-E) ****

Session V Chair: **Kevin Shuford,** Baylor University

8:30 am *Charge Carriers in Solar Energy Conversion: Insights into Structure, Dynamics, and Reactivity from Multiscale Modeling*

Michel Dupuis, University at Buffalo

9:00 am *Real-Time Electron Dynamics of Large Chemical Systems: Theory and Practice*
Bryan Wong, University of California, Riverside

9:30 am *Understanding Molecular Scale Chemical Transformations at Solid-Liquid Interfaces – Computational Investigation of Electrolyte Oligomerization and the Role of Additives*
Jim Pfaendtner, University of Washington

10:00 am **** Break ****

Session VI Chair: **Michael Fayer,** Stanford University

10:30 am *Long-Range Ion-Ion Correlations in Water*
John Fulton, Pacific Northwest National Laboratory

11:00 am *Reversed Interfacial Fractionation of Carbonate and Bicarbonate Evidenced by X-ray Photoemission Spectroscopy and Theory*
Richard Saykally, Lawrence Berkeley National Laboratory

11:30 am *Mapping Electron Delocalization during Ultrafast Charge Transfer*
Munira Khalil, University of Washington

12:00 pm **** Working Lunch (Salons A-E) ****

1:00 pm–1:45 pm Free/Discussion Time

Session VII Chair: **Geraldine Richmond,** University of Oregon

1:45 pm *The Molten Salts in Extreme Environments Energy Frontier Research Center (MSEE)*
James Wishart, Brookhaven National Laboratory

2:15 pm *Imaging Chemical Dynamics in Electrolyte Solutions*
Amber Krummel, Colorado State University

2:45 pm *Atomistic Modeling of Electronic Spectroscopy for Organic Chromophores in Solutions*
Liang Shi, University of California, Merced

3:15 pm **** Break ****

Session VIII **Overview of New Projects**

Chair: **Greg Kimmel,** Pacific Northwest National Laboratory

3:30 pm *Using Ultrafast Entangled Photon Correlations to Measure the Temporal Evolution of Molecular Excited States*
Scott Cushing, California Institute of Technology

3:45 pm *Exploring New Diamond Surfaces with Precision Chemistry and Quantum Spectroscopy*
Nathalie de Leon, Princeton University

4:00 pm *Following Photochemical Reactions in Complex Environments with Quantum Transition Path Sampling*
David Limmer, University of California, Berkeley

4:15 pm **** Break ****

4:30 pm *Catalysis Driven by Confined Hot Carriers at the Liquid/Metal/Zeolite Interface*
Bin Wang, University of Oklahoma

4:45 pm *Small is Beautiful: Engineered Defects on Ultra-Nano TiO_2*
Mary Jane Shultz, Tufts University

5:00 pm *Elucidating the Formation Mechanisms of Zeolites Using Data-Driven Modeling and In-Situ Characterization*
Valeria Molinero, University of Utah
and **Ilke Arslan**, Center for Nanoscale Materials, Argonne National Laboratory

5:30 pm **** Reception (No Host, Lobby Lounge) ****

6:00 pm **** Dinner (on your own) ****

Wednesday, November 6

7:30 am **** Continental Breakfast (Salons A-E) ****

Session IX Chair: **Aaron Holder**, DOE BES/Chemical Sciences, Geosciences, and Biosciences Division

8:30 am *The Center for Scalable and Predictive methods for Excitations and Correlated phenomena (SPEC): interpreting the spectra obtained at BES' light sources*
Sotiris Xantheas, Pacific Northwest National Laboratory

9:00 am *Applying Deep Learning Methods to Develop New Models of Charge Transfer, Nonadiabatic Dynamics, and Nonlinear Spectroscopy in the Condensed Phase*
Christine Isborn, University of California, Merced

9:15 am *Tuning the Properties of Two-Dimensional Materials toward Efficient Photocatalysis*
Kevin Shuford, Baylor University

9:30 am *Chemical Reactivity in Complex Environments*
Teresa Head-Gordon, Lawrence Berkeley National Laboratory

10:00 am **** Break ****

10:30 am *Molecular Based Analysis of Solvation Processes*
Marat Valiev, Pacific Northwest National Laboratory

11:00 am *Theory of Crystallization vs. Vitrification*
Kranthi Mandadapu, Lawrence Berkeley National Laboratory

11:30 am **** Meeting Adjourns ****

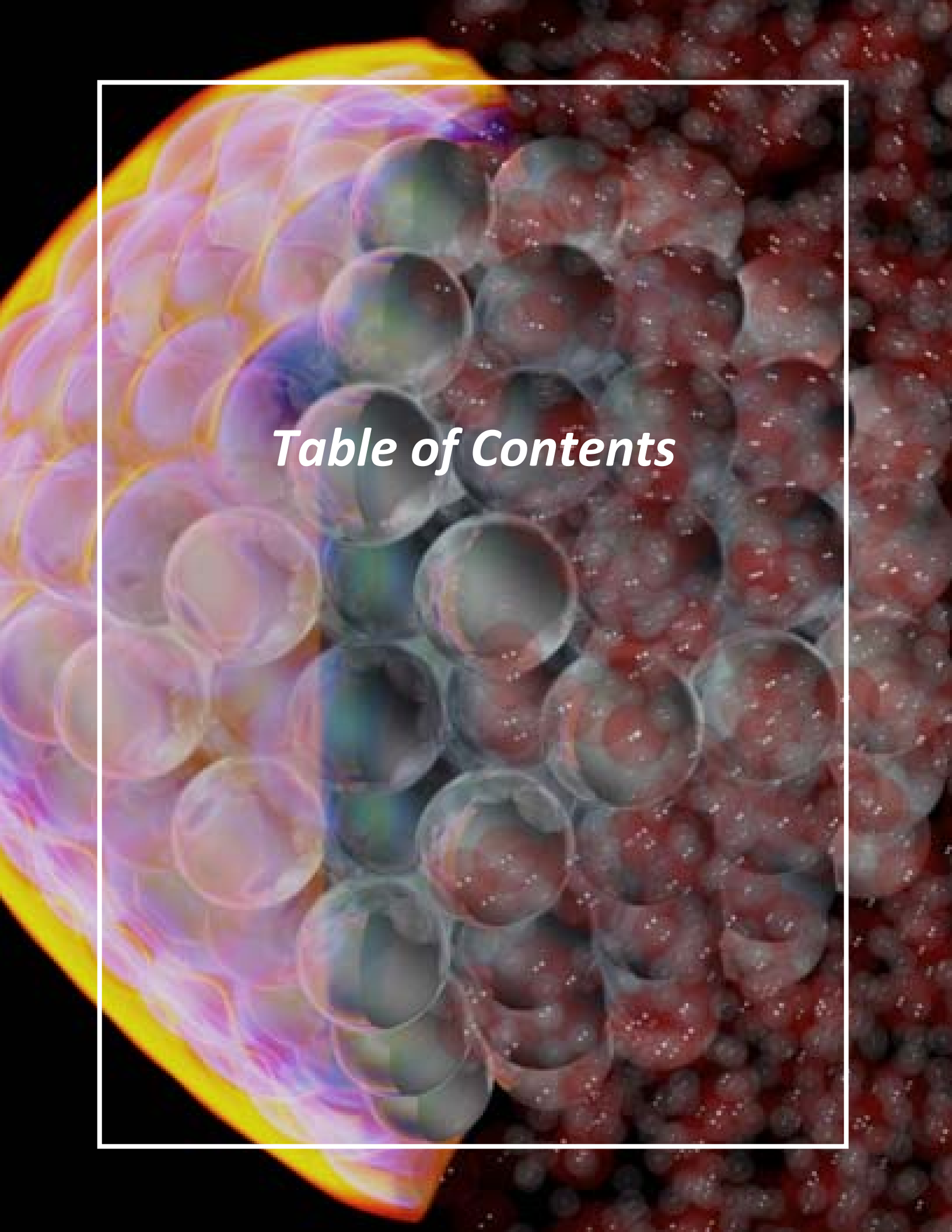

Table of Contents

TABLE OF CONTENTS

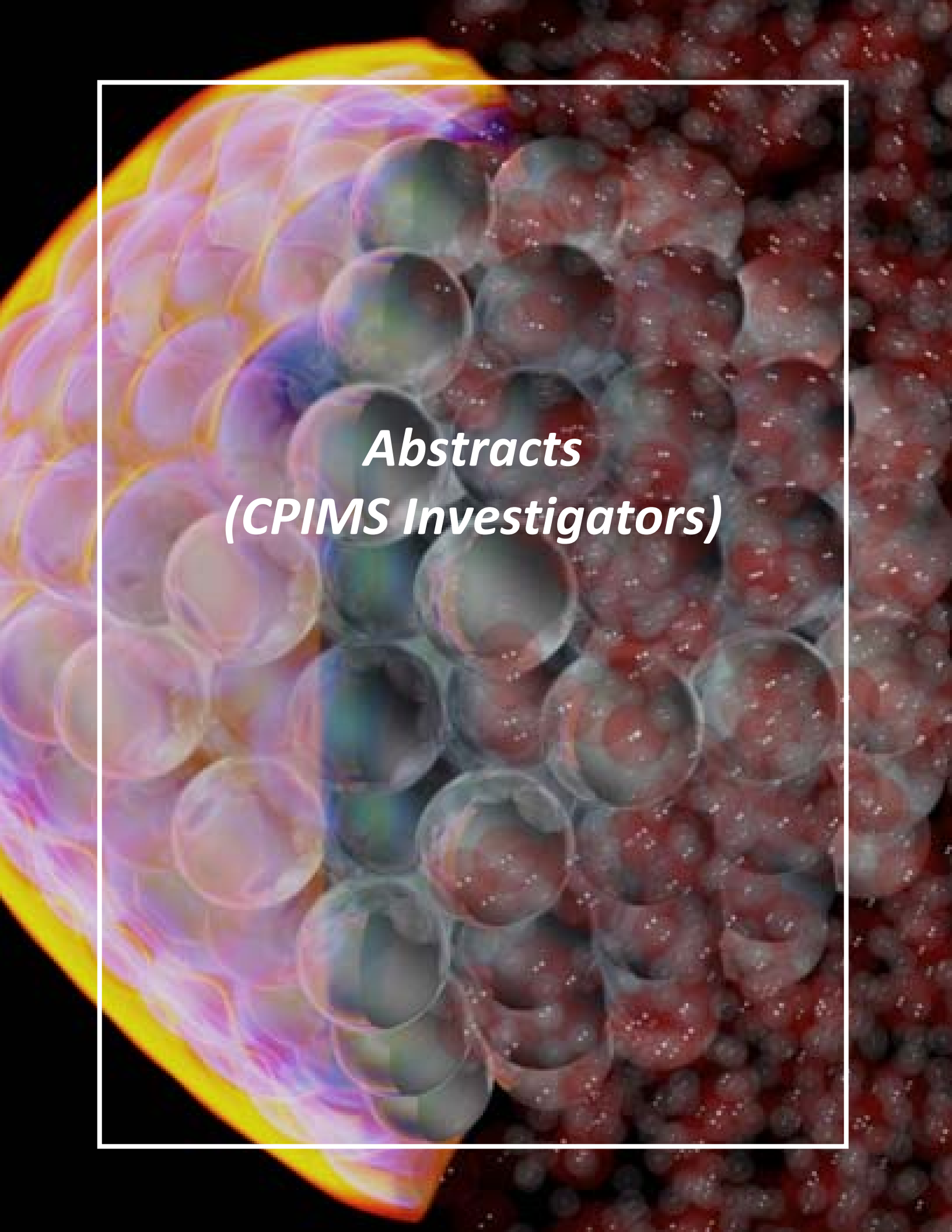

Abstracts (CPIMS Investigators)

Chemical Transformations in Bulk Aqueous Solutions and Near Interfaces

Musahid Ahmed (mahmed@lbl.gov), Phillip Geissler (geissler@berkeley.edu)
Teresa Head-Gordon (TLHead-Gordon@lbl.gov), Kevin Wilson (krwilson@lbl.gov)
Lawrence Berkeley National Laboratory, Chemical Sciences Division,
One Cyclotron Road, Berkeley, CA 94720

Program Scope

The ability to control or accelerate a chemical reaction is of great importance in basic energy science related to hydrogen production, energy conversion in fuel cells, or artificial photosynthesis technologies, and synthetic catalysts. Inspired by the fact that the activity of encapsulated enzymes and their active sites, or that organometallic reactions are accelerated when encapsulated within the cavities of nanoscale water-soluble metal clusters, a particularly promising strategy to guide chemical reactions is the use of interfaces and confinement. While there are multiple examples for exploiting nanoconfined spaces for catalytic purposes, including nanoporous materials, supramolecular hosts, or microdroplets, the mechanisms underlying the enhanced reactivity are not fully understood. What may unify these case-specific success stories is a more fundamental aspect – the altered physical properties of the solvent due to the confining interfaces – that could be more generally developed to regulate chemical reactions in the condensed phase.

Progress Report

Probing non-covalent interactions in chemically reactive systems. Non covalent interactions such as hydrogen bonding, electrostatics, and van der Waals forces play a crucial role in driving chemical reactivity – particularly in liquids such as water where most synthesis occurs. The Ahmed group has employed a multimodal experimental approach that combines synchrotron based mass spectrometry and photoelectron spectroscopy coupled with state-of-the-art electronic structure calculations, in collaboration with Krylov (USC), to show that water plays a crucial role in directing the stability and charge states of arginine peptide system in aqueous environments.[1] The vibrational spectroscopy of water under confined conditions were studied by probing the uptake of water on microporous silica nanoparticles developed by a reverse micro-emulsion method utilizing zinc nanoclusters encapsulated dendrimers. In collaboration with Jones at Caltech, the Ahmed lab used electron microscopy to decipher how the combination of copper-lanthanum core-shell cathode demonstrates reversible partial fluorination and defluorination reactions in a tetraalkylammonium salt-fluorinated ether electrolyte solution at room temperature.[2]

Chemical Reactivity in Confined Systems. Head-Gordon and coworkers have been developing rational, physical concepts that are more predictive in designing desired catalytic outcomes, by calculating electric fields relevant to the reactant and transition states of different types of catalysts.[3] Part of that understanding is understanding the basic principles of nature's best catalysts – enzymes.[4-5] We have extended these concepts to consider supramolecular assemblies, which have gained tremendous attention due to their apparent ability to catalyze reactions with the efficiencies of natural enzymes.[6] More recently using Born-Oppenheimer molecular dynamics and density functional theory, we identify the origin of the catalytic power of the supramolecular assembly $Ga_4L_6^{12-}$ on the reductive elimination reaction from gold complexes. By comparing the catalyzed and uncatalyzed reaction in explicit solvent to identify the reaction free energies of the reactants, transition states, and products, we determine that the catalysis arises from an encapsulation of a catalytic moiety- a primary water molecule – that is unlike the biomimetic scenario of catalysis through direct host-guest interactions. At the same time the nanocage host

preconditions the transition state for greater sensitivity to electric field projections onto the breaking carbon bonds to complete the reductive elimination reaction with greater catalytic efficiency.

We have also mapped the free energy and mechanisms of two retro-Diels-Alder reactions, in the gas phase, in bulk water, and in water nanoconfined[7] by parallel graphene sheets. We find that both bulk and nanoconfined aqueous environments accelerate the reactions to a very similar degree. Furthermore, we observe nearly identical activation free energies for systems in bulk water at very different densities. The mechanism underlying the acceleration in all cases is the stabilization of the transition state through enhanced hydrogen bonding between the carbonyl groups of the dienophiles and water. Despite that the systems studied here are broadly different at a nanoscale level, the hydrogen bonding behavior of the carbonyl groups, which governs the catalytic acceleration, remains largely unchanged regardless of solvent density or nanoconfinement state. Our results suggest that the local environment surrounding the carbonyl groups exclusively governs the acceleration of aqueous Diels-Alder reactions, and that observations of orders of magnitude acceleration of reactions under confinement are not operative for Diels-Alder reactions.

This general conclusion from the Head-Gordon group that confinement effects on reactivity are small for Diels-Alder reactions also resonates with the recent work of the Wilson group, who independently explored recent reports on dramatic acceleration (up to 10^6 times) for the phosphorylation reaction of sugars in nanosized droplets. While this reaction was recently reported to greatly accelerated in droplets, careful control experiment in our laboratory[8] have revealed in all likelihood that the observed reaction products and acceleration factors have significant contributions from gas phase ion molecule chemistry. Using a newly develop quadrupole electrodynamic trap we have further investigated confinement effects on a synthesis reaction using a fluorescent product. This approach allows precise control over droplet size (10 – 80 microns in diameter) and avoids some of the ambiguities of electrospray mass spectrometry. The rate coefficient for the reaction of *o*-phthalaldehyde (OPA) with alanine in the presence of dithiolthreitol was found[9] to be 25% larger than the equivalent reaction in the bulk, suggesting moderate effects of confinement on the bimolecular reaction. The droplet size used for this reaction was still rather large (~40 micron diameter) and future efforts will be dedicated to examine the droplet size dependence of this reaction.

Amphiphilic self-assembly and reactivity at interfaces. Wilson and Hendrik Bluhm (past member of the LBNL CPIMS program) continue to work on combing Langmuir troughs with ambient pressure X-ray photoelectron spectroscopy, allowing for the study the reactivity of organic monolayers at liquid interfaces. Although the packing and orientation of the stearic acid molecules on water have been investigated in the past using surface pressure measurements, often combined with infrared spectroscopy, ambient pressure X-ray photoelectron spectroscopy (APXPS) provides complementary information on the chemical composition and density of the surfactant layer and can also be used in future experiments to investigate the abundance and surface propensity of ions in solution as a function of surfactant chemistry and packing. In the present proof-of-principle study we demonstrate that changes in the packing density and orientation of the molecules can be directly determined from APXPS data, which correlate well with the compression curves from surface tension measurements. In addition, APXPS provides information on the distribution of the stearic acid molecules beyond the breakdown compression threshold, which is difficult to gain using other characterization methods.

The Wilson and Geissler groups continue to examine photochemically driven self-

assembly in which we have completed a set of measurements of 9-oxo-nonanoic acid. This molecule is soluble in water and when excited creates double tail reaction products that spontaneously form monodisperse 100 nm structures. While the molecular building blocks have been well characterized by us, together we are endeavoring to understand the overall mechanism that controls the self-assembled size, dynamics and composition.

Future Plans

Amphiphilic self-assembly and reactivity at interfaces. The Wilson lab will continue collaborative work with Geissler on the photochemically driven self-assembly of oxo-acids. In the future we will focus on obtaining high quality electron microscopy images to ascertain and guide the theory development on the structure details of the self-assembled products. We will examine how the self-assembled size depends ionic strength and upon protonation or deprotonation of the acid group. Wilson and Mandadapu will collaborate on understanding how simple binary mixtures of glass forming organics impact interfacial reactions. Current work is focused on providing Mandadapu experimental data to refine theories of diffusion in glass forming aqueous systems.

In related work, Ahmed will explore self-assembly of natural or synthetic amphiphiles to build well defined-nanostructures with controllable function at the molecular level are driven by non-covalent interactions where the solvent can play a major role. Ahmed will use arginine as a template, since it has a flexible molecular structure, composed of a guanidinium head group and an alpha amino acid tail held together by an aliphatic hydrocarbon backbone. We will use terahertz time domain spectroscopy and dynamic light scattering to probe the initial growth processes of arginine with hydrocarbon fatty acids. The terahertz spectra informs on the rate of chemical reaction and the changes in the hydrogen bond network of the system, while the light scattering should reveal the dynamics of particle formation as a function of pH, concentration and temperature. To track the very early part of the nucleation and molecular growth processes, we propose to use small angle X-Ray scattering to capture dynamics while the reactivity components will be imaged via synchrotron based IR microscopy.

Nanoconfinement on Carbon Reductive Elimination and Diels-Alder type reactions. The Head-Gordon lab will consider different metals and nanocage functionalization to predict whether we can predict accelerated reactivity for the reductive elimination chemistry (which is modest by biocatalytic standards) using electric fields as guidance as we have done previously for synthetic enzymes.[5] Furthermore, although the transition state free energy stabilization for Diels-Alder is not perturbed by the confinement conditions we have examined, we do see changes in mechanism such as asynchronicity in the breaking of first vs. second bond, bifurcation of the transition state, and alternate pathways being discovered that have not been observed in earlier theoretical studies. These have implications for general understanding and control of chemical reactivity in the condensed phase to create new products (such as diradicals) that are only observed at high temperature in bulk water.

The Wilson group will focus on making robust measurements to ascertain the possible mechanism for explaining (modest) rate enhancements in small droplets. For the OPA systems we will measure the rate coefficient as a function of droplet size down to 5 micron in radius. Additionally we will focus on another simple reaction involving acid degradaton of tetracycline (flourescent) in collaboration with Head-Gordon. This reaction has been previously studied in Leidenfrost droplets (millimeter sized droplets) and substantial acceleration over the bulk has been observed. We will measure this reaction down to 5 microns and obtain the relevant scaling data for the rate coefficient as a function of droplet size.

Publications Acknowledging DOE support (2018-present):

1. Barrozo, A.; Xu, B.; Gunina, A. O.; Jacobs, M. I.; Wilson, K.; Kostko, O.; Ahmed, M.; Krylov, A. I. To Be or Not To Be a Molecular Ion: The Role of the Solvent in Photoionization of Arginine. *J Phys Chem Lett* **2019,** *10* (8), 1860-1865. doi.org/10.1021/acs.jpclett.9b00494
2. Davis, V. K.; Bates, C. M.; Omichi, K.; Savoie, B. M.; Momcilovic, N.; Xu, Q.; Wolf, W. J.; Webb, M. A.; Billings, K. J.; Chou, N. H.; Alayoglu, S.; McKenney, R. K.; Darolles, I. M.; Nair, N. G.; Hightower, A.; Rosenberg, D.; Ahmed, M.; Brooks, C. J.; Miller, T. F., 3rd; Grubbs, R. H.; Jones, S. C. Room-temperature cycling of metal fluoride electrodes: Liquid electrolytes for high-energy fluoride ion cells. *Science* **2018,** *362* (6419), 1144-1148.doi: 10.1126/science.aat7070
3. Vaissier Welborn, V.; Pestana, L. R.; Head-Gordon, T. Computational Optimization of Electric Fields for Better Catalysis Design. *Nature Catalysis* **2018**. DOI:10.1038/s41929-018-0109-2
4. Welborn, V. V.; Head-Gordon, T. Fluctuations of Electric Fields in the Active Site of the Enzyme Ketosteroid Isomerase. *J Am Chem Soc* **2019,** *141* (32), 12487-12492. DOI: 10.1021/jacs.9b05323
5. Vaissier, V.; Sharma, S. C.; Schaettle, K.; Zhang, T.; Head-Gordon, T. Computational Optimization of Electric Fields for Improving Catalysis of a Designed Kemp Eliminase. *ACS Catalysis* **2018,** *8* (1), 219-227. DOI: 10.1021/acscatal.7b03151
6. Vaissier Welborn, V.; Head-Gordon, T. Electrostatics Generated by a Supramolecular Capsule Stabilizes the Transition State for Carbon-Carbon Reductive Elimination from Gold(III) Complex. *J Phys Chem Lett* **2018,** *9* (14), 3814-3818. DOI:10.1021/acs.jpclett.8b01710
7. Pestana, L. R.; Felberg, L. E.; Head-Gordon, T. Coexistence of Multilayered Phases of Confined Water: The Importance of Flexible Confining Surfaces. *ACS Nano* **2018,** *12* (1), 448-454. DOI: 10.1021/acsnano.7b06805
8. Jacobs, M. I.; Davis, R. D.; Rapf, R. J.; Wilson, K. R. Studying Chemistry in Micro-compartments by Separating Droplet Generation from Ionization. *J Am Soc Mass Spectrom* **2019,** *30* (2), 339-343.http://doi.org/10.1007/s13361-018-2091-y
9. Jacobs, M. I.; Davies, J. F.; Lee, L.; Davis, R. D.; Houle, F.; Wilson, K. R. Exploring Chemistry in Microcompartments Using Guided Droplet Collisions in a Branched Quadrupole Trap Coupled to a Single Droplet, Paper Spray Mass Spectrometer. *Anal Chem* **2017,** *89* (22), 12511-12519.http://doi.org/10.1021/acs.analchem.7b03704
10. S. Belsare, V. Pattni, M. Heyden, T. Head-Gordon (2018). Solvent Entropy Contributions to Catalytic Activity in Designed and Optimized Kemp Eliminases. *J. Phys. Chem. B* 122, 5300−5307. DOI: 10.1021/acs.jpcb.7b07526.
11. L. Ruiz Pestana, O. Marsalek, T. E. Markland, T. Head-Gordon (2018). The Quest for Accurate Liquid Water Properties from First Principles. *J. Phys. Chem. Lett.* 9 (17) 5009-5016. DOI: 10.1021/acs.jpclett.8b02400
12. L. Ruiz Pestana, N. Minnetian, L. Nielsen Lammers, T. Head-Gordon (2018). Dynamical inversion of the energy landscape promotes non-equilibrium self-assembly of binary mixtures. *Chem. Sci.* 9, 1640. DOI: 10.1039/c7sc03524a
13. K. Schaettle, L. Ruiz Pestana, T. Head-Gordon, L. Nielsen Lammers (2018). A structural coarse-grained model for clays using simple iterative Boltzmann inversion. *J. Chem. Phys.*148, 222809, DOI:10.1063/1.5011817
14. E. Jurrus, D. Engel, K. Star, K. Monson, J. Brandi, L. E. Felberg, D. H. Brookes, L. Wilson, J. Chen, K. Liles, M. Chun, P. Li, D. W. Gohara, T. Dolinsky, R. Konecny, D. R. Koes, J. E. Nielsen, T. Head-Gordon, W. Geng, R. Krasny, G. Wei, M. J. Holst, J. A. McCammon, N. A. Baker, (2018), Improvements to the APBS biomolecular solvation software suite. *Pro. Sci.*, 27: 112-128. DOI::10.1002/pro.3280

Ensemble representation for the realistic modeling of cluster catalysts at heterogeneous interfaces

PI: Anastassia N. Alexandrova[1,3]
co-PI: Philippe Sautet[1,2,3]

[1]Department of Chemistry and Biochemistry, and [2]Chemical and Biomolecular Engineering, University of California, Los Angeles, [3]California NanoSystems Institute, 607 Charles Young Drive East, LosAngeles, CA 90095-1569, USA
e-mail: ana@chem.ucla.edu, sautet@ucla.edu

Program scope

When a catalytic interface is amorphous and dynamic, reaction conditions set it in motion. Under the influence of high temperatures and partial pressures of gasses, a strong restructuring of the interface can take place, and the motion continues concurrently with the catalyzed reaction. This opens hundreds of possibilities for how the surface may look like, and what active sites it may expose and use in catalysis at any instance. Modeling this reality requires a paradigm shift toward statistical mechanics and ensemble representation of heterogeneous catalytic interfaces.

The goal of our project is to develop new approaches for computational characterization of surface-deposited cluster catalysts that would capture their realistic ensemble nature. With this, we aim to explain existing experimental data and make new testable predictions regarding size-activity dependencies of surface-deposited cluster catalysts. We focus on the catalytic activation of C-H bonds on Pt clusters and CuO_x clusters deposited on alumina (in link with experiments by Dr. Stefan Vajda).

The objectives are:

1. To adapt and develop the essential computational tools for modeling the ensemble of low energy isomers for supported cluster catalysts
2. To determine ensemble average properties for supported cluster catalysts: catalytic activity, and spectra (XANES, XPS, IR), compare to in situ experiments, and validate or improve our models.
3. To study the kinetics of cluster isomerization and determine whether the isomerization dynamics can couple to the reaction or adsorption dynamics.
4. To provide guidelines for cluster catalysts with improved activity or selectivity. Predictions will be tested experimentally.

Recent progress

Methodological advances:

The modeling of supported sub-nano clusters in conditions of catalysis of oxidative and non-oxidative dehydrogenation of hydrocarbons is challenging due to the large configuration space involving the cluster, the adsorbates, and the support (Publication 2). Our systems also exhibit thermal isomerization and possible dynamic coupling between the reaction and isomerization as well as adsorbate rearrangement. Several codes have been developed or adapted for modeling these phenomena:

i) The Basin-Hopping (BH) global optimization in a core/shell separate scheme was developed for adsorbate-covered Pt clusters on alumina. It is a perturbation procedure for Pt cluster as a core, and H/molecules as a shell. Sampling is performed separately and with different length steps. The application of this scheme to $Pt_7H_{10}(CH_3)$ shows that we can successfully find the typical low-energy Pt_7 core geometries and describe a relatively complete static picture of both the isomerization and H/CH_3 rearrangement of low-energy isomers.

ii) The grand canonical Basin-Hopping (GCBH) method was adapted, to simultaneously optimize the cluster geometries and compositions in terms of model free energies at a given P_{O2}. This method is used for clusters not amendable to the core-shell paradigm. GCBH was applied to Cu_4O_x and also Pt_8H_x clusters on α-Al_2O_3(0001), γ-Al_2O_3(100) and γ-Al_2O_3(110). Structure and coverage are explored under reaction conditions of ODH, hydrogenolysis, and thermal dehydrogenation.

iii) We proposed symmetry-adapted root-mean-square-distance for determining the similarity between isomers, based on which the NEB method has been used to find the barrier heights for all isomerization and rearrangement processes, first without the kinetic content.

iv) We introduced an exploratory algorithm that samples the system directly at the transition state of the catalyzed reaction, in order to find possible reaction paths that involve cluster isomerization in a thermodynamic sense.

v) To see kinetic effects and energy transfer between the incoming or reacting molecule and the cluster, we performed ab initio molecular dynamics (AIMD) simulations with a simple model in which an average treatment of initial energy is used to assign the initial velocities and the displacements from the equilibrium position, and the molecule is assigned an extra translational velocity pointing towards the cluster. For a realistic statistical representation of the system, we improved the model for the clusters from a classical Boltzmann distribution at a given temperature, and using quasi-classical trajectories for molecules.

vi) Cu_4O_x clusters are difficult for electronic structure calculations. Since we cannot afford better methods, we chose to determine the optimal Hubbard U for d orbital of Cu and the chemical potential of $O_{2(gas)}$ at standard conditions, to agree with HSE06 results. The optimal combination is 2.0 eV and -5.34 eV, respectively.

vii) We developed a high dimensional neural network potential (HDNNP) on Pt clusters of size 6 to 20. The potential reproduces the difference between a fast low level PBE minimal basis set DFT calculation and a more accurate but expensive level, using a hybrid functional or non-local vdw functional and a plane wave basis set. Such a differential approach (named ΔHDNNP) can deliver very accurate and fast predictions (error < 10 meV/atom) of the high level DFT method energies. The overall speedup can be as large as 900 for 20 atom Pt cluster. Tests on 25 and 55 atoms clusters show a very good transferability (publication 3).

New chemistry, new phenomena at cluster-decorated catalytic interfaces:

i) Five structures for supported subnanometer Pt_7 cluster can participate in dehydrogenation catalysis. The energy spectra of low-energy isomers of $Pt_7H_{10}CH_3$ on α-Al_2O_3 was determined, as a model of catalytic cluster in conditions of alkane dehydrogenation reaction. The addition of adsorbates stabilizes some low-energy isomers with very different Pt_7 shapes, compared to the bare cluster case. 58 local structure minima are found in the low-energy range (up to 0.4 eV above the energy of putative global minimum (GM)) and can be classified into 6 categories according to their Pt_7 core geometries. At reaction temperature (700-900 K), 5 of these Pt_7 geometries have a similar probability of presence (Fig 1). Hence any or all of these isomers could be relevant for the catalytic mechanism. The two most probable structures in the ensemble are used to study of pathways of methane C-H bond cleavage and hydrogen rearrangement on these clusters. These pathways suggest a small amount of coupling between the cluster and adsorbate motion.

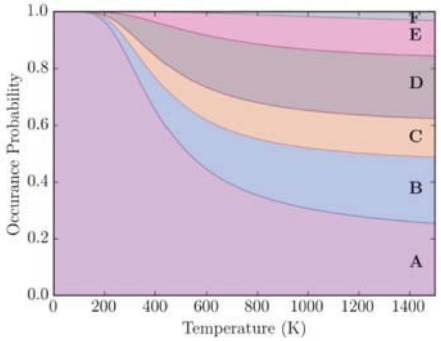

Fig1 : Occurrence probability of Pt_7 core shapes (A to F) for $Pt_7H_{10}CH_3$ on alumina vs temperature.

ii) Supported Pt clusters do rearrange as a function of H coverage and this rearrangement is support-dependent:

Pt_8H_x on different supports were globally optimized at 600 °C, 0.1 bar of H_2, and at 25 °C and 1 bar, using a grand canonical global optimization approach, where the structure of the cluster and the H coverage are simultaneously optimized, for a given T and P condition. On α-Al_2O_3, Pt_8 is mostly 3D but very fluxional in structure at low H coverage and converts to open one-layer 2D structures with minimal functionality at high H coverage, whereas on γ-Al_2O_3(100), the exact opposite occurs, and Pt_8 clusters present one-layer 2D shapes at H coverage and switch into compact 3D shapes under high H coverage (Fig. 2), during which the Pt_8 cluster preserves moderate fluxionality.

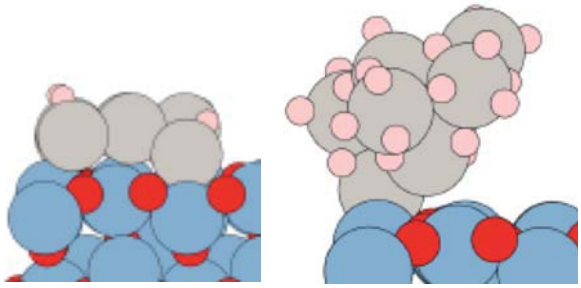

Fig 2 : Pt_8 on γ-Al_2O_3 at low (left) and high (right) H coverage

iii) Different binding sites on the support can contribute to structural diversity in the ensemble, and produce different activities: Cu_4O_x on amorphous Al_2O_3 was shown to exhibit high activity for selective ODH of propane. Based on experimental conditions, GCBH free energy optimization was done at 200 °C and 0.5 bar of O_2. The low free energy Cu_4O_x clusters can be located at two regions on the alumina surface, where they have different redox properties.

iv) Reducibility is a proposed metric of activity in ODH: We calculated the oxygen removal free energy for Cu_4O_x, finding that most O atoms are difficult to remove in the global minimum structure, but that metastable geometries or higher O coverage structures are much easier to reduce. Hence metastable structures of the catalyst are key for ODH.

v) Cluster-molecule kinetic energy exchange: The coupling between reaction or adsorption and cluster isomerization depends on the timescales of these processes. In order to study the possible coupling, we chose two contrasting systems. For dissociative chemisorption of CH_4 on Pt_{13} cluster, the interaction between the cluster and the molecule is weak; while in the other case the interaction between O_2 and Cu_4O_x cluster is strong. We performed AIMD simulation to study the reactivity and dynamic coupling between metal cluster transformation and reaction on the cluster. We found that in the process of methane approaching and immediately dissociating on or scattering from the Pt_{13} cluster, the cluster transformation is not coupled to methane dissociation, and the fluctuation in Pt_{13} is due to the thermal effects (Fig 3). Three types of trajectories were found: dissociative, trapped, and scattered. The transformation of the Pt_{13} cluster induced by CH_4 is tiny while methane is dissociating, because of the short time-scale. However, after methane dissociates or leaves the cluster, unique methane-induced isomerization follows. Hence, reaction and cluster isomerization proceed in a step-wise manner.

vi) We show that the data obtained from X-ray absorption near edge structure (XANES), which has been widely used as a robust tool for catalyst characterization, should be interpreted carefully when it comes to fluxional surface-supported nanoclusters. Extracting such information for these clusters might be complicated thanks to the fluxional behavior of the cluster, presence of different compositions on the support, and the inherent size effect. We investigate the computed and experimental XANES of copper oxide

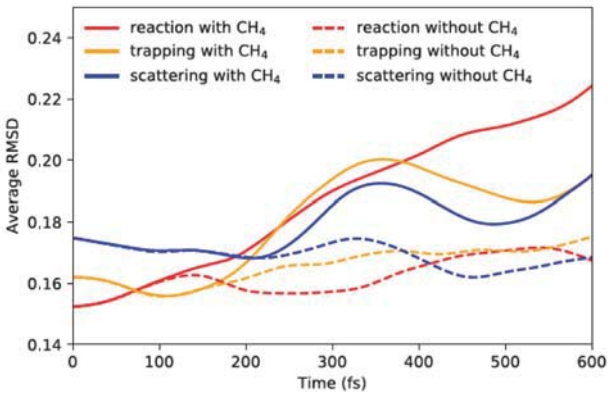

Fig 3 : AIMD of methane on Pt_{13}. Average RMSD on Pt over each type of trajectories at 400 K.

clusters with different compositions, Cu_4O_x (x = 2–5) and Cu_5O_y (y = 3, 5), deposited on amorphous alumina and ultrananocrystalline diamond (UNCD) respectively. The computed XANES shows that the geometry of the cluster can sometimes significantly affect the position of the peaks in the spectrum which means that one should take into account all thermally-accessible isomers in reaction conditions to interpret XANES, otherwise one might arrive at misleading conclusions.

vii) Cluster catalysts break scaling relations: Pt clusters can break the scaling relationships between chemically-related molecular fragments in ORR, thanks to their highly dynamic behavior (clusters easily adapt their structures upon changing the adsorbate or coverage). Hence, small clusters present opportunities for outstanding catalytic performance (Publication 1).

vii) We also explored smaller metallic entities. A collaboration with the Bowen group at Johns Hopkins, aims at understanding gas-phase catalysis of CO_2 reduction. The bimetallic hydride anionic cluster $PdCuH_4^-$ was shown by the Bowen group to produce complexes of formate ($HCOO^-$) and formic acid (HCOOH), and $PdCuCO_2H_4^-$ clusters when exposed to CO_2. Computations were used to identify the structures of the anionic cluster and determine what the most likely reaction pathway for the production of formate and formic acid is. In collaboration with experiments in the group of Ning Yang in Singapore, we modelled atomically dispersed Pt1-polyoxometalate catalysts. Using a series of polyoxometalates supported Pt catalysts, we find that despite the Pt_1-support interactions being different, the reaction pathways of various Pt1-polyoxometalate catalysts are very similar and their effective reaction barriers are close to each other and as low as 24 kJ/mol, indicating the possibility of obtaining SACs with improved stability without compromising activity (publication 4).

Future plans

The method development part of the project is essentially complete, and we are now in the production stage. We will perform numerous reactivity studies on discovered ensembles of clusters on surfaces in corresponding reaction conditions. From reactivity studies we will begin developing descriptors of activity of different sites simultaneously present at the interface (of which there may be hundreds), in order to streamline the assessment of activity of the interface, bypassing the massive amount of calculations. We will accumulate and analyze a wealth of statistics on the semiclassical trajectories that will elucidates the extent of dynamic coupling between various events at hot and pressurized interface in catalysis. From this, we may derive new rules concerning the definition of reaction coordinate in cluster catalysis, and other fundamentally new possibilities. We will also pursue explicit and exhaustive finding of reaction pathways that involve cluster isomerization or adsorbate rearrangement as part of the reaction coordinate, in addition to the reaction event itself.

Publications that acknowledge the program

1) Zandkarimi, B.; Alexandrova, A. N. Dynamics of subnanometer Pt clusters can break the scaling relationships in catalysis. 2019, J. Phys. Chem. Lett., 10, 460-467

2) Zandkarimi, B.; Alexandrova, A. N. Surface-supported cluster catalysis: ensembles of metastable states run the show. 2019, WIRES, advanced review, DOI: 10.1002/wcms.1420

3) Geng Sun and Philippe Sautet, Toward Fast and Reliable Potential Energy Surfaces for Metallic Pt Clusters by Hierarchical Delta Neural Networks, J. Chem. Theory Comput. In press 2019, DOI: 10.1021/acs.jctc.9b00465

4) Bin Zhang, Geng Sun, Shipeng Ding, Hiroyuki Asakura, Jia Zhang, Philippe Sautet, Ning Yan, Atomically Dispersed Pt1−Polyoxometalate Catalysts: How Does Metal−Support Interaction Affect Stability and Hydrogenation Activity? J. Am. Chem. Soc. 2019, 141, 8185−8197

Condensed Phase and Interfacial Molecular Science

Heather C. Allen
Ohio State University, Department of Chemistry and Biochemistry
100 West 18th Ave, Columbus OH 43210

Program Scope

Controlling Aqueous Interfacial Phenomena of Redox-Active Ions with External Electric Fields. There is a critical need to develop a thorough mechanistic understanding of interfacial hydration of redox ions and solvent organization with and without externally applied fields. Iron (II) / iron (III) is one such redox couple that is pervasive in our natural environment. Furthering our understanding of water-mediated iron speciation at interfaces provides fundamental knowledge relevant to geochemical and energy-related phenomena including mineral dissolution and energy infrastructure. Literature precedents suggest that an externally applied electric field will influence ion hydration properties, ion pairing, ion speciation and complexation, and interfacial water organization at the air/aqueous interface. We know that, of the studied alkali and alkaline earth metal ions, ions and water are not distributed homogeneously at interfaces, and it is therefore the current expectation that multivalent cations with co-anions will spontaneously form an electrical double layer, thereby aligning water in the diffuse layer. This phenomenon is explored with aqueous iron salts. Here we also study iron ions and their preferred speciation including the role interfacial water has on mediating the speciation process, in addition to the solvation shell water within the interface, and in the bulk. An additional goal for the proposed research is to show beyond proof of concept experiments, a fundamental understanding of the organization of, and induced by, redox ions Fe(II) and Fe(III) with and without externally applied electric fields at the hydrophobic air /water interface. In these studies we design and employ vibrational sum frequency generation (VSFG) spectroscopic, glancing angle, and polarized Raman spectroscopic, surface tension and ^{241}Am-based surface potentiometric experiments. Expected outcomes include instrumentation development important to understanding redox ions at aqueous surfaces, electric field effects, and advances in surface-sensitive spectroscopy, and constant depth reflection spectroscopy.

Recent Progress

Despite the importance of iron throughout all forms of life on earth and beyond, a complete molecular level understanding of the solvation of ferric ions has not been realized. Solvated Fe(III) is difficult to study due to the process of complexation to the counter anion and hydrolysis of the coordinated solvent molecules leading to a heterogeneous solution with diverse speciation. In our recent work, ferric chloride and nitrate complexes in aqueous solution were studied to first understand their bulk behavior as it related to water mediated ion pairing interactions. We used

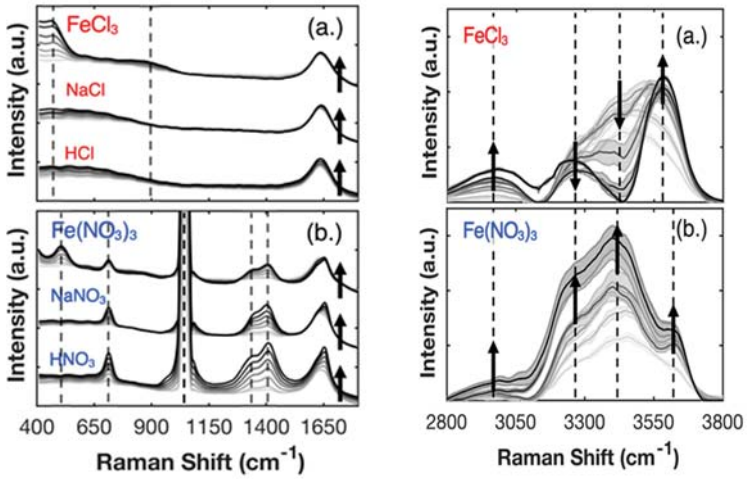

***Figure 1: Left Panel**: Unpolarized lower frequency Raman spectra of (a.) $FeCl_3$, NaCl, and HCl solutions and (b.) $Fe(NO_3)_3$ nitrate, $NaNO_3$, and HNO_3 solutions from 0.05 to 0.6 m. **Right Panel**: Unpolarized perturbed-water-spectra of (a.) $FeCl_3$ and (b.) $Fe(NO_3)_3$ with HCl spectra as 'solvent' over a concentration series from 0.05 to 0.6 m (light to dark grey). Arrows indicate increasing concentration.*

polarized and unpolarized Raman spectroscopy to study these salts as a function of their concentration in water, and at room temperature, and we referenced the spectra to their respective sodium salt or mineral acid.[1] Perturbed-water-spectra were generated using multivariate curve resolution-alternating least squares (MCR-ALS) to reveal the spectral response uniquely contributing to that of the ferric salts. Despite increased acidity of the ferric nitrate solutions, the water molecules in these solutions exhibit similarities to solvated sodium nitrate solutions whereas ferric chloride solutions were found more similar to hydrochloric acid solutions with respect to hydrogen bonding organization. These results revealed concentration dependent changes to the hydrogen bonding network, changes to the water symmetry, and changes to the relative abundance of solvent shared ion pairs. Ferric nitrate retains its water mediated ion pairing configuration; thhis is significantly different behavior compared to ferric chloro solution species. In Fig. 1, the Raman spectra of bulk solutions utilized in this analysis are shown. In the Left Panel separate spectra were obtained for the ferric salt and their associated sodium salt and acid to be used for PWS analysis. The Right Panel reveals the significant solvation response from the perturbed-water-spectra.

In other research that we also published in 2019, both aqueous and glycerol $FeCl_3$ solution surfaces were investigated with polarized vibrational sum frequency generation (SFG) spectroscopy.[2] In this work, we collaborated with CPIMS PI Robert Baker to elucidate the existence of Fe(III) at the surface and near surface regions of glycerol $FeCl_3$ solutions, where glycerol was used as a high vacuum compatible proxy for water. At higher concentrations in water, SFG revealed that the electric double layer (EDL) that was evident at lower concentrations of $FeCl_3$ in both water and glycerol solutions was substantially repressed, suggestive of Fe(III) complex enrichment and dominance of a centrosymmetric Fe(III) species that is surface active. In addition, a significant vibrational red-shift of the dangling OH from the water molecules that straddle the air-water interface revealed that the second solvation shell of the surface active Fe(III) complex permeates the topmost layer of the aqueous interface. Interesting at the surface of the glycerol solutions of $FeCl_3$, given a similar dielectric relative to water, yet much bulkier with hydrophobic moieties, the OH stretching modes were amplified at low $FeCl_3$ concentration and at high concentration, just as in the water solutions, was suppressed suggesting highly similar iron complexation with the chloro and OH (of glycerol) at the air- water interface.

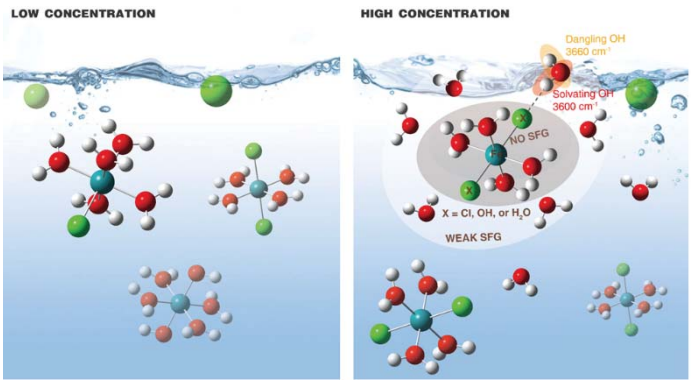

Figure 2. Iron complexation of centrosymmetric species dominate at higher $FeCl_3$ concentrations.

In our work on instrumentation development for surface potential measurements, we recently demonstrated that the surface potential of the air-aqueous salt interface of various simple salts exhibits significant magnitude increases with concentration. We are also currently working on measuring the surface potential of calibration molecules where the calibrant has a defined surface activity such that upon monolayer coverage the surface potential can also be easily calculated. This will then allow an absolute voltage value to be reported from the aqueous salt surfaces after comparison to the calibrant monolayer surface potential measurements. Just as in a pH meter calibration, 2 points are necessary at a minimum to calibrate the measurements. This approach is a significant departure from the few prior works in the literature, and although it is a simple concept, does present difficulties upon its implementation. We have

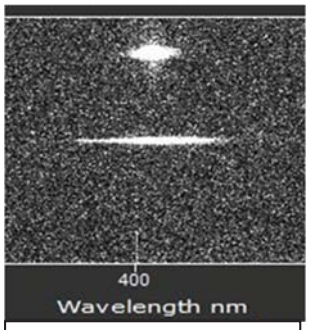

Figure 3. Second harmonic generation signal from the aqueous surface relative to simultaneous acquisition of the reference channel for signal calibration.

also completed a series of measurements of pure solvents that follow the predicted response using a simple model that incorporates dielectric constant and surface charge.

Surface potential values can also be derived from second harmonic generation (SHG) measurements from the air-aqueous salt interfaces. We have made significant progress in our SHG instrumentation to allow referenced SHG data from air-aqueous salt interfaces. A CCD image is shown in Fig. 3 revealing reference channel SHG response with the response from the solution surface.

Future Plans

We will continue to design experiments for the study of hydration and complexation of iron species at aqueous surfaces and in the bulk solution. We are continuing our research at the air-aqueous interface of simple salt solutions for comparisons to iron salts using SFG, SHG, surface potential measurements and Raman spectroscopy. Iron speciation is far more complex than non transition metal salts; yet, these simpler systems allow a series of reference values. In addition, for even the simplest salt NaCl, water mediation and solvation is not well understood, in particular details on the distributions of the ion pairing types (solvent shared vs solvent separated for example). We are continuing our work on surface potential instrumentation as discussed above, and are planning additional control experiments to ensure we understand the reported surface potential values and their meaning as they relate to water dipole orientation and speciation at the air-water interface. For example, we are currently testing noble gases in the air space, purging CO_2 from the solution phase, and also testing different electrode materials to test that our methods are robust. Surface potential instrument development using the Americium alpha decay source continues to be a major thrust. We have begun experiments in applying an electric field across the air-aqueous interface while probing with SHG, and preliminary data has been obtained. Yet, deconvoluting induced chemistry is nontrivial. We will be continuing work in this area. Future work also includes further developing a phase sensitive SHG instrument for revealing the sign of the surface potential.

Publications

1. S. M. Baumler, W. H. Hartt V, H.C. Allen; Hydration of Ferric Chloride and Nitrate in Aqueous Solutions: Water-mediated Ion Pairing Revealed by Raman Spectroscopy, *Phys. Chem. Chem. Phys.* **2019**, 21, 19172-19180 DOI: 10.1039/C9CP01392J

2. L. Lin, J. Husek, Jakub; S. Biswas, S. Baumler, T. Adel, K. C. Ng, L. R. Baker, H. C. Allen; Iron(III) Speciation Observed at Aqueous and Glycerol Surfaces: Vibrational Sum Frequency and X-Ray, *J. Am. Chem. Soc.* **2019**, 141, 34, 13525-13535.

Size-Selected Sub-Nano Electrocatalysis

Scott L. Anderson (anderson@chem.utah.edu), Chemistry Department,
University of Utah, 315 S. 1400 E., Salt Lake City, UT 84112

Anastassia N. Alexandrova (ana@chem.ucla.edu), Chemistry and Biochemistry,
Philippe Sautet (sautet@ucla.edu), Chemical Engineering
University of California Los Angeles, Los Angeles, CA 90095

Program Scope

This project, which started September 1, 2019, uses a combination of experimental studies of size-selected electrocatalysts with closely coupled theory, to probe the effects of catalytic site size, catalyst- support interactions, and the coverage of the sub-nano catalytic centers, on activity for several fundamental, relatively simple electrocatalytic reactions. Previous DOE-funded experiments showed order of magnitude effects of varying cluster size, affecting both activity and product branching, with effects clearly related to size-dependent electronic structure in some cases, and to catalytic site size in others.[1-4] In this new project, an expanded experimental tool set is coupled with detailed theory, to extract enhanced mechanistic insight.

Approach

The proposed research exploits Anderson's ability to make size-selected electrodes with controlled coverage of sub-nanometer catalytic centers, by depositing mass-selected metal clusters on atomically clean electrode supports in UHV. After characterization with surface science tools *in situ*, electrodes are transferred into an attached UHV-compatible antechamber that allows several types of experiments. The antechamber can be vented with UHP argon, and then electrocatalytic properties can be studied using standard methods (e.g. cyclic voltammetry) *in situ* without air exposure. Alternatively, the sample can be transferred out of the antechamber either dry, under inert atmosphere, or wetted by a thin film of electrolyte, in either case protecting the electrode from contamination by species in air. The sample can also be saturated by CO in the UHV system before transfer to the antechamber, further protecting against contamination by adventitious adsorbates.

In addition to *in situ* surface science and electrochemical characterization, *ex situ* measurements include scanning electrochemical cell microscopy (SECCM) and *operando* scanning transmission electron microscopy (STEM) to probe the effects of cluster proximity and aggregate formation on electrocatalytic activity, and to study cluster diffusion and sintering. *Operando* X-ray scattering and spectroscopy will probe cluster size and oxidation state changes under electrochemical potentials. SECCM and X-ray experiments will be in collaboration with Henry S. White (Utah) and Sungsik Lee (Argonne), respectively.

Density Functional Theory (DFT) by Alexandrova and Sautet will study small clusters under adsorbate loading and electrochemical potentials. To maximize experiment-theory coupling, hence mechanistic insight, the work will focus on fundamental reactions on relatively simple electrodes. The combination of detailed experimental results with DFT-based simulations will provide molecular level understanding of the factors that control electrochemical activity and selectivity.

There are no publications to report at this time.

References cited

[1] S. Proch *et al.*, J. Am. Chem. Soc. **135** (2013) 3073−3086.
[2] A. von Weber *et al.*, Phys. Chem. Chem. Phys. **17** (2015) 17601.
[3] A. von Weber *et al.*, J. Phys. Chem. C. **119** (2015) 11160.
[4] A. von Weber, and Scott L. Anderson, Acc. Chem. Res. **49** (2016) 2632.

Probing Electrochemical Reactivity Under Nanoconfinement Using Molecularly Pillared Two Dimensional Materials

Veronica Augustyn (vaugust@ncsu.edu)
Dept. of Materials Science and Engineering
North Carolina State University
Raleigh, NC 27695

Program Scope

The goal of this research is to understand how the confinement of liquid phase reactants within the layers of a two dimensional material influences their electrochemical reaction kinetics. The hypothesis driving this research is that there will be an optimum interlayer spacing of layered materials to enable electrochemical reactivity in the interlayer. Layered and 2D materials have broad applications in catalysis and electrocatalysis, where it is hypothesized that the catalytically active sites reside at edges and surface defects. This research will investigate how the nanoconfined interlayer of these materials can be made accessible for electrocatalytic activity. Nanoconfinement has been shown to affect the physical properties of molecules and solvents and may be utilized to further tune electrochemical activity. Importantly, the research will utilize a materials chemistry approach to define the nanoconfinement environment via molecular pillars – molecules of defined length anchored within the interlayer. In order to test this hypothesis, the research will investigate how molecular pillaring of a prototypical layered material, MoS_2, influences the electrocatalysis of the hydrogen evolution reaction (HER), a critical step in the electrochemical synthesis of hydrogen fuel. The objectives of this research include: (1) the synthesis of MoS_2 with nanoconfined fluids and controlled interlayer spacing; (2) characterization of the structure, chemical composition, and dynamics of the interlayer confined molecules; and (3) characterization and mechanistic understanding of a liquid-phase electrochemical reaction under nanoconfinement by these hybridized layered materials. The understanding developed over the course of this research will be applicable to both fundamental and applied energy research, from electrochemistry and materials chemistry, to fuel cells and electrolyzers.

Recent Progress

Our recent progress has focused on assembling the research team, which included the hiring of a graduate student and postdoctoral fellow. We are now beginning the synthesis of the molecularly-pillared two dimensional materials using MoS_2 as a model, electrocatalytically active host. We are investigating two synthesis protocols: one for thin films, that will be suitable for electrochemical and spectroscopic studies, and one for bulk materials, that will provide samples suitable for the physical characterization techniques.

Future Plans

Our immediate future plans for this year are to synthesize the molecularly pillared MoS_2 materials using, initially, a variety of alkyl amines as the pillars. After synthesis, we will perform physical characterization to determine the nature (chemistry, content) of the intercalated species and their dynamics. We will also investigate the electrochemical reactivity of a simple 1 electron redox process under nanoconfinement.

Publications

There are currently no publications to report for this new award, which began September 1, 2019.

Visible light photo-catalysis in charged micro-droplets
DE-SC0016044
Abraham Badu-Tawiah
Department of Chemistry and Biochemistry, The Ohio State University. Columbus, OH 43210
badu-tawiah.1@osu.edu

Program Scope

This research program seeks to establish the use of charged micro-droplet environment as a medium for studying excited-state chemistry. The confined droplet environment has capacity to accelerate chemical reactions using only picomoles (10^{-12} mol) of reactants. The hypothesis is that the effect of electric fields used during charged droplet generation, the effect of concentration achieved by solvent evaporation from the resultant charged droplets, and the effect of droplet exposure to a highly intense and coherent visible laser source will enable the production of unique, reactive photo-chemical species for novel pathways that might be difficult to access in traditional bulk, condensed-phase conditions. Unlike traditional gas-phase reactions conducted under reduced pressure, the ionic environment of the charged droplets exists at the interface of solution-phase and the gas-phase, yielding information that is directly transferrable to large scale chemical synthesis. The main focus of our work has been the development of novel devices for charged droplet manipulation and real-time product detection by mass spectrometry (MS). Chemical systems of interest involve the study of interfacial oxidation of amines.

Recent Progress

We have developed a novel contained-electrospray (ES) ionization device that is capable of (i) reactant confinement in charged droplets, and (ii) manipulation of the droplet reaction environment with a variety of stimuli (photons, electrical discharge, and heat). Progress is reported on the effects of photons, electrical energy, and heat on electrosprayed charged droplet reactivity.

By coupling a portable laser source with nESI MS, we established the first MS-based picomole-scale real-time photoreaction screening platform.[1,2] With this approach, we discovered an effective photocatalytic pathway involving the dehydrogenation of 1,2,3,4-tetrahydroquinolines (THQ) to the corresponding quinolines. The reaction was catalyzed by the common visible-light-harvesting complex [Ru-(bpy)$_3$]Cl$_2$ (bpy=2,2'-bipyridine) under ambient conditions. Mechanistic studies revealed that the main active species in the droplet interfacial reaction environment to involve superoxide anions ($O_2^{\bullet-}$) produced during the process of photo-catalyst regeneration. Under this photocatalytic pathway, we observed marked reactivity difference between tetrahydroquinolines and tetrahydroisoquinolines. While tetrahydroquinolines (THQ) underwent full dehydrogenated via the removal of four hydrogen atoms to yield quinolones (>86% yield), tetrahydroisoquinoline (THiQ) produced the dihydroisoquinoline intermediate irrespective of visible light exposure time. Surprisingly, although this reactivity difference between the isomers THQ and THiQ is well-known, the factors governing this inconsistency are incompletely known.

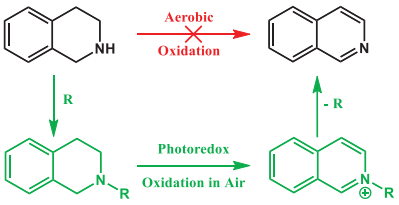

Scheme 1. Schematic representation of rationally designed synthetic method for THiQ, involving three steps: step I – activation of THiQ via N-substitution, step II – aerobic oxidative dehydrogenation using Ru(bpy)$_3^{2+}$ photo catalyst, step III – regeneration of isoquinolines by removing substitute

Detailed mechanistic investigations using DFT calculation and our real-time reaction screening revealed a high-speed electronic interconversion bottleneck caused by hyper-conjugation. We observed that N-substitution with *pi* and *sigma* donors relieved the hyper-conjugation, freeing THiQs to undergo full hydrogenation. By this insight, a new photocatalytic synthetic strategy was rationally designed to enable large-scale production of isoquinolines from THiQ. This new producer involves three simple steps (Scheme 1): (i) N-substitution of a suitable auxiliary to reduce hyper-conjugation, (ii) photoredox oxidation of N-substituted THiQ using off-the-shelf, visible light harvesting $Ru(bpy)_3Cl_2$ complex under ambient conditions, and (ii) removal of N-substituted auxiliary to generate isoquinoline.

We have since realized that the active $O_2^{\bullet-}$ generated by the photochemical reactions can also be produced by other sources such as corona discharge. Therefore, we studied the reactivity of amines and compared their behavior with photochemical reaction. The results revealed that the exposure of an aqueous-based liquid drop containing amines and graphite particles to plasma generated by a corona discharge resulted in heterogeneous aerobic dehydrogenation reactions. The presence of graphite particles introduced heterogeneous interfacial/surface effects, which enabled efficient sampling of the reactive species in the plasma. The dehydrogenation reactions reached >96% yields in less than 2 minutes of reaction time.[3] Interestingly, primary amines produced the corresponding nitriles. This is contrary to conventional reactions (photochemical and thermal) which tend to yield self-coupled imine products from primary amines (Scheme 2). This graphite catalyzed dehydrogenation reaction was performed on hydrophobic paper substrates, prepared in-house to control the interfacial forces between the analyte solution and the paper surface. Contact angles typically used for estimating surface energies performed poorly on the rough porous paper substrate. Therefore, we developed a novel spray method to enable us characterize the surface energy of the prepared hydrophobic paper.[4]

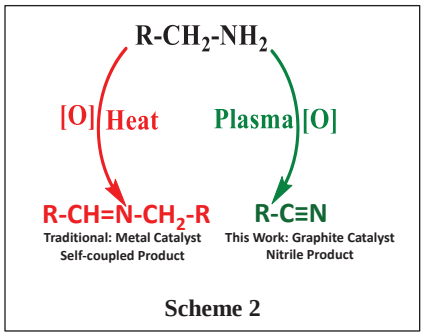

Scheme 2

We have achieved similar dehydrogenation products via electrochemical reactions using inert platinum electrode for the electrospray process.[5]

We have also studied the competitive oxidation between two different functional groups using excited-state chemistry in the droplet environment. Here, we used bi-functional substrates such as amino alcohols and their expected reaction is illustrated in Scheme 3. Both the OH and NH_2 groups could act as electron donors for reaction with excited photocatalyst so we seek to study their cooperativity within a single substrate under the droplet reaction conditions. Our expectation was to form strained rings using the reactive droplet environment. This interest is motivated by the fact that small and strained N-heterocycles such as those found in penicillin offer the prospects of new drug leads. However, less progress has been made for benzazetidines, an azetidine core flanked by benzene ring, due to the significant ring strain in these four-membered scaffolds. In our experiments, we observed that the excess charge at the droplet surface actually facilitates dehydration reactions leading to the expected strained-ring products without the use of a photocatalyst. In other words, this uncatalyzed interfacial charge directed reaction leading to

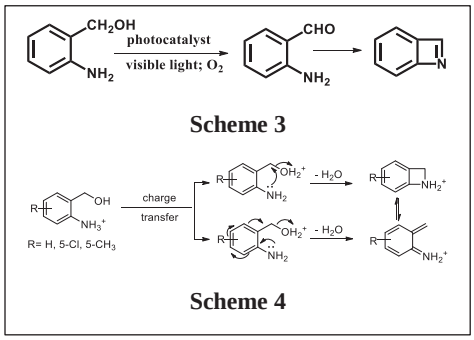

dehydration (Scheme 4) occurs faster than dehydrogenation induced by excited state chemistry. Detail mechanistic experiments using isotope-labeled substrates have confirmed that the hydrogen atom from amine functional group in involved in this dehydration reaction.

Future Plans

The focus of our work will remain (i) the development and refinement of methodologies to "process" ions at atmospheric pressure, where processing includes ion formation, ion stimulation, ion reaction, and product collection, and (ii) attempts to advance understanding of the fundamentals of ion chemistry at interfaces and atmospheric pressure, using these new methodologies. Of particular interests include the creation of novel devices to enhance interfacial effects of charged microdroplets and the elucidation of the complete mechanism governing their reactivity.

For example, we are developing a new apparatus (Scheme 5) to enable non-equilibrium interfacial reactions in charged microdroplets. With this setup, we plan to be able to deposit reagents directly at the droplet surface without relying on surface enrichment via solvent evaporation. This new experimental setup for enhanced interfacial reactions is expected to create opportunities to access multiple reaction landscapes by operating under non-equilibrium conditions.[6]

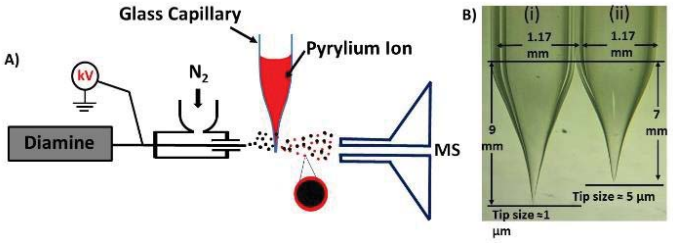

Scheme 5. A) Experimental setup for depositing reaents (e.g. pyrilium ion) onto the surface of charged microdroplets containing reagents to be reacted (e.g., diamine) via a droplet pick-up mechanism. Reaction products are subsequently detected by the mass spectrometer in real-time. **B)** Photograph showing a typical nano-electrospray ionization pulled glass capillary (i) compared with capillary for our experiment (ii) used for containing reagent to be deposited onto droplet surface.

Due to its speed and surface immediate enrichment, we believe this setup will provide the platform needed to fully characterize the source of the $O_2^{\bullet-}$ reactive species in droplet-based photochemistry by capturing transient intermediates and other reaction pathways that cannot be accessed under the typical equilibrium conditions (e.g., in situations where reagents are premixed before electrospray).

We are particularly interested in bi-functional reagents to evaluate intramolecular versus intramolecular competitive reactions. While the enhanced surface/interfacial properties will limit solvent effects, we plan on studying the corresponding atmospheric pressure gas-phase reactions to effectively calculate enhancement factors achieved in the droplet environment.

By controlling the position of the non-equilibrium reactions, we plan to enable *in-situ* preparation of active catalysts from simple salts (e.g., $CuBr_2$) and free ligands (e.g., 2,2'-bipyridine). For example, a previous report on a systematic investigation of the effect of different components in the Cu salt/bpy catalytic system showed better performance under basic (e.g., N-methylimidazole (NMI)) and stable radical (e.g., 2,2,6,6-tetramethylpiperidinyloxy (TEMPO)) conditions. Spectroscopic investigation suggested the presence of $[Cu(bpy)(NMI)O_2]^+$ and oxygen-bound dimer, $[Cu(bpy)(NMI)(O_2)Cu(bpy)(NMI)]^{2+}$, all indicating the importance of reactive oxygen species. By changing the polarity of the electrospray droplet, and depositing selected reagents at the surface, we will simplify the compositional complexity of this catalytic system and create opportunities for catalyst synthesis and reaction screening in a single

experimental step. Here too, solvent effects will be studied systematically on-line using the contained-ES apparatus.[7,8] That novel and highly reactive chemical species can be generated under the charged micro-droplet environment motivates us to screen other first row transition metal salts including those of Ni and Fe. We have unique opportunity to vary a multitude of reaction conditions within a short time period. For this, we will electrospray various selected halides from different solvent compositions. Effects from confinement, photon and electrical discharge is expected to generate different micro-solvated $[ML_n]^{n+}$ species (L = halide, H_2O, CH_3CN, OCH_3, $OHCH_3$, etc.) with various oxidation states, some of which will be expected to have catalytic activities. Intermediate detection and characterization will be achieved by using a novel non-equilibrium reaction setup.

References and Recent Publications

1. Suming Chen, Qiongqiong Wan and Abraham K. Badu-Tawiah "Picomole-Scale Real-Time Photoreaction Screening: Discovery of the Visible-Light-Promoted Dehydrogenation of Tetrahydroquinolines under Ambient Conditions" *Angew. Chem. Int. Ed.* **2016**, *55*, 9345
2. Savithraa Jayaraj and Abraham K. Badu-Tawiah "N-Substituted Auxiliaries for Visible Light-Mediated Dehydrogenation of Tetrahydroisoquinolines: A Theory-Guided Rational Catalytic Design Supported by Real-time Electrospray-based Photoreaction Screening" *Scientific Reports* **2019**, 9, 11280
3. Kathryn M. Davis and Abraham K. Badu-Tawiah "Direct and Efficient Dehydrogenation of Tetrahydroquinolines and Primary Amines using Ionic Wind Generated on Ambient Hydrophobic Paper Substrate" *J. Am Soc. Mass Spectrom.*, **2017**, 28(4), 647–654
4. Damon, D. E.; Maher, Y. S.; Allen, D. M.; Baker, J.; Chang, B. S.; Maher, S.; Thuo, M. M.; Badu-Tawiah, A. K. "Determining Surface Energy of Porous Substrates by Spray Ionization" **Submitted, 2019**
5. Qiongqiong Wan, Suming Chen, and Abraham K. Badu-Tawiah "An integrated mass spectrometry platform enables picomole-scale real-time electrosynthetic reaction screening and discovery *Chemical Science*, **2018**, 9, 5724
6. Sahraeian, T.; Kulyk, D.S.; Wan Q.; **Badu-Tawiah, A.K**. "Droplet Imbibition Enables Non-Equilibrium Interfacial Reactions in Charged Microdroplets" **Submitted, 2019**
7. Colbert F. Miller, Dmytro S. Kulyk, Jongin W. Kim, and Abraham K. Badu-Tawiah "Re-configurable, Multi-mode Contained-electrospray Ionization for Protein Folding and Unfolding on Milliseconds Time Scale" *Analyst*, **2017**, 142, 2152-2160
8. Colbert F. Miller, Benjamin Burris and Abraham K. Badu-Tawiah "Spray Mechanism of Contained-Electrospray Ionization" **Submitted, 2019**
9. Sierra Jackson, Devin J. Swiner, Patricia C. Capone and Abraham K. Badu-Tawiah "Thread Spray Mass Spectrometry for Direct Analysis of Capsaicinoids in Pepper Products" *Analytica Chimica Acta*, **2018**, 1023, 81-88

Probing Ion Solvation and Charge Transfer at Electrochemical Interfaces Using Nonlinear Soft X Ray Spectroscopy

L. Robert Baker
100 W. 18th Ave. Newman-Wolfrom Laboratory
Department of Chemistry and Biochemistry
The Ohio State University, Columbus, OH 43210
baker.2364@osu.edu

1. Program Scope

Fundamental understanding of interfacial charge transfer is an important challenge with both scientific and technological relevance because these processes are responsible for the performance of batteries, fuel cells, acid–base catalysts, and other electro and photochemical systems. Improving the efficiency of these energy conversion technologies requires a detailed understanding of the molecular-level processes occurring at interfaces that drive electrochemical energy conversion. In electrochemical systems, charge transfer may occur as the bias-driven motion of electrons or holes from a solid electrode to a liquid phase reactant, or as ion de-solvation, injection, and intercalation across the electrode/electrolyte interface. Probing the interfacial charge transfer dynamics with chemical specificity, ultrafast time resolution, and surface sensitivity is crucial for developing detailed understanding of these processes and, subsequently, for engineering materials with desirable optical and electronic properties.

To elucidate surface charge carrier dynamics at surfaces, we have constructed a tabletop extreme ultraviolet (XUV) spectrometer that operates in reflection at near grazing incidence angle.[1-2] XUV spectroscopy is well suited for studying charge carrier dynamics because of it is element specific and sensitive to oxidation state, and spin-state, and coordination geometry, and because these experiments can be performed in the laboratory with femtosecond time resolution.[3] Unlike transmission measurements, XUV reflection-absorption (RA) is not limited by sample thickness which extends the use of XUV spectroscopy to functional materials without restriction to sample thickness or substrate. Moreover, reflectivity offers the advantage of surface specificity having a measured probe depth of only a few nm, indicating that this technique can specifically follow charge transfer dynamics at the surface of a material.[4]

We have applied this technique to identify the chemical nature of defect states in NiO which mediate charge carrier recombination in this material.[5] Direct observation of small polaron formation and transport has remained elusive due to unavailability of spectroscopic techniques that are sensitive to this process. Detailed understanding of the photoexcited charge carrier trapping via small polaron, diffusion of the polaron to the defect site, and subsequent defect-mediated recombination is crucial for the design of NiO based energy conversion materials.

We have also studied the dynamics of charge separation at the heterojunction of NiO/Fe_2O_3 by probing the changes in the electronic structure and lattice environment of both Ni and Fe centers simultaneously.[6] These measurements showed the ability to independently resolved exciton dissociation in photoexcited Fe_2O_3 and subsequent hole injection into an NiO layer. These results were the subject of a DOE science highlight and were featured on the cover of *Physical Chemistry Chemical Physics*. These measurements provide relevant insights into the surface properties of a material that control the efficiency of charge separation at interfaces.

Ongoing work includes the investigation of spin crossover dynamics in thin film cobalt ferrite ($CoFe_2O_4$). Cobalt ferrite is a ferromagnetic insulator at room temperature which has shown promise for controlling spin transport at interfaces. Using XUV spectroscopy, we can follow ultrafast spin crossover dynamics at the surface of this material with element-specific resolution. In a separate direction, we have also recently extended the use of XUV reflection spectroscopy to study solvated ions at the surface of liquid glycerol.

2. Recent Progress

Direct Observation of Ultrafast Hole Localization in Metal Oxide Semiconductors

Using XUV-RA spectroscopy, we have recently demonstrated the ability to detect both photoexcited electrons in metal *3d* states as well as holes in oxygen *2p* states.[3] In a series of first row transition metal oxides, Fe_2O_3, Co_3O_4, and NiO, we directly observe the electron and hole localization on the ultrafast time scale by probing the metal $M_{2,3}$-edge (*3p* → *3d* transition) and oxygen L_1-edge (*2s* → *2p* transition), respectively. We observe that the hole localizes to O *2p* valence band states within the instrument response time (~100 fs) following photoexcitation.[3] Signature of the hole at the O L_1-edge enables the comparison of excited state electronic structure of the hybridized valence band that correlates with water oxidation efficiency in Fe_2O_3, Co_3O_4, and NiO.

Bohr Radii of Charge Transfer Excitons

Poor charge carrier mobility is one of the major reasons of losses experienced during energy conversion in first row transition metal oxide semiconductors. The charge carrier mobility and catalytic efficiency of these materials are closely related to the interaction between the photoexcited electron–hole and the localization of the exciton. Using pump fluence dependent study of the transient XUV-RA intensity, we find that the photoexcited electrons and holes are separated by approximately one M–O bond length in Fe_2O_3, Co_3O_4 and NiO.[7] The observed saturation behavior of the transient signal has been fitted by the saturable absorber model. From this model, we can calculate the exciton Bohr radius for each of the metal oxides and find that the exciton Bohr radii are on the order of one M–O bond length, suggesting a highly localized nature of the exciton. This picture is consistent with the Frenkel exciton model, where excitons tend to be localize within a single unit cell. Gradual increase of the exciton size correlates with the red shifts of the O L_1-edge peak position from Fe_2O_3, Co_3O_4 to NiO. This observation suggests that excitons prefer to delocalize with increasing M–O bond covalency. Accordingly, these results indicate that the photoexcitation basically occurs across a single M–O bond where hole is localized on O *2p* valence band states with electron localized on metal *3d* conduction band states. This work was highlighted in Advances in Engineering.

Defect-Mediated Charge Carrier Recombination in NiO

We have used XUV-RA spectroscopy to identify the nature of the surface defect states, ultrafast charge carrier trapping, and defect-mediated recombination dynamics in NiO thin film.[5] Complimentary study using XPS has been used to support findings of XUV-RA measurements. Several thin films of NiO were prepared by varying the annealing temperature (100–500 ^oC) to control the thermal oxidation of nickel thin film. Using XUV-RA and XPS measurements we have identified two different kinds of defect sites in these thin films: a) Sub-surface grain boundary between Ni metal and thin NiO layers b) Ni vacancy defect associated with Ni^{3+}. The density of these defects depends on the annealing temperature and have significant effects on the photoexcited charge carrier recombination dynamics.

Static XUV-RA spectra of nickel thin film annealed at different temperatures are dominated by a strong peak at 64.8 eV which corresponds to Ni^{2+} $M_{2,3}$-edge transition, confirming the presence of NiO at the surface of each sample. A small shoulder present at 59 eV for the low-temperature annealed samples (100, 200, and 300 °C) is assigned as Ni metal since our previously assigned peak for Ni^+ lies at 62 eV and this features is at even lower energy. These observation identifies both Ni^{2+} and Ni metal is supported by XPS spectra and suggests the presence of grain boundary defect sites. Furthermore, to confirm the presence on Ni^+ we rely on detecting oxygen vacancies associated with undercoordinated Ni^+ metal centers by fitting O 1*s* XPS spectra.

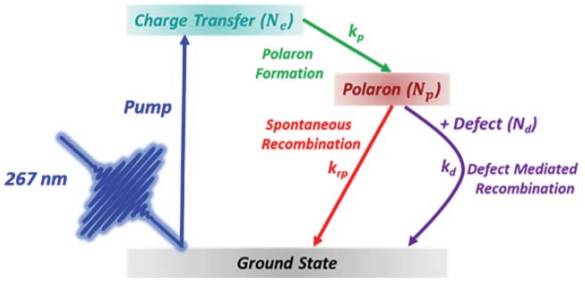

Figure 1: Schematic of the kinetic model depicting the decay pathways of charge-transfer states (N_e) in the presence of defects states (N_d).

Figure 1 schematically depicts the kinetic model used to understand the charge carrier dynamics in NiO thin films annealed at different temperatures.

Photoexcitation by a 267 nm pump pulse leads to the generation of a charge-transfer excited state (N_e) within the instrument response time (100 fs). This charge-transfer state decays into the polaron state (N_p) with a rate constant of k_p. This polaron state can decay either through spontaneous recombination (k_{rp}) or defect mediated recombination (N_d) with a bimolecular decay constant of k_dN_d. Since this decay rate is bimolecular, the dominant effect on the polaron recombination rate should scale linearly with either the concentration of oxygen vacancies (Ni^+) or grain boundaries (Ni metal). We find that grain boundaries serve to increase the polaron recombination rate while oxygen vacancies play a minor role in recombination dynamics.

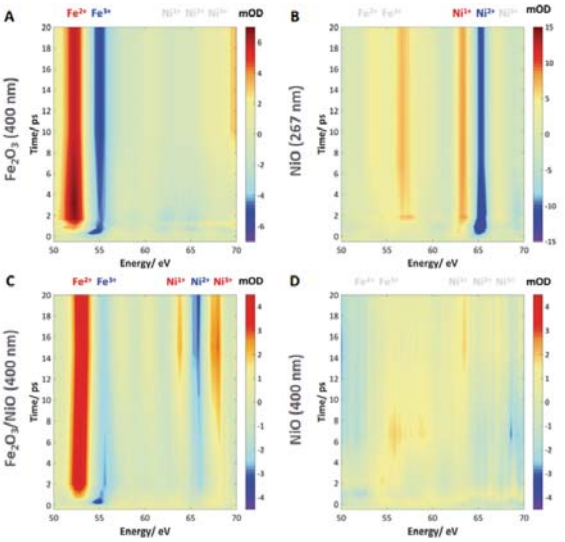

Figure 2: Contour plots showing transient XUV-RA data of Fe_2O_3 (A), NiO_x/Fe_2O_3 (C) and NiO (D) pumped at 400 nm and NiO (B) pumped at 267 nm

Interfacial Charge Transfer in NiO_x/Fe_2O_3 Heterojunctions

Charge carrier dynamics at a NiO_x/Fe_2O_3 heterojunction with respect to pure NiO and pure Fe_2O_3 are important to understand its catalytic activity for water oxidation. Additionally, the valence band offset of these two materials is well suited for transferring photoexcited holes from Fe_2O_3 to NiO to produce spatially separated electrons and holes in this metal oxide heterojunction. To investigate the charge carrier dynamics across the type II heterojunction of NiO and Fe_2O_3, photoexcited carrier dynamics of pure NiO, pure Fe_2O_3 and the heterojunction have been performed.[6]

Figure 2 shows the transient XUV-RA data for pure Fe_2O_3, pure NiO and the heterojunction excited at 400 nm (Fig. A, C and D) and pure NiO excited at 267 nm (Fig. B). The dynamics of pure Fe_2O_3 and NiO have been performed previously,[6,9] where samples undergo a LMCT process after photoexcitation. Due to the wide band gap (~ 4 eV) of NiO compared to Fe_2O_3 (~ 2 eV) it is expected that the photoexcitation of the heterojunction at 400 nm light will selectively excite the charge carriers in Fe_2O_3 and not NiO. Figs. C and D confirm this prediction showing a delayed response from the Ni edge for the heterojunction and no excitation for pure NiO at 400 nm. This delayed formation of Ni^{3+} after photoexciting at 400 nm indicates excitation of the underlying Fe_2O_3 substrate and subsequent hole transfer to NiO valence band states composed of significant Ni 3*d* character. To the best of our knowledge, this is the first element specific observation of ultrafast interfacial hole migration in heterojunction material causing this data to be featured as a cover article for PCCP.

3. Future Plans

Spin Crossover in Cobalt Ferrite Thin Films

We have performed transient XUV-RA experiments on cobalt ferrite ($CoFe_2O_4$) thin films in order to probe the photo-induced spin dynamics in this material. Figure 3 shows the the transient XUV-RA spectrum of this material where we see similar features previously reported for Fe_2O_3 and Co_3O_4. The Fe^{3+} bleach (55.6 eV) and Co^{2+} bleach (61 eV) along with positive features corresponding to Fe^{2+} (52.8 eV) and Co^{3+} (~ 68 eV) indicate a one electron charge transfer from cobalt to iron centers. Ground state cobalt ferrite has native Co^{2+} in a high spin state configuration and photoexcited Co^{3+} can either adopt the high- or low-spin state. Simulations of the transient spectrum

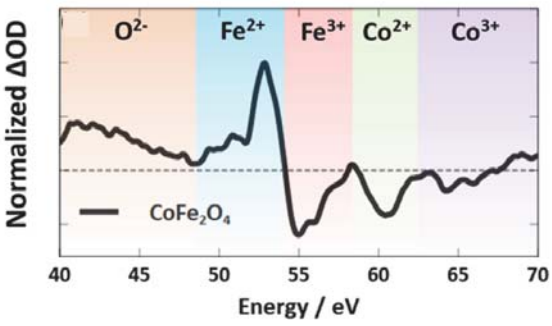

Figure 3: Transient XUV-RA spectrum of cobalt ferrite. Shaded regions represent the O L-edge, Fe M-edge, and Co M-edge demonstrating the ability to probe oxidation and spin state changes with element specificty on the femtosecond time scale in this ternary oxide.

corresponding to high- and low-spin configuration of Co^{3+} (not shown) reveal that the Co3+ metal centers transition from high to low spin upon photoexcitation. Ongoing analysis suggests the driving force for spin crossover is the formation of a hole polaron that compress the lattice around Co^{3+}, increasing the crystal field splitting of cobalt 3*d* orbitals and driving a high spin to low spin transition.

Detecting Solvated Ions at Liquid Interfaces

Finally, we seek to extend XUV-RA spectroscopy to probe the dynamics of solvated ions at liquid surfaces. Figure 4 compares the normalized XUV-RA ground state spectra of $FeCl_3$ glycerol solutions with solid Fe_2O_3. As can be seen, we detect Fe^{3+} ions at the glycerol surface with excellent signal-to-noise even at sub-molar concentrations. Traditionally XUV spectroscopy of transition metal complexes has proven challenging owing to the very short penetration depth of XUV light in solution. The ability to obtain these spectra at good signal-to-noise in a reflection geometry will open future opportunities for measuring the dynamics of solvated ions at interfaces. This work represents the beginning of a collaboration with CPIMS PI, Heather Allen, where we utilize this technique to investigate Fe speciation at liquid interfaces.[7] We anticipate that in the near future these studies may be extended to probe the ultrafast dynamics of solvated ions at liquid interfaces.

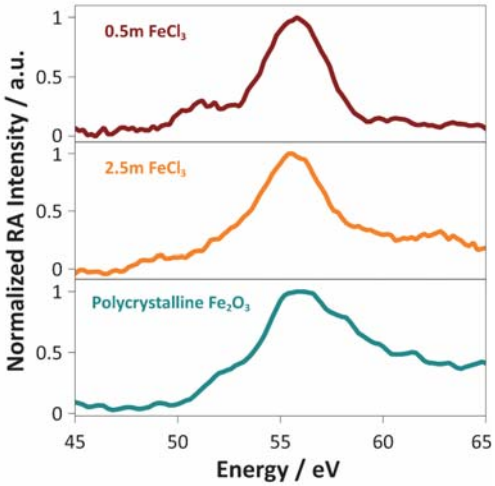

Figure 4: Ground state XUV-RA spectra of thin film $FeCl_3$ solution for low and high concentrations

4. Publications Acknowledging This Award:

1. Cirri, A.; Husek, J.; Biswas, S.; Baker, L. R., Achieving Surface Sensitivity in Ultrafast XUV Spectroscopy: $M_{2,3}$-Edge Reflection–Absorption of Transition Metal Oxides. *The Journal of Physical Chemistry C* **2017,** *121* (29), 15861-15869.
2. Biswas, S.; Husek, J.; Baker, L. R., Elucidating ultrafast electron dynamics at surfaces using extreme ultraviolet (XUV) reflection–absorption spectroscopy. *Chemical Communications* **2018,** *54* (34), 4216-4230.
3. Biswas, S.; Husek, J.; Londo, S.; Baker, L. R., Highly Localized Charge Transfer Excitons in Metal Oxide Semiconductors. *Nano Letters* **2018,** *18* (2), 1228-1233.
4. Husek, J.; Cirri, A.; Biswas, S.; Baker, L. R., Surface electron dynamics in hematite (α-Fe_2O_3): correlation between ultrafast surface electron trapping and small polaron formation. *Chemical Science* **2017,** *8* (12), 8170-8178.
5. Biswas, S.; Husek, J.; Londo, S.; Baker, L. R., Ultrafast Electron Trapping and Defect-Mediated Recombination in NiO Probed by Femtosecond Extreme Ultraviolet Reflection–Absorption Spectroscopy. *The Journal of Physical Chemistry Letters* **2018,** *9* (17), 5047-5054.
6. Biswas, S.; Husek, J.; Londo, S.; Fugate, E. A.; Baker, L. R., Identifying the acceptor state in NiO hole collection layers: direct observation of exciton dissociation and interfacial hole transfer across a Fe2O3/NiO heterojunction. *Physical Chemistry Chemical Physics* **2018,** *20* (38), 24545-24552.
7. Lin, L.; Husek, J.; Biswas, S.; Baumler, S. M.; Adel, T.; Ng, K. C.; Baker, L. R.; Allen, H. C., Iron(III) Speciation Observed at Aqueous and Glycerol Surfaces: Vibrational Sum Frequency and X-ray. *Journal of the American Chemical Society* **2019,** *141* (34), 13525-13535.

Methods for addressing strongly heterogeneous and far-from-equilibrium systems

Monika Blum (mblum@lbl.gov), Phillip L. Geissler (plgeissler@lbl.gov),
Teresa Head-Gordon (thg@berkeley.edu), Kranthi Mandadapu (kkmandadapu@lbl.gov), and
Kevin Wilson (krwilson@lbl.gov)

Lawrence Berkeley National Laboratory, Chemical Sciences Division
1 Cyclotron Road, Berkeley, CA 94720

Program Scope

A significant gap exists between basic studies of molecular chemical physics and the operation of real devices and natural systems. This effort aims to establish the chemical methods and insight that will enable understanding of systems that are profoundly complex in composition, heterogeneity, preparation, and organization.

Theoretical and computational aspects of this effort are advanced by Geissler, Head-Gordon, and Mandadapu. Their work provides general techniques for addressing microscopic organization under conditions that profoundly challenge conventional approaches of simulation and analysis. Such behavior typically also presents formidable challenges for experimental measurement. Complementary method development in the laboratory is thus an important partner to these efforts. Like theory, experimental advances are needed to develop novel ways for observing reactions in liquids and at their surfaces. In particular, liquids present a substantial challenge for detecting short lived reaction intermediates produced in thermal reactions. Furthermore, in many realistic systems, reactants reside both at the interface as well as the fully coordinated environment of the bulk solution. Blum and Wilson are developing new laboratory strategies for these purposes.

Recent Progress

We are advancing computational techniques that systematically explore the space of dynamical trajectories. Accessing dynamical behavior on time scales much longer than those of basic microscopic motions (say, ps to ns) is a ubiquitous challenge in molecular simulation. A variety of methods have been developed for one-step transformations in relatively simple environments, e.g., elementary chemical reactions in solution. These focus on the existence of a well-defined barrier whose crossing determines long-time dynamics. For much more complex situations that are not dominated by a single barrier, these computational approaches generally fail. From glassy systems to self-assembling nanostructures to systems driven out of equilibrium, examining typical trajectories is a challenge, and examining atypical yet especially informative trajectories is deeply problematic.

Geissler is building a new generation of path sampling techniques to explore atypical trajectories of long duration. In the context of self-assembly, successful trajectories of a poorly designed system may be rare, hindering the assessment of essential improvements. More broadly, modern understanding of fluctuating systems is grounded in an appreciation of their extreme fluctuations, which reveal strong response to external forces. Accessing atypical trajectories in computer simulations requires some kind of bias, and correcting for this bias in long trajectories creates profound sampling inefficiencies. We have made strides in developing methods that resample limited segments of long trajectories, bridges whose endpoint constraints introduce significant

technical complications. In this way we can impose strong biases without compromising efficiency. Application to a classic model of strongly driven systems (asymmetric exclusion processes) demonstrates the soundness of this approach and a potential to access important limits that have up to now been very difficult to explore.

Mandadapu and co-workers developed a theory for the glassy dynamics of supercooled liquid mixtures. Given the relaxation behavior of individual supercooled liquids, this theory predicts the relaxation times of their mixtures as temperature is decreased. The model is based on dynamical facilitation theory for glassy dynamics, which provides a physical basis for the relaxation and vitrification of a supercooled liquid. This is in contrast to empirical linear interpolations such as the Gordon-Taylor equation typically used to predict glass transition temperatures of liquid mixtures. The theory can now predict transport properties and glass transition temperatures of mixtures of glassy materials in excellent agreement with all of the available experimental data on binary mixtures of glass formers. Mandadapu also studied the pre-transitions effects in glass formers and demonstrated that active and inactive phases in glass formers are pre-transition effects of the nearby non-equilibrium dynamical phase transition in trajectory space.

Head-Gordon has continued to perform theoretical studies on ion-exchange mechanisms in model layered charged interfaces as model systems for strongly heterogeneous and far-from-equilibrium systems. Last year we proposed that the sharp ion exchange fronts observed within an interlayer arises from a process in which the relaxation dynamics of one of the ions induces a metastable phase for the other ion, giving rise to a new non-equilibrium idea we have termed “dynamical inversion of the energy landscape” (DIEL). DIEL led to the observed sharp exchange fronts seen experimentally in charged systems such as illite clays, which cannot be explained by simple diffusion. Ion-exchange between charged layers also creates interesting “interstratification” patterns, where interlayers are fully replaced by larger ions that intercalate in non-trivial ways with interlayers still occupied by small ions. To gain insight into the process of interstratification, which now involves multiple interlayers that are mechanically coupled through the particular pattern of ions, we are developing a lattice model where a kinetic Monte Carlo routine (KMC) is used to evolve the ion dynamics when coupled to a mechanical network model that determines the interlayer spacing at each lattice site as a function of the spatial configuration of the ions and the bending rigidity of the layers. In the mechanical network each layer is represented by a 2-D mesh of discrete nodes that is inextensible but that can bend to accommodate the ions. The bending rigidity of the layers is captured by harmonic angle potentials between three adjacent nodes. Each layer is coupled to its neighboring ones through vertical springs that represent the ions in the interlayer sites. The vertical springs have different equilibrium lengths to represent the different sizes of the ions. The potential energy of the system is minimized to find the interlayer spacing at each occupied site, and giving the particular distribution of large and small ions or unoccupied states with respect to an associated interlayer spacing.

Direct detection of reaction intermediates is an important step in unraveling complex mechanisms in condensed and interfacial systems. Colliding microdroplet reactors, currently under development by Wilson, show some promise of achieving very fast inertial mixing times in the microsecond range, which would allow short lived reactive intermediates to be observed directly either by spectroscopy or mass spectrometry. We have completed an initial study of a prototype colliding droplet reactor. To quantify mixing dynamics, we collide two streams of 40 ± 5 μm diameter droplets. One droplet stream contains an acid and the other a Rhodamine dye. When

they collide the fluorescence is acid quenched. Mixing times are then recorded by measuring the decay in fluorescence using a camera. The quenching rate is fast (i.e. instantaneous) relative to the much slower mixing timescales. Mixing times were found to be influenced not only by the velocity at which microdroplets collide but also the impact parameter of the collision (i.e., head-on vs off-center collision). We achieve submillisecond mixing times ranging from ~900 μs at a collision velocity of 0.1 m/s to <200 μs at ~6 m/s. At collision velocities >7 m/s, droplet fragmentation occurred, resulting in incomplete mixing. We benchmark our reactor using iron-catalyzed hydroxyl radical production from hydrogen peroxide (Fenton's reaction) and subsequent aqueous-phase oxidation of organic species in solution. Kinetic simulations of our measurements show that quantitative agreement can be obtained using known bulk-phase kinetics for bimolecular reactions in our colliding-droplet microreactor.

Future Plans

Mandadapu will extend studies of effects of glassy dynamics on mixing/demixing transitions involving binary and ternary mixtures of glass formers (including water), with particular applications to aerosol particles. This work will be done in collaboration with Kevin Wilson's experimental group. To this end, Mandadapu proposes to study formation and melting of glasses driven by changes in temperature as well as changes in relative humidity. Increase in humidity has been shown to increase diffusion within a material while a decrease in humidity decreases diffusion. Depending on the rate of drying, the material can be a viscous liquid in equilibrium, or an out-of-equilibrium, amorphous solid (i.e., a glass). While there exist several robust, theoretical interpretations of the temperature-driven glass transition, there is no concrete physical basis for the understanding of glass formation in multi-component systems driven by a change in composition and relative humidity. The prevalent interpretation of mixtures of the viscous materials and water in the literature relies on empirical formulae without any microscopic basis. Mandadapu proposes to apply the model for glassy behavior in mixtures to aerosol mixtures. The predictions from the model, can be tested in experiments performed by Wilson, who has measured the diffusion of water molecules using Raman spectroscopy on levitated droplets of mixtures to ensure rapid mixing times and contactless measurements. Future work also plans to identify the dominant physical mechanisms at small and large length scales, i.e., the competition between surface and bulk effects in droplets of aerosols and the crossover between the two regimes.

Head-Gordon plans to explore multi-layer 2D charged interface materials, with control on the inter-plane confinement distances, to simultaneously consider how the sharp ion exchange fronts and interstratification occur dynamically and out-of-equilibrium. This will require further development of the chemomechanical model, in which we wish to observe and explain interstratification patterns.

Geissler will extend bridge bias sampling of trajectories to more realistic molecular systems that connect directly with experimental efforts, such as Wilson's studies of amphiphile assembly. Model processes of amphiphile reorganization, like desorption of a lipid molecule from a lipid bilayer and the fusion of lipid vesicles, will be important and challenging mid-term targets.

Our objective with the colliding droplet reactor is to achieve sub-100 μs mixing times. Wilson is continuing to pursue this goal by exploring asymmetric collisions (i.e. a collision of 1 large droplet with a smaller one). We are also developing branched electrodynamic guides to better constrain the droplet collision event and reliability in order to allow more complex spectroscopic probes (i.e. Raman and X-ray Absorption Spectroscopy) to be used to eventually study intermediates.

Collaborative efforts with Moni Blum are envisioned to develop new approaches to couple these fast mixing devices (colliding droplets and jets) to synchrotron based spectroscopies. In parallel, we are also working on single droplet mass spectrometry techniques for the detection of fast kinetics, products and intermediates. An IR laser will be focused to specific locations (e.g. 1 mm or 100 microseconds after the droplet collision) to vaporize the droplet contents for subsequent ionization by DART or electrospray followed by mass spectrometry analysis. By flash vaporizing the droplets at different distances mass spectra as function of reaction time will be collected during the reaction. We are also collaborating with Junko Yano's (LBNL) group to use colliding droplets to examine fast enzymatic-substrate reactions.

Blum is setting up a dedicated colliding flat jet system combined with ambient pressure x-ray photoelectron spectroscopy (APXPS) at the Advanced Light Source and will work with other LBNL experimentalists (Wilson, Ahmed, Saykally, and Crumlin) to utilize the system for a number of intermixing chemical reactions. The system will enable the controlled intermixing of two liquids and solutions in a stable sample environment in respect of flow, temperature, pH, etc. and short lived reactive intermediates can be observed at the intermixing point and changes of the mixing pattern while scanning over the liquid "sheets". In addition to x-ray spectroscopy the endstation will be combined with mass and IR spectroscopy. Blum will use the system for understanding the solvation mechanism and the reaction of ions with small molecules. The jet system will be modular to also be used for droplets and will work well with the groups previous and future efforts to study self-assembly chemistry at the droplet interface.

Publications Acknowledging DOE support:

G. M. Rotskoff and P. L. Geissler. "Robust nonequilibrium pathways to microcompartment assembly", Proc Natl Acad Sci USA 115, 6341 (2018), doi: 10.1073/pnas.1802499115.

L. R. Pestana, K. Kolluri, T. Head-Gordon, and L. Nielsen Lammers (2017). Direct exchange mechanism for interlayer ions in non-swelling clays. *Environ. Sci. & Tech.* 51 (1), 393–400

L. R. Pestana, N. Minnetian, L. Nielsen Lammers, T. Head-Gordon, (2017). Dynamical inversion of the energy landscape promotes non-equilibrium self-assembly of binary mixtures. *RSC Chemical Science*, 9, 1640 - 1646.

K. Schaettle, L. R. Pestana, T. Head-Gordon, L. Nielsen Lammers (2018). A structural coarse-grained model for clays using simple iterative Boltzmann inversion, *J. Chem. Phys.* 148, 222809.

Katira, S.; Garrahan, J. P.; Mandadapu, K. K., Solvation in Space-Time: Pre-transition Effects in Trajectory Space, Phys. Rev. Lett. 2018, 120, 260602. DOI:10.1103/PhysRevLett.120.260602

Katira, S., Garrahan, J. P., and Mandadapu, K. K., Theory for glassy behavior of supercooled liquid mixtures, Phys. Rev. Lett., 2019, 123, 100602. DOI:10.1103/PhysRevLett.123.100602

Davis, R.D., et al., Colliding-Droplet Microreactor: Rapid On-Demand Inertial Mixing and Metal-Catalyzed Aqueous Phase Oxidation Processes. Analytical Chemistry, 2017. 89(22): p. 12494-12501.

Discovering the Mechanisms and Properties of Electrochemical Reactions at Solid/Liquid Interfaces

Ethan J. Crumlin
Lawrence Berkeley National Laboratory
Chemical Sciences Division (Sponsor for DOE ECA)
and Advanced Light Source
1 Cyclotron Road, MS 6R-2100, CA, 94702
EJCrumlin@lbl.gov

Program Scope

We aim to probe the molecular interactions at solid/liquid electrochemical interfaces through a unique multi-modal approach that combines novel spectroscopy and state-of-the-art microscopy techniques with advanced theoretical modeling and computational science techniques. Our overarching *hypothesis is that discovering the mechanisms governing interfacial electrochemical properties, in particular the chemistry and electric potentials, will inform the development of more selective, stable, and efficient interfaces for reactions such as water splitting, CO_2 reduction, and N_2 reduction.* Combining experimental approaches with theory, we will iteratively explore the complex molecular interactions of a solid/liquid interface, a strategy that will expedite the discovery of new knowledge enabling future material and device innovations. First, we will conduct iterative multi-modal *operando* experiments and theoretical investigations of model solid/gas and solid/liquid systems. Progressing to the investigating the electric potential across the solid/liquid interface under non-idealized conditions—namely, reactive conditions—to understand how the potential profile deviates from the predictions of conventional theory. We also explore non-metal surfaces, such as those with absorbed surface species and oxide passivation layers. Finally, we will apply the foundational insight and methodology established to specifically study the alkaline metal and halide ion promotion mechanisms involved in important energy conversion reactions such as CO_2 reduction. We will directly examine the interplay of electrodes with different ions to distinguish the chemical and electrical potential properties governing the selectivity and efficiency of these electrochemical reactions.

Recent Progress

As we build out our approach for studying *in situ* and *operando* solid/liquid interface studies, we have started to merge our theory and experimental characterization pipeline using solid/gas models. These initial studies are part of our research plan for progressing experimental, theoretical, and technique development to the most complex interactions we will be probing. In anticipation for studying CO_2 electrochemistry, we investigated how CO_2 adsorbs onto an Ag silver and how that adsorption changes in the presence of water.[1] This study combined experimental investigations from APXPS combined with computational DFT to provide synergistic insight into this interface.

We find that physisorbed linear (*l*-) and chemisorbed bent (*b*-) CO_2 are *not* stable on pure Ag (111) surface, in contrary to what's observed on Cu surface.[1-2] While subsurface O (which stabilized both the *l*- and *b*-CO_2 in the Cu system) is not stable on Ag (111) surface, instead subsurface O moves without a barrier to a three-fold site on the top layer as a surface O. The surface O cannot stabilize both the *l*- and *b*- CO_2 on the Ag surface, but rather gaseous CO_2 reacts with the surface O to form a chemisorbed surface species ($O{=}CO_2^{\delta-}$) with a $C{=}O_{up}$ double bond pointing up while the other two O bind to adjacent three fold Ag(111). Interestingly, we find this surface chemisorbed adsorbent is *not* an ionic carbonate possessing three similar O atoms. In fact, the total charge of $O{=}CO_2^{\delta-}$ is $-1.26e^-$ with a charge on C is +1.46. We find $O{=}CO_2^{\delta-}$ is the only stable species on the Ag surface when exposed solely to CO_2 (no H_2O is present), while adding H_2O and CO_2 leads to up to four water attaching on ($O{=}CO_2^{\delta-}$) and two water attaching onto and stabilizing *b*-CO_2 on the surface. These theoretical thermodynamics are tested and validated through APXPS experiments. We find a very different and much more favorable mechanism involving the $O{=}CO_2^{\delta-}$ and

H_2O molecules on Ag compared to that involving *b*-CO_2 on Cu. This work highlights that the charge transfer configurations are responsible for the tunability of CO_2 adsorption on the metal catalyst surface. Each metal surface modifies both the chemical speciation and the respective adsorption energies, thus providing a new basis for tuning CO_2 adsorption behavior to facilitate selective product formations.

From this study, we recognized there was an additional opportunity to develop some of our theoretical capabilities for understanding interfaces. We noticed experimentally the clear pressure and temperature dependence for water adsorption and surface reaction chemistries present on the surface. Essentially a surface chemistry phase diagram. Recognizing this, we utilized our computational DFT results to synergistically determine the surface chemistries on the Ag surface.[3] Additionally, by developing and deploying a chemical reaction network model, we were able to establish a clear temperature and pressure phase diagram for the surface chemical species. This model fit our experimental data very well confirming our study.

The importance of this first of its kind study, is that it lays the foundation for directly linking experimental results to theory in both a determination of the chemical species, but also their population and surface chemistry kinetics. In the future, this will allow us to build out tools to more efficiently analyze data and existence of species, but also allow us to develop machine learning approaches to expedite our interfacial characterization data points needed to generate a surface chemistry phase diagram. To further expand upon these studies and continue our progress we are conducting additional studies for how CO_2 and water or hydrogen interact with Pt, Pd, and Ni surfaces. This will help to complement our understanding of these interactions and generate a diverse data set to support future theoretical investigations and refine our understanding of the interfacial chemistry. This will also help us to develop a data set that we can use to train future machine learning approaches for the solid/gas interface in preparation for creating an approach in the future for solid/liquid interfaces.

With respect to probing solid/liquid electrochemical interfaces we have made a lot of progress in this direction. We have several systematic studies underway probing how halide anions impact the water oxidation reaction and the interfacial properties that include the formation of various oxide/hydroxides/etc. Most of our experimental results have focused on using tender APXPS to probe the solid/liquid interface under *operando* conditions. One study focuses on how a platinum electrode is influenced by a chloride ion on the electrochemistry in an alkaline electrolyte using *operando* APXPS. The current hypothesize we are exploring is that we are observing chloride ion adsorption on platinum and/or forming a complex with dissolved platinum ion and chloride ion ($PtCl_x^{n-}$). Additional analysis will be followed to understand how the ratio of chloride ion and hydroxide ion would affect the platinum surface and the following electrochemistry. We have also explored Ni metal electrodes using *operando* APXPS to detect the solid/liquid interface in the mixed electrolyte of KOH and KX (Halides, X= F^-, Cl^-, Br^-, I^-) at different electrochemical conditions, which gives us direct evidence of the Ni phase transform. Our data analysis is in the prelimnary stages however we clearly observed that some precipitates formed for some various electrolyte and potential combinations. Thus, identifying an ideal platform to develop our multi-modal approach for probing the dissolved complexes and their precipitate formation using mass spectroscopy. Currently we are developing a detailed library for all our control electrolytes, possible salt complexes formed, and then will run *ex situ* measurements of the used electrolyte. This will lay the foundation for our development of operando mass spectroscopy measurements that we hope to develop throughout this research program.

Future Plans

The interaction of water with metal surfaces is at the heart of electrocatalysis. But there remain enormous uncertainties about the atomistic interactions at the electrode–electrolyte interface. On the theory side, we will choose water adsorption and interaction on metal surfaces as a starting point, expand our chemical reaction network, and bridge the gap between solid/gas and solid/liquid interfaces. The first challenge in

the field is a lacking of correct description of the liquid phase water, as most of the current force field methodologies would underestimate the complexity of vibrational, translational and rotational entropic contribution due to the hydrogen bond network when water molecules are sufficiently close. The second challenge is the unclear linkage between the constant potential in most electrochemical experiments and the theoretical description of such potential bias. One way to walk around these problems would be using the grand canonical approach to simulate a mean field of solution with a fixed potential term on the solid/liquid interface while letting the electrons freely fluctuate, as implemented in the joint DFT code jDFTx.[4] Once the thermodynamics calculations are trustworthy in a solvation environment under potential, we would be able to correlate the electronic structures with APXPS BE measurement and correlate the population with APXPS peak area analysis.

We will also continue the studies of CO_2 adsorption and activation on electrode surfaces. We will explore the solid/gas and solid/liquid interfacial properties involving surface with multi-metal components and metal-metal oxide layered structure exposed to a range of electrolytes to continue our investigations into the cation and anion effects. We will further explore the solid/liquid interfaces to create the "interfacial" Pourbaix diagrams that can directly predict the phases changes at the interfaces under *operando* conditions. In order to reach higher current density measurements at the solid/liquid interface a two-chamber-like cell will be constructed. This kind of cell will be beneficial to study the electrochemistry reactions involving both gases and liquids, for the water splitting, CO_2 reduction, and N_2 reduction reactions. We will continue our efforts for introducing more multimodal characterizations into our program including scanning probe microscopy, IR, and Raman, that will further our ability to study *in situ/operando* the electronic and geometric information at the solid/liquid and solid/gas interfaces under various reaction conditions.

Publications Acknowledging Support of the DOE Office of Science Early Career Award:

i. Ye, Y., Yang, H., qian, J., Su, H., Lee, K.-J., Cheng, T., Xiao, H., Yano, J., Goddard, W. A. I. & Crumlin, E. J. Dramatic differences in carbon dioxide adsorption and initial steps of reduction between silver and copper. *Nature Communications*, 1875, doi:10.1038/s41467-019-09846-y (2019).

ii. Qian, J., Ye, Y., Yang, H., Yano, J., Crumlin, E. J. & Goddard, W. A. I. Initial Steps in Forming the Electrode-Electrolyte Interface: H2O Adsorption and Complex Formaiton on the Ag(111) Surface from Combining Quantum Mechanics Calculations and X-ray Photoelectron Spectroscopy. *Journal of the American Chemical Society*, 6946 - 6954, doi:10.1021/jacs.8b13672 (2019).

References

1. Ye, Y.; Yang, H.; qian, J.; Su, H.; Lee, K.-J.; Cheng, T.; Xiao, H.; Yano, J.; Goddard, W. A. I.; Crumlin, E. J., Dramatic differences in carbon dioxide adsorption and initial steps of reduction between silver and copper. *Nature Communications* **2019,** (10), 1875.
2. Favaro, M.; Xiao, H.; Cheng, T.; Goddard, W. A.; Yano, J.; Crumlin, E. J., Subsurface oxide plays a critical role in CO2 activation by Cu(111) surfaces to form chemisorbed CO2, the first step in reduction of CO2. *Proceedings of the National Academy of Sciences of the United States of America* **2017,** *114* (26), 6706-6711.
3. Qian, J.; Ye, Y.; Yang, H.; Yano, J.; Crumlin, E. J.; Goddard, W. A. I., Initial Steps in Forming the Electrode-Electrolyte Interface: H2O Adsorption and Complex Formaiton on the Ag(111) Surface from Combining Quantum Mechanics Calculations and X-ray Photoelectron Spectroscopy. *Journal of the American Chemical Society* **2019,** (141), 6946 - 6954.
4. Sundararaman, R.; Letchworth-Weaver, K.; Schwarz, K. A.; Gunceler, D.; Ozhabes, Y.; Arias, T. A., JDFTx: Software for joint density-functional theory. **2017,** *6*, 278 - 284.

Observing the Molecular & Dynamic Pathway of Water Oxidation on Titania Surfaces

Principal Investigator: Tanja Cuk
Associate Professor, Chemistry Department, University of Colorado, Boulder
Faculty Fellow, Renewable and Sustainable Energy Institute, University of Colorado, Boulder
4001 Discovery Drive, Boulder, Colorado 80303
Email: tanja.cuk@colorado.edu

Overview

While elements of heterogeneous water oxidation have been revealed previously by investigating catalysis spectroscopically and *in-situ*, the causal pathway requires truly dynamic probes of diverse molecular reactants and intermediates. In this proposal, multiple dynamic probes that begin at the earliest time steps of the reaction will target the different actors (e.g., trapped charge carriers, radical intermediates, and adsorbed water species) involved in evolving O_2. The strategy is based on merging multi-color, ultrafast transient (optical, mid-infrared, resonance Raman, & X-ray) spectroscopy with highly efficient photo-electrochemistry of the water oxidation reaction. The research aims to reveal the critical steps along the pathway to O_2 evolution and the factor—whether a specific bond breaking event or the surrounding environment—that limits the rate at which each step proceeds to the next.

A major outcome of this DOE grant would be a paradigm by which to resolve how reactant chemical bonds are broken and re-made into the chemical bonds of the product during electrochemical reactions, such that the speed and distribution of evolved products can be tailored. Depending on the pathway(s) resolved, the tailorable properties include materials choice, electrolyte conditions, and device design, among others. While the focus here is on the water oxidation reaction, this model system provides the critical seed for broader investigations of heterogeneous catalysis at the molecular and dynamic level. It also targets the unique properties of water, important for both energy storing reactions and as a medium for many chemical and life processes.

Recent Progress

An optical setup for transient reflectivity using a broadband source that covers from 350 nm to 700 nm (CaF_2) was constructed. The setup includes a special referencing technique which reduces the background issues with transient optical reflectance. This is the first step to constructing the full Raman experiments. This setup uses the recently purchased PIXIS CCD Detector and Princeton Instruments Isoplane Spectrometer with sufficient sensitivity and spectral resolution, respectively, for time-resolved stimulated resonance Raman spectroscopy.

With the broadband probe that extends into the UV, we are able to take a more extended spectrum of the data from the titania surface under catalytic conditions. This is especially important for the UV emission that results from charge-trapping intermediates at the surface. With the extended range, higher sensitivity, and better data collection techniques, we will complete the work on the

formation of the charge-trapping intermediates and their decay—as seen by mid-gap levels in $SrTiO_3$. Figure 1 shows recent data taken on the ps-ns time scale from the ~ 350 nm to 700 nm for a wide range of pH, at closed circuit (during catalysis) and open circuit (no current). Recent analysis shows that these spectra—at the entire range of reaction conditions shown—can be decomposed into two principal components, reflecting the existence of two primary species: VB holes and mid-gap hole traps on O-sites. Coherent oscillations under closed circuit conditions, due to acoustic phonons (coherent longitudinal acoustic phonons-CLAPs) that propagate into the sample as a result of the impulse created by charge separation at the semiconductor-liquid interface, are subtracted out of the data set. These CLAPs were accurately modeled by the acoustic dispersion in $SrTiO_3$, as shown in Figure 2. Current work is focused on understanding and quantifying the clear pH dependence seen in the data. This will be done by creating linear combinations of the principal components with physically relevant input from the "ends" of the data set, dominated by either VB holes or mid-gap levels, and will also be informed by steady state PL measurements. The CLAP data will be analyzed to understand the strain generated at the solid-liquid interface by efficient and permanent charge-separation. The above experiments and analysis were guided by a postdoctoral fellow, Ilya Vinogradov, and a research associate, Aritra Mandal, supported by this grant. They were supported also by two graduate students, Hanna Lyle and Suryansh Singh.

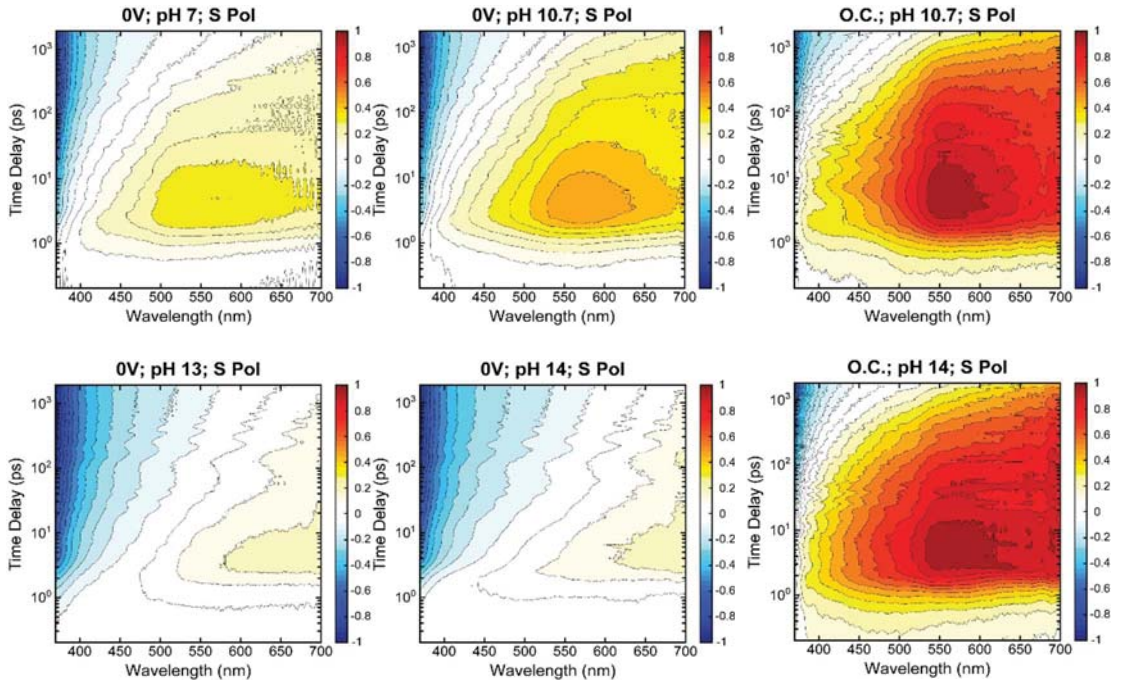

Figure 1: UV-VIS reflectance of catalytic surface from ps to ns at closed circuit (0V) and open circuit (OC) for a range of pH in s-polarization of the incoming white light probe. Emission is in blue, absorption is in red. The pH dependence of the emission suggests that the termination of the surface with hydroxyl or water groups influences the production of water oxidation intermediates—holes trapped at surface oxygen sites—at these time-scales.

Further, collaborations have been setup with a staff scientist at RASEI (Sadegh Yazdi). The purpose is to obtain TEM, SEM, and EDAX of the sample surface after catalysis has been run with the same light source used for the pump-probe experiments. Recent experiments have

implemented several different sample-scan methods for data collection, which will also be informed by this surface-sensitive microscopy.

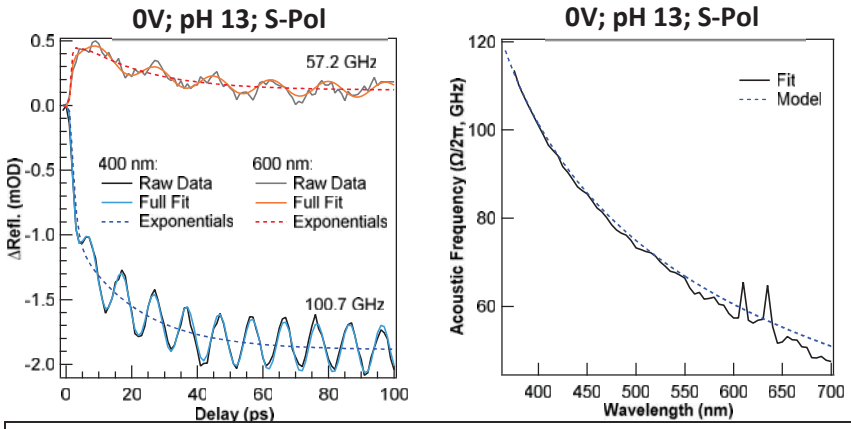

Figure 2: Coherent longitudinal acoustic phonons generated efficiently at closed circuit with efficient and long-lasting charge-separation. The oscillations are generated by a Raman process, and detected by the probe wave that interferes with the propogating phonon into the material. The dispersion relation of acoustic phonons STO (right) can be readily extracted.

Two manuscripts have been published based on the work in the group previously at UC Berkeley/LBNL and funded by a CPIMS grant. The first is on the water oxidation reaction at microsecond time-scales, entitled "Selecting between two transition states by which water oxidation intermediates on an oxide surface decay", published in *Nature Catalysis*[1]. This manuscript delineates the reaction-dependent decay of water oxidation intermediates (on STO) through two competing transition state pathways. The second is on visualizing the electric double layer of a battery electrolyte through potential-dependent vibrational spectroscopy, coupled with molecular dynamics simulations (through a collaboration with Oleg Borodin and Jenel Vatamanu). The manuscript, "Probing Electric Double Layer composition via in-situ Vibrational Spectroscopy and Molecular Simulations", was recently published in *J. Phys. Chem. Lett*[2].

Currently, there is a manuscript in preparation on the AP-XPS spectroscopy on water and hydroxyl groups absorbed to $SrTiO_3$[3]. This is coupled with DFT and MD calculations by Sri Pemmaraju. The goal is to show how quantitative the agreement between AP-XPS experiments and appropriate calculations can be. This work is also in collaboration with Hendrik Bluhm.

Future Work

- The broadband data of the catalytic surface discussed above will extended to the microsecond time scale. For the full time range, a ~ 800 ps pulsed laser will be purchased, such that there are no baps in time. In particular, we will focus on the loss of polarization from the picosecond to the 10's of nanosecond regime, which implies that initially localized intermediates have become mobile.

- The Raman pump will be set up such that vibrational dynamics can be extracted from the reaction-dependent kinetics of the mid-gap levels. In the *Nature Catalysis* manuscript, the kinetics associated with these mid-gap levels obey canonical transition state theory. We therefore would like to resonant on them electronically, while collecting vibrational data associated with chemical events, such as reaching a particular transition state (*i.e.* two oxyl radicals next to eachother) and the formation of a chemical bond (O-O). The current

spectrometer and detector are setup for these experiments. What is being collected now is the extended broadband range of the catalytic surface—i.e. regular transient reflectance—as input. Secondly, the Raman pump, which resonantes on the UV edge of this spectrum, needs to be setup, along with the associated electronics and programming which combines data collection from the three beams. We expect to complete this in FY2020, and hopefully have initial stimulated Resonance Raman data.

- Data from the TEM, SEM, EDAX, and XPS will be analyzed holistically and in the context of the transient measurements taken. We may discover that the long-time reconstructions inform us about the water oxidation process, including degradative processes on the percent level compared to the O_2 evolution.

- The plan is also to continue to analyze and take AP-XPS data on different STO surfaces, including doped and light activated. Some of this data has already been taken, and is awaiting the completion of the analysis above. My group hopes to do this in collaboration with scientists at the AP-XPS beamline at LBNL.

Publications

1. X. Chen, D. Aschaffenburg, and T. Cuk, "Selecting between two transition states by which water oxidation intermediates on an oxide surface decay", *Nature Catalysis*, 2019, 2, 820.
2. J. Raberg, J. Vatamanu, S. Harris, C. H. M. van Oversteeg, A. Ramos, O. Borodin and T. Cuk, "Probing Electric Double Layer Composition via in-situ Vibrational Spectroscopy and Molecular Simulations", *J. Phys. Chem. Lett.* 2019, 10, 3381.
3. D. Aschaffenburg, S. Kawasaki, S. Choing, C.D. Pemmaraju, H. Bluhm, and T. Cuk, "The First Hydration Layer of Hydroxylation and Water Absorption on $SrTiO_3$ Surfaces: Experiment (AP-XPS) and Theory", in-preparation.
4. T. Cuk, "Forwarding Molecular Design of Heterogeneous Catalysts," *ACS Central Science (First Reactions)*, 2018, 4, 1084 (invited).

Using Ultrafast Entangled Photon Correlations to Measure the Temporal Evolution of Optically Excited Molecular Entanglement

Scott Cushing
Division of Chemistry and Chemical Engineering, California Institute of Technology
1200 E California Blvd, Pasadena CA 91125
scushing@caltech.edu

Program Scope: The goal of this project is to measure how a molecular system evolves when photoexcited by an entangled photon. The preservation of an optically-excited, entangled state is critical for applying chemical systems in quantum information, computing, and sensing technologies. A superposition between one entangled photon of a biphoton pair and the spin state of a photoexcited molecule can be created. The second entangled photon from the biphoton pair is then interfered with this state using a variable time-delay. The measured decoherence or preservation of the entangled state gives insight into the spin-vibronic coupling and other relaxation mechanisms that occur. Entangled photons are also proposed to have non-classical spectroscopic benefits. First, the spectral and temporal properties of the entangled photons are not Fourier-limited, potentially allowing femtosecond entangled probes with MHz or lower linewidths. Second, a pulsed laser is not needed to measure time-resolved interactions. The entangled beam from a CW laser has a finite interaction time which is experimentally controllable. Finally, the entangled photon beams are easily separated from classical backgrounds and can have sub-shot noise limits.

A high-flux entangled photon spectrometer is currently being designed and built. In the past, the flux of entangled photon experiments was limited by a weak conversion efficiency in standard nonlinear crystals and non-multiplexed photon counting. Our setup will use a chirped, nonlinear waveguide capable of creating µW of entangled photons and multiplex the detection in a photon counting CCD (Figure 1). The entangled photon experiments will take place on a series of intersystem crossings (single-triplet, doublet-quartet, singlet fission) in inorganic molecules with and without a solid-state interface. Through these transitions, it will be understood if the superposition between an entangled photon and spin state can be optically read out. The non-classical spectroscopic benefits of entangled photons will also be tested.

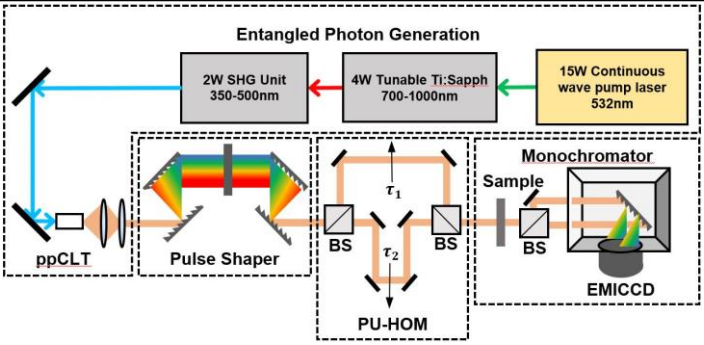

Figure 1. *Schematic of the entangled photon spectrometer. The ppCLT is a periodically poled congruent lithium tantalate waveguide; BS is a beam splitter; EMICCD is an intensified electron multiplying camera, PU-HOM is a simplified schematic of a phase-unlocked Hong-Ou-Mandel interferometer.*

Publications: There are no publications to report because this is a new award with a start date of September 1st, 2019.

Chemical stability and dynamical evolution of nanostructured alloys under voltage

Ismaila Dabo (dabo@matse.psu.edu) and Susan B. Sinnott (sinnott@matse.psu.edu)
Department of Materials Science and Engineering
The Pennsylvania State University, University Park, PA 16802

Program scope

The goal of the project is to apply and further develop embedded quantum-mechanical models and classical force fields to study the chemical stability and dynamical evolution of nanostructured alloys. The focus is on understanding the voltage-dependent dissolution and corrosion of Au and Pt nanoalloys. Experimental data for prototypical Au- and Pt-based catalytic systems will be used to assess and validate the electrochemical models.

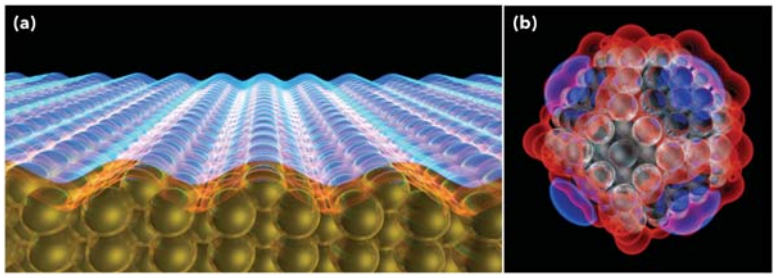

Figure 1 | (a) Quantum–continuum model of reconstructed Au(110) using an implicit description of the ionic electrolyte, which enables us to effectively represent interface polarization under electrical potential. **(b) Quantum-continuum model of a truncated octahedral Pt particle** showing the polarization potential at the negatively charged edges, which compensates the dangling bonds of undercoordinated Pt atoms. The charge redistribution strongly influences electrochemical corrosion.

First-principles simulations have been widely applied to deliver atomistic insights into the environmental effects that limit catalytic durability. To date, much attention has been devoted to understanding the role of adsorption and finite temperature on the stability of alloy surfaces, providing an effective assessment of catalyst durability under vacuum conditions. The objective of the project is to address the limitations of conventional first-principles analyses and consider the influence of the electrochemical environment on the durability of nanocatalysts. To this end, we are implementing voltage-dependent continuum solvation models and charge-optimized many-body force fields, which account for the solvation and electrification contributions that control surface and particle stability in representative aqueous electrolytes (**Figure 1**).

As illustrated in **Figure 2**, this work is organized around two main tasks: **(I)** predicting the size- and morphology-dependent dissolution and oxygen-driven restructuring via place exchange and passivation of single-component catalytic nanoparticles in aqueous environments, and **(II)** understanding the dealloying behavior of multicomponent surfaces under applied voltage.

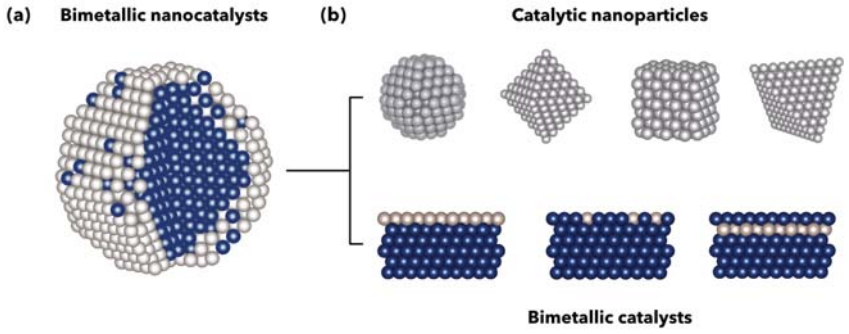

Figure 2 | (a) Au- and Pt-based bimetallic nanoparticles are the main focus of this project. **(b)** The computational study of these complex nanoalloys is broken down into (I) predicting the morphology- and size-dependent durability of pure nanoparticles, and (II) simulating alloying and dealloying at bimetallic surfaces as a function of voltage and pH.

Recent Progress

The stability of electrocatalytic systems is primarily controlled by the electrification phenomena which occur in the interfacial region separating the electrode from the electrolyte — the *electrical double layer*. The expertise of our team is in the development of voltage-dependent solvation methods and charge-optimized many-body force fields to predict molecular interactions at solid-liquid interfaces as a function of the applied voltage and ionic activities (**Figure 3**).

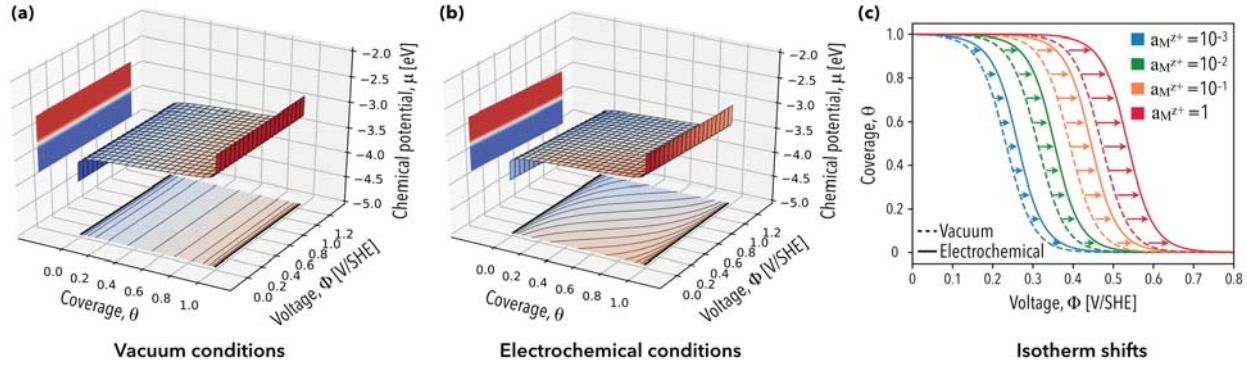

Figure 3 | Effects of surface electrification on the stability of electrodeposited transition metals on gold. Chemical potential surfaces of chemisorbed Cu atoms in (a) vacuum conditions and (b) electrochemical conditions. Introducing surface electrification leads to large shifts (c) in the adsorption isotherms as a function of the activity of the metal ions. We are leveraging these computational capabilities to predict, understand, and ultimately control the electrochemical stability of multi-component nanostructured electrocatalytic systems in realistic aqueous environments.

In Task **(I)**, these computational capabilities have been used to predict the dissolution of metal cations from facets, corners, and edges of nanoparticles. Drawing on these predictions, novel trends were found for the corrosion of Pt nanocatalysts, showing a high sensitivity of metallic dissolution with respect to voltage, specifically in the water stability window, as illustrated in **Figure 4**. In contrast, simulations of neutral nanoparticles do not predict any Pt dissolution. These conclusions are confirmed by explicit classical simulations of nanoparticles, which were performed using the charge-optimized many-body (COMB3) potential. The preliminary COMB3 results are comparable to density-functional theory calculations; notably, the new generation of force fields predicts charge distributions at Pt surfaces in close agreement with first-principles calculations.

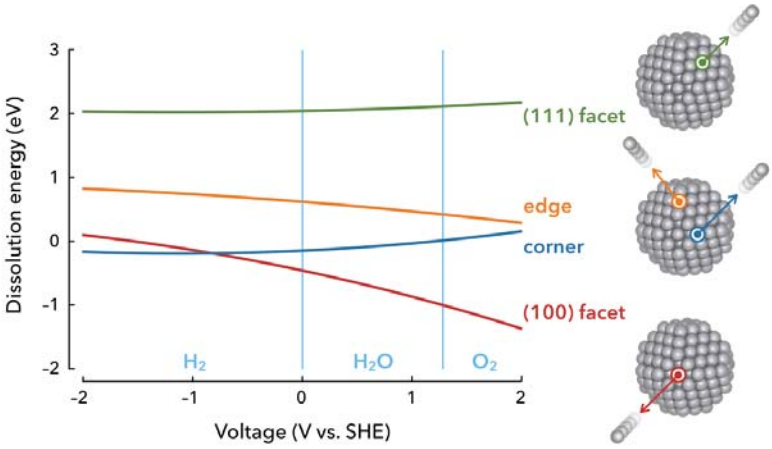

Figure 4 | Early stages of metal dissolution at solvated Pt nanoparticles. Embedded quantum-mechanical calculations of the site-dependent free energy of dissolution have been carried for 1.9-nm truncated octahedral nanoparticles using the self-consistent continuum solvation (SCCS) model. In the water stability window, Pt on (100) facets is unexpectedly seen to dissolve preferentially compared to lower coordinated sites.

In Task (II), the surface alloying behavior of core-shell nanoparticles has been investigated using an in-house interfacial cluster expansion (ICE) code. Motivated by the experimental observation of an anomalously high activity of Pd monomers at Au electrodes, the alloying behavior of other catalytic systems (Pt, Ag, Cu, Ir, Ru with Au) is being assessed. In the Ag/Au system, preliminary observations suggest a significant increase in the density of Ag monomers at high voltages (**Figure 5**). Although these findings motivate further study into fuel-cell electrocatalytic alloys, current results already provide some insights into related catalyst applications such as industrial organic oxidation. In fact, the partial oxidation of ethylene and other organics require highly selective catalysts. The selectivity of these reactions is controlled by the morphology of the active surface multimers. Our results show that the equilibrium density of these multimers is extremely sensitive to the voltage, causing large changes in the overall selectivity. Based on these initial calculations, further in-depth studies of specific catalytic reactions are underway. The thermodynamic data generated for these analyses are systematically stored in the automated interactive infrastructure and database for computational science (AiiDA) to ensure data availability and reproducibility. These data will be also used for subsequent fitting of the classical force-fields to simulate the time evolution of Au and Pt nanoparticles.

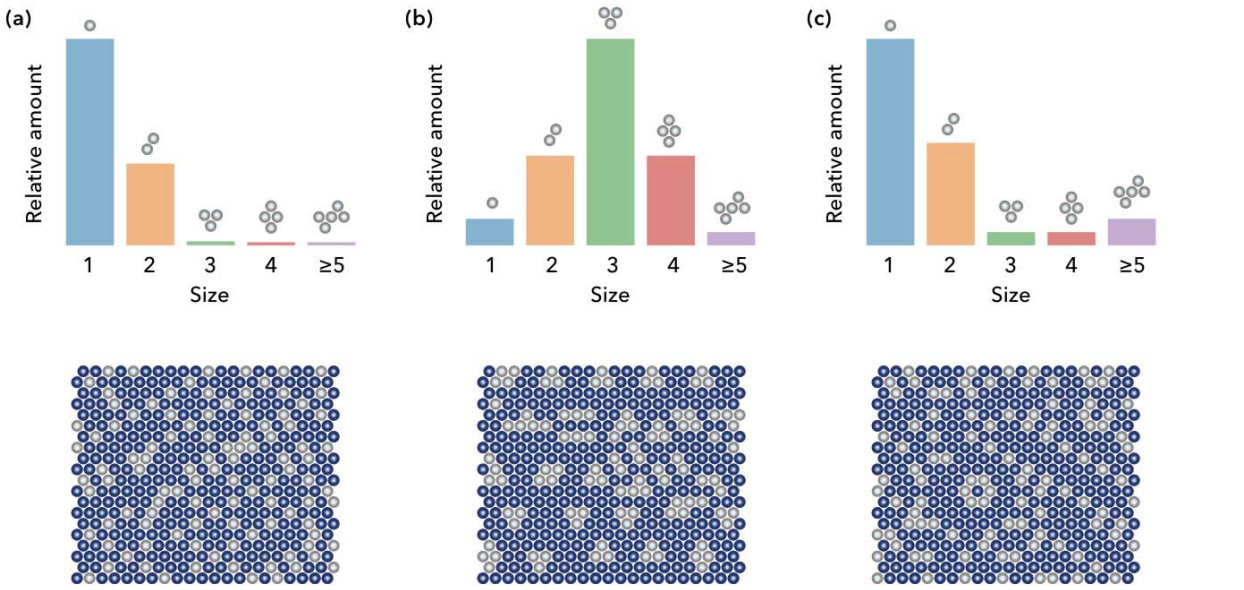

Figure 5 | Equilibrium surface configurations of $Ag_{0.25}Au_{0.75}$ surface alloys at various voltages: (a) 0.2 V vs. SHE, (b) 0.4 V vs. SHE, (b) 0.9 V vs. SHE (standard hydrogen electrode). Following the coloring convention of Fig. 2, subsurface Au atoms are shown in blue and Ag atoms are shown in grey. The cluster expansions used in these simulations were constructed without the effects of the continuum solvent. Yet, these preliminary trends already show that the amounts of monomers, dimers, and trimers vary largely with voltage. Simulations that include the dielectric response of the medium for Pt, Ag, Cu, Ir, Ru on Au surfaces, and for Ag, Cu, Ir, Ru on Pt surfaces are currently being carried out.

Future plans

Experimental studies of platinum nanoparticles show various levels of oxidation as a function of facet orientation. Voltammetric measurements suggest that different amounts of surface and subsurface oxidation can facilitate or prevent dissolution at specific potentials. The expected sensitivity of electrode durability to oxygen adsorption motivates us to study Pt and O co-adsorption and co-dissolution under applied voltage. We are thus developing multicomponent cluster expansions that will enable us to analyze the electro-dissolution behavior of Pt-O systems.

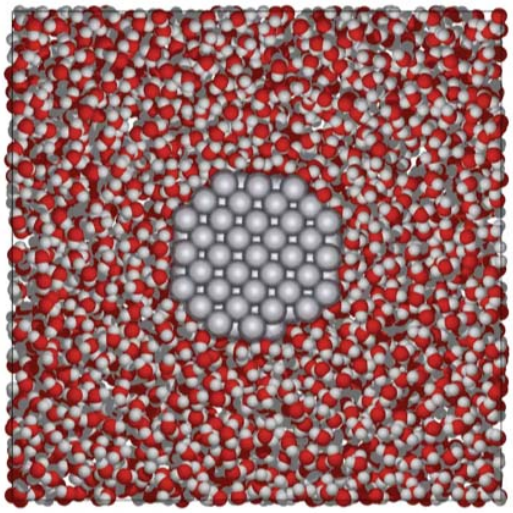

Figure 6 | Explicit simulation of a nanoparticle using the COMB3 charge-optimized force field. In these simulations, the electronic charge is allowed to redistribute freely across the system to account for the effects of charge transfer. In the continuation of this work, the voltage will be simulated by imposing an electronegativity offset to adjust the oxidation state of the metal atoms, and surrounding molecules and ions (eCOMB).

In parallel, classical molecular dynamics simulations using the COMB3 model will be employed to determine the reconstruction of Au and Pt electrodes due to metal-oxygen place exchange (**Figure 6**). These COMB3 results will be compared to quantum-continuum predictions for the same nanoparticles. Pt electrodes in contact with an electrolyte with varying ionic concentrations will also be simulated and ion displacement maps will be generated to determine the influence of electrical driving forces at the electrode-electrolyte interface. These results will be used to improve the accuracy and broaden the applicability of the COMB3 potential and its voltage-dependent counterpart (eCOMB) with a focus on understanding the effects of surface disorder and particle size. We will also analyze the influence of the applied voltage and surface concentration on the stability of the electrode-electrolyte interface. In practical terms, it is expected that the reconstruction of the surface upon adsorption should reduce the local depletion of charge and enhance the durability of the electrocatalyst.

Publications

1. S. E. Weitzner and I. Dabo, Voltage effects on the stability of Pd ensembles in Pd–Au/Au(111) surface alloys, *Journal of Chemical Physics* **150**, 041715 (2019).
2. S. E. Weitzner and I. Dabo, First-principles simulations of electrified interfaces in electrochemistry, in *Heterogeneous Catalysts: Emerging Techniques for Design, Characterization and Applications* (*Wiley-VCH)* edited by W. Y. Teoh, A. Urakawa, Y. H. Ng, P. H.-L. Sit (2019).
3. J. M. Goff, S. B. Sinnott, I. Dabo, Effects of interfacial charge and particle size on the dissolution of platinum nanocatalysts using the COMB3 and self-consistent continuum solvation models, submitted to *Journal of Chemical Physics* (special issue on *Interfacial Structure and Dynamics for Electrochemical Energy Storage*) (2019).
4. R. E. Slapikas and S. B Sinnott, Optimized utilization of the COMB3 reactive potentials in LAMMPS, *Journal of Chemical Theory and Computation*, to be submitted (2019).

Exploring new diamond surfaces with precision chemistry and quantum spectroscopy

Nathalie de Leon (npdeleon@princeton.edu)
Assistant Professor of Electrical Engineering, Princeton University, 50 Olden Street, Princeton, NJ 08544

Program Scope: The aim of the research program is to develop new processing and spectroscopy methods for diamond surfaces, with the goal of creating entirely new surface terminations that are inaccessible with current techniques. Developing new surface terminations for diamond would enable a wide range of future applications based on this material, from classical applications (power electronics, biocompatible devices, electrochemistry, cathodes) to quantum applications (quantum sensors, quantum communication networks, quantum simulators). However, diamond surfaces are particularly difficult to functionalize because the material is chemically inert and difficult to polish. Our approach is to develop a new method of surface termination by first preparing a high quality, reactive, bare surface by thermal annealing in ultrahigh vacuum (UHV) conditions and subsequently exposing the surface to neutral atoms. In order to study these new reactions, we will perform *in situ* measurements using two complementary suites of spectroscopy tools: (1) traditional photoelectron spectroscopy and electron diffraction to study fundamental reaction kinetics, structure, and chemical termination, and (2) quantum spectroscopy using nitrogen vacancy (NV) centers in diamond to probe nanoscale order and magnetic interactions between surface atoms. This project will be enabled by a novel, home-built, UHV cluster tool, which is currently under construction in our group. Leveraging our controlled surfaces, we also aim to explore new wet chemical functionalization techniques for single crystal diamond.

Prior Related Work: Our recent work has focused on developing high quality, oxygen-terminated, diamond surfaces to create NV centers within nanometers of the surface that have ultralong coherence times. Many groups have observed that NV spin coherence degrades within 100 nanometers of the surface, suggesting that diamond surfaces are plagued with ubiquitous defects. Prior work on characterizing and reducing near-surface noise has primarily relied on using NV centers themselves as probes; while this has the advantage of exquisite sensitivity, it provides only indirect information about the origin of the noise.

We have taken a different approach: using NV-based nanoscale spectroscopy and traditional surface spectroscopy methods as complementary diagnostic tools to identify sources of noise at the diamond surface. Using this approach, we determined that surface morphology is crucial for realizing reproducible chemical termination, and we used this information to achieve a highly ordered, oxygen terminated surface with suppressed noise and correspondingly longer coherence times for shallow NV centers. Specifically, we have realized a near-atomically smooth oxygen termination that yields NV centers within 5 nm of the surface with coherence times exceeding 100 μs, more than an order of magnitude improvement in performance over prior demonstrations [Phys. Rev. X 9, 031052, 2019].

Recent Progress: Surface chemistry in diamond is difficult because diamond is hard, chemically inert, and sterically hindered. Most available methods involve plasma, which damages the surface morphology. We will develop new techniques for terminating diamond in UHV in a unique apparatus that is currently under construction. UHV allows for the preparation of bare, dangling bond surfaces, which can then be exposed to low energy neutral atoms, minimizing surface damage. Novel surfaces can be prepared and then probed without breaking vacuum, yielding nanoscale information about magnetic and electric field noise at the surface. This instrument is the first of its kind, and it will enable precise chemical control and correspondingly precise spectroscopic interrogation of the diamond surface. Leveraging our ability to prepare pristine surfaces, we aim to study the fundamental reactivity of the diamond surface, devise new strategies for functionalization, and study the interactions between the surface and shallow NV centers. In year 1, our specific proposed plan was to work on four topics: (1) The preparation of pristine surfaces in UHV, (2) the study of oxygen desorption kinetics from the diamond surface, (3) the exploration of wet chemical functionalization methods starting with our smooth surfaces, and (4) measuring the charge state dynamics of shallow NV centers.

(1) Preparing pristine surfaces in UHV

After designing the cluster tool over 2016-2018, the first phase of construction and instrumentation installation began in January 2018, and we completed the first phase of the project—building the surface preparation and spectroscopy chamber—by September 2018. Using this first chamber, we have developed a procedure for thermally annealing the diamond in order to remove adventitious carbon, and then to desorb oxygen to prepare a bare, dangling bond surface. Upon heating to 1000˚C, we are able to observe almost complete oxygen desorption from the surface using X-ray photoelectron spectroscopy (XPS), as well as subsequent 2x1 reconstruction of the dangling bond surface using low energy electron diffraction (LEED). We are also able to observe detailed changes in the O1s XPS peak at intermediate temperatures, indicating that different oxygen terminations can form at the surface with incomplete oxygen coverage.

(2) Oxygen desorption kinetics at the diamond surface

We have also studied the kinetics of oxygen desorption in detail by performing time-resolved XPS. When we apply a continuous ramp in temperature, we observe that the background-subtracted area of the O1s peak decreases monotonically. However, surprisingly, we also see an apparent pause in the desorption rate around 650-800˚C, contrary to what would be expected for a single activation energy. To quantify this pause in the desorption, we looked at the time dependence of the O1s signal at particular temperatures. At each temperature, we see a time dependence that is consistent with first-order kinetics, but we also see that the rate varies dramatically. The desorption starts at a low rate at low temperatures, then increases by more than a factor of 2 at 550˚C, and then decreases again to a similar rate to the low temperature regime at 700˚C. The rate then increases again at higher temperatures. One hypothesis is that the surface termination is heterogeneous, and the different activation energies correspond to different species. This would be consistent with the observation that the fitted time dependence has an offset for each curve. We plan to perform detailed chemical shift scans on the steady-state surfaces to test this hypothesis.

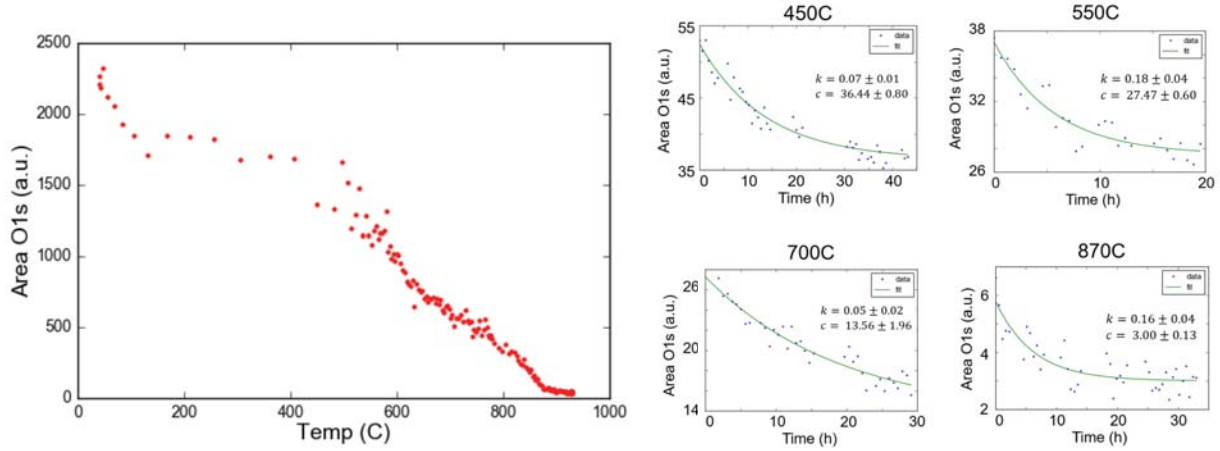

Figure 1: (Left) Integrated area of the O1s peak in XPS as the temperature is ramped. A pause in desorption is apparent around 650˚C. (Right) Detailed time-resolved measurements of desorption at particular temperatures, verifying the pause at 700˚C. The data are fitted to a single exponential, with the rate constant k and offset c shown in each subpanel.

(3) Wet chemical functionalization

Starting with our ultra-smooth, oxygen-terminated surfaces, we have developed methods in collaboration with Ania Jayich (UCSB) to generate smooth, hydrogen-terminated surfaces that can be used for subsequent functionalization. In collaboration with Robert Knowles (Princeton Chemistry), we have explored the application of photoredox catalysis to the diamond surface. In order to search this space, we established methods for verifying that new species at the surface result from chemical attachment rather than physisorption, using cleaning methods, AFM, and XPS. Figure 2 shows an

example of a successful hit: fluorination followed by cleaning in heated solvents results in a F1s XPS peak, with no evidence of other heteroatoms from the precursor (N, S), as well as identical surface roughness, indicating no physisorbed surface contamination. Near-edge X-ray absorption fine structure (NEXAFS) spectroscopy at NSLS-II will be used to further verify that we have formed a C-F bond at the surface.

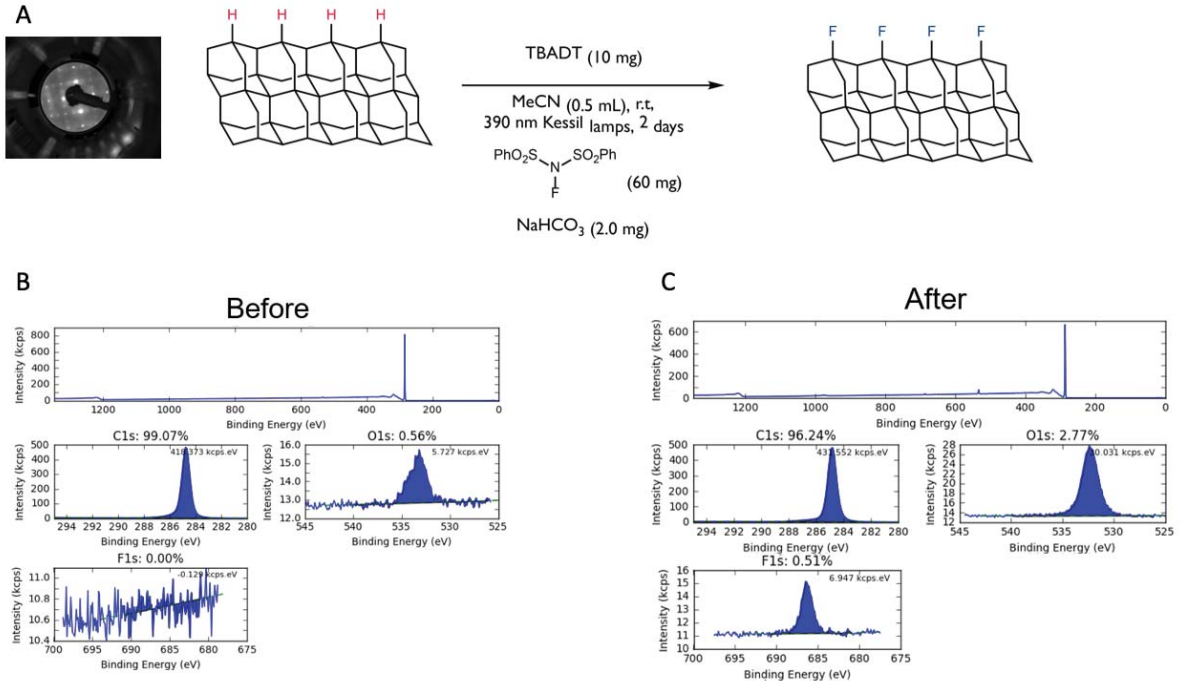

Figure 2: Wet chemical functionalization of the diamond surface. (A) Reaction scheme starting with hydrogen terminated diamond (as verified by LEED and XPS) to fluorinate the diamond surface using a photoredox catalyst. (B) Before and (C) after XPS scans showing around 10% fluorine coverage of the surface.

(4) Charge state dynamics of shallow NV centers

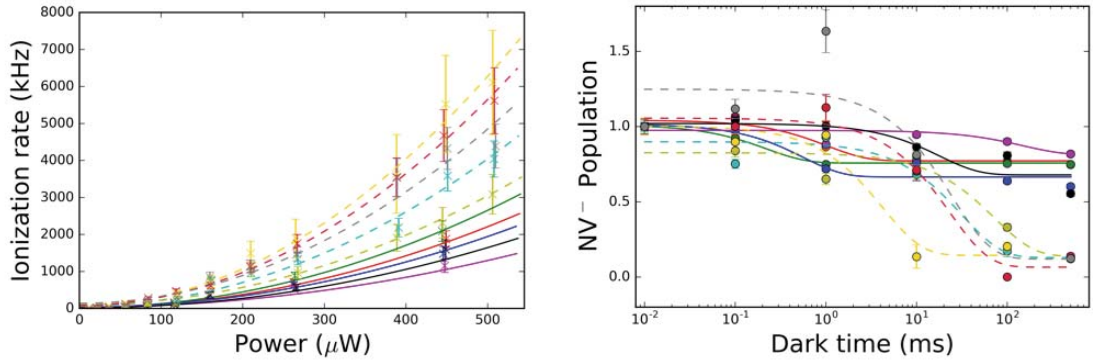

Figure 3: Ionization rate under green excitation of varying power (left) and in the dark (right) for NV^- centers within 10 nm of the diamond surface. The dashed lines represent individual NV centers under a surface that has been processed while contaminated with boron, while solid lines represent individual NV centers under an optimized, oxygen-terminated surface.

NV centers can exist in at least two charge states, negative and neutral. The negatively charged NV is useful for quantum sensing and quantum information processing, while the neutral NV center exhibits short spin coherence times. We have investigated the influence of the surface on the charge dynamics of NV centers. In the bulk, NV ionization rates are well-understood, and the NV^- is

thermodynamically stable. We observe that under certain surface terminations, the ionization rate can be enhanced, and that ionization in the dark can be observed, indicating that NV^0 is the more stable charge state (Figure 3). We have also investigated the detailed time-dependent photoluminescence of single NV^- centers after preparing the spin in $m_s = 0$ and -1, and we find that we can only account for the power dependence of the time traces with a model that incorporates ionization to and recombination from a "dark" state. Extracting these ionization and recombination parameters (Figure 4), we find dramatic differences in both the power dependence and relative rates when we compare NV centers under different surfaces. Our on-going investigations will include studying the effects on steady-state charge populations, free carrier concentrations, and the implications for quantum sensing.

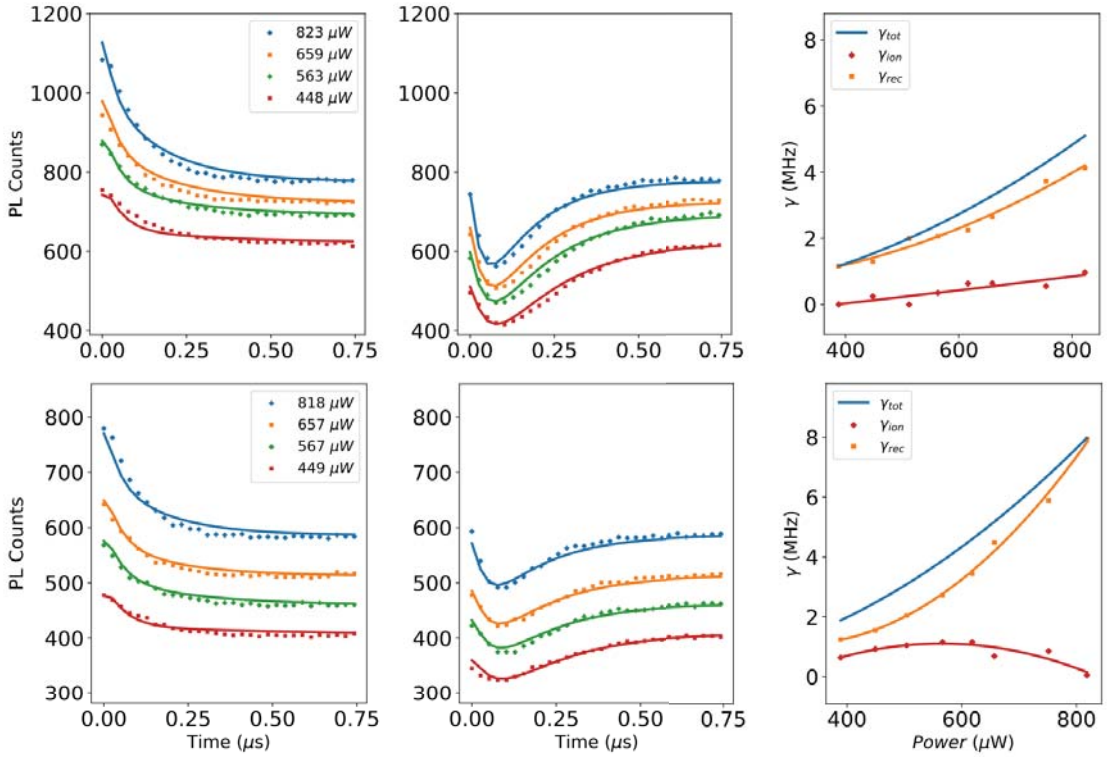

Figure 4: Time-dependent photoluminescence from representative NV centers in the optimized (top row) and contaminated (bottom row) samples. Solid lines correspond to fits that incorporate known NV photophysics, as well as power-dependent ionization and recombination. The right column shows the extracted ionization and recombination rates, constrained by the measured total rate (blue).

Future plans: Over the next year, we plan to study the reactivity of the bare diamond surface using a thermal gas cracker attached to the chamber to introduce new heteroatoms. We will further optimize wet chemical functionalization techniques, and will perform synchrotron spectroscopy at NSLS-II to fully characterize these surfaces. We have also recently completed construction on the second chamber of the UHV cluster tool, a cryogenic confocal microscope for performing NV-based surface spectroscopy, and will begin to perform charge state detection and photoluminescence excitation spectroscopy on NV centers under novel surfaces. Our final construction stage will involve incorporating microwave control of single NV centers, which we plan to begin this winter.

There are no publications to report at this time.

Charge Carrier Space-Charge Dynamics in Complex Materials for Solar Energy Conversion: Multiscale Computation and Simulation

Michel Dupuis
Department of Chemical and Biological Engineering
Computational and Data-Enabled Science and Engineering Program
University at Buffalo, Buffalo USA
mdupuis2@buffalo.edu

Program Scope:

The long term objective of our project is the fundamental characterization of processes and efficiencies in solar energy-to-fuels conversion systems in the three stages of 'light absorption', 'carrier transport', and 'carrier reactivity' (Figure 1). Our current efforts focus 'carrier transport' to understand, characterize, and ultimately control the factors that lead to enhanced separation of photo-generated electron and holes toward higher solar energy-to-fuel conversion efficiency. Our approach to modeling the space-charge distribution dynamics and the redox activity of charge carriers, combines first-principles atomistic computation and mesoscale kinetics simulation. We develop tools that we validate against experimental data. We apply these tools to identify design principles toward enhanced carrier transport and conversion efficiency.

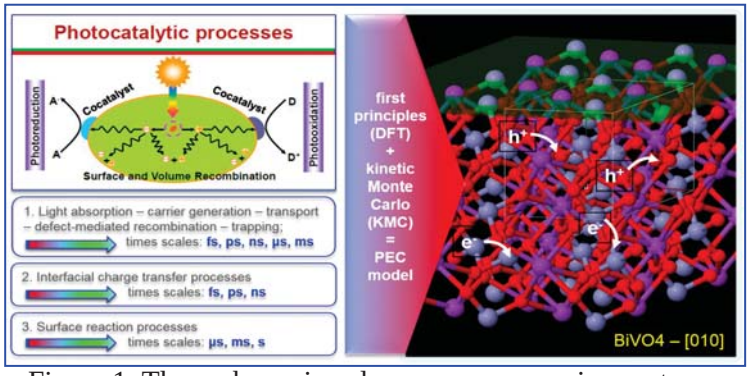

Figure 1. Three phases in solar energy conversion systems. Our project focuses on 'carrier transport' toward enhancing electron-hole separation and solar energy conversion efficiency.

This overall research program deals with timely societal challenges in renewable energy, i.e. the efficient and cost-effective conversion of solar energy to electrical and chemical energies. Current conversion efficiencies, including for solar water splitting, are far from the level needed for practical applications. At the most fundamental level, the research addresses how the flow of charge carriers in complex crystalline environments of single phase, multi-phase, and multi-materials semiconductor systems can be tailored to enhance redox reactivity in photo-electro-chemical conversion. This research is aligned with BES' CSGB Division focus areas of 'charge transport and reactivity' and 'chemistry at complex interfaces'. Currently our efforts focus on two main activities:

1. *Method developments*: The developments include quantum mechanical (QM) electronic structure tools to characterize electron/hole (e/h) carrier transfer in the solid state. They include also a lattice-based kinetic Monte Carlo (KMC) code to study the dynamics of carrier distribution in mesoscale models.
2. *Mesoscale transport studies*: we use the QM-derived e/h energetics and transfer rates to build mesoscale models of cation- and anion-doped photocatalysts at experimentally relevant scale. We study carrier transport and strategies for enhanced carrier separation.

Semiconductors that are our current focus are materials, doped and undoped, with highest water oxidation efficiency to date, such as bismuth vanadate $BiVO_4$ (BVO), tantalum nitrite Ta_3N_5, and other materials that exhibit the intriguing phenomenon of *facet selectivity* for oxidation and reduction. One goal is be to establish the theoretical foundation for facet selectivity and other strategies to enhance carrier separation and improve solar energy conversion performance. The combined QM+KMC mesoscale modeling has already proven essential to understand the nature of intrinsic carrier transport and the role of cation and anion doping in manipulating transport properties. The insights from mesoscale modeling can offer a step toward *screening of photo-active materials* with superior photocatalytic performance. Structural and chemical descriptors of 'good' transport and carrier separation ability are starting to emerge.

Recent Progress:

✓ *Mesoscale transport dynamics in $BiVO_4$*: We recently completed a study of carrier transport in BVO. DFT calculations indicated that thermodynamic stability is not a factor in facet selectivity. An exhaustive characterization of electron and hole hopping pathways in BVO yielded activation energies ~ 0.36 eV for electrons, and as low as ~ 0.17 eV for holes. Mesoscale KMC modeling revealed that hole transport is not nearly as efficient as the low barrier would suggest. Hole transport is *bi-modal*, with very fast but not transport-efficient hops ('rattling' motion) and slower but transport-efficient hops. [Liu-2018] It emerged from this work that strategies to eliminate hole 'rattling' will improve hole transport efficiency and water oxidation performance. This work illustrates also how mesoscale kinetic modeling is critically important as it captures the connection between elementary hopping rates and material structure and topology. Interpretations based on elementary hop characterization alone, even if at the quantum level of theory, have the potential to be misleading.

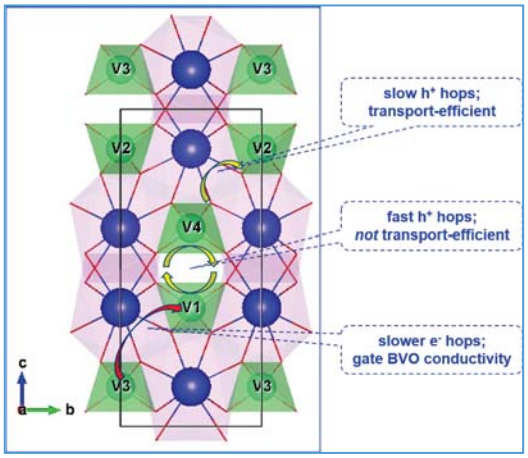

Figure 2. Bimodal h^+ transport in BVO; h^+ transport gates BVO redox activity.

Cation and anion doping in $BiVO_4$: cation doping of BVO with W/Mo has been shown to enhance conversion efficiency in BVO-based devices. We studied how W/Mo doping of BVO affects carrier mobility and electric conductivity. [Pasumarthi-2019] W/Mo doping results in a small decrease in electron mobility. However, the increase in carrier density upon doping overshadows the marginal decrease in electron mobility, resulting into an increased electronic conductivity. Work in progress deals with modeling homo-junctions, layered systems with a gradient of W-doping concentration. Anion doping of BVO with sulfur, up to a level of concentration of ~ 25%, has been shown to enhance charge separation. Calculations in progress are starting to reveal how hole transport in S-doped BVO involves S-to-S hoping only and that hole 'rattling' is eliminated in S-doped BVO.

✓ *Method and program developments*:

a. *Lattice-based KMC code for charge carrier transport:* We continued the development of a python code for lattice-based KMC simulation of charge carrier transport. (Figure 3) The new capability deal with the 'model engine' to include specific features for systems of interest, such as models 2D-periodicity, fine particle models, non-uniform doping, carrier generation, carrier recombination, carrier redox reactivity.

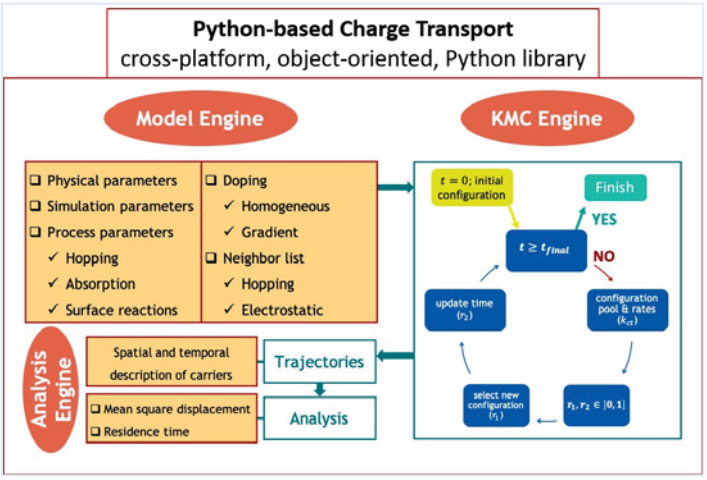

Figure 3. Flow chart of PyCT, a Python code for lattice-based Kinetic Monte Carlo for carrier transport.

b. *New method for polaron transfer calculation in the solid state*: we created a new module in the electronic structure code CP2K for the rigorous calculation of the electronic coupling $H_{AB} = < \Psi_A \mid H \mid \Psi_B >$ between polaron states ('initial' and 'final' non-orthogonal quasi-diabatic Marcus/Holstein states) in solid-state (periodic) DFT systems. The implementation takes advantage of the massively parallel capabilities of CP2K. Other tools include a/ the fast determination of phonon spectrum via compressed sensing of molecular dynamics trajectories. b/ an internal coordinate-based determination of the "anti-phase symmetric stretch" vibrational mode underlying the electron transfer. c/ the extension of accelerated meta-dynamics to polaron transfer using the anti-phase symmetric stretch coordinate as collective meta-dynamics coordinate to reduce dimensionality.

We presented the above research to the community on several occasions during the current funding period. PI Dupuis was an invited speaker at an international meeting on 'Solar Fuel-Solar Cells' and at the Fall meeting of ACS 2018. He is an invited speaker at the Fall meeting of the MRS 2019. Student Viswanath Pasumarthi was selected for contributed presentations at the ACS Spring meeting 2019, at the ACS Fall meeting 2019, and at the MRS Fall meeting in 2019. At MRS Fall 2019, student Pavan Behara will present a poster of the periodic DFT code developments for electronic coupling $\mathbf{V_{AB}}$ calculation, for compressed sensing in phonon calculations, and for metadynamics modeling of polaron transfer.

Future Plans:

We are presently extending the initial application work to investigate homo-junctions of layered BVO with a gradient of W/Mo dopant concentration. Indeed the electronic features of metal doping are more appreciable when controlling the spatial distribution of doping concentrations. Such is the case for homo-junctions of gradient (W/Mo)-doped BVO that enhance charge carrier separation. We are also completing the modeling of S-doped BVO. S-doping eliminates inefficient 'hole rattling' in BVO and enhances hole transport, carrier separation, and water oxidation performance. Future efforts will focus modeling finite size shape-selected BVO nanoparticles, with account of the processes associated with surface reactions (oxidation and reduction). Such modeling will offers a more 'complete' picture of photocatalytic systems.

CPIMS-sponsored Publications (2018-2019) –

1. T. Liu, **V. Pasumarthi, C. LaPorte**, Z. Feng, Q. Li, J. Yang, C. Li, and **M. Dupuis**, "*Bimodal hole transport in bulk $BiVO_4$ from computation*", J. Mater. Chem. A 6, 3714 (2018).
2. **V. Pasumarthi**, T. Liu, **M. Dupuis**, and C. Li, "*Charge carrier transport dynamics in W/Mo-doped $BiVO_4$: first principles-based mesoscale characterization*", J. Mater. Chem. A, 7, 3054 (2019).
3. N.A. Deskins, P.M. Rao, and **M. Dupuis**, "*Charge Carrier Management in Semiconductors: Modeling Charge Transport and Recombination*", Springer Handbook of Inorganic Photochemistry, 2019.
4. **P. K. Behara** and **M. Dupuis**, "*Electron Transfer in the Solid State: a Periodic Density Functional Theory Implementation*", Phys. Chem. Chem. Phys., accepted (2019).

CPIMS-sponsored Presentations (2018-2019) –

1. **M. Dupuis**, invited speaker, "*Multiscale characterization of carrier transport in photocatalytic materials: Application to $BiVO_4$*", 256th ACS National Meeting, symposium on "*Computational Photocatalysis*", Boston MA, August 2018.
2. **M. Dupuis**, invited speaker, "*Computational Photo-Electro-Chemical Catalysis (PEC): electronic structure, carrier transport, and redox reactivity*", The 6th International Symposium on "*Solar Fuels and Solar Cells*", Dalian National Laboratory for Clean Energy, Dalian, China, October 2018.
3. **M. Dupuis**, invited speaker and session chair, "*Recent method and application advances in multiscale characterization of carrier transport in materials for water splitting, such as cation- and anion-doped bismuth vanadate*", 258th MRS National Meeting, symposium on "*Materials Science for Efficient Water Splitting*", Boston MA, December 2019.
4. **V. Pasumarthi**, contributed oral presentation, "*Multiscale modeling of carrier transport in photocatalytic materials: Application to bismuth vanadate BiVO4*", 257th ACS National Meeting, symposium on "*Light-Driven Chemistry: Photoelectrochemistry & Photocatalysis*", Orlando FL, April 2019.
5. **V. Pasumarthi**, contributed oral presentation, "*Multiscale modeling of carrier transport in photocatalytic systems towards enhanced charge separation*", 258th ACS National Meeting, symposium on "*Understanding of Energy Materials with Advanced Computation & Characterization*", San Diego CA, August 2019.
6. **V. Pasumarthi**, contributed oral presentation, "*Multiscale Modeling of Charge Carrier Dynamics in Complex Metal Oxides for Solar Water Splitting: The Case of Anion Doping in BiVO4*", 258th MRS National Meeting, symposium on "*Materials Science for Efficient Water Splitting*", Boston MA, December 2019.
7. **P. K. Behara**, poster presentation, "*Electron transfer in the solid state: extension of the corresponding orbitals transformation for calculating electron transfer parameter V_{AB} to periodic systems*", 258th MRS National Meeting, symposium on "*Materials Science for Efficient Water Splitting*", Boston MA, December 2019.

Chemical Kinetics and Dynamics at Interfaces

Visualizing Local Optical Fields and Chemistry at Complex Interfaces

Patrick Z. El-Khoury (PI) and Alan G. Joly

Physical Sciences Division
Pacific Northwest National Laboratory
P.O. Box 999, Mail Stop K8-88
Richland, WA 99352, USA
patrick.elkhoury@pnnl.gov

Additional collaborators include: Kevin T. Crampton (PNNL), Andrey Krayev (Horiba Scientific), Libor Kovarik (PNNL), Edoardo Apra (PNNL), Eric Bylaska (PNNL), Niri Govind (PNNL), Irina Novikova (PNNL), James Evans (PNNL), Markus Raschke (University of Colorado at Boulder), Scott Lea (PNNL), Brian O'Callahan (PNNL), Jiguang Zhang (PNNL).

Program Scope

Photons can be converted into nanoscale optical fields in the form of localized and propagating surface plasmons. Such fields may be used to drive and monitor (photo)chemical and (photo)physical processes at interfaces with joint nanometer spatial and femtosecond temporal resolution. We address the challenges associated with generating spatiotemporally tailored plasmons to enable optical field manipulation and visualization over the relevant length and time scales. In this regard, the conversion between localized and propagating plasmon modes is of principle interest. In the context of interfacial plasmon driven chemistry, the dynamic interplay between molecular matter and localized optical fields strongly influences the (photo)physical and (photo)chemical properties of molecules. To this end, we strive to develop a fundamental molecular-level understanding of the interactions between molecular systems and enhanced local optical fields in their immediate vicinity, with emphasis on plasmon-induced chemical transformations at realistic (i.e., heterogeneous) interfaces. Overall, the conceptual and technological advances enabled through this fundamental research thrust provide the basis for understanding complex solid-air and solid-liquid interfaces that are often encountered in biological, catalytic, and electrochemical processes of current interest to DOE.

Approach

Our approach can be distilled into several objectives: (1) develop spatiotemporally tailored tip- and nanostructure-sustained plasmons for the delivery of well-defined and tunable nanoscale optical-fields, (2) investigate the fundamentals of plasmon-driven chemical transformations and reactivity at interfaces through tailored plasmons and model molecular systems (resonant and non-resonant Raman reporters), and (3) understand the operative physics underpinning metal–molecule coupling through increasingly sophisticated theoretical treatments. In practice, we combine time-resolved photoemission electronic microscopy (tr-PEEM) with tip-enhanced Raman spectroscopy (TERS) and imaging to address both localized and propagating surface plasmons with

femtosecond temporal and nanometer spatial resolution. Our two main experimental techniques are complimented by several microscopic and spectroscopic tools, including (i) electron and ion microscopy and lithography, and (ii) polarization-resolved optical dark-field spectral imaging to characterize the resonances of lithographically patterned plasmonic constructs and nanostructures.

Recent Progress

Surface Plasmon Coupling and Control Using Spherical Cap Structures. Surface plasmon polaritons (SPPs) launched from a protruded silver spherical cap structure were visualized using PEEM driven by s-polarized femtosecond laser excitation.[1] The resulting SPPs were comparable in intensity to SPPs launched with p-polarized excitation but produced distinct spatial profiles. The spatiotemporal properties of the nascent SPPs were determined by splitting the femtosecond pulse into a spatially separated pump–probe pair of orthogonal polarizations. The s-polarized pump pulse was used to initiate the SPP, which was subsequently visualized using a spatially and temporally separated p-polarized probe pulse. The s-polarization-launched SPP displayed a bifurcated spatial structure with an antisymmetric mirror plane; it may thus be regarded as two spatially distinct, temporally phase-locked wave packets.

Direct Visualization of Counter-Propagating Surface Plasmons in Real Space-Time. We deployed two-dimensional nanohole arrays as resonant SPP couplers that enable counter-propagation and excitation field interference-free imaging of SPP wave packets.[2] We monitored the spatiotemporal evolution of the resulting SPPs using two-color photoemission electron microscopy. The measurements track the electric field envelope of the SPPs in real space and time and enable direct characterization of their spatiotemporal properties in a regime where the SPP wave packet is the principal observable. We provided an analysis of the observables for both the co- and counter-propagating directions via SPP trajectories that are recorded in tandem. Our results highlight the advantages of isolating SPPs through counter-propagation, where excitation field–SPP interactions are suppressed.

Local Optical Field and Chemical Reaction Imaging of Complex Interfaces via TERS. We very recently developed a methodology that may be used to visualize local optical fields[3] and chemistry[4] at complex interfaces *via* TERS. Our approach allows fast (0.2 s/pixel) nanoscale chemical imaging of solid-air and solid–liquid interfaces with nm spatial resolution. This important technical breakthrough allowed us to record chemical reaction images, namely plasmon-induced chemical transformations, at solid–liquid interfaces for the first time.[4] The same modality allowed us to demonstrate that molecular TERS spectra and nanoscale images report on plasmon-enhanced local optical fields with nanometer spatial resolution under ambient laboratory conditions.[3] In the realm of chemistry at interfaces, we directly demonstrated that not all regions of optical field nano-localization and enhancement are suitable sites for chemical transformations on plasmonic metals. Using a model plasmon-driven chemical process, i.e., the dimerization of p-nitrothiophenol (NTP) to dimercaptoazobenzene (DMAB), we found that TERS maps at vibrational resonances corresponding to NTP trace the optical fields that are maximally enhanced toward the edges of the gold platelets.[3,4] Conversely, simultaneously recorded product maps revealed that the dimerization process occurs only at specific sites on our substrate. Overall, our results showed that molecular crowding and steric effects play a key role in our case of plasmon-driven NTP dimerization at the

gold–water interface. This finding challenges a previously accepted notion, whereby chemical reactivity was exclusively associated with optical field localization and enhancement. To rigorously understand our experimental observables, we continue to develop advanced theoretical treatments[5] that may be used to simulate ultrasensitive/high-resolution TERS spectra and images. These involve Raman spectral simulations from *ab initio* molecular dynamics as well as novel approaches to simulating ensemble averaged and non-ergodic Raman scattering on equal footing.[5]

Future Plans

Spatiotemporally Tailored Local Optical Fields. Our recent progress in generating and observing counter-propagating SPPs[2] relies on the resonant coupling of the incident field(s), which modifies the SPP spectrum. Combining this principle with our ongoing tr-PEEM efforts provides a direct route to interference-free surface plasmon microscopy and spectroscopy. The advantages of generalizing the concept into the limit of counter-propagating SPP excitation are multifold. Counter-propagation requires resonant coupling that modifies the SPP spectrum, in contrast to the forward direction spectrum that is nearly identical to the laser pulse. In effect, this provides a route to both generating tailored (energy, direction, phase) SPPs and investigating the elementary electronic processes in metals that govern resonant SPP coupling. The latter represents an inversion of the conventional forward problem in that SPPs may be utilized to extract the optical properties of plasmonic constructs in the near-field, and *vice versa*. In addition to the coupling and characterization schemes described above, the proposed experiments suggest alternate avenues with regard to SPP manipulation and delivery. Namely, tailored optical pulses translate into modified SPPs. The modality would be vastly expanded through the addition of a pulse shaper. In this scheme, pump-pulse pairs may be relatively tuned to synthesize test and reference SPP pairs. Phase, frequency, and polarization modifications to the test pulse may then be utilized to alter the plasmon spatiotemporal profile and to introduce or compensate for temporal dispersion. Correlated far-field measurements of SP resonances (hyperspectral dark field reflectance and scattering) will complement these proposed PEEM efforts.

Enhanced Multimodal Nanoscale Chemical Imaging. One of our immediate goals is to understand the difference between resonant (nile blue, rhodamine dyes) and non-resonant (functionalized aromatic thiols) Raman reporters in the context of local optical field imaging via TERS, which is a current subject of debate in scientific literature. To this end, nanoscale maps of molecularly excited electronic states (akin to UV-Vis measurements but on the nanometer scale) in combination with TERS chemical and chemical reaction imaging will allow us to understand the correlation between optical absorption at interfaces on one hand and chemical reactivity on the other. Nanoscale extinction spectroscopy and imaging will also allow us to directly measure the spatially varying tip–sample nanojunction resonances. Herein, polarization-resolved spectral imaging of native plasmonic nanoparticles and lithographically patterned substrates will be performed. Overall, correlated extinction and Raman maps of native and chemically functionalized substrates will be deployed to understand the operative chemistry and physics throughout the course of plasmon-enhanced chemical transformations at complex interfaces.

References to publications of DOE BES sponsored research (October 2017 to present)

1. Joly, A. G.; Gong, Y.; El-Khoury, P. Z.; Hess, W. P. "Surface Plasmon-Based Pulse Splitter and Polarization Multiplexer" *J. Phys. Chem. Lett.*, **2018**, *9*, 6164.

2. Crampton, K. T.; Joly, A. G.; El-Khoury, P. Z. "Direct Visualization of Counter-Propagating Surface Plasmons in Real Space-Time" *J. Phys. Chem. Lett.* **2019**, *10*, 5694.

3. Bhattarai, A.; Crampton, K. T.; Joly, A. G.; Kovarik, L.; Hess, W. P.; El-Khoury, P. Z. "Imaging the Optical Fields of Functionalized Silver Nanowires through Molecular TERS" *J. Phys. Chem. Lett.* **2018**, *9*, 7105.

4. Bhattarai, A.; El-Khoury, P. Z. "Nanoscale Chemical Reaction Imaging at the Solid-Liquid Interface via TERS" *J. Phys. Chem. Lett.* **2019**, *10*, 2817.

5. Aprà, E.; Bhattarai, A.; El-Khoury, P. Z. "Gauging Molecular Orientation through Time Domain Simulations of Surface-Enhanced Raman Scattering" *J. Phys. Chem. A* **2019**, 123, 7142.

Nanoporous Materials and Ionic Liquids: Dynamics, Structure, and Interactions

Michael D. Fayer

Department of Chemistry, Stanford University, Stanford, CA 94305-5080; fayer@stanford.edu

This program is investigating structural dynamics and intermolecular interactions in complex molecular systems that have mesoscopic structure. The effects of nanoconfinement on the dynamics of liquids are being investigated. Water in the nanopores of porous SiO_2 is an ideal system because of the uniform pore structure with well-defined sizea. Nanoporous SiO_2 is important in many applications. Other important systems in which water exists in confinement are hydrogels and polyelectrolyte fuel cell membranes. Room temperature ionic liquids (RTILs) are also being studied. RTILs are salts that are liquids at room temperature. They are generally composed of complex organic cations and inorganic anions. The complex structure of the cations and anions inhibit crystallization. The cations frequently have long alkyl chains that cause the liquids to segregate into ionic and apolar organic regions, giving the liquids structure on mesoscopic distance scales. In addition to bulk RTILs, RTILs in the pores of polymer membranes in the context of Supported Ionic Liquid Membranes for CO_2 capture were investigated. The principal experimental tools for the investigations are ultrafast nonlinear IR methods particularly 2D IR and polarization selective pump-probe experiments (PSPP), fast fluorescence experiments, and optical heterodyne detected optical Kerr effect (OHD-OKE) experiments.

Many of water's remarkable properties arise from its tendency to form an intricate and robust hydrogen bond network. Understanding the dynamics that govern this network is fundamental to elucidating the behavior of pure water and water in biological and physical systems. In ultrafast nonlinear IR experiments using a water hydroxyl probe, the accessible time scales are limited by water's rapid vibrational relaxation (1.8 ps for dilute HOD in H_2O), precluding interrogation of slow hydrogen bond evolution in non-bulk systems. Hydrogen bonding dynamics in bulk D_2O were studied from the perspective of the much longer lived (36.2 ps) CN stretch mode of selenocyanate ($SeCN^-$) using PSPP experiments, 2D IR spectroscopy, and molecular dynamics simulations. The simulations made use of the empirical frequency mapping approach, applied to $SeCN^-$ for the first time. The PSPP experiments and simulations showed that the orientational correlation function decays via fast (2.0 ps) restricted angular diffusion (wobbling-in-a-cone) and complete orientational diffusive randomization (4.5 ps). Spectral diffusion, quantified in terms of the frequency-frequency correlation function (FFCF), occurred on two timescales. The initial 0.6 ± 0.1 ps timescale is attributed to small length and angle fluctuations of the hydrogen bonds between water and $SeCN^-$. The second 1.4 ± 0.2 ps measured timescale reports on the slower collective reorganization of the water hydrogen bond network around the anion. These values are the same as measured using the OH stretch of HOD as the vibrational probe in bulk D_2O. The experiments and simulations provided details of the anion-water hydrogen bonding and demonstrated that $SeCN^-$ is a reliable vibrational probe of the ultrafast spectroscopy of water.

Nanoporous silica materials are important in catalysis, energy, and materials applications in which water is an essential component. System performance is intimately connected to the water dynamics occurring in confined environments. However, the dynamics and associated structures of water in mesoporous silica are challenging to measure or predict. Water dynamics subject to nanoscale confinement were examined via ultrafast infrared spectroscopy on $SeCN^-$ dissolved in the hydrated 2.4 nm silica nanopores of MCM41. As discussed above, $SeCN^-$ is an excellent probe of water dynamics with a sufficiently long lifetime to measure the slow dynamics created by nanoconfinement. Polarization selective pump-probe and two-dimensional infrared measurements on the CN stretching mode of $SeCN^-$ were used to probe the effect of confinement on orientational relaxation and spectral diffusion dynamics. The measurement on $SeCN^-$ provide information on water hydrogen bond dynamics. The long CN stretch lifetime (~36 ps), relative to the water hydroxyl stretch (< 2 ps), significantly extended the timescales that could be accessed. Complete orientational relaxation ($C_2(t)$, orientational correlation function) and spectral

diffusion ($C_\omega(t)$, frequency-frequency correlation function) dynamics were measured and compared to the simulated time correlation functions in a model silica pore of the same size. The simulations were done in collaboration with Professor Ward Thompson, University of Kansas. A slow decay component not present in the bulk liquid was observed in both experiments, indicating that the hydrogen bond dynamics were significantly altered by confinement. The simulations did a very good job of reproducing the observables. The simulations revealed a qualitative difference in the functional dependence of $C_2(t;d)$ and $C_\omega(t;d)$ on d, the distance from the interface. The former becomes exponentially faster with distance from the surface while the latter makes an abrupt transition from slower to faster dynamics midway between the surface and pore center, $d \cong 6$ Å.

Polymeric hydrogels have wide applications including electrophoresis, biocompatible materials, water superadsorbents, and contact lenses. The properties of hydrogels involve the poorly characterized molecular dynamics of water and solutes trapped within the three-dimensional cross-linked polymer networks. We applied 2D IR and PSPP spectroscopies to investigate the ultrafast molecular dynamics of water and a small molecular anion solute, $SeCN^-$, in polyacrylamide hydrogels. For all mass concentrations of polymer studied (5% and above), the hydrogen bonding network reorganization (spectral diffusion) dynamics and reorientation dynamics reported by both water and $SeCN^-$ solvated by water were significantly slower than in bulk water. As the polymer mass concentration increased, molecular dynamics in the hydrogels slowed further. The magnitudes of the slowing, measured with both water and $SeCN^-$, were similar. However, the entire hydrogen bonding network of water molecules appeared to slow down as a single ensemble, without a difference between the core water population and the interface water population at the polymer-water surface. This uniformity was attributed to the fact that acrylamide, like water, is both an H-bond donor and acceptor, with acrylamide/water H-bonds similar in bond strengths to water/water. In contrast, the dissolved $SeCN^-$ exhibited two-component dynamics, where the major component was assigned to the anions fully solvated in the confined water nanopools. The slower component has a small amplitude which was correlated with the polymer mass concentration, and was assigned to adsorbed anions strongly interacting with the polymer fiber networks. The interaction of the $SeCN^-$ with the polymer is quite different than its interaction with water.

Proton transfer in water is ubiquitous and a critical elementary event which, via proton hopping between water molecules, enables protons to diffuse much faster than other ions. The problem of the anomalous nature of proton transport in water was first identified by Grotthuss over 200 years ago. In spite of a vast amount of modern research effort, there are still many unanswered questions about proton transport in water. An experimental determination of the proton hopping time has remained elusive due to its ultrafast nature and the lack of direct experimental observables. We used 2D IR spectroscopy to extract the chemical exchange rates between hydronium and water in HCl acid solutions using a vibrational probe, the CN stretch of methyl thiocyanate (MeSCN). These were the first direct observations of a proton moving from a hydronium to a water molecule and of a water molecule receiving a proton from a hydronium. *Ab initio* molecular dynamics (AIMD) simulations, done in collaboration with my colleague Professor Tom Markland, demonstrated that the chemical exchange is dominated by proton hopping. The observed experimental and simulated acid concentration dependence then allowed us to extend the measured single step proton hopping time to the dilute limit, which, within error, gave the same value as inferred from indirect measurements using proton mobility and NMR linewidth analysis. In addition to obtaining the proton hopping time in the dilute limit from direct measurements and AIMD simulations, the results indicated that proton hopping in dilute acid solutions is induced by the concerted multi-water molecule hydrogen bond rearrangement that occurs in pure water. This proposition on the dynamics that drive proton hopping was confirmed through the use of a variety of experimental results from the literature.

Proton transfer in the nanoscopic water channels of polyelectrolyte fuel cell membranes was studied using a photoacid, 8-hydroxypyrene-1,3,6-trisulfonic acid sodium salt (HPTS) into the channels. Three fully hydrated membranes, Nafion (DuPont) and two 3M membranes, were studied to determine the impact of different pendant chains and equivalent weights on proton transfer. Fluorescence anisotropy and excited state population decay data were measured to characterize the local environment of the fluorescent probes and proton transfer dynamics. Measurements of the HPTS protonated and deprotonated fluorescent bands' population decays provided information on the proton transport dynamics. The decay of the protonated band from ~0.5 ns to tens of ns is determined by dissociation and recombination with the HPTS, providing information on the ability of protons to diffuse in the channels. The dissociation and recombination was manifested as a power law component in the protonated band fluorescence decay. The results showed that equivalent weight differences between two 3M membranes resulted in a small difference in proton transfer. However, differences in pendant chain structure did significantly influence the proton transport, with the 3M membranes displaying more facile proton transfer than Nafion.

The ion transport behavior of RTILs is pivotal for a variety of applications, especially when RTILs are used as electrolytes. Many aspects of the transport dynamics of RTILs remain to be understood. The RTIL 1-butyl-3-methylimidazolium bis(trifluoromethylsulfonyl)imide ($BmimNTf_2$), was studied with molecular dynamics simulations. Building on previous work that employed ion cage models, it was found that the diffusion dynamics of the cations and anions were well described by a hopping process random walk where the step time is the ion cage lifetime obtained from the decay of the ion cage correlation function. It was determined that the temperature dependent cation and anion diffusion constants could be determined quantitatively form the cage correlation function. Detailed analysis of the ion cage structures indicated that the electrostatic potential energy of the ion cage dominates the diffusion dynamics of the caged ion. The ion orientational relaxation dynamics showed that ion reorientation is a necessary step for ion cage restructuring. The dynamic ion cage model description of ion diffusion presented can be useful for designing RTILs to control their transport behavior.

Water and ions dynamics in concentrated LiCl solutions were studied using ultrafast 2D IR spectroscopy with the MeSCN CN stretch as the vibrational probe. The IR absorption spectrum of MeSCN has two peaks, one peak for water-associated with the nitrogen lone pair of MeSCN (W) and the other peak corresponding to Li^+ associated with the lone pair (L). 2D IR Chemical Exchange Spectroscopy was used to measure the interchange of water to Li^+ and vice versa. To extract the structural dynamics (spectral diffusion) reported by the probe for the W and L species, we developed a method that isolates the peak of interest by subtracting the 2D Gaussian proxies of multiple interfering peaks. This is an important new analysis method that will have wide ranging applications. Center line slope data (CLS – normalized frequency-frequency correlation function) for 2D bands from the W and L species are fit with triexponential functions. The fastest component (~1.5 ps) is assigned to local hydrogen bond length fluctuations. The intermediate timescale (~4.0 ps) corresponds to the hydrogen bond network rearrangement. These values vary somewhat with concentration. The slowest component decays in ~40 ps and corresponds to ion pair and ion cluster dynamics, that is, the time for the ion cloud to randomize its structure. Orientational relaxations of the W and L species were extracted using a new method to eliminate the effects of overlapping peaks. A Stark coupling model was used to extract the rms average electric field produced by the ion clouds along the CN moiety as a function of concentration.

Publications

"Proton Transfer in Perfluorosulfonic Acid Fuel Cell Membranes with Differing Pendant Chains and Equivalent Weights," Joseph E. Thomaz, Christian M. Lawler, and Michael D. Fayer J. Phys. Chem. B 121, 4544-4553 (2017).

"Water-Anion Hydrogen Bonding Dynamics: Ultrafast IR Experiments and Simulations," Steven A. Yamada, Ward H. Thompson, and Michael D. Fayer J. Chem. Phys. 146, 234501 (2017).

"Carbon Dioxide in a Supported Ionic Liquid Membrane: Structural and Rotational Dynamics Measured with 2D IR and Pump-Probe Experiments," Jae Yoon Shin, Steven A. Yamada, and Michael D. Fayer J. Am. Chem. Soc. 139, 11222-11232 (2017).

"Ultrafast to Ultraslow Dynamics of a Monolayer at the Air/Water Interface: 2D IR Spectroscopy," Chang Yan, Joseph E. Thomaz, Yong-Lei Wang, Jun Nishida, and Michael D. Fayer J. Am. Chem. Soc. 139, 16518-16527 (2017).

"The Influence of Mesoscopic Confinement on the Dynamics of Imidazolium-Based Room Temperature Ionic Liquids in Polyether Sulfone Membranes," Joseph E. Thomaz, Heather E. Bailey, and Michael D. Fayer J. Chem. Phys. 147, 194502 (2017).

"Influence of Water on Carbon Dioxide and Room Temperature Ionic Liquid Dynamics: Supported Ionic Liquid Membranes vs. the Bulk Liquid," Jae Yoon Shin, Steven A. Yamada, and Michael D. Fayer J. Phys. Chem. B 122, 2389-2395 (2018).

"Water Dynamics in Polyacrylamide Hydrogels," Chang Yan, Patrick L. Kramer, Rongfeng Yuan and Michael D. Fayer J. Am. Chem. Soc. 140, 9466-9477 (2018).

"Dynamics and Vibrational Coupling in a Pb-I-SCN Layered Perovskite," Jun Nishida, John P. Breen, Daiki Umeyama, Hemamala I. Karunadasa, Michael D. Fayer J. Am. Chem. Soc. 140, 9882-9890 (2018).

"Extraordinary Slowing of Structural Dynamics in Thin Films of a Room Temperature Ionic Liquid," Jun Nishida, John P. Breen, Boning Wu, and Michael D. Fayer ACS Central Science 4, 1065-1073 (2018).

478. "Ion-Molecule Complex Dissociation and Formation Dynamics in LiCl Aqueous Solutions from 2D IR Spectroscopy," Rongfeng Yuan, Chang Yan, and Michael D. Fayer J. Phys. Chem. B 122, 10582-10592 (2018).

"Orientational Pair Correlations in a Dipolar Molecular Liquid: Time-Resolved Resonant and Nonresonant Pump-Probe Spectroscopies," Steven A. Yamada, Heather E. Bailey, and Michael D. Fayer J. Phys. Chem. B 122, 12147-12153 (2018).

"Water Dynamics in Nanoporous Silica: Ultrafast Vibrational Spectroscopy and Molecular Dynamics Simulations," Steven A. Yamada, Jae Yoon Shin, Ward H. Thompson, and Michael D. Fayer J. Phys. Chem. C 123, 5790-5803 (2019).

"Imidazole and 1-Methylimidazole Hydrogen Bonding and Non-hydrogen Bonding Liquid Dynamics: Ultrafast IR Experiments," Jae Yoon Shin, Yong-Lei Wang, Steven A. Yamada, Samantha T. Hung, and Michael D. Fayer J. Phys. Chem. B 123, 2094-2105 (2019).

"Fast Dynamics of a Hydrogen-Bonding Glass Forming Liquid: Chemical Exchange-Induced Spectral Diffusion in 2D IR Spectroscopy," David J. Hoffman, Sebastian M. Fica-Contreras, and Michael D. Fayer J. Chem. Phys. 150, 124507 (2019).

"Reorientation-Induced Stokes Shifts Caused by Directional Interactions in Electronic Spectroscopy: Fast Dynamics of Poly(methyl methacrylate)," Joseph E. Thomaz, Patrick L. Kramer, Sebastian M. Fica-Contreras, David J. Hoffman, and Michael D. Fayer J. Chem. Phys. 150, 194201 (2019).

"Tracking Aqueous Proton Transfer by 2D-IR Spectroscopy and Ab Initio Molecular Dynamics Simulations," Rongfeng Yuan, Joseph A. Napoli, Chang Yan, Ondrej Marsalek, Thomas E. Markland, and Michael D. Fayer ACS Cent. Sci. 5, 1269-1277 (2019).

"Dynamics of Water Molecules and Ions in Concentrated Lithium Chloride Solutions Probed with Ultrafast 2D IR Spectroscopy," Rongfeng Yuan and Michael D. Fayer J. Phys. Chem. B 123, 7628-7639 (2019).

"Dynamical Properties of a Room Temperature Ionic Liquid: Using Molecular Dynamics Simulations to Implement a Dynamic Ion Cage Model," Maolin Sha, Xiaohang Ma, Na Li, Fabao Luo, Guanglai Zhu, and Michael D. Fayer J. Chem. Phys. accepted (2019).

Size Dependence of Liquid-Liquid Phase Separation in Aerosol Particles

Miriam Freedman
Department of Chemistry & Department of Meteorology and Atmospheric Science
205 Chemistry Building, The Pennsylvania State University, University Park, PA 16802
Email: maf43@psu.edu

Program Scope:

The overarching goal of this proposal is to understand how confinement affects phase transitions in particles. We are specifically interested in liquid-liquid phase separation (LLPS) in aerosol particles composed of salts and organic compounds. In these systems, LLPS can occur due to salting out of the organic component, resulting in an organic-rich phase and a salt-rich phase. In experiments, we induce salting out by drying the particles. As the relative humidity surrounding the particles decreases, the salt concentration within the particle increases, driving the phase separation process. We have previously determined that phase separation is inhibited for particle sizes < 50 nm because small particles cannot overcome the activation barrier needed to form a new phase. We focused this initial work on three model systems. Results from these studies have application to understanding myriad processes of aerosol particles in the environment such as heterogeneous chemistry, new particle growth, cloud droplet nucleation, optical properties, etc. At the same time, they have general application to understanding the physical chemistry of this phase transition which results in the formation of an interface within a liquid.

The specific goals of this project are as follows: 1) to extend our initial findings to systems composed of complex mixtures of organic compounds mixed with salts; 2) to investigate LLPS in polymer mixtures to investigate the role of the radius of gyration and the interaction energies on the phase separation behavior; 3) to explore the role of viscosity in the inhibition of phase separation; and 4) to develop experimental phase diagrams for liquid-liquid phase separation as a function of particle size by identifying the approximate location of the binodal curves and the critical point where the binodal and spinodal meet. We have previously captured particles for analysis once phase separation is complete and the particles are dry. We proposed here to capture particles wet and flash freeze them prior to imaging to obtain information on where phase separation occurs as a function of relative humidity. Complementary measurements of surface tension and viscosity of the systems of interest were also proposed. We have currently completed the two years of this grant.

Recent Progress:

Phase Separation in Systems Containing Multiple Organic Compounds and Ammonium Sulfate: We have previously demonstrated that liquid-liquid phase separation is absent at small particle sizes. Our initial systems were succinic acid, pimelic acid, or polyethylene glycol-400 (PEG-400) mixed with ammonium sulfate. We have expanded to systems containing complex organic mixtures with ammonium sulfate. These complex mixtures include multiple dicarboxylic acids, a mixture of alkyl and aromatic compounds with acid and alcohol functional groups, and the water soluble products of the dark ozonolysis of α-pinene. For every system studied, a size dependence of the morphology is observed, in which small particles remain homogeneous while

large particles phase separate (**Fig. 1**). This result suggests that the size dependence of morphology is important for ambient particles, which could impact for the formation of cloud condensation nuclei and the growth of new particles.

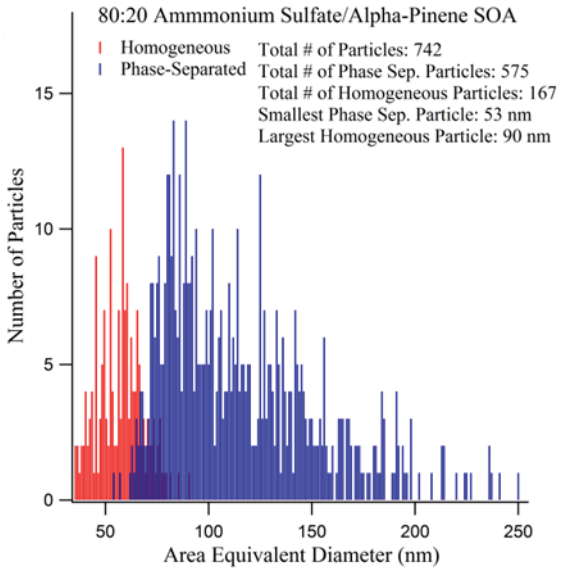

Figure 1. Size dependence of liquid-liquid phase separation for aerosol particles composed of ammonium sulfate and the water soluble components of the dark ozonolysis of alpha-pinene.

The Effects of Viscosity on the Phase Transitions of Supermicron Droplets: Aerosol particles that are composed of salts and organic compounds can vary widely in viscosity, depending on their composition and water content. To examine the role of viscosity on the phase transitions of aerosol particles, we studied supermicron droplets composed of ammonium sulfate or sodium chloride, an organic compound (dicarboxylic acid, polyol, or poly(ethylene glycol)), and sucrose. The addition of sucrose of different weight percents was used to alter the viscosity of the solution. The systems were investigated with optical microscopy. Sucrose had little impact on water uptake and crystallization of particles, but had a significant effect on the relative humidity at which liquid-liquid phase separation takes place (separation relative humidity). The separation relative humidity decreases with increasing viscosity until the point at which phase separation is inhibited (**Fig. 2**). The higher the starting separation relative humidity with no sucrose added, the higher the concentration of sucrose needed to arrest the phase separation. The identity of the salt also impacts the amount of sucrose required to arrest phase separation and is controlled more strongly by the identity of the anion. Our results suggest that phase separation may be inhibited in viscous aerosol.

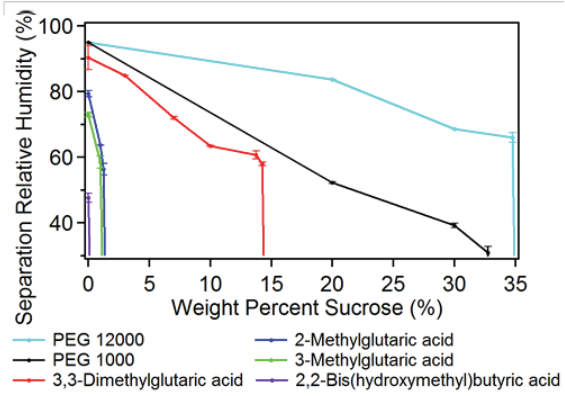

Figure 2. Separation relative humidity for droplets composed of an organic compound and ammonium sulfate as a function of sucrose weight percent.

Phase Separation in Polymer Nanoparticles: The phase separation of polymers has been studied for decades in many different systems. Our research is unique because we study the phase separation of water-soluble polymers in one dimension through the creation of aerosolized polymer nanoparticles. These experiments can provide insight into the mechanisms behind polymer phase separation and could have potential applications to the energy and medical sciences. The experiments are performed by atomizing aqueous solutions of water-soluble polymers. The particles are dried and impacted on transmission electron microscopy (TEM) grids and imaged using cryo-TEM. The first system studied was polyethylene glycol (PEG) and Dextran, which is a well characterized polymer aqueous two-phase system. Particles composed of PEG-6k and Dextran-10k were found to have a size dependent morphology where particles < 85 nm in diameter

are homogeneous and particles > 56 nm in diameter are phase separated. Note that these cutoffs yield three size regimes: only homogeneous particles are found at the smallest diameters, a mixture of homogeneous and phase separated particles are found at intermediate sizes, and only phase separated particles are observed at the largest diameters. By keeping the ratio of the polymers the same and changing the molecular weight, we can explore the role of the interaction energy χN on the size dependence of the morphology. As the molecular weight is increased, we observe that the smallest phase separated particles shift to smaller sizes. We have shown this effect for both PEG and Dextran mixtures and polyvinyl alcohol (PVA) and sodium polystyrene sulfonic acid salt (PSS) mixtures (**Fig. 3**). Using Flory-Huggins theory, we can show that this is the expected result as the molecular weight increases.

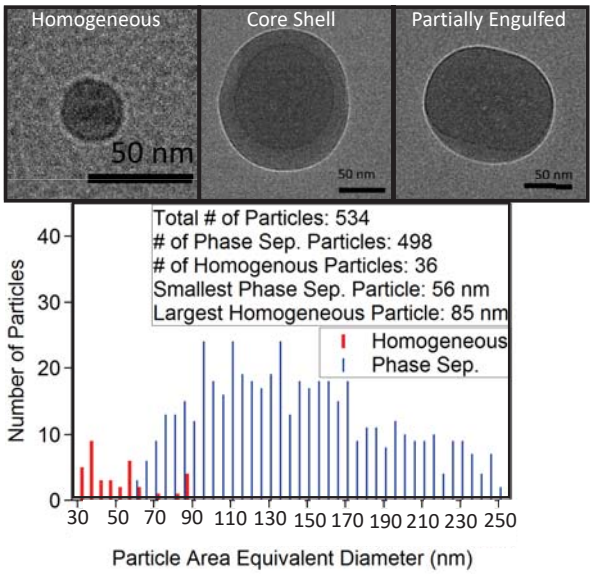

Figure 3. Size dependence of phase separation in submicron PEG/Dextran aerosol particles.

Vitrifying Aerosol Particles to Obtain the Submicron Separation Relative Humidity: We have built a flow chamber to flash freeze particles at a given relative humidity, deposit them on TEM grids, and image using cryo-TEM. We have calibrated the relative humidity in the chamber using potassium salts. Our results for liquid-liquid phase separating systems are unexpected. To run these samples, we equilibrate particles at different relative humidities and then capture them for imaging. Small particles remain homogeneous at any relative humidity probed. Larger particle sizes phase-separate randomly as a function of their diameter, until sufficiently low relative humidity, when all eventually are phase separated (**Fig. 4**). This stochastic behavior is indicative of a first order phase transition. The submicron separation relative humidity differs from the supermicron separation relative humidity for most systems. This result is significant because it indicates that the parameterizations that have been created for supermicron particles do not accurately represent the relative humidities at which the phase transition occurs for submicron particles.

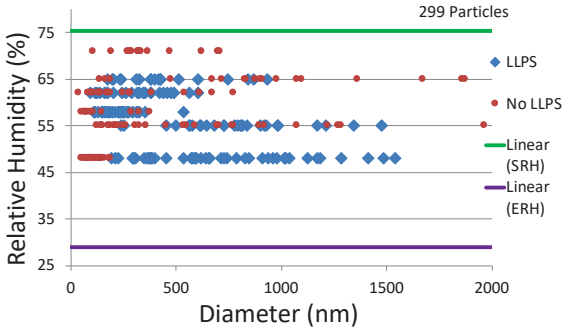

Figure 4. Phase separation of aerosol particles composed of 2-methylglutaric acid and ammonium sulfate as a function of relative humidity.

Future Plans:

All of the above studies are submitted or in preparation. Our primary goal in the next months is to publish this work. In addition, there are several aspects of this project that we would like to explore further:

Experimentally Constructed Phase Diagrams as a Function of Particle Size: One of our initial goals of this project was to experimentally construct phase diagrams as a function of particle size. For our systems presented above (with the exception of the complex organic mixtures project), we have generally focused on one ratio of organic to inorganic components. We plan to start to vitrify particles at a range of different ratios to better understand the submicron phase diagram for these systems.

Effect of Viscosity on Size Dependence of Phase Separation in Submicron Aerosol: We are interested in determining how the diameter below which all particles are homogeneous shifts as the viscosity of the system is increased. We plan to work with PEG and ammonium sulfate. We will change viscosity in three ways: 1) changing the ratio of the organic to inorganic components, 2) changing the molecular weight of PEG, and 3) adding sucrose to the system.

Effect of Salt Identity on Size Dependence of Phase Separation in Submicron Aerosol: Each salt exhibits a different degree of salting out of the organic compounds, which may also shift the diameter below which all particles are homogeneous. We plan to work with PEG and a range of different salts to explore this behavior.

DOE-Sponsored Publications (since 2017):

D. J. Losey, E.-J. E. Ott, M. A. Freedman, Effects of High Acidity on Phase Transitions of an Organic Aerosol, *Journal of Physical Chemistry A* **2018**, *122*, 3819-3828. doi: 10.1021/acs.jpca.8b00399

M. A. Freedman, E.-J. E. Ott, K. E. Marak, Role of pH in Aerosol Processes and Measurement Challenges, *Journal of Physical Chemistry A* **2019**, *123*, *1275-1284.*

T. M. Kucinski, J. N. Dawson, M. A. Freedman, Size Dependent Liquid-Liquid Phase Separation in Atmospherically Relevant Complex Systems, *submitted.*

Chemical Kinetics and Dynamics at Interfaces

Fundamentals of Solvation under Extreme Conditions

John L. Fulton

Physical Sciences Division
Pacific Northwest National Laboratory
902 Battelle Blvd., Mail Stop K2-57
Richland, WA 99354
john.fulton@pnnl.gov

Collaborators: S. M. Kathmann, G. K. Schenter, C. J. Mundy, N. Govind.

Program Scope

The primary objective of this project is to describe, on a molecular level, the solvent/solute structure and dynamics in fluids such as water under extremely non-ideal conditions. The scope of studies includes solute–solvent interactions, clustering, ion-pair formation, and hydrogen bonding occurring under extremes of temperature, concentration and pH. The effort entails the use of spectroscopic techniques such as x-ray absorption fine structure (XAFS) spectroscopy, high-energy x-ray scattering, coupled with theoretical methods such as molecular dynamics (MD-XAFS), and electronic structure calculations in order to test and refine structural models of these systems. In total, these methods allow for a comprehensive assessment of solvation and the chemical state of an ion or solute under any condition. The research is answering major scientific questions in areas related to energy, environmental and biological processes including specific areas of relevance to DOE such as mixed hazardous waste processing, power plant chemistry, and geologic carbon dioxide sequestration. This program provides the structural information that is the scientific basis for the chemical thermodynamic data and models in these systems under non-ideal conditions.

Recent Progress

Long range ordering of ions in water.

The overwhelming majority of scattering studies (X-rays, neutrons, photoelectrons (EXAFS)) have probed the local structure about ions up to approximately 0.5 nm. However, electrostatic forces order ions to much longer distances. Length scales up to about 5 nm can be quantitatively related to (1) important thermodynamic properties such as ion activity coefficients and osmotic pressure, (2) are important to the formation of pre-nucleation clusters at near-saturation conditions and (3) to long range ion ordering affecting mesoscale processes. High-energy X-ray diffraction measurements can be used to probe this long-range ordering of ions in water.

Figure 1a shows XRD measurements (11-ID-C, APS) for a set of monovalent and divalent salts. These g(r) plots in the region from about 0.1 to 0.5 nm illustrate the well-known structure of water hydrating cations and anions. The progression of peaks between 0.15 and 0.25 nm correspond to the first-shell, ion/water distances of Al^{3+}, Mg^{2+}, Na^{+}, Mg^{2+}, respectively. There is the contribution from water-water, $g_{OO}(r)$, at about 0.28 nm. The Cl^{-} and Br^{-} first-shell waters reside at about 0.3 to 0.34 nm. Finally, the divalent cations form solvent-shared ion pairs (SSIP) with their respective anion as a series of peaks just below about 0.5 nm. The peaks at longer range, between 0.5 to 1.5 nm, are assigned to ion-ion ordering occurring at much longer length scales.

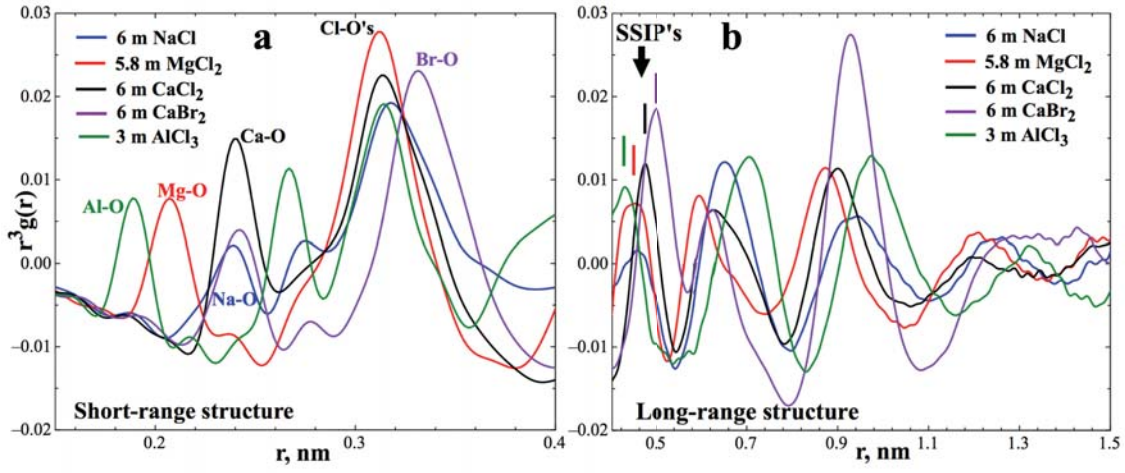

Figure 1. XRD distribution functions, $g^x(r)$, for monovalent, divalent and trivalent salts near their saturation points. The r^3-weighted distribution functions are shown for the short range (a) and long range (b) structures. In (b), the set of features near 0.5 nm can be assigned to SSIP's while the exact peak assignments at longer distances, from 0.6 to l.5 nm, are not yet known.

Early studies of electrolyte solutions by Debye, Hückel, Onsager and others were first to show that the macroscopic thermodynamic properties such as the osmotic pressure and ion activity coefficients were dominated by the long-range Coulombic forces between ions. More comprehensive theories have evolved that directly relate these properties to the full ion-ion and ion-water pair distribution functions. For example, Kirkwood-Buff theory directly relates how the assembly of different pair distribution functions of the electrolyte solution are used to directly calculate the ionic activity and osmotic pressure coefficients. The underlying fundamental quantities in this formalism are the Kirkwood-Buff integrals (KBI's) that are derived from the set of r^2-weighted pair distribution functions, $g_{ij}(r)$'s. This long-range emphasis (r^2-weighting) illustrates the importance of the measured structure in Figure 1b.

For x-ray diffraction, the measured x-ray total distribution function, $g^x(r)$, is composed of a weighted summation of the same set of pair-distribution functions that are used to determine the KBI's. Furthermore, the total $g^x(r)$ and the partials, $g_{ij}(r)$'s, can be simply and exactly calculated from a MD trajectory as shown by the example in Figure 2a. In Figure 2a we compare the experimental results with those from classical empirical intermolecular potentials (Smith/Dang and Joung/Cheatham). The use of empirical potentials (rather than DFT) is required to effectively sample long length scales. For this case of 6 m NaCl, there is good agreement between experiment and theory for the periodic ordering above about 0.5 nm that is believed to have a basis in the ion electrostatic repulsion.

In order to make the connection to the overall thermodynamic properties of interest, both short- and long-range length scales are important. These two regions are not decoupled, in that the short-range ion pair structure will have a strong impact on the ordering at longer length scales. For instance, a contact-ion pair, CIP, will appear as a "neutral" solute to a spectator ion at long distance whereas a SSIP will exert an electrostatic force on the spectator ion that is approximately proportional to the ion pair separation distance and thereby lead to long range ordering. .

More insights into the long-range ion ordering can be derived from the measured fluid structure factor, S(Q). As shown in Figure 2b, there is a transition region near 3 $Å^{-1}$ (blue) between a set of

3-4 diffraction-like peaks at lower Q, and the oscillating S(Q) feature at higher Q. In the standard XRD analysis it is the Fourier transformation of this high-Q structure that generates the familiar set of ion-water and water-water in the g(r). Less-well appreciated are the low-Q peaks, that generate the *periodic* structure in the g(r) upon FT transformation due to long-range periodic ordering of anions and cations. We have quantitatively predicted this long-range structure (both in $S^x(Q)$ and $g^x(r)$) from a MD trajectory using a 7 nm box size and empirical intermolecular potentials that have been optimized to predict the solution osmotic coefficients.

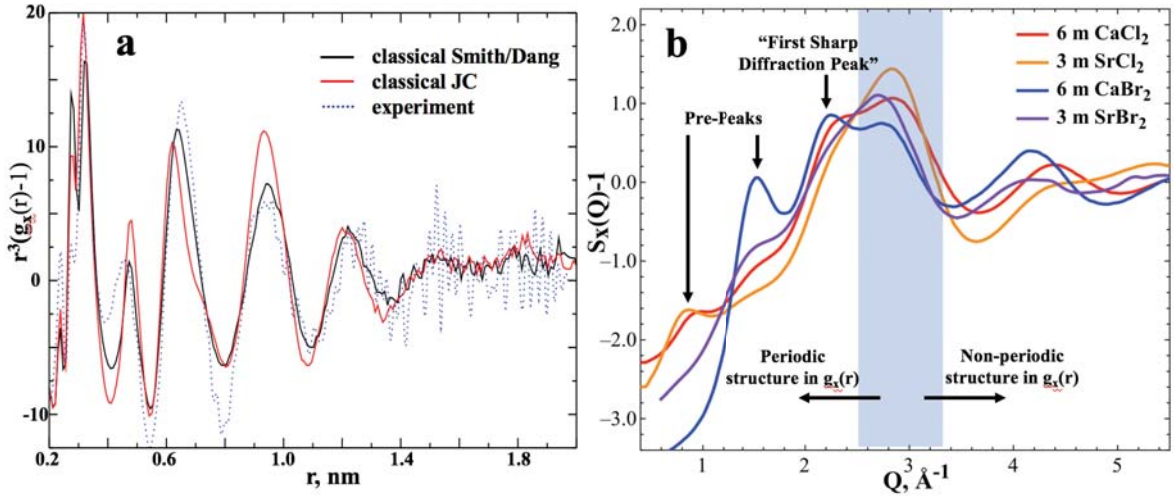

Figure 2. In (a), the r^3-weighted XRD distribution function, $r^3g^x(r)$, for 6 m NaCl is compared to MD simulated structure using two different classical potentials. Structure up to almost 2 nm is reproduced by the simulation. In (b), the structure factor, $S^x(Q)$, is shown for the Ca^{2+} and Sr^{2+} salts of chloride and bromide highlighting the diffraction-like peaks at $Q < 3$ Å^{-1}.

Future Plans

The objective is to gain a fundamental understanding of the molecular structure that provides the basis for understanding ion chemistry and dynamics. We propose exploring ion-water structure for systems in which the local structure has not yet been measured or the structure is not yet fully understood. Our goal is to identify the underlying structural factors that govern the macroscopic properties of ions that have so far eluded a comprehensive theoretical treatment. The proposed work also involves a comprehensive study of ion pairing in concentrated solutions and at high temperatures. The objective is to describe how the ion-pair structure is governed by a range of different types of solvent interactions.

References to publications of DOE sponsored research (2018 - present)

1. Zhuang, D.B.; Riera, M; Schenter, G.K.; Fulton, J.L.; Paesani, F. "Many-Body Effects Determine the Local Hydration Structure of Cs^+ in Solution" *J. Phys. Chem. Lett.* **2019** *10(3)* 406 10.1021/acs.jpclett.8b03829
2. Pham, VT; Fulton, JL "Contact ion-pair structure in concentrated cesium chloride aqueous solutions: An extended X-ray absorption fine structure study" *J. Electron Spec. Rel. Phenon.* **2018** *229(20).* 25 10.1016/j.elspec.2018.09.004

3. Galib, M; Schenter, GK; Mundy, CJ; Govind, N; Fulton, JL "Unraveling the spectral signatures of solvent ordering in K-edge XANES of aqueous Na^{+}" *J. Chem. Phys.* **2018** *149(12)* 124503. 10.1063/1.5024568
4. Wildman, A; Martinez-Baez, E; Fulton, J; Schenter, G; Pearce, C; Clark, AE; Li, XS. "Anticorrelated Contributions to Pre-edge Features of Aluminate Near-Edge X-ray Absorption Spectroscopy in Concentrated Electrolytes". *J. Phys. Chem. Lett.* **2018** *9(10)* 2444 10.1021/acs.jpclett.8b00642
5. Henzler, K; Fetisov, EO; Galib, M; Baer, MD; Legg, BA; Borca, C; Xto, JM; Pin, S; Fulton, JL; Schenter, GK; Govind, N; Siepmann, JI; Mundy, CJ; Huthwelker, T; De Yoreo, JJ "Supersaturated calcium carbonate solutions are classical". *Science Advances* **2018** *4(1).* eaao6283 10.1126/sciadv.aao6283

A cluster approach to understanding solvation effects on ion structure and photochemistry

DE-SC0018902

Etienne Garand

Department of Chemistry, University of Wisconsin-Madison, Madison, WI 53706

egarand@wisc.edu

Program scope

The aim of this proposal is to provide a detailed understanding of solvation effects on the structure and chemistry of molecular ions via spectroscopic interrogation of precisely assembled micro-solvated clusters. Many energy transformation, storage, and transport systems consist of interesting environments that differ from conventional bulk "liquid phase", e.g., porous materials with cavity on the nanometer scale. In such environments, chemical behaviors arising from partial solvation and interfaces can play a dominant role in the observed physical characteristics. Even the fundamental chemical properties of a molecule, such as its structure or its acidity, can differ significantly from those found in the isolated molecule or the bulk phase.

Studies of mass-selected charged solvated clusters are crucial in providing insights into the exact structure of an ion as well as ion-solvent and solvent-solvent interactions. The strength of such an approach lies in the presence of a well-defined molecular object in which these specific interactions can be highlighted and separated for study. The main challenge here lies in being able to study, at similar levels of detail, clusters with sufficient complexity such that the results from these model systems can be properly translated to condensed phase systems. Recently, experimental progresses made in our lab and others enabled the probing of increasingly complex ionic clusters that are more directly representative of partially solvated ions found at interfaces or of ions present in confined water in nanoscale pores. We have showed that temperature control in ion traps can be used to efficiently cluster solvent molecules onto almost any ion. Cluster sizes containing up to 50 water molecules can now be readily produced. This unprecedented versatility and cluster size accessibility enable systematic studies of stepwise solvation of illustrative model systems, making it possible for us to build up an in-depth molecular-level understanding of how solvation influence structures via competitive and cooperative interactions. These understandings can then be transferred to more complex systems of various sizes to explain observed phenomena, as these models contain all the basic elements of interactions that are present in the larger systems. Furthermore, results from the proposed studies can serve as crucial benchmarks for theory, where it is still difficult to accurately capture these combinations of non-covalent interactions.

There are several closely interrelated major scientific goals in this proposal. We aim to 1) develop the experimental toolkit necessary to extract molecular structure and non-covalent interaction information from spectroscopy of large solvated ionic clusters. 2) Develop a molecular-based understanding of cooperative and competitive hydrogen-bonding interactions that modulate the conformational space of flexible ions in the presence of water. 3) Understand how the species of the ion can influence the water hydrogen-bonding network surrounding the entire ionic adduct. 4) Probe how photodissociation yield, branching ratio and mechanism can change as a function of the solvation environment around an ionic chromophore.

Recent Progress

We have acquired the IR predissociation (IRPD) spectra of microsolvated glycine and L-alanine, $GlyH^+(H_2O)_n$ and $AlaH^+(H_2O)_n$, n=1-6. These are the two simplest amino acids─glycine does not have a side-chain while alanine has a simple methyl side-chain, as shown in Figure 1. The purpose of this study is to probe the effect of the hydrophobic methyl side-chain on the overall solvation interactions. The assignments of the solvation structures were aided by IR-IR double resonance spectroscopy and H_2O/D_2O substitution. These experimental methods were developed and implemented in our lab with the aim of being able to carry out more precise analysis and structural determination from the congested IRPD spectra, which are typical of increasing cluster sizes.

The IR-IR two-laser double resonance scheme allows us to isolate isomer-specific spectral signatures. The details of our IR-IR double resonance implementation are published in Ref [4]. Briefly, our setup has one laser focused directly inside the 10 K tagging trap, while the other functions as a typical predissociation laser. This allows for both an isomer-burning scheme as well as an ion-dip scheme, providing flexibility for tackling different systems of interest. In Ref[4], we applied our IR-IR ion-dip double resonance approach to disentangle the vibrational spectrum of Na^+(glucose), revealing the presence of 8 conformational and anomeric isomers, likely formed and trapped during the ESI process.

The H_2O/D_2O substitution approach takes advantage of the low-temperature environment in the reaction trap to produce D_2O clusters while preventing H/D exchange with the core ion. When D_2O is introduced at 300 K inside the reaction trap, we observed extensive H/D exchange of the N-H and O-H protons. At 80 K, the results indicate there is insufficient energy to allow for H/D exchange during the

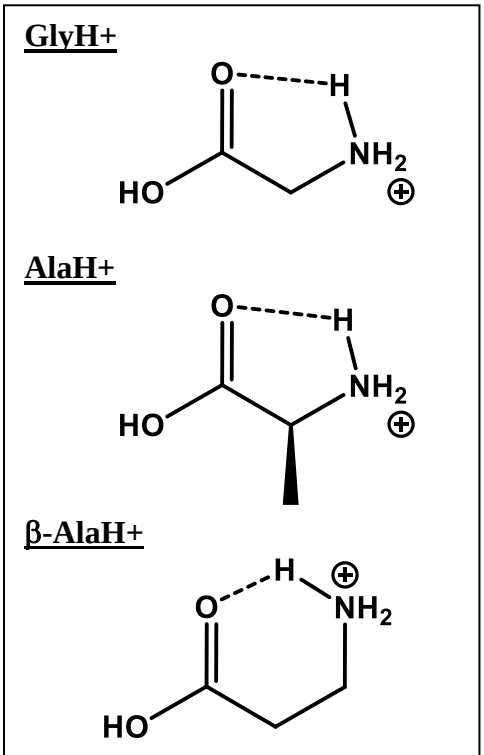

Figure 1. Structure of protonated Glycine, Alanine and β-Alanine.

~10 ms residence time of the ions inside the trap. Comparison of the IRPD spectra of the H_2O solvated clusters and D_2O solvated clusters thus allows for the direct identification and separation of the vibrational bands belonging to the ion core from those of the solvent molecules. Our initial spectroscopic results on $GlyH^+(H_2O)_n$ clusters was published in Ref [5].

The analysis $GlyH^+(H_2O)_n$ and $AlaH^+(H_2O)_n$ spectra, published in Ref[9], reveals the water-amino acid as well as the water-water interactions, and the subtle effects of the methyl side-chain in L-alanine on the solvation motif are also highlighted. Both bare amino acids exhibit an intramolecular hydrogen bond between the protonated amine and carboxyl terminals (see Fig. 1). In the n = 1-2 clusters, the water molecules preferentially solvate the protonated amine group. While glycine and L-alanine have similar solvation isomers, we observed clear differences in the relative isomer stabilities for the two amino acids. These differences are found to be due to electron donation from the methyl group weakening the intramolecular hydrogen-bond, rather than purely steric effect. This is highlighted in the n = 3 cluster, which shows a further preference for solvation of the carboxyl group in L-alanine, rather than breaking the intramolecular hydrogen-bond as in glycine. For n = 4-6 clusters, the solvation structure of the two amino acids is remarkably similar, with one dominant isomer present in each cluster size. The first solvation shell is completed at n = 4, evidenced by a lack of free NH and OH stretches on the amino acid, as well as the first observation of H_2O-H_2O interactions in the n = 5 spectra. Finally, we note that calculations at the DFT level show excellent agreement with the experiment for the smaller clusters. However, when water-water interactions compete with water-amino acid interactions in the larger clusters, DFT results show greater disagreement with experiment when compared to MP2 results.

Two important conclusions from this work are driving our current efforts. First, we are further probing the effect of intramolecular hydrogen-bond on the microsolvation structure by studying β-Alanine. This unnatural amino acid has a much stronger intramolecular hydrogen-bond due to the longer alkyl chain between the amine and carboxyl groups, as shown in Figure 1. Preliminary results show a marked difference between the microsolvated structure of glycine and β-Alanine. For instance, five water molecules are required to break the intramolecular hydrogen-bond in β-Alanine while only three are needed in glycine. We are currently developing a quantitative molecular model for the competition between ion-solvent and ion intramolecular interactions by using the amplitude of the redshifted (hydrogen-bond donating) OH stretch to determine the strengths of individual hydrogen-bonds.

Second, we are further investigating the electronic effect of alkyl side-chains on the intra-molecular hydrogen-bond. This effect was highlighted when we found different contributing structures for $(Gly)_3H^+$ and $(Ala)_3H^+$. We thus started a systematic study of all the possible Ala and Gly permutation in a tripeptide (i.e., Gly-Gly-Gly, Ala-Gly-Gly, Gly-Ala-Gly, etc). IR-IR double resonance spectroscopy is used to obtain quantitative information on the ratio of the three important conformations in these species. This study is revealing the complex effect of the methyl

side-chain on the strength of possible intramolecular hydrogen-bonds between the amine group and the various C=O groups.

Future Plans

We plan to continue our study of microsolvated amino acids and flexible peptides. In particular, we will continue to probe the effect of solvation on the structure of larger tri- and tetra-peptides (see Ref[8]) which feature a lot of conformational freedom. We will also study the effect of solvation on the acid-base behavior of these species, e.g., the solvent driven formation of zwitterionic structures. We are currently working on a major improvement of our ion source. The new source will feature two mass-selective reaction traps in series, which will enable the synthesis of more complex solvated clusters. We have made good progress in implementing mass-selectivity via digital waveform driven quadrupole ion trap. The next step will be to explore the careful transfer and preservation of fragile cluster structures between two ion traps.

Publications

1) S. J. Kregel, G. K. Thurston, J. Zhou and E. Garand, *A multi-plates velocity-map imaging design for high-resolution photoelectron spectroscopy*, **J. Chem. Phys.**, 147, 094201 (2017)

2) S. J. Kregel, G. K. Thurston, E. Garand, Photoelectron spectroscopy of anthracene and fluoranthene radical anions, **J. Chem. Phys.**, 148, 234306 (2018)

3) S. J. Kregel, and E. Garand, *Ground and Low-Lying Excited States of Phenoxy, 1-Naphthoxy and 2-Naphthoxy Radicals via Anion Photoelectron Spectroscopy*, **J. Chem. Phys.**, 149, 074309 (2018)

4) J. M. Voss, S. J. Kregel, K. C. Fischer, and E. Garand, *IR-IR conformation specific spectroscopy of Na^+(Glucose) adducts*, **J. Am. Soc. Mass Spectrom.**, 29, 42-50 (2018)

5) J. M. Voss, K. C. Fisher, and E. Garand, *Accessing the vibrational signatures of amino acid ions embedded in water clusters*, **J. Chem. Phys. Lett.**, 9, 2246-2250 (2018)

6) J. M. Voss, K. C. Fischer, and E. Garand, *Revealing the structure of isolated peptides: IR-IR predissociation spectroscopy of protonated triglycine isomers*, **J. Mol. Spec.**, 347, 28-34 (2018)

7) E. Garand, *Spectroscopy of Reactive Complexes and Solvated Clusters: A Bottom-Up Approach Using Cryogenic Ion Traps*, **J. Phys. Chem. A**, 122, 6479-6490 (2018)

8) K.C. Fischer, J. M. Voss, and E. Garand, *Probing the solvation-induced structural changes in conformationally flexible peptides: IR predissociation spectroscopy of $Gly_3H^+(H_2O)$*, **J. Phys. Chem. A**, 122, 8213-8221 (2018)

9) K. C. Fischer, S. L. Sherman, J. M. Voss, J. Zhou and E. Garand, *Microsolvation Structures of Protonated Glycine and L-Alanine*, **J. Phys. Chem A**. 123, 3355-3366 (2019)

10) G. K. Thurston, C. R. Sagan and E. Garand, *Vibrationally resolved photoelectron spectroscopy of oligothiophene radical anions*, **J. Chem. Phys.**, (in press)

Improved Methods for Modeling Functional Transition Metal Compounds in Complex Environments: Ground States, Excited States, and Spectroscopies

Hrant P. Hratchian (PI, hhratchian@ucmerced.edu), Christine M. Isborn (cisborn@ucmerced.edu), Aurora Pribram-Jones (apribram-jones@ucmerced.edu), Liang Shi (lshi4@ucmerced.edu), and David A. Strubbe (dstrubbe@ucmerced.edu)

University of California, Merced, 5200 N. Lake Rd., Merced, CA 95343

Abstract

Rapid advances in energy applications require new theory and computational models to provide guidance for interpretation of experimental results and mechanistic understanding. New theory development is necessary to treat systems of increasing complexity, size, and relevance to real applications. Functional transition metal compounds, including molecules, clusters, nanoparticles, surfaces, and solids, provide particular promise for magnetic, optical, and catalytic applications. However, such systems can be exceptionally challenging to model. To make progress in understanding and designing transition metal compounds for energy applications, theory must be able to simulate such systems in complex environments, as well as simulate the spectra of such complex systems to provide direct connections with experiment. Leveraging the independent expertise of the team's members, this project will make inroads to the theoretical and computational challenges associated with studying transition metal compounds, their reaction chemistry, photophysics and photochemistry, and response to spectroscopic interrogation. The team's recent work has focused on expanding the capabilities of ground and excited electronic structure methods and understanding the role of the environment in models of two-dimensional electronic spectroscopy (2DES), which is the focus of this abstract.

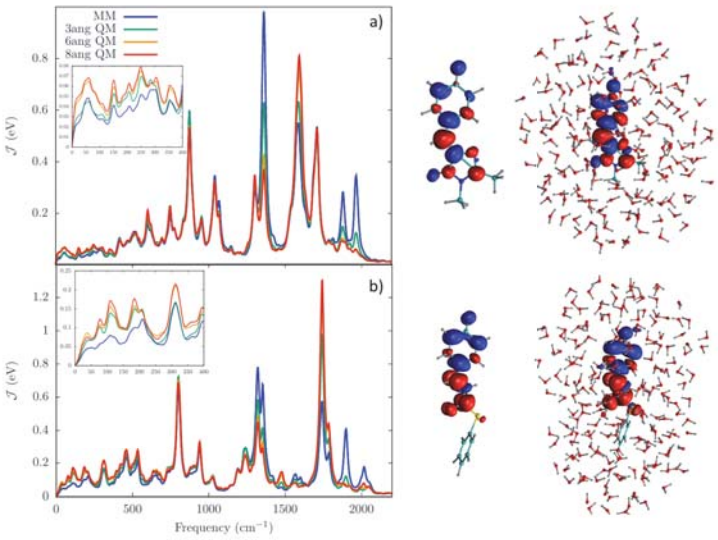

Figure 1. Spectral density of a) the GFP chromophore anion and b) the PYP chromophore anion in water for varying sizes of the QM region for the solvent sphere included in the TDDFT excited state computation. The inset shows a zoom-in of the low frequency region. Also shown are plots of the electron (red) hole (blue) difference densities of the S_1 state, as computed for a pure MM solvent environment and for an 8 Ang QM region of solvent.

To probe and simulate ultrafast relaxation of electronic excited states, work is underway to develop techniques and best practices for modeling two-dimensional electronic spectroscopy (2DES) in the condensed phase based on the cumulant expansion. Our initial results (see Figure 1) suggest that the quantum mechanical treatment of the environment plays a key role in controlling the spectral density and will likely also be key to accurately modeling 2DES and coupling between the electronic and vibrational degrees of freedom.

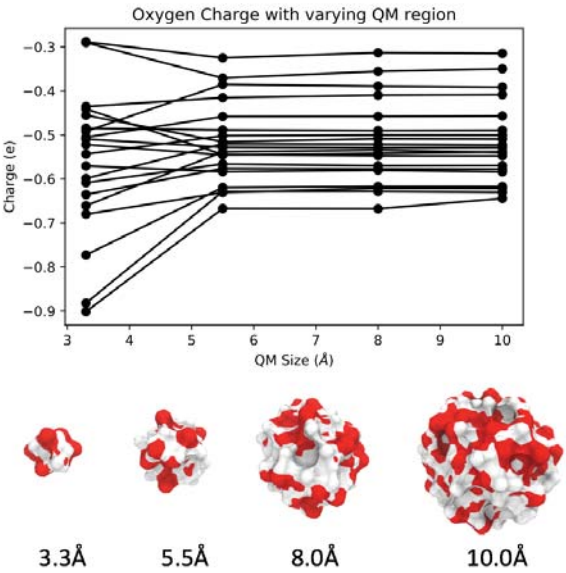

FIGURE 2. Oxygen charge of a randomly selected central water for 20 QM/MM liquid water configurations as a function of QM region radius. A snapshot of representative QM regions with varying sizes are shown using a surface representation (for clarity, MM waters not shown).

We also aim to develop new models for effective treatment of charge transfer in complex environments. We have been working on devising a reliable yet computationally efficient protocol to assign partial atomic charges of water molecules in condensed phases based on quantum chemistry calculations. We have assessed the effects of density functional, basis set, and population analysis methods against higher levels of theory (e.g., CCSD) and available experimental data (e.g., dipole moment) for isolated water and liquid water. The convergence of the atomic charges in liquid water with the size of explicit quantum-mechanical (QM) region is also scrutinized. Figure 2 shows some preliminary results using the ωB97XD/cc-pVDZ model chemistry and atomic-dipole-corrected Hirschfeld population analysis method. Our preliminary protocol shows relatively fast convergence with QM region size, and moderate sensitivity to local hydrogen bonding environment. We are currently benchmarking our protocol against more calculations, and will apply it to understand charge transfer in liquid water.

In the next year, our team will advance developments in ground and excited electronic structure methods and will pursue improved simulation of two-dimensional electronic spectroscopy.

Grant Number and Title

DE-SC0019053. Improved Methods for Modeling Functional Transition Metal Compounds in Complex Environments: Ground States, Excited States, and Spectroscopies.

Ph.D. Students: Bowan Han and Ali AbouTaka
Postdocs: Bradford Barker and Hector Corzo

Publications

While initial manuscripts are currently in preparation and under review, none have yet appeared in-press.

USING COMPOSITION-CONTROLLED CLUSTER ASSEMBLIES TO DECODE THE SPECTRAL DYNAMICS OF PROTON DEFECTS IN WATER AND LOCAL INTERACTIONS IN TAILORED IONIC LIQUIDS

DE-FG02-00ER15066 and DE-FG02-06ER15800

Program Managers: Dr. Mark Pederson and Dr. Gregory Fiechtner

K. D. Jordan (jordan@pitt.edu), Dept. of Chemistry, University of Pittsburgh, Pittsburgh, PA 15260

M. A. Johnson (mark.johnson@yale.edu), Dept. of Chemistry, Yale University, New Haven, CT 06520

Our joint program exploits size-selected clusters as a medium with which to unravel molecular level pictures of key, often transient species in condensed phase and interfacial chemistry. We have intensely focused our recent efforts to unravel the spectral signatures of excess protons in well-defined water networks and to clarify the role of hydrogen bonding in room temperature ionic liquids (ILs).

I. Capturing intrinsic, site-dependent spectral signatures and lifetimes of isolated OH oscillators in extended water networks

In this thrust for our program, we exploit the unique properties of the extended H-bonded water cages that are created when 20 water molecules are complexed with the hydronium ion (H_3O^+) to reveal the molecular-level mechanics that underlie the diffuse vibrational spectra of interfacial water. These are useful model systems because they allow us to eliminate ultrafast spectral diffusion arising from thermal fluctuations in the surrounding network to isolate the relaxation behavior due entirely to vibrationally excited state dynamics. In the past year, we determined the spectral responses of individual, isolated OH groups located at each of the spectroscopically distinct locations in the "magic number" $H_3O^+(H_2O)_{20}$ cluster. This system occurs with a distorted pentagonal dodecahedron (PD) structure, and was chosen for this study because the H_3O^+ ion is accommodated on the surface of the cage, thus providing opportunity to explore the possibility of monitoring the migration of the charge defect at a microscopic surface. Using isotopomer-selective, two color IR-IR photobleaching of cryogenically cooled, mass-selected ions, we determined how the lineshapes of the OH stretching vibrational fundamentals and associated combination band activities depend on their positions in the spectrum. This information was masked in our recent (2019) *Science* paper in which we used another variation of the isotopic dilution and double resonance method to establish the correlation between the frequencies of the two OH oscillators on an intact H_2O molecule embedded in the otherwise perdeuteratred water cage around Cs^+. Here we report a surprisingly simple trend in the linewidths displayed by isolated OH oscillators (decoupled by insertion of one HDO molecule into the heavy water cages) in both Cs^+ and H_3O^+ cluster systems in which the bell shaped, homogeneous band contours systematically broaden with increasing red-shift, thus

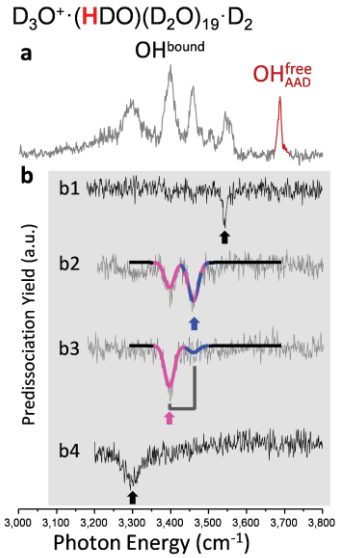

Fig. 1. Application of isotopomer-selective, IR-IR double resonance spectroscopy to the $D_3O^+\cdot(HDO)(D_2O)_{19}\cdot D_2$ cluster identify the linewidths and multiplet structures derived from the excitation of single, isolated OH oscillators in the distorted pentagonal dodecahedron structure.

revealing intrinsic relaxation times on the order of 75 fs for the most red shifted bands. We also report a fascinating observation that OH oscillators in both systems that reside near the center of the diffuse OH stretching envelope do not appear as isolated features. In contrast to the universally accepted ansatz used in simulations of water spectra, the OH fundamentals occur with a weaker combination band above them associated with excitation of a soft mode of the cage. The fact that these dynamics are in play at very low temperature suggests that the underlying mechanics are driven by vibrational zero-point displacements. The manuscript describing these results has been provisionally accepted for publication in *Nature Chemistry* (ref. 3).

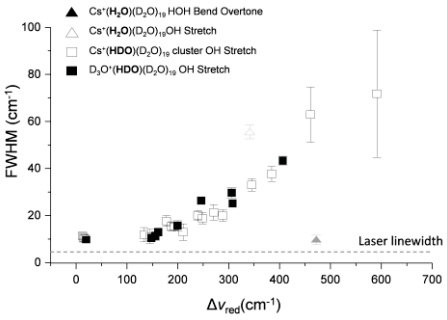

Fig. 2. Dependence of experimental linewidths of OH stretch features on the red shift of the OH frequency from the gas phase, uncoupled free OH stretch value at 3607 cm^{-1}.

We are presently extending the double resonance experiments to elevated temperatures in order to measure the onset of the migration of the proton defect on the surface of the $H^+(H_2O)_{21}$ cage. We are accomplishing this by tracking time evolution of the OH features associated with specific $H^+(D_2O)_{21}$ isotopomers. Interpretation of these results requires an intense theoretical analysis to reveal the character of the low energy region of the potential energy surface describing this motion. Although there is consensus that the charge defect lies on the surface, there has not been a detailed analysis of the H-bonding arrangements of the various low-energy isomers of this cluster, and little is known about the pathways for interconverting the low-energy isomers. The Jordan group has therefore developed strategies for generating various H-bonding arrangements of PD $H^+(H_2O)_{21}$ and have optimized the resulting structures at the B3LYP+D3/6-311+G(2d,p) with subsequent refinement at the at the DF-MP2/aug-cc-pVTZ level of theory. In addition, pathways for interconversion of the low energy isomers and their isotopomers have been mapped out with the same approach. In the process of this work we identified nine low-energy classes of isomers of $H^+(H_2O)_{21}$ based on the PD structured motif. The lowest energy class (I) consists of ten isomers, seven of which had been identified in earlier theoretical studies.* These ten isomers are calculated to lie within 0.2 kcal/mol of one another. Thus, all ten type I isomers would be expected to have significant population in one low-temperature (~20 K) experiments of the Johnson group. Significantly, the ten isomers of class I are found to have nearly identical vibrational spectra in the harmonic approximation.

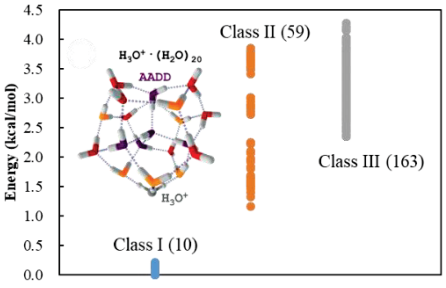

Fig. 3. Distribution of energies of the isomers in the three lowest energy classes of isomers of $H^+(H_2O)_{21}$ obtained from B3LYP+D3/6-311+G(2d,p) level of theory. The number of isomers in each class is indicated in parentheses.

The isomers in the other classes are calculated to lie at 1.0 kcal/mol or more above the class I isomers, and thus are not expected to have significant population at low temperature (i.e., ~20 K)) experiments. We find that the pathways connecting the various type I isomers involve isomers from the higher energy classes as intermediates, with the overall activation energies being 6 kcal/mol or more. While these barriers are surmountable with the amount of energy associated with OH stretch vibrational excitation (with energies greater than ~3000 cm^{-1}), energy randomization from IVR is likely to be sufficiently fast that such excitation is unlikely to lead to interconversion of type I isomers on the time scale of the experiment. On the other hand, the barriers to go from the type I to the type II isomers are calculated to be as low as 2.4 kcal/mol. (after inclusion of vibrational ZPE), leading us to conclude that I → II

isomerization could occur upon OH stretch excitation of the cold $H^+(H_2O)_{21}$ cluster.

II. Spectroscopic assessment of intra- and intermolecular hydrogen bonding in functionalized ionic liquids

A second thrust for our efforts is the elucidation of the local interactions that underlie macroscopic behavior of room temperature ionic liquids (ILs). In a collaboration with CPIMS colleagues at Brookhaven National Lab (led by James Wishart), we have an ongoing program to address the observation that the replacement of alkyl substituents on IL cations with ether-functionalized ones dramatically reduces their viscosity, thereby improving the transport properties for important applications. Theoretical simulations revealed that the positions and numbers of ether oxygens in the chain should have profound effects on the intra- and intermolecular hydrogen bonding patterns that control molecular-scale and bulk transport properties. This scenario thus provided an excellent opportunity to explore the local hydrogen-bonding interactions in these systems through direct analysis of the vibrational spectra obtained using cryogenic ion spectroscopy. In our first study, reported in ref. 2, we established the affinities of the ether groups for various binding sites of the imidazolium ring in the isolated cations, and in ternary assemblies with the BF_4^- anion where the ethers must compete with the anion for binding sites. These microscopic observations support the inferences drawn from simulations about the effects of ether chain structure on intra- and intermolecular H-bonding patterns in the ionic liquid phase. It is important to note that this joint effort was initiated by the Wishart team precisely because this information was not available from any other experimental approach.

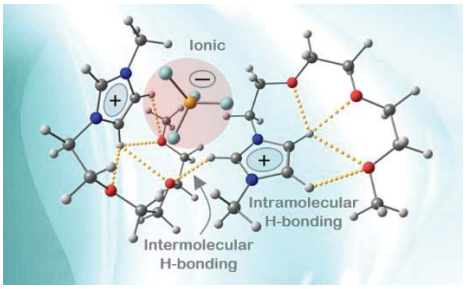

Fig. 4. Lowest energy calculated isomer of the ether-functionalized IL ternary ion complexes with two cations and one BF_4^- anion.

We look forward to next study the ternary clusters with a series of different anions (X^- = NTf_2^-, BF_4^- and I^-) and monitoring the strengths of H-bonding to the imidazolium ring sites. The methylated-$C_{(2)}$ derivatives of these ether cations is another point of interest, since they could potentially encourage interactions involving the weaker binding sites of the imidazolium ring.

Another class of ILs that we are also working on is the hydroxy-functionalized ILs with Ralf Ludwig (U. of Rostock). In those studies, we demonstrated that cooperative H-bonding between the OH groups leads to direct contacts between the nominally repulsive cations. This was accomplished by resolving the isomer-selective spectra of ternary cationic clusters (ref. 9) as well as the observation of the telltale red shifts arising from the cyclic homodromic OH···OH···OH···X^- motif in a quinary cation cluster (ref. 7). Furthermore, incorporation of neutral molecular mimics of the cation to the IL led to the formation of stable positively charged cyclic structures, which was reported in ref. 6. Our next manuscript (ref. 12) addresses the propensity to form such cooperative H-bonding interactions by extension of the hydroxyalkyl chain of the cations.

V. Plans for the next year

Over the past year, the groundwork has been laid for our long-standing goal of monitoring the pathways for proton translocation though a water network, with our first experimental paper from Yale describing the spectra of single OH oscillators just provisionally accepted for publication in *Nature Chemistry*. We next plan to merge this experimental effort with the theoretical predictions by the Jordan group, and follow the temperature-dependent onset for site-to-site migration of a proton defect in size-selected water cages. At the same time, we will be expanding the part of our program aimed at understanding the molecular level interactions at play in functionalized, room temperature ionic liquids, which is an on-going collaboration with CPIMS colleague James Wishart. Of particular interest in this area will be to address how trace water is incorporated in the otherwise ionic assemblies, and quantify the degradation pathways leading to chemical activation of these solvents.

VI. Papers in the past two years under this grant:

1. **"Disentangling the Complex Vibrational Mechanics of the Protonated Water Trimer by Rational Control of Its Hydrogen Bonds"**, C. H. Duong, N. Yang, M. A. Johnson, R. J. DiRisio, A. B. McCoy, Q. Yu, and J. M. Bowman, *J. Phys. Chem. A*, **123**, 7965-7972, (2019).
2. **"Spectroscopic Assessment of Intra- and Intermolecular Hydrogen Bonding in Ether-Functionalized Imidazolium Ionic Liquids"**, H. J. Zeng, M. A. Johnson, J. D. Ramdihal, R. A. Sumner, C. Rodriguez, S. I. Lall-Ramnarine, and J. F. Wishart, *J. Phys. Chem. A*, ASAP (As Soon As Publishable), (2019).
3. **"Capturing the Intrinsic, Site-Dependent Spectral Signatures and Lifetimes of Isolated OH Oscillators Embedded in an Extended Water Network at 20 K"**, N. Yang, C. H. Duong, P. J. Kelleher, and M. A. Johnson, *Nature Chem.*, *Provisionally accepted, Sept. 26,* (2019).
4. **"Molecular-Level Origin of the Carboxylate Head Group Response to Divalent Metal Ion Complexation at the Air-Water Interface"**, J. K. Denton, P. J. Kelleher, M. A. Johnson, M. D. Baer, S. M. Kathmann, C. J. Mundy, B. A. Wellen Rudd, H. C. Allen, T. Choi, and K. D. Jordan, *Proc. Natl. Acad. Sci. U. S. A.*, **116**, 14874-14880, (2019).
5. **"One-Dimensional Adiabatic Model Approach for Calculating Progressions in Vibrational Spectra of Ion–Water Complexes"**, B. V. Henderson and K. D. Jordan, *J. Phys. Chem. A*, **123**, 7042-7050, (2019).
6. **"Cooperatively Enhanced Hydrogen Bonds in Ionic Liquids: Closing the Loop with Molecular Mimics of Hydroxy-Functionalized Cations"**, T. Niemann, A. Strate, R. Ludwig, H. J. Zeng, F. S. Menges, and M. A. Johnson, *Phys. Chem. Chem. Phys.*, **21**, 18092-18098, (2019).
7. **"Spectroscopic Evidence for an Attractive Cation–Cation Interaction in Hydroxy-Functionalized Ionic Liquids: A Hydrogen-Bonded Chain-Like Trimer"**, T. Niemann, A. Strate, R. Ludwig, H. J. Zeng, F. S. Menges, and M. A. Johnson, *Angew. Chem., Int. Ed.*, **57**, 15364 (2018).
8. **"Tag-Free and Isotopomer-Selective Vibrational Spectroscopy of the Cryogenically Cooled $H_9O_4^+$ Cation with Two-Color, IR-IR Double-Resonance Photoexcitation: Isolating the Spectral Signature of a Single OH Group in the Hydronium Ion Core"**, C. H. Duong, N. Yang, P. J. Kelleher, M. A. Johnson, R. J. DiRisio, A. B. McCoy, Q. Yu, J. M. Bowman, B. V. Henderson, and K. D. Jordan, *J. Phys. Chem. A*, **122**, 9275-9284, (2018).
9. **"Structural Motifs in Cold Ternary Ion Complexes of Hydroxyl-Functionalized Ionic Liquids: Isolating the Role of Cation-Cation Interactions"**, F. S. Menges, H. J. Zeng, P. J. Kelleher, O. Gorlova, M. A. Johnson, T. Niemann, A. Strate, and R. Ludwig, *J. Phys. Chem. Lett.*, **9**, 2979 (2018).
10. **"Communication: Spectroscopic Characterization of a Strongly Interacting $C_{(2)}H$ Group on the $EMIM^+$ Cation in the $(EMIM^+)_2X^-$ (X = BF_4, Cl, Br, and I) Ternary Building Blocks of Ionic Liquids"**, O. Gorlova, S. M. Craig, and M. A. Johnson, *J. Chem. Phys.*, **147**, 231101, (2017).
11. **"Disentangling the Complex Vibrational Spectrum of the Protonated Water Trimer, $H^+(H_2O)_3$, with Two-Color IR-IR Photodissociation of the Bare Ion and Anharmonic VSCF/VCI Theory"**, C. H. Duong, O. Gorlova, N. Yang, P. J. Kelleher, M. A. Johnson, A. B. McCoy, Q. Yu, and J. M. Bowman, *J. Phys. Chem. Lett.*, **8**, 3782-3789, (2017).

In preparation

12. **"Chain Length Dependence of Hydrogen Bond Linkages between Cationic Constituents in Hydroxy-Functionalized Ionic Liquids: Tracking Bulk Behavior to the Molecular Level with Cold Cluster Ion Spectroscopy"**, H. J. Zeng, F. S. Menges, T. Niemann, A. Strate, R. Ludwig, and M. A. Johnson, (2019).
13. **"Bend-Stretch Combination Band of the 'Magic' Number $H_3O^+(H_2O)_{20}$ Cluster in Near IR as a Site-Specific Population Probing Tool"**, N. Yang, C. H. Duong, A. B. McCoy, and M. A. Johnson, (2019).

Nucleation Chemical Physics

Shawn M. Kathmann
Physical Sciences Division
Pacific Northwest National Laboratory
902 Battelle Blvd.
Mail Stop K1-83
Richland, WA 99352
shawn.kathmann@pnl.gov

Program Scope

The objective of this work is to develop an understanding of the chemical physics governing nucleation. The thermodynamics and kinetics of the embryos of the nucleating phase are important because they have a strong dependence on size, shape and composition and differ significantly from bulk or isolated molecules. The technological need in these areas is to control chemical transformations to produce specific atomic or molecular nanoparticles with specific properties. Computing reaction barriers and understanding condensed phase mechanisms is much more complicated than those in the gas phase because the reactants are surrounded by solvent molecules and the configurations, energy flow, quantum and classical electric fields and potentials, and ground and excited state electronic structure of the entire statistical assembly must be considered.

Recent Progress and Future Directions

Voltage and Field Fluctuations as Crystallization Order Parameters

The observations of luminescence during crystallization as well as electric field induced crystallization suggest that the process of crystallization may not be purely classical but also involves an essential electronic structure component. Strong electric field and/or voltage fluctuations may play an important role in this process by providing the necessary driving force for the observed electronic structure changes. The importance of electric field fluctuations driving electron transfer has been a topic of intense research since the seminal work of Marcus. The main objective of this work is to provide basic understanding of the fluctuations in charge, electric potentials, and electric fields, both classically and quantum mechanically, for concentrated aqueous NaCl electrolytes.

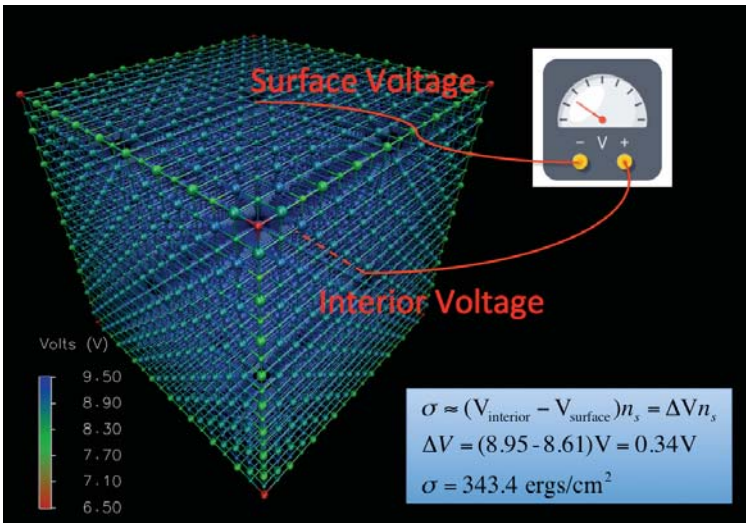

Figure 1. Interfacial surface energy of NaCl (18^3) crystal derived from difference in interior and surface voltages. Interfacial water will lower ΔV to 0.071V yielding an aqueous interfacial surface energy of σ = 67.5 ergs/cm^2.

The stability of each ion in a finite cluster depends upon the Madelung voltages of the individual ions, each sensitive to its own crystalline or amorphous environment – see Figure 1, 2 and 4. As the salt clusters approach their ultimate crystal cubic symmetry, they may pass through various non-cubic distorted or amorphous configurations, including the presence of trapped water molecules. Since a unique Madelung potential exists for each stable crystalline polymorph, then the Madelung voltages for each ion

within a salt cluster may be used as an order parameter (in addition to other order parameters e.g., the distance between ions, the angle between ion triplets, and electric fields at the ion sites) characterizing their progress along various nucleation pathways leading to those polymorphs. Interfacial surface energies can be obtained from differences between interior and surface voltages, including the influence of interfacial water – see Figure 1. Figure 2 shows the progression of Madelung voltages experienced by Na^+ and Cl^- ions due to all other charges within the cubic nanocrystals in a vacuum – large potentials are more stable. By the symmetry of perfect NaCl crystals, the potentials for the Na^+ ions are equal and opposite to Cl^- ions such that the magnitude of both potentials coincide. Conveniently, the size dependent potentials and fields (to be discussed later) can be split into subgroups corresponding to their location in the crystal: interior (*i*), faces (*f*), edges (*e*), and corners (*c*).

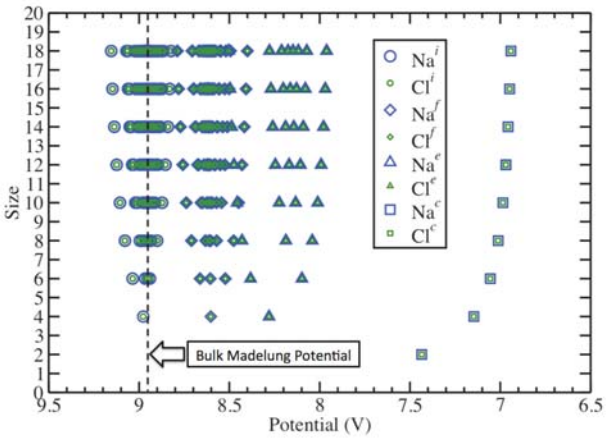

Figure 2. Madelung potentials experienced by ions (Na^+ = blue symbols, Cl^- = green symbols) within even-sized NaCl nanocrystals (# of ions = $Size^3$) showing how the electric properties vary with size and subgroup (*i*, *f*, *e*, *c*). Lattice ion-ion distance is 2.81Å.

Our previous classical molecular dynamics studies of concentrated aqueous NaCl electrolytes showed that the distribution of voltages for all the ions in the solution, including those ions trapped within salt clusters, spanned a broad range that included the bulk Madelung voltages (±8.95V for ion charges of ±1.0e). But, in that study we did not separate the voltage distributions between solvated ions and those

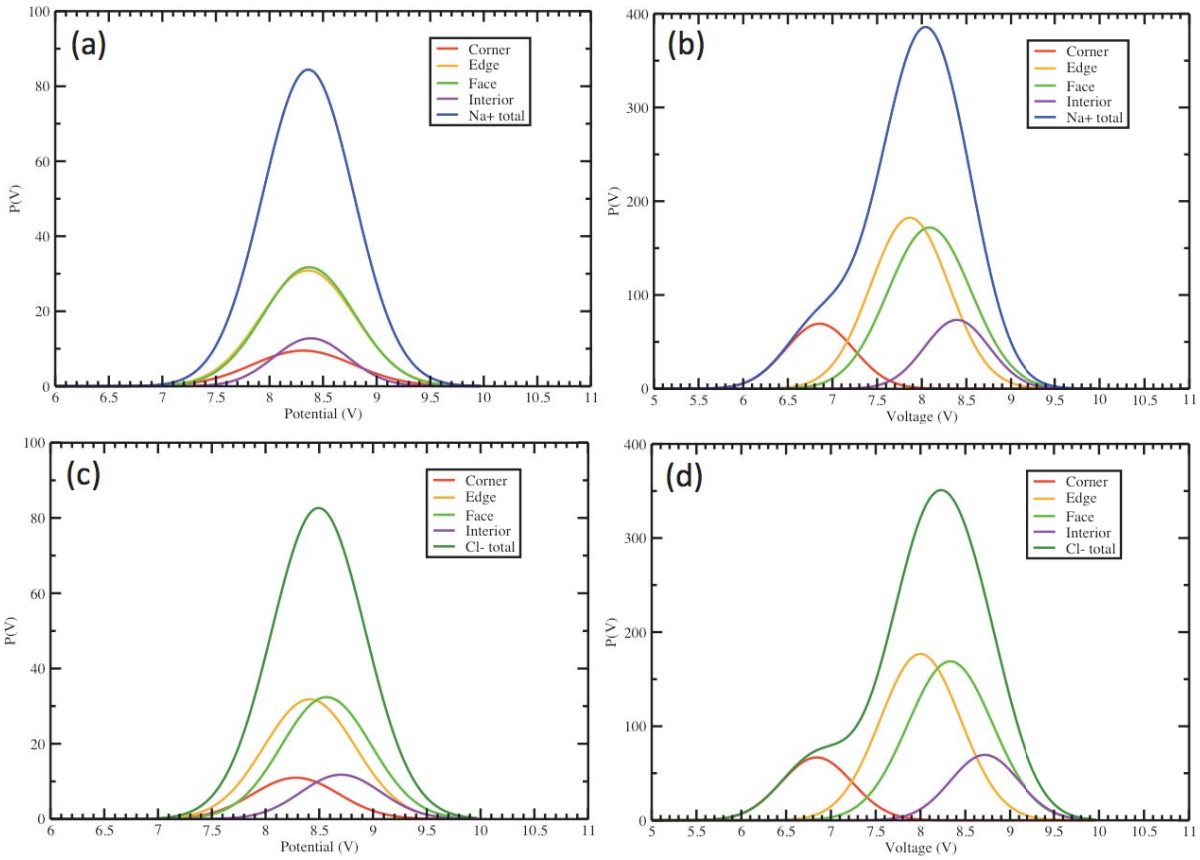

Figure 3. Madelung potentials experienced by ions (Na^+ = blue, Cl^- = green) in a 4^3 NaCl nanocrystal with [Na^+(a) and Cl^-(c)] and without [Na^+(b) and Cl^-(d)] the influence of the water. The voltage axis is inverted w.r.t. Figure 2.

ions involved in salt clusters. Here we present our results showing how the Madelung voltages are modified for a 4^3 crystal in water taken from a ns trajectory at 300K using the SD + SPC/E interactions. Figure 3 shows the distribution of potentials for Na^+ and Cl^- in water. From these voltage differences we find an aqueous interfacial surface energy of σ = 67.5 ergs/cm^2 including water and an interfacial surface energy of σ = 329.3 ergs/cm^2 without the influence of water. Both of these surface energies compare very well with published simulation and experimental values. Here the water plays a key role in lowering the interfacial surface energy by increasing the voltages on the ions on the crystal faces by 0.35V.

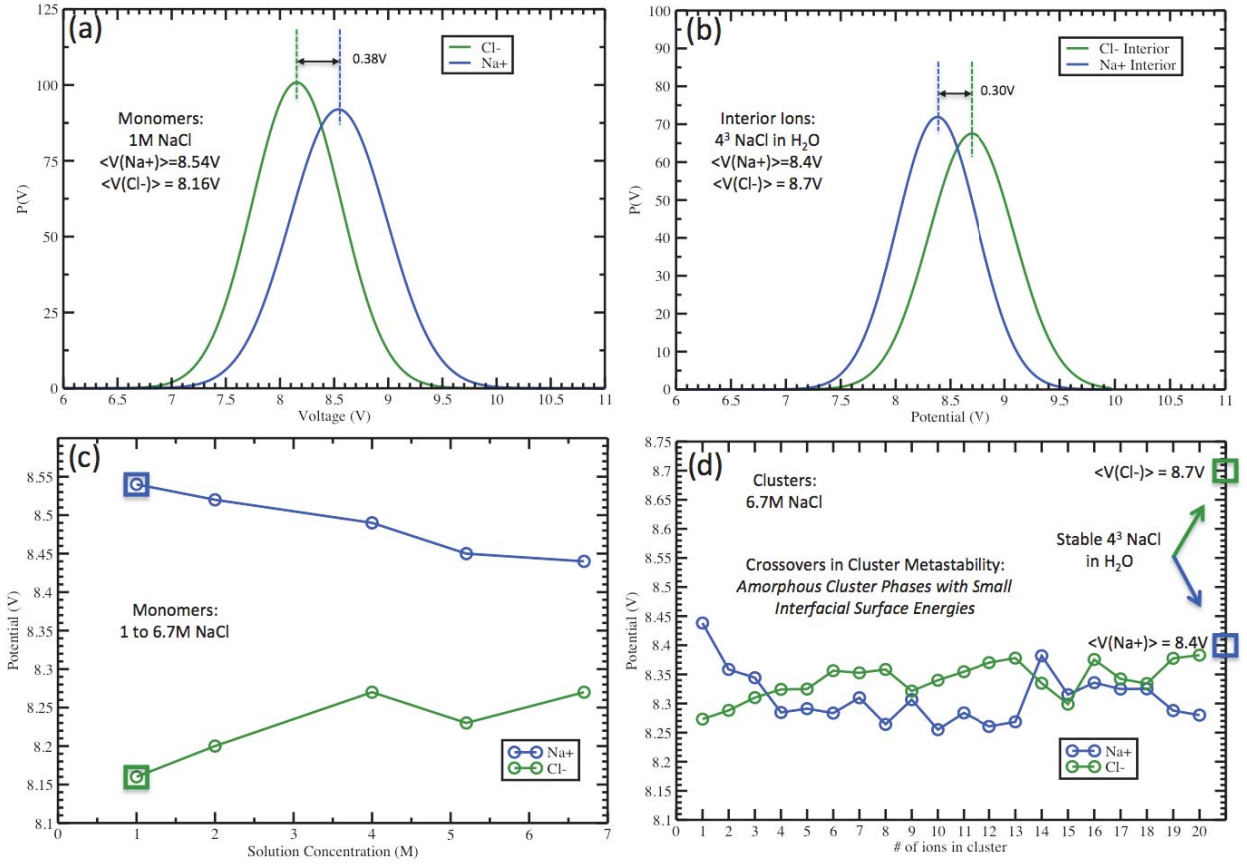

Figure 4. Madelung potentials experienced by ions (Na^+ = blue, Cl^- = green): (a) monomer ions in a 1M NaCl, (b) Interior ions in a 4^3 NaCl nanocrystal in water, (c) monomer ion voltage concentration dependence, and (d) ions in metastable clusters in 6.7M NaCl showing crossover effects compared to a stable 4^3 NaCl nanocrystal in water.

An order parameter, or cluster definition, provides a low-dimensional means of understanding the mechanism of crystallization while differentiating between various amorphous or crystalline pre-critical clusters leading to different nucleation pathways. Furthermore, we anticipate that these order parameters are very sensitive indicators of the structure of salt clusters underlying crystallization.

There is increasing evidence from both simulation and experiment that nanoscale amorphous complexes and phases may play important roles in crystallization. In Figure 4 (a)-(d) we present how the Madelung voltages provide key insights into the metastable pathways leading to crystallization. Fig. 4a shows the voltage distributions for the Na+ and Cl- ions in 1M NaCl showing that Na^+ lies at a higher voltage than Cl^- by 0.38V → 8.74 kcal/mol. Fig. 4b shows that, in contrast, in a 4^3 NaCl nanocrystal in water the Na^+ lies at a lower voltage than Cl^- by -0.30V → -6.9 kcal/mol. Thus, at some intermediate point(s) the voltages experienced by the Na^+ and Cl^- ions must crossover each other. That the ions tend to do so can already be seen in the monomer ions as a function of solution concentration shown in Fig. 4c.

Figure 4d shows the voltages experienced by Na^+ and Cl^- within the clusters in 6.7M NaCl. Clearly, one can see several voltage crossovers as a function of the # of ions in the clusters compared to the voltages experienced by Na^+ and Cl^- ions in the interior of a stable 4^3 NaCl nanocrystal in water. Here, we define clusters to be those ions within a distance of 3.5Å (i.e., within the 1st peak of the Na-Cl radial distribution function determined from the simulated aqueous electrolytes). Thus, (1) as a function of concentration the ion monomers of Na^+ tend to lower voltages and Cl^- to higher voltages with the Na+ remaining at a higher voltage than Cl^-, (2) they crossover each other as a function of cluster size, and (3) they finally switch with the Cl^- at a higher voltage than Na^+ in the 4^3 NaCl crystal. A similar crossover between the Na^+ and Cl^- ions is seen in the electric field distributions where Na^+ monomer ions experience stronger fields than Cl^- ions in 1M NaCl by about 0.1 V/Å whereas in the 4^3 NaCl nanocrystal in water the Cl^- ions experiences a greater field by about 0.1 V/Å.

Our calculations and analyses provide the first steps toward understanding the magnitude and fluctuations of charge, electric potentials and fields in aqueous electrolytes and what role these fields may play in driving charge redistribution/transfer during crystallization as well as inducing crystal formation itself. Using the Madelung potential and its deviations provide a convenient order parameter to explore various pre-critical amorphous salt clusters and the pathways they take to their ultimate crystalline polymorphs. Moreover, we can use the differences in voltages experienced by the ions in the clusters to quantify the interfacial surface energies to connect with continuum approaches like classical nucleation theory as well as the statistical mechanical formulation of cluster free energies and distribution functions.

It still remains an outstanding challenge to directly connect simulation and experiment. No experiment to date has directly measured the production of critical clusters to yield a true nucleation rate. The particle size distributions relevant to the nucleation event, i.e., those critical clusters being produced as they come over the top of the nucleation barrier, from simulation still remain out of experimental reach. These freshly nucleated particles still need to undergo growth and coagulation to reach the length and times scales probed by conventional laboratory methods. Simulating these processes atomistically quickly becomes computationally intractable. Instead, it is possible to take the particle size distributions relevant to nucleation and model the combined nucleation, growth and coagulation processes through the general dynamic equation. This allows simulators to reach the length and time scales relevant to Small Angle X-ray Scattering (SAXS). On the experimental SAXS side, getting particle size distributions as a function of time suffers from the inverse scattering problem. Current DOE synchrotron X-ray beams as well as the new free electron laser sources of X-rays may be the only way to achieve consistency between measurement and theory of crystallization in condensed phase chemical physics.

Direct PNNL collaborators on this project include G.K. Schenter, C.J. Mundy, S.S. Xantheas, M. Valiev, X. Wang, J. Fulton, L. Dang, and M. Baer and current postdoctoral fellow Evgenii Fetisov. Outside collaborations with Kristian Molhave at the Technical University of Denmark on the connections between electron holography and voltages inside and at the interface of liquid water, Mark Johnson at Yale on connections between electric fields and vibrational spectroscopy have been beneficial.

Acknowledgement: This research was performed in part using the DOE NERSC facility. Battelle operates PNNL for DOE.

Publications of DOE Sponsored Research (2016-present)

C.T. Wolke, J.A. Fournier, E. Miliordos, **S.M. Kathmann**, S.S. Xantheas, and M.A. Johnson, "Isotopomer-selective spectra of a single intact H_2O molecule in the $Cs^+(D_2O)_5H_2O$ isotopologue: Going beyond pattern recognition to harvest the structural information encoded in vibrational spectra", *Journal of Chemical Physics*, **144**, 074305 (2016).

J.A. Soltis, W.C. Isley III, M. Conroy, **S.M. Kathmann**, E.C. Buck, G.J. Lumetta, "In situ microscopy across scales for the characterization of crystal growth mechanisms: the case of europium oxalate", *CrystEngComm*, **20**, 2822 (2018).

Chemical Kinetics and Dynamics at Interfaces

Structure and Reactivity of Ices, Oxides, and Amorphous Materials

Bruce D. Kay (PI), R. Scott Smith, and Zdenek Dohnálek
Physical Sciences Division
Pacific Northwest National Laboratory
P.O. Box 999, Mail Stop K8-88
Richland, Washington 99352
bruce.kay@pnnl.gov

Collaborators include: G.A. Kimmel, N.G. Petrik, Y. Xu, and C. Yuan

Program Scope

The objective of this program is to examine physiochemical phenomena occurring at the surface and within the bulk of ices, oxides, and amorphous materials. The microscopic details of physisorption, chemisorption, and reactivity of these materials are important to unravel the kinetics and dynamic mechanisms involved in heterogeneous (i.e., gas/liquid) processes. This fundamental research is relevant to solvation and liquid solutions, glasses and deeply supercooled liquids, heterogeneous catalysis, environmental chemistry, and astrochemistry. Our research provides a quantitative understanding of elementary kinetic processes in these complex systems. For example, the reactivity and solvation of polar molecules on ice surfaces play an important role in complicated reaction processes that occur in the environment. These same molecular processes are germane to understanding dissolution, precipitation, and crystallization kinetics in multiphase, multicomponent, complex systems. Amorphous solid water (ASW) is of special importance for many reasons, including the open question over its applicability as a model for liquid water, and fundamental interest in the properties of glassy materials. In addition to the properties of ASW itself, understanding the intermolecular interactions between ASW and an adsorbate is important in such diverse areas as solvation in aqueous solutions, cryobiology, and desorption phenomena in cometary and interstellar ices. Metal oxides are often used as catalysts or as supports for catalysts, making the interaction of adsorbates with their surfaces of much interest. Additionally, oxide interfaces are important in the subsurface environment; specifically, molecular-level interactions at mineral surfaces are responsible for the transport and reactivity of subsurface contaminants. Thus, detailed molecular-level studies are germane to DOE programs in environmental restoration, waste processing, and contaminant fate/transport.

Our approach is to use molecular beams to synthesize “chemically tailored” nanoscale films as model systems to study ices, amorphous materials, supercooled liquids, and metal oxides. In addition to their utility as a synthetic tool, molecular beams are ideally suited for investigating the heterogeneous chemical properties of these novel films. Modulated molecular beam techniques enable us to determine adsorption, diffusion, sequestration, reaction, and desorption kinetics in real-time. In support of the experimental studies, kinetic modeling and simulation techniques are used to analyze and interpret the experimental data.

Recently, in collaboration with Greg Kimmel, we have developed a pulsed laser heating method to investigate deeply supercooled liquids by producing transiently heated films, which

become liquids that last for approximately 10 ns per laser pulse. Subsequent rapid cooling due to the dissipation of the heat pulse into the metal substrate effectively quenches the liquid dynamics until the next laser heating pulse arrives. The rapid heating and cooling allow the system to reach previously unattainable supercooled liquid temperatures and return to the amorphous state before significant crystallization can occur. Recent research in this area has focused on quantifying homogeneous nucleation rates in deeply supercooled liquid water as described in the abstract by Greg Kimmel and in references [1] and [6].

Recent Progress and Future Directions

Desorption Kinetics of Carbon Dioxide from a Graphene-Covered Pt(111) Surface The interaction of carbon dioxide with surfaces has long been of interest in many areas of research, in particular catalysis. More recently, there has been a renewed interest in the interactions of CO_2 with graphene and modified graphene for applications in photocatalysis, adsorbent materials, sensors, and separations. Adsorbate−graphene interactions are also important as models to understand weak molecular interactions and to astrophysicists interested in adsorbate adsorption on astrophysical bodies composed of carbon. In all of the above-mentioned research areas, the geometry of the adsorbate on the surface will affect its interaction energy and possibly its chemical behavior. For example, the adsorbate geometry can affect the electrical response and selectivity of graphene-based sensors. In weakly bound systems small changes in geometry can have large effects on the interaction energies.

In a recent paper [5], we focused on the interactions of CO_2 with a pristine (nonmodified) graphene-covered Pt(111) surface. Molecular beam dosing, temperature-programmed desorption (TPD), and reflection absorption infrared spectroscopy (RAIRS) were employed in the investigation. The TPD technique is used to determine the CO_2 binding energy and RAIRS is used to determine the geometry of CO_2 on the graphene surface. The CO_2 TPD spectra show monolayer and multilayer desorption peaks; however, the multilayer peak is not well-separated from the monolayer peak. The TPD spectra for submonolayer and multilayer coverages align on separate common leading edges. This alignment is a signature of zero-order desorption kinetics. In general, zero-order kinetics indicates that the rate of a given process is independent of the amount of the species of interest. In this case, it means that the desorption rate is independent of the coverage. While it may seem counterintuitive for submonolayer coverages, zero-order kinetics can occur if isolated adsorbates diffusing on the surface interact in equilibrium with two-dimensional islands.

The RAIRS spectra for submonolayer coverages have a relatively sharp peak at ∼2350 cm^{-1}, which is assigned to the ν3 asymmetric stretch. The peak is observed at the onset of CO_2 adsorption, and the area of the peak increases linearly with coverage. This suggests that CO_2 does not lie flat on the surface but instead has a component of its bond axis perpendicular to the graphene surface. For second and multilayer coverages, a second peak is observed that is blue shifted from the monolayer. The appearance of the second infrared peak only after the coverage exceeds 1 ML supports the idea of layer-by-layer growth which is consistent with the TPD filling curves. The

observation of the two separate peaks is consistent with the monolayer interacting with the graphene layer and the second layer interacting with the CO_2 monolayer.

The desorption and infrared results provide a quantitative reference for future theoretical and experimental studies on both pristine and modified graphene surfaces. For theorists these results provide data to benchmark the calculations of weak interactions (CO_2 with graphene) that are important in many areas and are difficult to quantify. For experimentalists these results provide a reference for CO_2 behavior on pristine graphene in order to compare with its behavior on modified graphene surfaces. Future work will focus on quantifying various CO_2 binding energies and structure on other substrates including metals and oxides.

Crystallization growth rates and front propagation in amorphous solid water films

Amorphous solid water (ASW) has been the subject of research for many reasons including its importance in astrophysical environments and its role as a model system in understanding the behavior of supercooled liquid water. In the laboratory, ASW can be created in a vacuum chamber by vapor deposition onto a cold substrate ($T < 130$ K). Metastable ASW films will eventually transform to the lower energy crystalline phase where the kinetics will depend on the temperature. The crystallization kinetics for ASW have been studied by a number of groups using a variety of techniques. In many cases, the crystallization kinetics were used to extract nucleation and growth rates for the formation of crystalline ice (CI) from deeply supercooled liquid water. The extraction of the nucleation and growth rates from the crystallization kinetics requires knowledge of, or an assumption about, the crystallization mechanism. In most of the prior work, a random bulk nucleation mechanism was used in the analysis.

We have previously probed the role of the vacuum interface in ice nucleation by comparing the isothermal crystallization of 1000 ML ASW films with ("capped") and without ("uncapped") a decane layer on top of the film. We found that the crystallization rate for the "uncapped" films was about eight times faster than that for the "capped" films. We also showed that crystallization for "uncapped" films begins at the ASW/vacuum interface. The plausible explanation for more facile surface nucleation is that molecules at the surface are less constrained than those in the bulk and likely have a lower energy barrier for nucleation. A "top-down" crystallization mechanism was proposed in which, once formed, the outer crystalline layer acts as a template that results in a crystallization growth-front that propagates into the bulk.

In some recent work, we measured the growth rate of crystalline ice (CI) in amorphous solid water (ASW) films using reflection absorption infrared spectroscopy [7]. Two different experiments were set up to measure rates of the crystallization front propagation from an underlying crystalline template upward and from the vacuum interface downward. In one set of experiments, layers of ASW (5% D_2O in H_2O) were grown on a CI template and capped with a decane layer. In isothermal experiments from 140 to 150 K, crystallization was observed from the onset (no induction time) and the extent of crystallization increased linearly with time. In a second set of experiments, uncapped ASW films without a CI template were studied. The films were created by placing a 100 ML isotopic layer (5% D_2O in H_2O) at various positions in a 1000 ML

ASW (H_2O) film. The CI growth rates obtained from the two configurations (capped films with a CI template and uncapped films without a CI template) are in quantitative agreement. The results support the idea that for ASW films in a vacuum, a crystalline layer forms at the surface that then acts as a CI template for a growth front that moves downward into the film. The growth rate activation energy of 40 ± 3 kJ/mol is in good agreement with the value of 43 ± 3 kJ/mol obtained from recently published data. These values are lower than many other values in the literature where the crystallization kinetics were measured using the adsorption and desorption of an inert gas on the ASW surface and thus were measuring only the crystallization of the surface layer. The higher growth activation energies could be the result of not accounting for surface nucleation in the analysis of the crystallization kinetics.

The crystalline ice growth rates obtained in this work should be useful in estimating bulk nucleation rates from the crystallization kinetics in capped ASW films. Future work will also explore the role of surface nucleation in the crystallization of other amorphous solids including that of methanol and ethanol.

References to Publications of DOE sponsored Research (October 2017 - present)

1. Xu, YT, NG Petrik, RS Smith, BD Kay, and GA Kimmel, "Homogeneous Nucleation of Ice in Transiently-Heated, Supercooled Liquid Water Films" *Journal of Physical Chemistry Letters* **8**, 5736 (2017).
2. Smith, RS and BD Kay, "Desorption Kinetics of Benzene and Cyclohexane from a Graphene Surface" *Journal of Physical Chemistry B* **122**, 587 (2018).
3. Smith, RS and BD Kay, "Desorption of Benzene, 1,3,5-Trifluorobenzene, and Hexafluorobenzene from a Graphene Surface: The Effect of Lateral Interactions on the Desorption Kinetics" *Journal of Physical Chemistry Letters* **9**, 2632 (2018).
4. Smith, RS, NG Petrik, GA Kimmel, and BD Kay, "Communication: Proton Exchange in Low Temperature Co-Mixed Amorphous H_2O and D_2O Films: The Effect of the Underlying Pt(111) and Graphene Substrates" *The Journal of Chemical Physics* **149**, 081104 (2018).
5. Smith, RS and BD Kay, "Desorption Kinetics of Carbon Dioxide from a Graphene-Covered Pt(111) Surface" *J Phys Chem A* **123**, 3248 (2019).
6. Kimmel, GA, YT Xu, A Brumberg, NG Petrik, RS Smith, and BD Kay, "Homogeneous Ice Nucleation Rates and Crystallization Kinetics in Transiently-Heated, Supercooled Water Films from 188 K to 230 K" *Journal of Chemical Physics* **150**, 204509 (2019).
7. Smith, RS, CQ Yuan, NG Petrik, GA Kimmel, and BD Kay, "Crystallization Growth Rates and Front Propagation in Amorphous Solid Water Films" *Journal of Chemical Physics* **150**, 214703 (2019).
8. Chen, L, SJ Zhang, RR Persaud, RS Smith, BD Kay, D Dixon, and Z Dohnalek, "Understanding the Binding of Aromatic Hydrocarbons on Rutile TiO_2(110)" *Journal of Physical Chemistry C* **123**, 16766 (2019).

Probing and Controlling Electronic Correlations and Vibronic Coupling During Ultrafast Intramolecular Electron Transfer in Solvated Mixed Valence Complexes

Munira Khalil
Department of Chemistry, University of Washington, Seattle, WA 98195-1700, mkhalil@uw.edu
Niranjan Govind
Environmental Molecular Sciences Laboratory, Pacific Northwest National Laboratory, P.O. Box 999, Richland, WA 99352.
Robert W. Schoenlein
Linac Coherent Light Source, SLAC National Accelerator Laboratory, Menlo Park, CA 94025

This is a new award (DE-SC0019277) starting in September 2018 and funded under the solicitation, "Research at the Frontiers of X-ray Free Electron Laser Ultrafast Chemical and Material Sciences (DE-FOA-0001904)." The central goal of this project is to directly visualize and quantify how electronic correlations, vibronic couplings, and local solute-solvent interactions control intramolecular electron motion on the femtosecond time scale. The research program will focus on solvated Ruthenium (Ru) based mixed-valence complexes, a prototypical class of transition-metal complexes, which are of significant interest for their potential applications in photochemical energy conversion. Electron movements following photochemical excitation are closely coupled with atomic/vibrational and solvent motion. To disentangle these various components requires tools designed to directly probe electron correlations and vibronic coupling (coherently coupled motions of electronic and vibrational coordinates) on the timescale of electron motion in the solution phase.

The proposed X-ray absorption, emission and resonant inelastic X-ray scattering (RIXS) spectroscopy experiments will make use of the new technical capabilities of LCLS-II and related upgrades to LCLS, which will provide access to chemical dynamics on the 10s of femtosecond timescale using X-ray pulses in the tender X-ray region (1.5~3 keV) with higher repetition rate and increased spectral stability. The research program will exploit emerging nonlinear X-ray capabilities of XFELs such as stimulated X-ray emission and double-core-hole spectroscopy to achieve new insights into excited-state charge dynamics and correlated phenomena. Along with X-ray experiments, we will utilize new multidimensional vibronic spectroscopies developed by the Khalil group to probe vibronic coupling between the cyanide bridging ligand and the intervalence charge transfer between the Ru sites.

Our ability to extract microscopic details from the X-ray experiments hinges on our ability to simulate the linear and non-linear X-ray signals. This project includes the development of computational tools to simulate spectroscopic observables from non-equilibrium chemical dynamics of transition metal mixed valence systems on photo-excited electronic states accounting for explicit solute-solvent interactions.

The combined experimental and computational studies will produce data which can be used to develop and validate theoretical models that treat coherent electronic and nuclear dynamics on an equal footing to describe non-equilibrium photochemical dynamics in molecular systems. Below we will outline the progress we have made towards the goals outlined above.

- ***Synthesis of Ru complexes.*** We have synthesized a series of Ru dimer and trimer complexes following procedures outlined in the procedures outlined in the literature. These include: (i) $[Ru^{II}(trpy)(bpy)(\mu\text{-}CN)Ru^{II}(bpy)_2CH_3CN](PF6)_3$, referred to as Ru-dimer-ACN, (ii)

$[Ru^{II}(trpy)(bpy)(\mu\text{-}CN)Ru^{II}(bpy)_2Cl]Cl_2$, referred to as Ru-dimer-Cl, and (iii) $[Ru^{II}(DMAP)_4\{(\mu\text{-}CN)Ru^{II}(py)_4Cl\}_2](PF_6)_2$, referred to as Ru-trimer-DMAP, where (py=pyridine and DMAP=4-dimethylaminopyridine).

Transient IR spectroscopy of Ru complexes. The transient IR experiments were performed on Ru dimer samples, dissolved in acetonitrile. The samples were excited with 400 nm excitation and probed in the cyanide stretching region with IR pulses. The instrument time resolution was sub-80 fs. Upon optical excitation in the Ru-dimer-ACN complex, we see a strong transient absorption CN stretching feature, which is 50 cm^{-1} red-shifted from the ground state peak at 2110 cm^{-1}. This absorption feature is the proposed signature of a mixed valence excited state. The experiments find the formation of the state on a 1.2 ps timescale and it has a lifetime greater than 10s of ns. The experiments on the Ru-dimer-Cl complex, also indicated the formation of a mixed valence excited state, but on slower timescale of 6.2 ps. We are currently analyzing the data to understand the differences in the mixed valence excited state formation by careful fitting of the data and performing polarization-selective experiments in the next few months.

Equilibrium X-ray Absorption and X-ray Emission Spectroscopy of Ru complexes at the Ru L-edge. In order to understand the 4*d* electronic configuration in the ground state of the Ru transition metal complexes, we have obtained equilibrium X-ray absorption (XAS), X-ray emission (XES) and RIXS spectra in solution and powder form on a series of Ru(II) and Ru(III) single metal, dimer and trimer complexes. We were awarded a short beamtime in April 2019 at ALS BL 10.3.2 to perform Ru $L_{2,3}$-edge XAS spectra in fluorescence mode probing the $2p \rightarrow 4d$ transitions in $[Ru^{II}Bpy_3]Cl_2$ and Ru-dimer-ACN. The samples were flowed in a 50 μm thick jet and this was the first demonstration of the Ru L-edge XAS in solution at BL 10.3.2 at ALS. We continued with our equilibrium studies at the Ru L_3-edge studies at SSRL Beamline 14 in July 2019. We obtained high S/N XAS spectra in solution of a series of Ru(II) and Ru(III) single metal complexes and the two Ru dimer complexes. We have also obtained non-resonant valence-to-core XES and $L_3L\alpha$ RIXS spectra of a series of Ru(II) and Ru(III) single metal complexes and the two Ru dimer complexes in powder form at SSRL Beamline 6 in June 2019. The valence-to-core (VtC) XES data reports on the $4d \rightarrow 2p$ transitions and help details the local ligand environment around the Ru center. The $L_3L\alpha$ RIXS spectra report on 4*d*-3*d* CT excitations, which are optically inactive. The successful collection of equilibrium Ru XAS and XES spectra will allowed us to validate parameters in the simulation/computational codes for correctly modelling the electronic structure of the solvated Ru(II) and Ru(III) single and multi-metal complexes.

Femtosecond XAS and XES spectroscopy at the Ru L-edge at SwissFEL in July 2019. We successfully competed for beamtime to perform fs X-ray experiments at the Ru L-edge which is in the tender X-ray region. The experiment was conducted at the ESA Prime instrument of the Alvra hutch at SwissFEL from July 21st to July 29th 2019 in 5 (24 hours) shifts total. The samples (RuDimerACN, and RuDimerCl) were dissolved in acetonitrile (~20mM) and flowed through a 50 μm cylindrical liquid jet in a chamber filled with He and at a pressure of 250mBar. Tender X-rays from SwissFEL with pulse durations of <50 fs were focused to ~8x8 μm. Optical pumping was accomplished by ultrafast pulses (<50 fs, ~1 μJ) at 400 nm with a ~ 70 fs (FWHM) focal spot size at the liquid jet. X-ray absorption measurements at the Ru L_3-edge were made in total fluorescence yield (TFY) by scanning the Si (111) monochromator in the 2830-2852eV range and using a Si-PIN diode placed inside the sample chamber. L_α ($3d \rightarrow 2p_{3/2}$) X-ray emission was

collected simultaneously by using a Von Hamos spectrometer. VtC XES ($4d \rightarrow 2p_{3/2}$) was collected in pink beam above the L_3 absorption edge. Data was taken at pump-probe delay times of 600 fs and 10 ps. Kinetic traces at specific energies (resonant with spectral features) were also measured with delays of -5 ps to 25 ps. Preliminary analysis of the data reveals time-resolved changes in the ligand environment following MLCT excitation. We are in the process of analyzing the data to extract signatures of electron delocalization and excited state mixed valency in the Ru complexes.

Nonlinear X-ray Emission Spectroscopy on Transition Metal Complexes: Double Core Hole Valence-to-Core X-ray Emission Spectroscopy. With the help of newly developed x-ray free-electron laser (XFEL) sources, creating double core holes simultaneously at the same or different atomic sites in a molecule has now become possible. Double core hole (DCH) x-ray emission is a new form of X-ray nonlinear spectroscopy, where the absorption of one photon is accompanied by the ejection of two core electrons. In this process the correlation between the two ejected core electrons plays an important role. We have theoretically explored the metal K-edge valence-to-core (VtC) x-ray emission spectroscopy (XES) of metal/metal and metal/ligand double core hole states in a series of 3d transition metal complexes with time-dependent density functional theory. Specifically, we considered mono- and binuclear transition metal model complexes. For the binuclear complexes with metal-metal direct bonds, VtC-XES signals of the metal 1s DCHs at different sites were studied. Mononuclear complexes with different Mn oxidation states (II, III) have been used to investigate the emissions of the metal-1s/ligand-1s DCH states, from which the information about the chemical bonds between the metal center and the coordinating atoms can be revealed. We have compared our simulated DCH VtC-XES signals with conventional single core hole (SCH) XES signals. The energy shifts and intensity changes of the DCH emission lines with respect to the corresponding SCH-XES features are like fingerprints of the coupling between the second core hole and the occupied orbitals around the DCHs that contain important chemical bonding information of the complex. We have demonstrated that DCH XES provides subtle information on the local electronic structure around metal centers in transition metal complexes beyond conventional linear XES. Our predicted changes from calculations between SCH-XES and DCH-XES features should be detectable with modern XFEL sources. We have submitted a paper detailing these results. Further DCH studies are planned on 4d Ru transition metal complexes at the L-edge, where we expect larger shifts.

DOE Supported Publications

1. B. E. V. Kuiken, M. R. Ross, M. L. Strader, A. A. Cordones, H. Cho, J. H. Lee, R. W. Schoenlein, and M. Khalil, "Picosecond sulfur K-edge x-ray absorption spectroscopy with applications to excited state proton transfer", *Structural Dynamics* 4 (2017) 044021.
2. S. Eckert, J. Norell, P. S. Miedema, M. Beye, M. Fondell, W. Quevedo, B. Kennedy, M. Hantschmann, A. Pietzsch, B. E. Van Kuiken, M. Ross, M. P. Minitti, S. P. Moeller, W. F. Schlotter, M. Khalil, M. Odelius, and A. Fohlisch,"Ultrafast independent N-H and N-C bond deformation investigated with resonant inelastic x-ray scattering", *Angew. Chem. Int. Ed.* **56** (2017) 6088-6092.
3. J. D. Gaynor, and M. Khalil, "Signatures of vibronic coupling in two-dimensional electronic-vibrational and vibrational-electronic spectroscopies", *J. Chem. Phys.* **147** (2017) 094202.
4. Y. Zhang, J. R. Rouxel, J. Autschbach, N. Govind, and S. Mukamel, “X-ray circular dichroism signals: a unique probe of local molecular chirality”, *Chemical Science*, **8** (2017) 5969-5978.

5. D. R. Mortensen, G. T. Seidler, J. J. Kas, N. Govind, C. P. Schwartz, S. Pemmaraju, and D. G. Prendergast, "Benchmark results and theoretical treatments for valence-to-core x-ray emission spectroscopy in transition metal compounds", *Phys. Rev. B.* **96** (2017) 125136-125145.
6. K. Henzler, E. O. Fetisov, M. Galib, M. D. Baer, B. A. Legg, C. Borca, J. M. Xto, S. Pin, J. L. Fulton, G. K. Schenter, N. Govind, J. I. Siepmann, C. J. Mundy, T. Huthwelker, J. J. De Yoreo, "Supersaturated calcium carbonate solutions are classical", *Science Advances*, **4** (2018), eaao6283, DOI: 10.1126/sciadv.aao6283
7. M. Ross, A. Andersen, Z. W. Fox, Y. Zhang, K. Hong, J-H. Lee, A. Cordones, A. M. March, G. Doumy, S. H. Southworth, M. A. Marcus, R. W. Schoenlein, S. Mukamel, N. Govind, M. Khalil, "Comprehensive experimental and computational spectroscopic study of hexacyanoferrate complexes in water: from infrared to x-ray wavelengths", *J. Phys. Chem.* B, **122**, (2018) 5075-5086
8. M. Galib, G. K. Schenter, C. J. Mundy, N. Govind, J. L. Fulton, "Unraveling the spectral signatures of solvent ordering in K-edge XANES of aqueous Na^+, *J. Chem. Phys.*, **149**, (2018), 124503.
9. Z. W. Fox, T. J. Blair, R. B. Weakly, T. L. Courtney, and M. Khalil, "Implementation of continuous fast scanning detection in femtosecond Fourier-transform two-dimensional vibrational-electronic spectroscopy to decrease data acquisition time." *Rev. Sci. Instr.* **89**, 113104 (2018).
10. Y. Zhang, U. Bergmann, R. Schoenlein, M. Khalil, N. Govind, "Double Core Hole Valence-to-Core X-ray Emission Spectroscopy: A Theoretical Exploration Using Time-Dependent Density Functional Theory." *J. Chem. Phys*, accepted for publication (2019)

Chemical Kinetics and Dynamics at Interfaces

Non-Thermal Reactions at Surfaces and Interfaces

Greg A. Kimmel (PI) and Nikolay G. Petrik

Physical Sciences Division
Pacific Northwest National Laboratory
P.O. Box 999, Mail Stop K8-88
Richland, WA 99352
gregory.kimmel@pnnl.gov

Collaborators include: BD Kay, RS Smith, and Y Xu

Program Scope

The objectives of this program are to investigate 1) thermal and non-thermal reactions at surfaces and interfaces, and 2) the structure of thin adsorbate films and how this influences the thermal and non-thermal chemistry. Energetic processes at surfaces and interfaces are important in fields such as photocatalysis, radiation chemistry, radiation biology, waste processing, and advanced materials synthesis. Low-energy excitations (e.g. excitons, electrons, and holes) frequently play a dominant role in these energetic processes. In photocatalysis, non-thermal reactions are often initiated by holes or (conduction band) electrons produced by the absorption of visible and/or UV photons in the substrate. In addition, the presence of surfaces or interfaces modifies the physics and chemistry compared to what occurs in the bulk.

We use quadrupole mass spectroscopy, infrared reflection-absorption spectroscopy (IRAS), and other ultra-high vacuum (UHV) surface science techniques to investigate thermal, electron-stimulated, and photon-stimulated reactions at surfaces and interfaces, in nanoscale materials, and in thin molecular solids. Since the structure of water near interface plays a crucial role in the thermal and non-thermal chemistry occurring there, a significant component of our work involves investigating the structure of aqueous interfaces. A key element of our approach is the use of well-characterized model systems to unravel the complex non-thermal chemistry occurring at surfaces and interfaces. This work addresses several important issues, including understanding how the various types of low-energy excitations initiate reactions at interfaces, the relationship between the water structure near an interface and the non-thermal reactions, energy transfer at surfaces and interfaces, and new reaction pathways at surfaces.

In collaboration with Bruce Kay and Scott Smith, we have developed a pulsed laser heating method that allows us to investigate deeply supercooled liquids by transiently heating nanoscale films. Heating transforms the films from amorphous solids to liquids that last for approximately 10 ns per laser pulse. Subsequent rapid cooling due to the dissipation of the heat pulse into a metal substrate effectively quenches the liquid dynamics until the next laser heating pulse arrives. The rapid heating and cooling allows the system to reach previously unattainable supercooled liquid temperatures and return to the amorphous state before significant crystallization can occur.

Recent Progress

Homogeneous Nucleation of Ice in Transiently-Heated, Supercooled Liquid Water Films

Ice nucleation in supercooled liquid water is one of the most common and important processes occurring on Earth. However, our understanding of fundamental aspects of ice nucleation, such as the maximum rate of nucleation, the temperature at which this maximum occurs, and the size and initial morphology of the ice nuclei, is still incomplete. Developing a detailed understanding of ice nucleation is impeded by the existence of "no man's land," the temperature range from approximately 160 to 230 K in which spontaneous

crystallization occurs too fast for most experimental techniques to observe. It is also challenging for molecular dynamics simulations to study ice nucleation due to the low probabilities for forming ice nuclei and the large number of possible molecular configurations.

In collaboration with Bruce Kay and Scott Smith, we recently used our pulsed heating technique to investigate the nucleation and growth of crystalline ice in transiently heated water films in nanoscale water films for 188 K < T_{max} < 230 K, where T_{max} was the maximum temperature obtained during a heat pulse.[5] The water films, which had thicknesses ranging from approximately 15 – 30 nm, were adsorbed on a Pt(111) single crystal. Because the ice growth rates have been measured independently, the ice nucleation rates could be determined by modeling the observed crystallization kinetics. The experiments show that the nucleation rate maximizes at T = 216 K ± 4 K, and the rate at the maximum is $10^{29\pm1}$ $m^{-3}s^{-1}$. The maximum nucleation rate reported here for flat, thin water films is consistent with recent measurements of the nucleation rate in nanometer-sized water drops at comparable temperatures. However, the nucleation rate drops rapidly at lower temperatures, which is different from the nearly temperature-independent rates observed for the nanometer-sized drops. At T ~ 189 K, the nucleation rate for the current experiments is a factor of ~10^{4-5} smaller than the rate at the maximum. The nucleation rate also decreases for T_{max} > 220 K, but the transiently-heated water films are not very sensitive to the smaller nucleation rates at higher temperatures. The crystallization kinetics were consistent with a "classical" nucleation and growth mechanism indicating that there is an energetic barrier for deeply supercooled water to convert to ice. This work extends our earlier experiments that explored ice nucleation in thicker (0.24 μm) water films.[2] Those experiments were designed to suppress nucleation at the water/metal and water/vacuum interfaces and thus measure the homogeneous nucleation rate for bulk water. We found that homogeneous nucleation rates of at least 10^{26} $m^{-3}s^{-1}$, and most likely ~$10^{29\pm2}$ m^{-3} s^{-1}, were needed to account for our observations. Future work will explore the structural transformations of deeply supercooled water prior to crystallization.

Crystallization Growth Rate and Front Propagation in Amorphous Solid Water Films

In collaboration with Bruce Kay and Scott Smith, the growth rate of crystalline ice (CI) in amorphous solid water (ASW) films was investigated using reflection absorption infrared spectroscopy [6]. Two different experiments were set up to measure rates of crystallization front propagation from a crystalline template on the substrate and from the vacuum interface toward the substrate. The CI growth rates obtained from the two configurations are in quantitative agreement. The results support the idea that for ASW films in a vacuum, a crystalline layer forms at the surface that then acts as a CI template for a growth front that moves downward into the film. The growth rate activation energy of 40 ± 3 kJ/mol is in good agreement with the value of 43 ± 3 kJ/mol obtained from recently published data. These values are lower than many other values in the literature where the crystallization kinetics were measured using the adsorption and desorption of an inert gas on the ASW surface and thus were measuring only the crystallization of the surface layer. The higher growth activation energies could be the result of not accounting for surface nucleation in the analysis of the crystallization kinetics.

Proton exchange in low temperature co-mixed amorphous H_2O and D_2O films: The effect of the underlying Pt(111) and graphene substrates

Proton exchange and mobility are of great importance in a wide range of scientific research areas including astrochemistry, biology, and fuel cell technology, to name a few. The transport of H^+ ions through solution, membranes, or ices is a critical step underlying many of these processes. The transport of protons has long been described by a Grotthuss or "structural" diffusion mechanism where a proton is passed between adjacent water molecules in a series of hops. The H/D exchange process is thought to occur via a two-step mechanism which involves a proton transfer (hop) followed by the migration of a Bjerrum L defect (turn).

Bjerrum defects, also known as orientational defects, are the places where the intermolecular hydrogen bonding is "defective", where either a hydrogen atom is missing between oxygens (L defect) or where there are two hydrogens (D defect).

In collaboration with Bruce Kay and Scott Smith, we studied isotopic exchange reactions in mixed D_2O and H_2O amorphous solid water (ASW) films using reflection absorption infrared spectroscopy.[4] Nanoscale films composed of 5% D_2O in H_2O were deposited on Pt(111) and graphene covered Pt(111) substrates. At 130 K, we found that the reaction is strongly dependent on the substrate with the H/D exchange being significantly more rapid on the Pt(111) surface than on graphene. At 140 K, the films eventually crystallized with the final products on the two substrates being primarily HOD on Pt(111) and a mixture of HOD and unreacted D_2O on graphene. The difference in the extent of proton exchange in the co-dosed films could be due to differences in the reactivity of the Pt(111) and graphene surfaces themselves. By pre-dosing H_2 and O_2 on Pt(111), we find that the observed differences in reactivity on the two substrates are likely due to the formation of hydrogen ions at the Pt(111) surface that are not formed on graphene. Once formed the mobile protons move rapidly through the ASW overlayer driving the H/D exchange reaction. Future work will focus on quantifying various aspects of the H/D exchange reaction kinetics and energetics.

References to publications of DOE-sponsored research (October 2017 – present)

[1] Rentao Mu, Arjun Dahal, Zhi-Tao Wang, Zdenek Dohnálek, Greg A. Kimmel, Nikolay G. Petrik, and Igor Lyubinetsky, "Adsorption and Photodesorption of CO from Charged Point-Defects on TiO_2(110)," *J. Phys. Chem. Lett.* **8**, 4565 (2017) (DOI: 10.1021/acs.jpclett.7b02052).

[2] Yuntao Xu, Nikolay G. Petrik, R. Scott Smith, Bruce D. Kay and Greg A. Kimmel, "Homogeneous nucleation of ice in transiently-heated, supercooled liquid water films," *J. Phys. Chem. Lett.* **8**, 5637 (2017), (DOI: 10.1021/acs.jpclett.7b02685).

[3] Nikolay G. Petrik, Rentao Mu, Arjun Dahal, Zhitao Wang, Igor Lyubinetsky and Greg A. Kimmel, "Diffusion and photon stimulated desorption of CO on TiO_2(110)," *J. Phys. Chem (C)*, **122**, 15382 (2018)**,** DOI: 10.1021/acs.jpcc.8b03418).

[4] R. Scott Smith, Nikolay G. Petrik, Greg A. Kimmel, and Bruce D. Kay, "Proton exchange in low temperature co-mixed amorphous H_2O and D_2O films: The effect of the underlying Pt(111) and graphene substrates," *J. Chem. Phys.* **149**, 081104 (2018), (DOI: 10.1063/1.5046530).

[5] Greg A. Kimmel, Yuntao Xu, Alexandra Brumberg, Nikolay G. Petrik, R. Scott Smith, and Bruce D. Kay, "Homogeneous ice nucleation rates and crystallization kinetics in transiently-heated, supercooled water films from 188 K to 230 K," *J. Chem. Phys.* **150**, 204509 (2019). (DOI: 10.1063/1.5100147)

[6] R. Scott Smith, Chunqing Yuan, Nikolay G. Petrik, Greg A. Kimmel, and Bruce D. Kay, "Crystallization Growth Rate and Front Propagation in Amorphous Solid Water Films," *J. Chem. Phys.* **150**, 214703 (2019). (DOI: 10.1063/1.5098481)

2D IR Microscopy—Technology for Visualizing Chemical Dynamics in Heterogeneous Environments

PI: Amber T. Krummel
Colorado State University, 200 W. Lake Street, Fort Collins, CO 80525
amber.krummel@colostate.edu

1. Program Scope

Chemistries crucial for energy technologies including battery technology, fuel cell technology, and enhanced oil recovery take place in heterogeneous environments. Understanding and predicting chemical dynamics, including solute-solvent interactions, adsorption processes, and transport processes, to name a few, requires the ability to probe these events directly and ultimately visualizing these processes via microscopy. The overarching goal of this project is to develop two-dimensional infrared (2D IR) imaging tools to directly probe chemical interactions in heterogeneous environments, with geochemical systems being our primary target in this project. A combination of experiments directed toward technology development, the exploration of fundamental chemical physics of large macrocycles and acidic oils, and culminating with the direct visualization of chemical interactions in model pore structures. This project builds from our expertise in fabricating IR compatible microfluidic structures, in developing a 100 kHz 2D IR spectrometer, and in probing the nanoaggregates of large macrocycles.

The large number of observables offered by 2D IR spectroscopy allows us to disentangle and quantify complex chemical interactions in ways that were not previously feasible. These observables include the direct measurement of the frequency-frequency correlation function, which is a direct measure of the homogeneous and inhomogeneous contributions to the vibrational lifetime; and the peak positions (both diagonal peaks and cross peaks) and intensities, which are a direct measure of molecular structure. Each of these observables can be spatially resolved. Below the progress made towards imaging dynamics with the 2D IR microscope will be discussed. During the past year, we have made significant progress toward investigating mesoscale dynamical behaviors in a model room temperature ionic liquid (RTIL). In addition, we have initiated 2D IR experiments focused on exploring the dynamic behaviors of carbonate mixtures and the solvation of cations by the carbonates. These results will add to our understanding of solvation in geochemical environments and battery technologies.

2. Recent Progress & Current Efforts

In the past 12 months we have completed initial 2D IR microscopy experiments on RTIL microdroplets. The 2D IR imaging experiments and the analysis of the data have revealed the chemical dynamics in the microdroplet changing over several micrometers. Our results open new questions regarding the unique dynamics that may exist in mesostructures of RTILs. In parallel, we have initiated 2D IR experiments to probe the solvation structures of carbonate mixtures. Our initial results reveal dramatic changes in the solvation structures when a fourth component is added to the carbonate mixtures. These results open new questions related to what is the influence of the fourth component and how do these new solvent structures influence the solvation of cations in the mixtures.

We have been able to improve acquisition rates of 2D IR microscopy images by taking full advantage of our 100 kHz mid-IR laser system that drives our 2D IR microscope. Currently we shape mid-IR pulses and detect the mid-IR signal fields at a 100 kHz repetition rate—the current speed limit of shaping and detection technology. In order to maintain these acquisition speeds we have designed a microscope head to utilize the point scanning geometry. The details of our 2D IR microscopy experiments are in a manuscript that has been submitted to the *Journal of Physical Chemistry*. In order to perform 2D IR microscopy, the IR output from the ZGP DFG stage is split into two lines using a $\lambda/2$ waveplate and wire grid polarizer. The polarizer reflects the probe pulse whose polarization is rotated by 90°, creating S-polarization. The P-polarized pump line passes through the polarizer and is sent to a high speed, mid-IR pulse shaper to generate the pump pulse pair with a variable delay at 100 kHz. The pump and probe pulses are recombined using a polarizer that transmits the pump pulses and reflects the probe pulse to create a

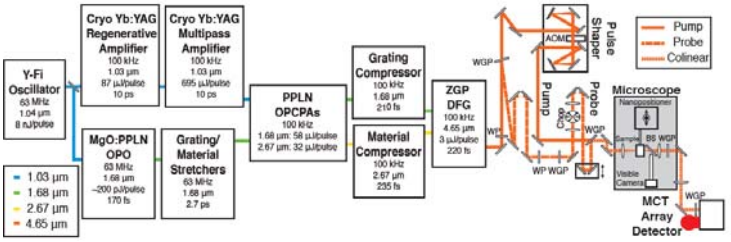

Figure 1. The general layout of 100 kHz mid-IR laser system and 2D IR microscope.

collinear geometry where 2D IR data is collected in the cross polarization (XXYY) configuration. The three pulses are focused into the sample by a Ge/Si achromatic lens and then re-collimated using a Si lens and sent to the detector. The spot size was measured by scanning a 10 µm pinhole in the X and Y direction at the focal plane and recording the integrated intensity. The full width at half maximum (FWHM) beam diameter was measured to be 19.5 µm in the Y direction and 14.2 µm in the X direction. The Rayleigh range of focus in the direction of propagation is approximately 140 µm. The two polarizers before the detector are used to block the pump pulses and transmit the probe and signal. The probe and signal fields are then passed through a monochromator and collected on a 1x64 element, mercury cadmium telluride (MCT) linear array detector operating at the speed limit of detection of 100 kHz. The 2D IR spectra shown in this report were all collected using a series of 510 pump pulse pairs delayed from 0 to 3.57 ps in 7 fs steps. Thus, the spectral resolution along the pump-axis (ω_{pump}) is 4.7 cm^{-1}. Spectra were acquired using a four-step phase cycling scheme with 2000 cm^{-1} rotating frame for background and scatter removal. The full 2D IR microscopy image of the RTIL microdroplet, shown in Figure 2a, is comprised of a data set of 476 2D IR spectra fully averaged 500 times. The pulse energies utilized were 70 nJ/pulse. The image shown in Figure 2a was collected in 120 minutes with an acquisition rate of 1984 individual 2D IR spectra per minute.

The RTIL microdroplet was produced by drop casting the RTIL in silicon oil. The droplets consisted of 1-ethyl-3-methylimidazolium tetrafluoroborate ($EmimBF_4$) and 1-ethyl-3-methylimidazolium tricyanomethanide (EmimTCM) RTILs. The EmimTCM is doped into the $EmimBF_4$ in a 1:500 volume ratio where TCM^- acts as a vibrational probe. A roughly spherical droplet is formed when a very small amount of RTIL (10-20 nL) is cast in silicon oil. The droplet becomes a pancake in shape when placed in between two CaF_2 substrates with a 100 µm spacer to set the sample thickness. The oil is used for stabilization of the RTIL microdroplet as well as removing scatter from the interface because the refractive index of the silicon oil is similar to the RTIL microdroplet. The chemical map generated by integrating the peak associated with the v=1→2 transition in the 2D IR spectra demonstrates that the TCM^- probe is evenly distributed across the microdroplet.

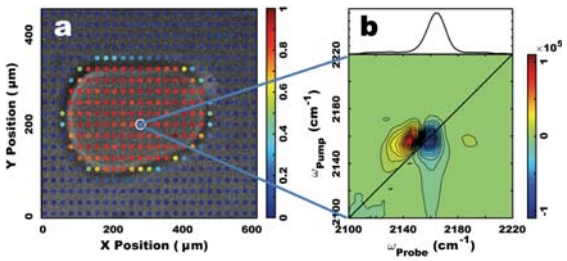

Figure 2. 2D IR image of the RTIL microdroplet (a). A representative 2D IR spectrum of TCM^- in the $Emim/BF_4$ RTIL. The chemical map is generated from integrating the intensity of the v=1→2 transition on the diagonal of the 2D IR spectrum collected at each point.

Using both the time and spatial resolution of 2D IR microscopy, dynamics information of different solvation regions across the microdroplet can be examined. In these experiments, the time delay (T_w) between the second and third pulses is varied and the solvent environment is allowed to evolve after pumping the system. A 2D IR microscopy experiment aimed at extracting the vibrational dynamics of the TCM^- probe was performed over a region of interest (ROI) of the RTIL microdroplet, where at each point 2D IR data were collected as a function of increasing T_w.

We performed nodal line slope analysis of the collected 2D IR spectra to characterize the spectral diffusion dynamics of TCM^- in an RTIL microdroplet. Spectral diffusion dynamics present some parameters, such as correlation times and the fluctuation amplitudes of the frequency fluctuation correlation functions (FFCFs). In Figure 3, the ROI selected is indicated with the white box and the nodal line slope values are plotted as a function of T_w, thus depicting the vibrational dynamics from interfacial and bulk environments within the ROI. It can be seen in Figure 3 that the decay curves at

bulk and interfacial regions are significantly different; the 95% confidence intervals for the bulk and interfacial regions are indicated by the gray shadow. In addition, NLS decays at intermediate regions exhibit a combined behavior of the bulk and the interface, but are not included in this plot for clarity. The decays were fit to a biexponential function following the model,

$$C(T_W) = a_1 exp(-T_W/\tau_1) + a_2 exp(-T_W/\tau_2) + b$$

The biexponential fit of the bulk region gives a τ_1 of 810 ± 100 fs and a τ_2 of 5.2 ± 1 ps. In contrast, the interface region produces a τ_1 of 210 ± 50 fs and a τ_2 of 2.8 ± 0.25 ps. Therefore, the time components indicate that the dynamics of spectral diffusion is markedly different at the interface than at the bulk environments within the RTIL microdroplets. The data representative of the intermediate regions were collected across the ROI in 2 μm steps from the interface, inside the microdroplet. The intermediate regions exhibit a combination of bulk and interfacial behaviors. For example, one such data set collected at 5 μm to the interior of the RTIL droplet produces a τ_1 of 650 ± 100 fs and a τ_2 of 5.0 ± 0.6 ps. Using the NLS curves, we can produce spatial models to describe how the dynamics might be evolving as the microdroplet is traversed.

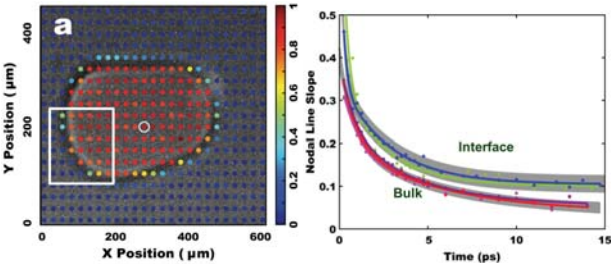

Figure 3. The ROI is indicated by the white box in (a). 2D IR spectra were collected as a function of T_w at 2 μm intervals across the ROI. The NLS decay curves reflecting the chemical dynamics within the ROI are shown in (b). NLS curves extracted from two representative interfacial points and two representative bulk environments are plotted with the associated 95% confidence intervals.

In order to model the data appropriately we must take into account the spatial distribution of the signal intensity for the third-order 2D IR signal, the dynamics as a function of sample location and the contribution from each spatial region within the beam profile. The details of this modeling are included in a manuscript we recently submitted, but it will be described briefly here. The 2D signal is assumed to be comprised of multiple environments along the horizontal direction away from the interface. Each region's NLS curve is modeled as a biexponential with an offset.

$$C_{NLS(X)} = \alpha_{1X}\exp\left(\frac{-T_w}{\tau_{1X}}\right) + \alpha_{2X}\exp\left(\frac{-T_w}{\tau_{2X}}\right) + offset_X$$

where X is the distance from the interface and T_w is the waiting time. The collected signal contains the signal from each spatial region weighted by the signal intensity in that region according to,

$$C_{NLS} = \sum_X \beta_X \left[C_{NLS(X)}\right]$$

where, β_X is the weighting factor at position X from the spatial distribution of the signal intensity. We assume the dynamics change continuously from interface to bulk dynamics with an unknown length scale and rate of change. No signal is generated in the silicon oil. A cartoon of the model is shown in Fig. 4a. The total RTIL microdroplet sample consists of silicon oil, interface and bulk regions. The interface and bulk are divided into spatial regions with their individual $C_{NLS(X)}$ and β_X. We consider several possible transitions from the interface to bulk dynamics in which the α_is and τ_is change from the interface values to the bulk values over the interface length. The shapes of the models are shown in Fig. 4a and an example of the fits to the data are shown in Figure 4b. The experimental data generating the NLS curves for three points in the ROI, interfacial region (red circles), bulk region (green circles), and an intermediate point (blue circles) are fit according to the spatial models briefly described above. Each spatial model produces a length scale over which the dynamics transition from interfacial behavior to bulk behavior.

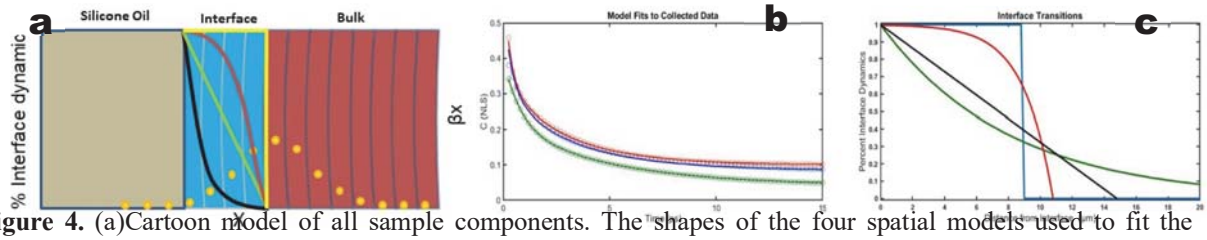

Figure 4. (a)Cartoon model of all sample components. The shapes of the four spatial models used to fit the experimental NLS decay curves from three points collected laterally across the ROI of the IL microdroplet. (b)Fits (lines) by the models to the experimental NLS data (open circles) from the interface (red), a point intermediate to the interface and bulk regions (blue), and the bulk region (green). (c) The functions describing the transition from interfacial dynamics to bulk dynamics as a function of distance from the interface by each model used: binary (blue), linear (black), exponential (green), and reverse exponential (red).

3. Future Plans

We have initiated experiments focused wholly on investigating solvation structures of carbonate mixtures. These experiments were born out of initial FTIR microscopy experiments in which we observed the spatial evolution of the linear IR spectrum of the carbonate mixture in the presence of an applied field. The carbonate mixture is representative of a commercially available organic electrolyte used in battery technologies. The fourth year of this project will be focused on characterizing the bulk solvent dynamics in this system and moving forward with 2D IR imaging experiments of the electrolyte solutions under an external voltage bias. These efforts will reveal fundamental physico-chemical interactions that are directly applicable to energy technologies.

4. Publications

1. Tibbetts, C.A., Luther, B.M., and Krummel, A.T., "**Approaches to Coherent Multidimensional Microspectroscopy**," an invited book chapter in the edited book entitled, Coherent Multidensional Spectroscopy, 2019, Springer Series in Optical Sciences 226, Springer Nature Publishing, pg. 311-337.

2. Tracy, K.M., Guchhait, B., Tibbetts, C.A., Luther, B.M., and Krummel, A.T., **Visualizing Chemical Dynamics in a Room Temperature Ionic Liquid Microdroplet**, *Journal of Physical Chemistry, B*, 2019, *submitted.*

3. Tracy, K.M., Guchhait, B., Tibbetts, C.A., Luther, B.M., and Krummel, A.T., **Perspective: 2D IR Microscopy—A Path to Spatially Resolved Ultrafast Chemical Dynamics**, *Journal of Chemical Physics*, 2019, *to be submitted.*

4. Guchhait, B., Tracy, K.M., Tibbetts, C.A., Luther, B.M., and Krummel, A.T., **Ultrafast Vibrational Dynamics of a Trigonal Planar Anionic Probe in Ionic Liquids: a 2D IR Spectroscopic Investigation**, *Journal of Chemical Physics,* to be submitted.

5. Tibbetts, C.A., Brantley, S., Gimble, N., Prieto, A.L., Corcelli, S., and Krummel, A.T. **The Structuring of Organic Battery Electrolytes with Fluoroethylene Carbonate**, *Energy Letters,* in preparation.

Mechanistic investigations of hot carrier induced electrocatalysis by single-particle spectroscopy

Christy F. Landes and Stephan Link
Department of Chemistry, Department of Electrical and Computer Engineering
Rice University, 6100 Main St. Houston, TX 77005
cflandes@rice.edu, slink@rice.edu

Program Scope

The goal of this project is to mechanistically understand the correlation of activity and stability of plasmonic electrocatalysts to nanoparticle morphology, surface chemistry, and 'hot' carrier physics using super-resolved single-particle spectro-electrochemical microscopy. The central hypothesis is that catalytic activity, selectivity, and stability of plasmonic electrocatalysts can be tuned by controlling the population and dynamics of excited charge carriers, and strongly depend on size, shape, crystal facet and surface chemistry. Furthermore, it is hypothesized that stability can be manipulated through the nanoparticle morphology and plasmon-induced hot carriers. State-of-the-art single-particle and single-molecule spectroscopic techniques with super-resolution capabilities are employed to probe electrocatalytic activities. Electro-generated chemiluminescence (ECL) microscopy will be used to image the spatial extent of active catalytic sites on single plasmonic nanoparticles and to correlate these sites with the nanoparticle morphology via scanning electron microscopy (SEM). Additionally, single-particle plasmon voltammetry is applied to probe electrocatalytic activity of nanoparticles with different morphologies characterized by SEM. Lastly, the kinetics of deactivation and morphology transformation of individual nanoelectrocatalysts is monitored with ECL and single-particle scattering microscopies. The following aims are being pursued:

(Aim 1) Investigate the effects of plasmon enhancement on the electrocatalytic activities of single metal nanoparticles and map intraparticle heterogeneity in catalytic activity via super-resolution microscopy.

(Aim 2) Combine single-particle voltammetry and super-resolved ECL microscopy to achieve unprecedented level of nanoscale understanding of catalysis using a model $Ru(bpy)_3Cl_2$ oxidation reaction.

(Aim 3) Explore the effects of plasmon induced instability of nanoelectrocatalysts and locate the most active and stable sites within particles using model quantum dots (QDs) and CO_2 reduction reactions.

Recent Progress

In the last year, we completed two projects aimed at characterizing the stability of plasmonic electrocatalysts, both in the absence and presence of light excitation to create hot carriers. While we reported initial results in our prior abstract, these projects have now been completed and published [1, 2]. The newest work addresses directly aim 3 and is summarized below. In addition, we have completed a study on the enhancement of ECL $Ru(bpy)_3Cl_2$ on plasmonic nanoparticle catalysts in accordance with the proposed experiments in aim 3. This work has just been accepted for publication [3].

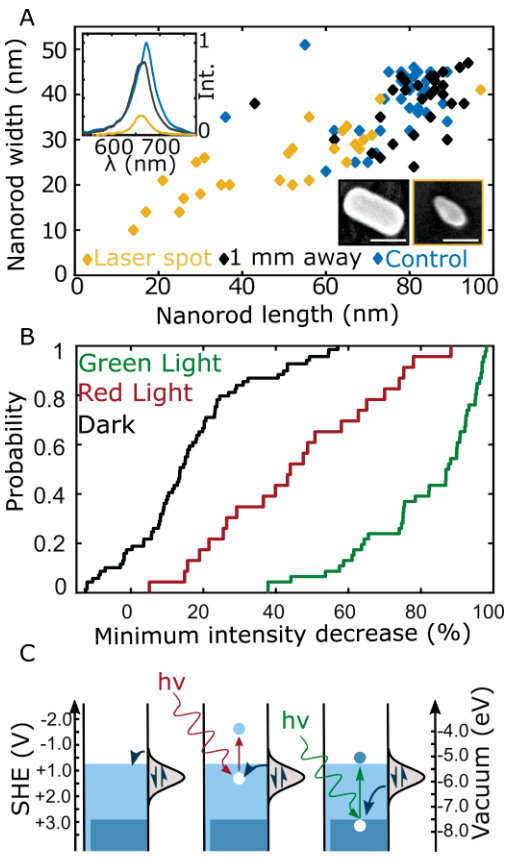

Figure 1: Hot hole enhanced nanorod dissolution A: nanorod length and width from SEM with and without light and a control from the same batch that had no potentials applied. The insets show representative spectra and SEM images. B: Intensity decrease of nanoparticles in the dark, and under red and green light illumination. C: Mechanistic diagram showing dissolution in the dark through slight overlap of the Fermi level with the chloride HOMO as well as the effect of hot holes from interband (red) and intraband (green) transitions.

To explore the effect of light induced hot carriers from plasmon damping and plasmon enhanced interband transitions on dissolution we employed snapshot hyperspectral imaging [2]. Upon illumination of gold nanoparticles at potentials just above the dissolution onset potential of 0.77 V vs. Ag/AgCl the nanoparticles dissolved, while nanoparticles in the dark did not show significant changes in scattering intensity (Figure, 1A inset), which was confirmed with correlated SEM (Figure 1A). Time dependent studies showed a highly heterogeneous 6 to 12 fold enhancement in dissolution rate, while surface temperature changes were calculated to be less than 3 K, strongly indicating the contribution of hot carriers to dissolution, rather than heating. When splitting the white light spectrum into a red (600 – 1000 nm) and green (400 – 550 nm) portion, we found that the green light drives nanoparticle dissolution at twice the rate of red light (Figure 1B). These findings indicate that plasmon enhanced interband transitions from green light illumination, which create hot holes in the d-band well below the Fermi level, drive oxidations more efficiently than the less energetic holes created from Landau damping of the longitudinal plasmon mode, which resides in the red part of the spectrum (Figure 1C). Our recently published results give new insight into hot hole driven photocatalysis on a single-particle level and demonstrate the importance of a single-particle approach for photocatalyst studies.

In completed work that was in progress last year, we've demonstrated that in the absence of light, the addition of low relative concentrations of certain oxoanions in chloride solutions increased the morphological stability of plasmonic gold nanorods under anodic potentials by altering the dissolution onset potential, particle reaction heterogeneity, and dissolution pathway [1]. Low relative concentrations (10%) of bicarbonate and phosphate oxoanions inhibited electrodissolution of gold nanorods by increasing the electrodissolution potential by 800 mV and 900 mV, respectively (Figure 2). Low relative concentrations of oxoanions also modified the heterogeneity of the electrodissolution statistics by reducing the emergence of distinct populations that occurred for chloride-only. By correlating SEM images with dark-field hyperspectral images, we determined that partially electrodissolved gold nanorods in chloride increased in average aspect ratio from 2.7 to 3.0 with a volume decrease of 36% (Figure 2C), whereas the aspect ratio in 90% chloride and 10% phosphate decreased to 2.1 with a volume decrease of 52% (Figure 2D). We examined the factors contributing to the inhibition of chloride mediated dissolution pathway of nanorods: ionicity,

coordination, oxoanion concentration, hydroxide concentration, and the oxoanion adsorption potential. Our interpretations of the observed trends suggest ionicity, pH, and the adsorption potential of the oxoanion have the greatest weight in terms of protection of gold nanorods in chloride electrolyte solution.

Regulating the electrochemical environment for metal nanoparticles is vital for their longevity in all electrochemical applications because they interface with enormously varied and complex chemical environments in technological settings. This range of environments poses critical challenges to corrosion and dissolution prevention in nanoparticle electronics, electrocatalysis, and electrochemical sensing, as no suitable overarching prevention strategy exists. Preventing dissolution is especially critical for expensive metals and for metal nanoparticles with properties that are strongly dependent on size and shape, such as plasmonic noble metal nanoparticles.

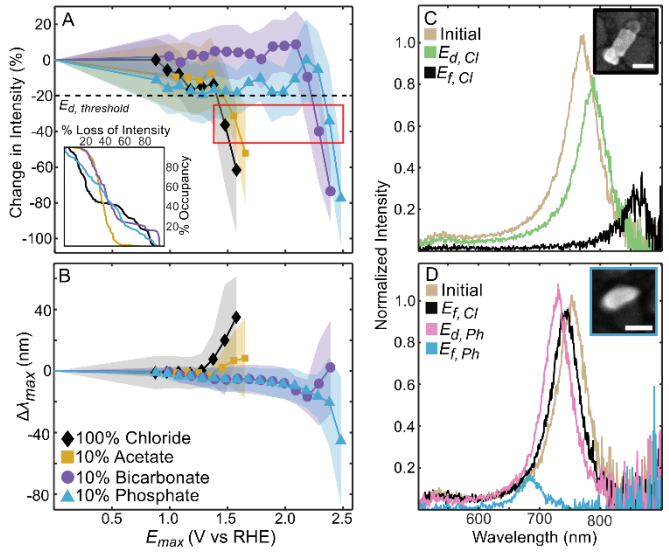

Figure 2. Spectroscopic changes of gold nanorods under electrodissolution in 90 mM NaCl solutions containing 10 mM of a competing oxoanion. (A) Average relative change in scattering intensity of the longitudinal plasmon resonance for multiple gold nanorods as a function of maximum anodic potentials, E_{max}. Negative values indicate a decrease in intensity. Shaded areas represent a range of one standard deviation on either side of the average. The dotted black line designates the threshold potential for electrodissolution (E_d). The inset shows the intensity cumulative distribution functions for each condition at E_d (red box). (B) Average change in resonance maximum λ_{max} as a function of E_{max}. Negative values indicate blue-shifts, and positive values indicate red-shifts in λ_{max}. (C) Spectral changes of a representative nanorod in 100% NaCl recorded initially, at E_d, and at the final potential (E_f). (D) Spectral changes of a representative nanorod in NaCl with 10% phosphate showing spectra at initial, E_d, and E_f conditions, along with the spectrum at $E_{f,Cl}$, for comparison. The insets are the correlated SEM micrographs after E_f was applied. All scale bars are 50 nm.

Our newest work on this project is a comprehensive study into the impact of nanoelectrode-emitter spectral overlap on ECL intensity, moving us closer to the goal of super-resolution ECL microscopy in aim 2 [3]. Single-particle microscopy revealed the influence of spectral overlap dependent signal enhancement, only previously hinted at in ensemble studies, by resolving heterogeneities arising from colloidal nanoparticle size and shape distributions. The single-particle ECL intensities and dark-field scattering spectra of 785 gold nanospheres and 177 gold nanotriangles were correlated to encapsulate spectral overlap over the entire emission spectrum of $Ru(bpy)_3Cl_2$ (Figure 3A). To isolate the influence of spectral overlap on emitter photon flux, other factors were minimized including background correction, removing surface ligands, using nanoparticles with similar crystal faceting, and normalizing for nanoparticle surface area and integration times. Upon minimizing these factors, nanoelectrode-emitter wavelength difference, $\Delta\lambda_{max}$, dependent photon fluxes showed a similar shape to the emission spectrum of $Ru(bpy)_3Cl_2$ and a 10-fold enhancement in photon flux

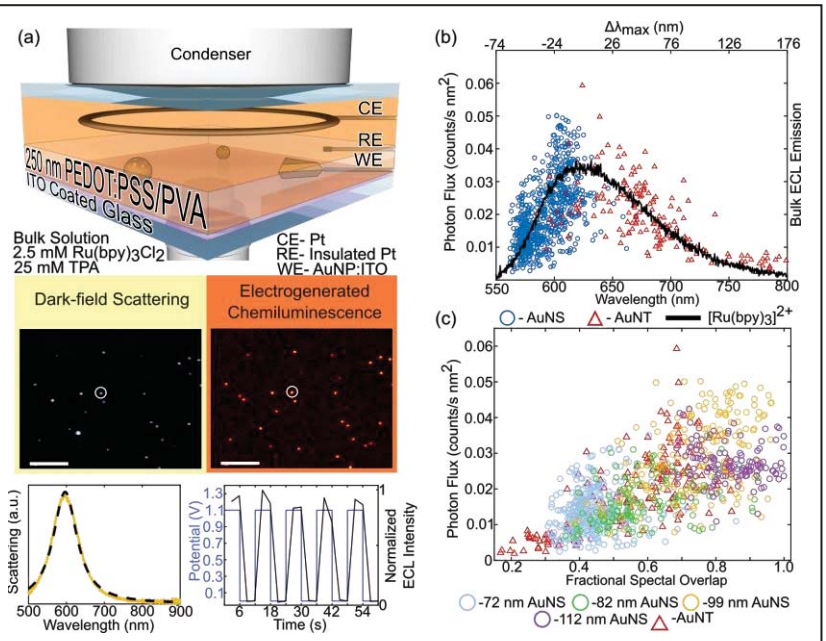

Figure 3. Nanoelectrode-Emitter Spectral Overlap Dependent Electrogenerated Chemiluminescence: (A) The scattering and electrogenerated chemiluminescence (ECL) intensity of 785 gold nanospheres and 177 gold nanotriangles are correlated. (B) Correcting scattering wavelength dependent ECL intensity for nanoparticle surface area results in an observed 10-fold enhancement in ECL intensity due to spectral overlap only. $\Delta\lambda = 0$ for 624 nm corresponds to the emission maximum of the $Ru(bpy)_3^{2+}$ ECL spectrum (C) A positive correlation between nanoparticle-emitter spectral overlap and photon flux is observed.

was observed (Figure 3B). The fractional spectral overlap between the nanoelectrode and emitter correlated positively with photon flux (Figure 3C). Gold nanospheres and gold nanotriangles, when corrected for surface area, demonstrated statistically similar spectral overlap dependences. The similar dependences indicated that there was no effect of shape for ECL. To maximize the absolute ECL signal, structures need both a large surface area, to allow for higher emitter concentration within the enhancement region, and a fractional spectral overlap close to unity. This study provided new mechanistic insight into plasmonic enhancement of ECL, as a step towards single molecule ECL detection on surfaces.

Future Plans

Future dissolution studies will focus on using directional re-shaping to identify hot carrier hot spots on gold nanorods. Preliminary results analyzing the plasmon resonance position showed red shifts for dissolution in the dark, whereas dissolution under illumination gave blue shifts, indicating preferential dissolution from the tips, which may be attributed to hot carrier hot spots on the tips. Our future ECL studies will focus on understanding the impact of electric fields on ECL intensity enhancement both experimentally and theoretically through studying the impact of gap sizes for gold nanodisk dimer structures. Super-resolving the emitted light will furthermore inform us about inter- and intra-particle heterogeneity of single-particle plasmonic electrocatalysts.

Publications

[1] C. Flatebo, S. S. E. Collins, B. S. Hoener, Y.-Y. Cai, S. Link, C. F. Landes. *Electrodissolution Inhibition of Gold Nanorods with Oxoanions.* J. Phys. Chem. C 2019, 123, 22, 13983–13992.

[2] A. Al-Zubeidi, B. S. Hoener, S. S. E. Collins, W. Wang, S. R. Kirchner, S. A. H. Jebeli, A. Joplin, W.-S. Chang, S. Link, C. F. Landes. *Hot Holes Assist Plasmonic Nanoelectrode Dissolution*. Nano Lett. 2019, 19, 2, 1301–1306.

[3] T. S. Heiderscheit, M. J. Gallagher, R. Baiyasi, S. S. E. Collins, S. A. H. Jebeli, L. Scarabelli, A. Al-Zubeidi, C. Flatebo, W.-S. Chang, C. F. Landes, S. Link. *Nanoelectrode-Emitter Spectral Overlap Amplifies Surface Enhanced Electrogenerated Chemiluminescence*. J. Chem. Phys. 2019, Accepted.

Understanding and controlling photoexcited molecules in complex environments

Principal Investigator: David T. Limmer, Assistant Professor
University of California, Berkeley CA 94610
dlimmer@berkeley.edu

Program Scope: This proposal aims to develop basic theoretical tools to understand how energy and matter can be controlled and transformed in small molecules, an example of which is sketched in Figure 1. The proposed research will explore basic physical principles, determine what limits exist in controlling matter at these fine scales, and develop numerical methods to extract the knowledge necessary for optimizing control under physical constraints. Specifically, using nonequilibrium statistical mechanics unified with contemporary views of open quantum systems, we will establish new ways to study how energy and material are converted from one form to another at a molecular level. The proposal will focus on molecules undergoing conformational or chemical changes in response to photoexcitation in the condensed phase, but the principles and methodologies will be broadly applicable.

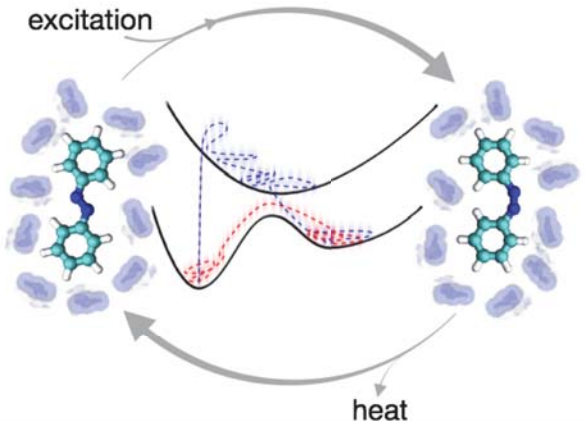

Figure 1: Representative illustration of the type of energy transduction processes to be studied under this proposal. Molecules of this type absorb energy in the form of light and subsequently relax, giving off heat to the environment. If this molecule is tethered to a surface, the conformation change has the potential to also do useful work. These simple examples of molecular machines fall outside the scope of traditional thermodynamics, and thus basic principles governing their efficiencies and controllabilities do not exist.

Specifically, to understand how energy and matter are transformed at the molecular scale, and how to ultimately control the outcomes and efficiencies of such processes, theoretical models can be constructed and studied. For molecules undergoing conformational changes or chemical reactions in response to photo-excitation, realistic models, full of molecular details, can be simulated on a computer, provided potential energy surfaces and equations of motion. Even when these can be constructed, however, importance sampling tools are needed to probe rare events, in order to clarify why certain conditions favor one outcome over another. The information content of a collection of such simulations is dense, and must be distilled in order for guiding principles to be discovered. This requires a theoretical framework with which to analyze results. These three areas–*model building, importance sampling, and analysis*–work synergistically, with constant feedback in order to eventually arrive at theoretically robust results. The focus of this proposal is to take these steps in the context of photo-induced conformational changes and chemistry, in specific instances where both nonequilibrium and nonadiabatic dynamics play important roles in determining the outcomes, or efficiencies, of reactivity.

There are no publications to report because this is a new award, with a start date of September 1, 2019

ION SOLVATION AND HYDROGEN BONDING IN LIQUID ELECTROLYTES

Mark Maroncelli[1] and Hyung Kim[2]

[1]Department of Chemistry, The Pennsylvania State University, University Park, PA 16802
maroncelli@psu.edu

[2]Department of Chemistry, Carnegie Mellon University, 4400 Fifth Ave., Pittsburgh, PA 15213
hjkim@cmu.edu

Program Scope: The goal of this project is to develop a better understanding of hydrogen bonding and solvation of simple ions in liquid electrolytes. The electrolytes considered include dilute salt solutions in conventional dipolar solvents, ionic liquids, and concentrated mixtures of ions and dipolar components such as deep eutectic solvents. Initial efforts will involve simple, well-known systems, but the ultimate targets are the more complex electrolyte systems of growing importance in many energy-related technologies, most notably in the areas of Li-ion and related batteries, supercapacitors, and electroplating. Three interrelated projects that combine infrared and NMR spectroscopy and computer simulation are planned.

The first and primary project entails the use of far-infrared (FIR) spectroscopy to study solvation of simple ions such as alkali metal salts in liquid electrolytes. FIR absorption bands of such ions result from rattling motions of the ions within the cage formed by surrounding solvent molecules. The spectra of these ion-solvent vibrations, when augmented with computer simulations, provide a direct window on their solvation structure and dynamics in different solvent environments. Although some work of this sort was initiated decades ago, improvements in instrumentation and computational power have greatly enhanced the quality of the spectra obtained as well as our ability to interpret them. Almost no such work has been reported in the more complex liquid electrolytes of interest here. This research will therefore explore what new insights can be gained when high-quality spectra in this region are interpreted with modern computational methods.

The second research area involves characterization and use of trialkylphosphine oxides (R_3PO) as mid-IR solvation probes. The PO bond ($P{=}O \leftrightarrow P^+\text{-}O^-$) is highly sensitive to the electrophilicity of its environment. In electrolyte solutions, both the ^{31}P chemical shift and the P-O stretching frequency are markedly affected by the availability of hydrogen-bond donating and cationic species within a solution. Whereas the trimethylphosphine oxide ^{31}P chemical shift has long been used to define solvent acceptor numbers, the promise of such molecules as vibrational probes has been largely ignored since the 1980s. Quantum chemical calculations and molecular dynamics simulations will be used to characterize the P=O stretch of trimethylphosphine oxide (TMPO) and create a spectroscopic map based on calibration against experimental data in a number of conventional solvents. IR spectroscopy of TMPO and related molecules will then be used to measure polarity and hydrogen bonding in the liquid electrolytes mentioned above. Classical molecular dynamics simulations, together with the spectroscopic map, will be used to interpret the observed spectra in terms of specific molecular interactions and dynamics.

The third final project is a minor extension of the FIR studies. Computer simulations undertaken for the FIR work will be extended to include calculation of the electric field gradient autocorrelation function (EFG ACF), which summarizes the dynamics relevant to quadrupole relaxation of atomic ions. These functions will be used to predict quadrupole relaxation times of

ions both in simple solvents, where experimental times are already available, as well as in electrolyte solvents, which have yet to be studied in this manner. New NMR measurements of relaxation rates will be performed as needed to test these predictions. Comparison of the EFG-ACFs to suitable representations of the dynamics underlying the FIR spectra will be made in order to better appreciate the different perspectives on ion solvation dynamics provided by FIR and NMR spectroscopies.

Recent Progress: The first year of the project was largely an induction period. Shortly after the start of funding, we learned of a vacuum FTIR spectrometer, similar to the one budgeted for purchase, was becoming available for use in a local user facility. Rather than purchase an entire instrument, we decided to retrofit this existing unit for FIR operation and shift the bulk of the equipment funds to instead purchase time at the facility and help support additional experimental personnel. After obtaining permission for this budget change late in 2018, a brief search was conducted and Kallol Mukherjee, already well versed ionic liquids and deep eutectics from his PhD experience, was hired into the Maroncelli group for a 1-year postdoc. He arrived in early August. Since his arrival, Kallol has begun learning how to obtain high-quality FIR spectra by benchmarking against aqueous alkali halide solutions, one of the few systems for which comparison data are available.[1] He has also recorded spectra of trimethylphosphine oxide (TMPO) in a variety of polar aprotic solvents, and in alcohols and water-acetonitrile mixtures. In the latter solutions he finds up to four distinct frequencies tentatively assigned to solvates having between 0 to 3 hydrogen bonds. We have initiated simulations of these TMPO solutions and made the first steps to constructing a spectroscopic map with which to help validate these assignments. We have also acquired initial spectra of TMPO in simple electrolyte solutions and again find multiple peaks tentatively assigned to solvates of different ion + solvent molecule compositions.

We have yet to begin the work of simulating FIR spectra. This part of the project will be performed by a postdoc in Kim's group, who was funded to begin in the second year of the project. Fangyong Yan has been hired for this position. He has been delayed somewhat by the visa process, but is expected to arrive in late October.

Future Plans: Experiments and simulations during the next year will continue the mid-IR studies of trialkylphosphine oxides, but emphasize the FIR work. After benchmarking against aqueous alkali-halide solutions, we will survey a broad range of electrolyte solutions, seeking the best cases for detailed computational study. First targets include alkali iodides and other lithium salts in nonaqueous solvents such as acetonitrile, dimethyl sulfoxide, and alkyl carbonates. Carbonate solvents are of particular interest, both due to their importance in battery applications and also because Kuroda and coworkers have recently provided detailed descriptions of these systems based on IR and 2D-IR measurements of mid-IR carbonate vibrations.[2] Simulations will likely begin with classical MD simulations of the sort employed by Kann and Skinner[3] for aqueous solutions in order to evaluate their accuracy in the case of nonaqueous solvents.

References:

1. D. A. Schmidt, O. Birer, S. Funkner, B. P. Born, R. Gnanasekaran, G. W. Schwaab, D. M. Leitner, and M. Havenith, "Rattling in the Cage: Ions as Probes of Sub-picosecond Water Network Dynamics," *J. Am. Chem. Soc.* **131,** 18512-18517 (2009). 10.1021/ja9083545

2. K. D. Fulfer and D. G. Kuroda, "Ion speciation of lithium hexafluorophosphate in dimethyl carbonate solutions: an infrared spectroscopy study," *Phys. Chem. Chem. Phys.* **20,** 22710-22718 (2018). 10.1039/c8cp03315c
3. Z. R. Kann and J. L. Skinner, "Low-frequency dynamics of aqueous alkali chloride solutions as probed by terahertz spectroscopy," *J. Chem. Phys.* **144,** 234501/234501-234501/234507 (2016). 10.1063/1.4953044

DOE-Sponsored Publications:

Marissa Saladin, Christopher A. Rumble, Durgesh V. Wagle, Gary A. Baker, and Mark Maroncelli, “Characterization of a New Electron Donor-Acceptor Dyad in Conventional Solvents and Ionic Liquids,” *J. Phys. Chem. B,* revision submitted in Sept. 2019.

Elucidating the Formation Mechanisms of Zeolites

Using Data-Driven Modeling and In-Situ Characterization

Valeria Molinero, *The University of Utah*
Subramanian Sankaranarayanan, *University of Chicago*
Ilke Arslan, *University of Chicago*

Program Scope and Plans. Zeolites are the main industrial solid catalysts. The presence of pores of molecular dimensions gives zeolites a selectivity that is key for their use in separations and catalysis. Organic cations are used to direct the synthesis towards specific zeolite polymorphs. However, the molecular mechanisms by which organic cations direct the nucleation towards specific zeolite crystals is not known.

The aim of this project is to develop and implement a synergistic, data-driven computational and experimental approach to resolve the molecular pathways of nucleation, growth, and polymorph selection of zeolites and unravel the role of organic cations in directing their formation. We will develop computationally efficient and accurate coarse-grained reactive models for the study of the nucleation and growth of pure silica zeolites in molecular simulations (Fig. 1) using machine learning with data gathered from high-resolution reactive force fields and experiments. Simulations with these models will be integrated with in-situ scanning tunneling electron microscopy (Fig 2), computer vision, and deep learning to unveil the molecular pathways of formation of silicalite-1 and other model zeolites.

Of particular interest in this project is to elucidate the role of amorphous precursors in the nucleation of the zeolite. Previous experiments indicate that silicalite-1 is born within non-crystalline aggregates in which the silicates and organic cations have local and medium range order similar to that of the zeolite. The organic cations that direct the formation of zeolites and those that direct the formation of ordered mesoporous silicas are similar. We hypothesize that the frustrated attraction that for large organic cations leads to the formation of stable mesophases that direct the synthesis of mesoporous silicas, could promote the formation of metastable mesophases that can assist in the nucleation and polymorph selection of zeolites. The simulations will allow us to investigate the role of the structure directing agents in building crystalline order, and whether there is mesoscopic pre-ordering that facilitates the nucleation and polymorph selection of the zeolite that could be detected with our sub-nm resolution in-situ imaging experiments. The enticing possibility of controlling the nucleation and polymorph selection of zeolites by tuning underlying metastable mesoscopic ordering of the silicates and structure directing agents would open the possibilities of controlling the synthesis of materials with ordering at multiple length-scales, while also providing a unifying framework for the mechanisms of formation of both crystalline zeolites and mesoporous silicas.

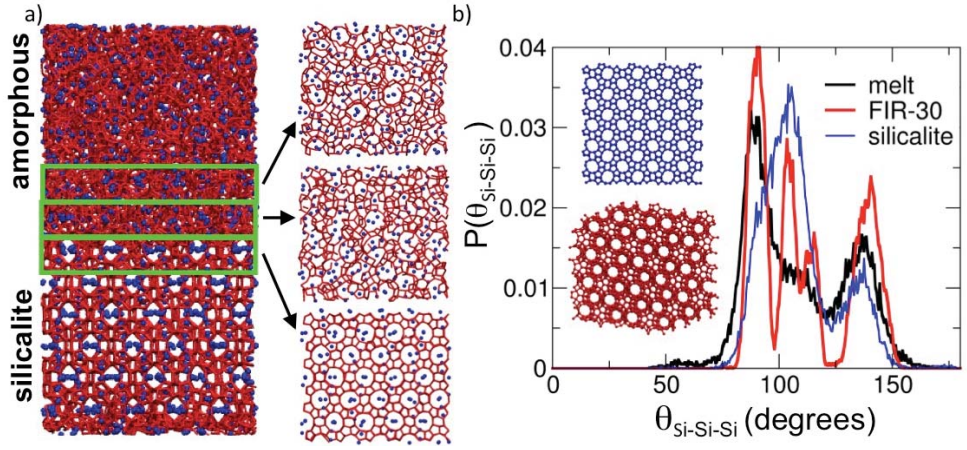

Figure 1. Molecular simulation of the silicalite/amorphous interface (panel a) and distribution of angles of the network former agent in silicalite, the melt, and a competing zeolite polymorph.

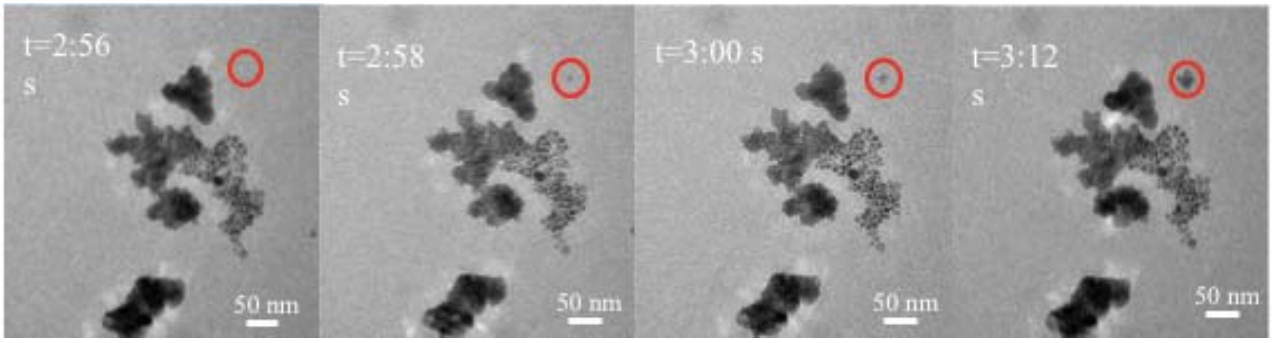

Figure 2. TEM imaging of in-situ growth of zeolite Y from reaction gel in hydrothermal synthesis, time in seconds. The red circle shows the locus of nucleation and growth of a new crystal.

Publications. There are no publications to report, because this is a new award with a start date of September 1 2019.

Intrinsic to collective properties of ions in solution

Christopher J. Mundy
Physical Sciences Division
Pacific Northwest National Laboratory
902 Battelle Blvd, Mail Stop K1-83
Richland, WA 99352
chris.mundy@pnnl.gov

Program Scope

The long-term objective of this research is to develop a fundamental understanding of processes, such as transport mechanisms and chemical transformations, at interfaces of hydrogen-bonded liquids. Liquid surfaces and interfaces play a central role in many chemical, physical, and biological processes. Many important processes occur at the interface between water and interfaces (liquid or solid). Separation techniques are possible because of the hydrophobic/hydrophilic properties of liquid/liquid interfaces. Reactions that proceed at interfaces are also highly dependent on the interactions between the interfacial solvent and solute molecules. The interfacial structure and properties of molecules at interfaces are generally very different from those in the bulk liquid. Therefore, an understanding of the chemical and physical properties of these systems is dependent on an understanding of both the bulk and interfacial solvation structure. The adsorption and speciation of ions at aqueous liquid interfaces are fundamental processes encountered in a wide range of physical systems. In particular, the manner in which solvent molecules solvate ions at the interface is relevant to problems in a variety of areas. Another major focus lies in the development of reduced models of interaction based on the potential of mean force (PMF) and solvation free energies to provide accurate descriptions of both single ion and ion-ion interactions. These reduced models can be used with appropriate simulation techniques for sampling statistical mechanical ensembles to obtain the desired collective properties such as nucleation.

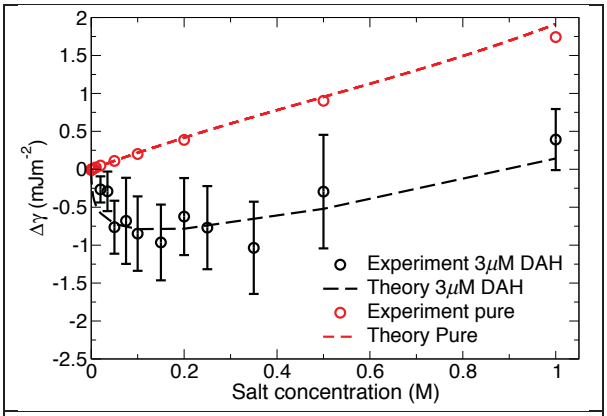

Figure 1: Experimental and theoretical fit of NaCl surface tensions in the presence of a dilute (but measurable) surfactant and the pure salt solution. Clear indication that the presence of a dilute surfactant gives rise to a Jones-Ray-like effect.

Progress Report

Towards a resolution of the Jones-Ray effect [5] The surface tension of dilute salt water is a fundamental property that is crucial to understanding the complexity of many aqueous phase processes. Small ions are known to be repelled from the air-water surface leading to an increase in the surface tension in accordance with the Gibbs adsorption isotherm. The Jones-Ray effect refers to the observation that at extremely low salt concentration the surface tension decreases in apparent contradiction with thermodynamics. Determining the mechanism that is responsible for this Jones-Ray effect is important for theoretically predicting the distribution of ions near surfaces. We use both experimental surface tension measurements and numerical

solution of the Poisson-Boltzmann equation to demonstrate that very low concentrations of surfactant in water create a Jones-Ray effect as shown in **Figure 1**. We also demonstrate that the low concentrations of surfactant necessary to create the Jones-Ray effect are too small to be detectable by surface sensitive spectroscopic measurements. The effect of surface curvature on this behavior is also examined and the implications for unexplained bubble phenomena is discussed. This work leaves open the possibility that the purity standards for water may be inadequate and that the interactions between ions with background impurities are important to incorporate into our understanding of the driving forces that give rise to the speciation of ions at interfaces.

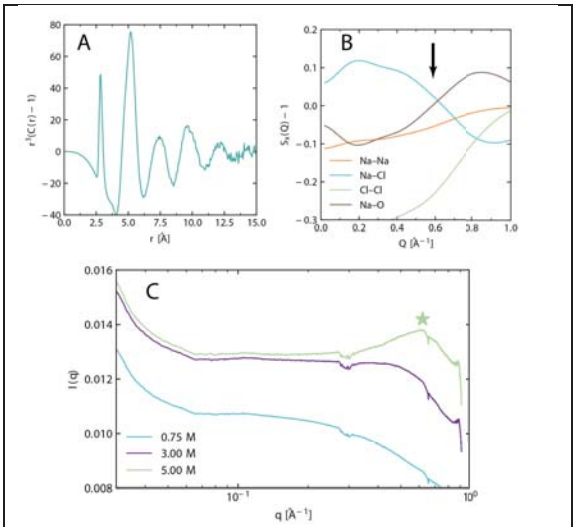

Figure 2: (A) Total correlation function (*C(r)*) obtained using molecular simulation of 6M NaCl depicting long-range oscillations. (B) The simulated structure factor (*S(Q)*) as determined from simulation broken down into single contributions. The arrow depicts the length scale at which all components sum to a maximum. (C) Experimental SAXS data obtained by Shawn Kathmann (PNNL) over a concentration range of NaCl solutions. The star depicts the emergence of long-range order at the precise length-scale given by that depicted in panel B.

Future directions

Probing long-range ion-ion correlation in electrolytes: The collective properties of concentration electrolytes form the basis of our understanding of phenomena in solution ranging from nucleation to formation of double layers in the vicinity of a dielectric surfaces. Many of our previous studies have focused on the role of short-range interactions informing our understanding clustering and the initial stages of nucleation. Recently, our group (in collaboration with John Fulton (PNNL) and Shawn Kathmann (PNNL) used modern light sources to probe the long-range collective properties of concentration electrolytes. To this end, modern small angle X-ray scattering (SAXS) experiments have been able to detect long-range correlation in electrolytes (see **Figure 2**) that show signatures of charge oscillations that can be connected to presence of a so-called Kirkwood line. Simply put, the Kirkwood line separates regions in concentration space that exhibit oscillatory decay of charge correlations as opposed to standard Debye-Huckel correlations. Although the presence of the Kirkwood line has been known theoretically for some time, its direct observation in bulk phase measurements and quantitative connection to molecular simulation has been elusive. The importance of the presence of the

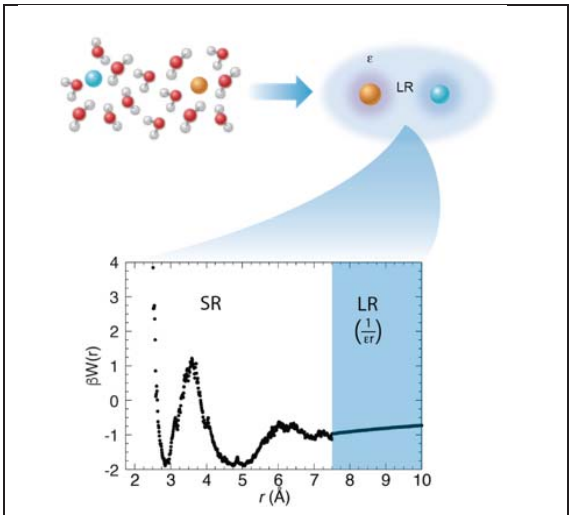

Figure 3: A schematic of the construction of a primitive model based on the potential of mean force. We combine short-range (SR) interactions as determined by molecular simulation with long-range (LR) dielectric response.

Kirkwood line is the relationship to clustering statistics, pathways to nucleation, in addition to understanding anomalous screening effects that have been measured using surface force apparatus.

To explore the origins of long-range charge oscillations our approach will be to initially construct reduced models of the aqueous electrolytes. We will use the potential pf mean force (PMF) as a tool to produce a model where water is reduced to a mean-field background (see **Figure 3**). A salient feature of this primitive model is that we have previously shown it can capture correlation effects to moderate concentrations through reproducing the experimentally observed osmotic coefficients. Questions regarding the nature of charge correlations using a primitive model versus an all-atom representation be investigated and directly compared to experimental measurement and theory.

Acknowledgements. This work was performed with Evgenii Fetisov (PNNL), Mirza Galib (PNNL), Santanu Roy (PNNL), Tim Duignan (PNNL), John D. Weeks (U. Maryland), Rick Remsing (Rutgers), Ilja Siepmann (U. Minn.), Greg Schenter (PNNL), Marcel D. Baer (PNNL), Shawn M. Kathmann (PNNL), Greg Kimmel (PNNL), and John Fulton (PNNL). We also acknowledge computer resources from NERSC. Battelle operates Pacific Northwest National Laboratory for the US Department of Energy. The Molecular Theory and Modeling FWP 16249 is co-managed by CTC and CPIMS programs of DOE Office of Basic Energy Sciences Division of Chemical Sciences, Geosciences, and Biosciences.

Publications with BES support (2018-present):

1. [**Invited**] Evgenii O. Fetisov, Marcel D. Baer, J. Ilja Siepmann, Gregory K. Schenter, Shawn M. Kathmann, and **CJM**, "The Statistical Mechanics of Solution-phase Nucleation: CaCO3 Revisited", (to appear in FOMMS 2018 volume of "Molecular Modeling and Simulation: Applications and Perspectives" edited by Ed Maginn)
2. Joanna K. Denton, Patrick J. Kelleher, Mark A. Johnson, Marcel D. Baer, Shawn M. Kathmann, **CJM**, Bethany A. Wellen Rudd, Heather C. Allen, Tae Hoon Choi, and Kenneth D. Jordan, "Molecular-level origin of the carboxylate head group response to divalent metal ion complexation at the air–water interface"**,** , PNAS July 23, 2019 116 (30) 14874-14880, https://doi.org/10.1073/pnas.1818600116
3. Marcel D. Baer**,** Halil I. Okur**, CJM,** Sylvie Roke**,** "The Diverse Nature of Ion Speciation at the Nanoscale Hydrophobic/Water Interface"**,** Evangelia Zdrali**, ,** *J. Phys. Chem. B* 2019 123 2414-2423, https://doi.org/10.1021/acs.jpcb.8b10207
4. Zhizhang Shen, Eugene S. Ilton, Micah P. Prange, **CJM**, and Sebastien N. Kerisit, "Diffusion Mechanism of Radiolytic Species in Irradiated Al (Oxy-)Hydroxides,", https://doi.org/10.1021/acs.jpcc.8b07809
5. Timothy T. Duignan, Mengsu Peng, Anh V. Nguyen, and Xiu Song Zhao, Marcel D. Baer, **CJM**, "Detecting the undetectable: The role of trace surfactant in the Jones-Ray effect," https://doi.org/10.1063/1.5050421
6. "Unraveling the spectral signatures of solvent ordering in K-edge XANES of Aqueous Na^{+}" M. Galib, G.K. Schenter, **CJM**, N. Govind, and J.L. Fulton, https://doi.org/10.1063/1.5024568
7. T. Duignan, MD Baer, and CJM, "Understanding the scale of the single ion free energy: A critical test of the tetra-phenyl arsonium and tetra-phenyl borate assumption," The Journal of Chemical Physics 148, 222819 (2018)

8. Z. Shen, J. Chun, K. Rosso, and **CJM "**Surface Chemistry Affects the Efficacy of the Hydration Force between Two ZnO(1010) Surfaces," *J. Phys. Chem. C*, 2018, 122 (23), pp 12259–12266
9. A. Prakash, MD Baer, **CJM**, and J. Pfaendtner, "Peptoid Backbone Flexibilility Dictates Its Interaction with Water and Surfaces: A Molecular Dynamics Investigation," *Biomacromolecules*, 2018, 19 (3), pp 1006–101
10. [**Frontiers Article**] S. Roy, M. Galib, G.K. Schenter, and **CJM**, "On the relation between Marcus theory and ultrafast spectroscopy of solvation kinetics," *Chemical Physics Letters,* 692, 417 (2018)
11. R. Remsing, T. Duignan, M.D. Baer, G.K. Schenter, **CJM**, and J.D. Weeks, "Water Lone Pair Delocalization in Classical and Quantum Descriptions of the Hydration of Model Ions" *J. Phys. Chem. B* 122, 3519 (2018)

Probing the Structure and Dynamics of Water Under Heterogeneous Nanoconfinement Through Ultrafast Vibrational Spectro/microscopy and Many-Body Molecular Dynamics

Francesco Paesani and Wei Xiong
Department of Chemistry and Biochemistry, University of California San Diego
La Jolla, CA 92093
Email: fpaesani@ucsd.edu; w2xiong@ucsd.edu

Program Scope

The goal of this research project is to gain a molecular-level understanding of the structure and dynamics of aqueous solutions in nanoporous materials by integrating state-of-the-art ultrafast vibrational spectroscopy/microscopy with advanced computer simulations based on many-body molecular dynamics.

Specific focus is on identifying the physical mechanisms and characterizing the underlying molecular interactions that determine the adsorption and transport processes of water and small solutes in metal-organic frameworks (MOFs) and β-cyclodextrin (β-CD) polymers - prototypical examples of inorganic porous materials and polymers, respectively, which have recently been proposed for technological applications in water purification. By combining bulk- and surface-sensitive, spatially resolved ultrafast vibrational spectroscopy with many-body molecular dynamics simulations, we aim at gaining broad insight into the structure and mobility of nanoconfined water in MOFs at various length scales. Analogous studies of salt solutions in MOFs will shed light on the molecular mechanisms as well as key solute-framework and water-framework interactions that govern the adsorption and transport of small ions through nanopores with different sizes, shapes, and degrees of hydrophobicy/hydrophilicity. Finally, measurements of spatially-resolved, surface-sensitive vibrational spectra will probe water heterogeneity in β-CD while many-body molecular dynamics simulations will be used to characterize domain-specific, structure-binding affinity relationships.

Recent Progress

From the experimental side, we have demonstrated the unique sensitivity of vibrational sum-frequency generation (VSFG) microscopy to probe strongly bonded water at the interface between water and self-assembled materials.[1] In the first proof-of-principle experiment, we investigated a guest-host self-assembled material composed of sodium dodecyl sulfide (SDS) and β-cyclodextrin (β-CD), SDS@2β-CD, using VSFG microscopy. Our measurements and associated analysis show that our hyperspectral microscope can differentiate individual self-assembled domains based on their spectral features, which unambiguously demonstrates the presence of spatial inhomogeneities that cannot be detected by ensemble-average spectroscopy. Our analysis also shows that the strong VSFG signal measured in our experiments is due to a combination of individual molecular chirality and highly coordinated ordering of the self-assembly, which gives rise to anisotropic signals (e.g., in measurements carried out using the SSS polarization combination). More importantly, we found that the strong interactions between water and the SDS@2β-CD assemblies effectively template the local structure of water, inducing ordering at the mesoscopic length scale.

From the theoretical side, we have combined infrared spectroscopy and many-body molecular dynamics (MB-MD) simulations to probe the structure and dynamics of confined water as a function of relative humidity (RH) within Co_2Cl_2BTDD, a metal-organic framework containing cylindrical pores lined with an ordered array of cobalt open coordination sites.[2] Building upon the agreement between the experimental and theoretical spectra, we demonstrated that water at low RH values initially binds to the open metal sites and subsequently forms disconnected

one-dimensional chains of hydrogen-bonded water molecules bridging between the cobalt sites. Upon further increase in relative humidity, these water chains nucleate pore filling, with water molecules occupying the entire pore interior before the relative humidity reaches 30%. Systematic analysis of the rotational and translational dynamics indicated heterogeneity in this pore-confined water, with water molecules displaying distinct levels of mobility as a function of the distance from the pore surface.

In our ongoing project, we have combined VSFG spectroscopy with MB-MD simulations to investigate the behavior of water adsorbed in ZIF-90, a zeolitic imidazolate framework. We have successfully demonstrated that D_2O molecules adsorbed in ZIF-90 adopts the same symmetry as the framework and give rise to unique spectral features. Building upon these observations, we have been able to resolve different peak positions by combining VSFG and FTIR spectra of D_2O in ZIF-90, under the same hydration conditions, which indicates that water molecules in the first adsorption layer in contact with the ZIF-90 framework experience different local hydrogen-bonding environments from water molecules located a few layers away from the framework. These experimental measurements have been accompanied by analogous MB-MD simulations. To this purpose, following our previous studies of breathing MOFs, a molecular model of ZIF-90 compatible with our MB-pol water model was developed from ab initio data. MB-MD simulations were then carried out as a function of relative humidity to characterize the adsorption process by monitoring the evolution of the different spectral features.

Future Plans

We are planning to continue the integration of experimental measurements and MB-MD simulations to gain fundamental insights into the properties of water in porous materials. Particular focus will be on performing transient VSFG measurements on ZIF-90 and MB-MD simulations to model VSFG spectra of both β-CD polymers and MOFs.

List of Publications

1. H. Wang, W. Chen, J.C. Wagner, W. Xiong, Local ordering of lattice self-assembled SDS@ 2β-CD materials and adsorbed water revealed by vibrational sum frequency generation microscope. *J. Phys. Chem. B* **2019**, 123, 6212-6221.
2. A.J. Rieth, K.M. Hunter, M. Dincă, F. Paesani, Hydrogen bonding structure of confined water templated by a metal-organic framework with open metal sites. *Nat. Commun.* **2019**, in press.

Understanding molecular scale chemical transformations at solid-liquid interfaces – computational investigation of electrolyte oligomerization and the role of additives

Jim Pfaendtner
University of Washington, Chemical Engineering (100% FTE)
PNNL, Senior Scientist (via UW/PNNL dual appointee program) (0% FTE)
Benson Hall | Seattle, WA 98195-1750 | jpfaendt@uw.edu

Program Overview. Understanding the molecular and nanoscale mechanisms of chemical reactions occurring at a liquid/solid interface is critically important to a huge range of processes. Compared with homogenous chemistry in a bulk condensed or gas phase, the modeling toolkit for predicting an interface-mediated reaction mechanism is far less developed, with many researchers falling back on individual reaction-by-reaction studies guided by chemical intuition. The proposed work will develop new computational approaches that address time scale limitations with a suite of enhanced sampling tools.

To date, our project has focused on a systematic study of reaction mechanisms of electrolyte degradation. We have developed reference mechanisms from gas phase mechanisms with implicit solvation, used MD to study electrolyte behavior under different types of interface functionalization, and implemented a reaction coordinate optimization scheme (aimless shooting with maximum likelihood maximization) in an automated approach that will greatly facilitate the use of this approach for determining reaction mechanisms in liquids at interfaces.

Recent Progress. A significant portion of the effort over the last year was devoted to the development of reference reaction mechanisms using MD simulations for eventual comparison to interfacial mechanisms that we predict. We studied the degradation of the model electrolyte ethylene carbonate (EC) and also compared the degradation of EC neat and in the presence of common additives fluoroethylene carbonate (FEC) and vinylene carbonate (VC). The role of FEC and VC is not yet been rationalized in terms of molecular scale reaction mechanisms impacting the evolution of the solid electrolyte interphase (SEI).

We used MD simulations enhanced with metadynamics to predict the most common reaction mechanisms from simulations of 2-4 molecules in the prescience of Li^+ and an extra reducing electron. An example of the early stage EC oligomerization mechanism is shown in Figure 1.

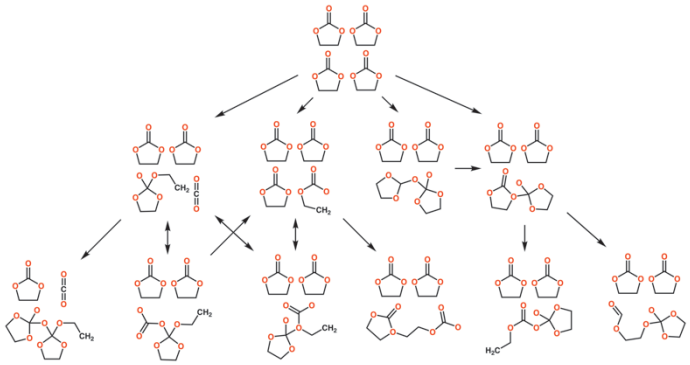

Figure 1: Reaction network of 4 EC molecules and 1 Li^+ with an extra reducing electron. Constructed from 56 separate reactive MD trajectories using mdstates[1]. Although the Li^+ was included in the simulations, it is not pictured in the reaction network.

The same process was repeated with 3 EC molecules and in the presence of a VC or FEC molecule in order to provide a systematic comparison. Since these results only used semi-empirical PM6, we performed a detailed analysis of the potential energy landscape with DFT level of theory for several of the competing pathways in order to understand how the additives change reaction energetics (Fig. 2)

[1] *mdstates* is an open source software package developed in this project to automatically harvest mechanisms from reactive MD trajectories

The results show that there is an energetic driving force for reaction between EC and common additives that is not present when EC reacts with itself and also that the barrier for reaction is slightly lowered. These reaction pathways also provide a mechanistic understanding for CO_2 evolution during SEI formation, which is still regularly debated in the literature.

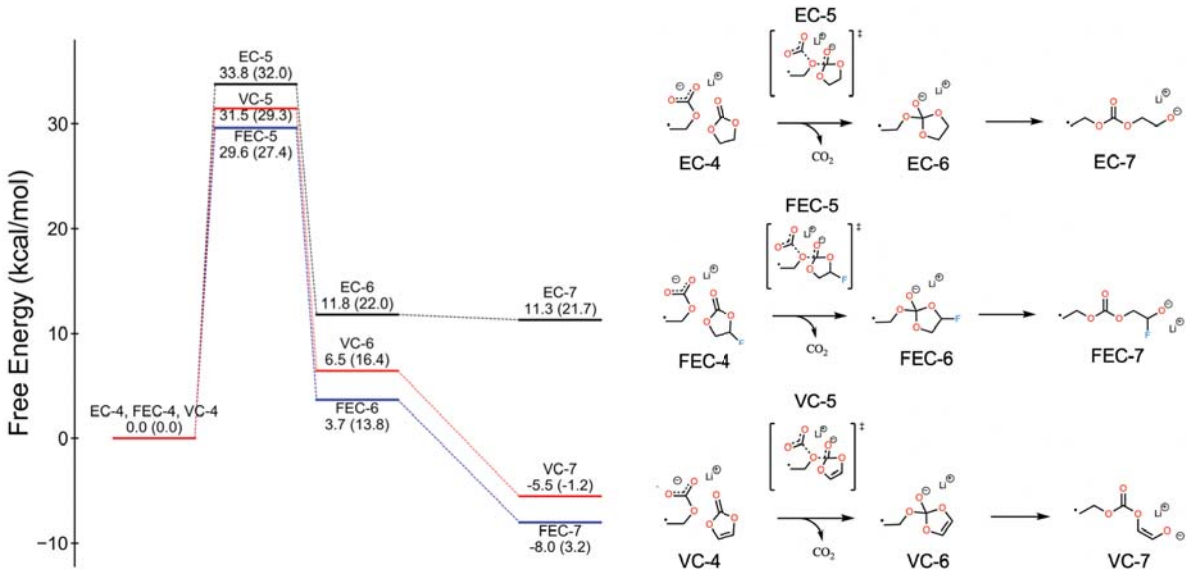

Figure 2: Left: Free energy diagram for S_N1 oligomerization for o-EC attacking EC (black), FEC (blue), and VC (red). Values in parentheses are enthalpy values in kcal/mol. Right: Reaction mechanisms for each species with each label marked on the free energy diagram.

The proposed S_N1 mechanism was compared against two different S_N2 reaction pathways that were proposed based on the MD studies described above and may not have been identified as CO_2 evolution pathways.

Future Plans. Based on the MD and DFT studies of the small clusters, we have selected the decarboxylation reaction as an initial comparison point for studying the role of interfacial chemistry on the mechanism and energetics. We are using classical MD to study the structure and dynamics of EC mixed with additives and a common lithium salt over model graphitic surfaces with varying terminal functionalization. At the same time we are beginning to use reaction coordinate determination methods determine the role of solvent CO_2 evolution during SEI formation.

There are two publications in preparation. Project state date was 9/15/18.

Probing Condensed-Phase Structure and Dynamics in Hierarchical Zeolites and Nanosheets for Catalytic Upgradation of Biomass

Neeraj Rai
330 Swalm Chemical, Mississippi State University, Mississippi State, MS, 39762
Email: neerajrai@che.msstate.edu

Program Scope

Understanding complex reactions at the molecular level in systems characterized by multi-scale collective coupling across time and space is a significant scientific challenge. This project is guided by the hypothesis that interactions of oligomers, solvents and active sites can be tailored by a suitable choice of solvent and also of pore architecture of solid-acid catalysts to promote chemical transformations during catalytic conversion of biomass. The architecture is determined by the choice of hierarchical zeolites, which provide large channels for macromolecule diffusion and small pores for catalysis. A multi-scale computational approach will be used to elucidate physical and chemical interaction across multiple spatial and temporal scales. Furthermore, advanced first principles Monte Carlo algorithms will be developed to efficiently sample configurational space. We will use advanced first principles Monte Carlo and molecular dynamics simulations, and electronic structure calculations to answer fundamental scientific questions pertinent to acid catalyzed hydrolysis and hydrogenolysis of cellulose and lignin, respectively, in ordered mesoporous zeolitic structures. One outcome will be a better understanding of the fundamental interactions of reactant and solid acid catalysts in the presence of solvents, enabling rational design of catalytic systems that can upgrade biomass in a selective and energy efficient manner. Another outcome will be the development of sampling tools essential to detangle interactions in complex, reactive phenomena.

Recent Progress

Diffusion of Glucose and solvent molecules in Nanopores of Faujasite in the Condensed Phase: Building up on our previous work on Beta zeolite, we have extended the work to new zeolite topologies such as Faujasite and MWW. We have conducted molecular dynamics simulations in *isothermal isobaric ensemble* to elucidate the diffusion mechanism as a function of pore topology. A model of zeolite supercell was generated and the dangling bonds were saturated with hydrogen atoms. Glucose and solvent molecules were subsequently added to the system. Simulations were were started with no solvent and glucose molecules in the nanopores. As the simulation progresses, solvent and glucose molecules diffuse in the pore till the equilibrium is reached. Figure 1) provides snapshot of the system after equilibration and simulation trajectory of a glucose and a water molecule. We find that glucose molecule traverses the system as the simulation progresses, however, once the glucose molecules enters a specific pore of the zeolite, the motion is localized within the pore due to collisions with the wall. It takes large number

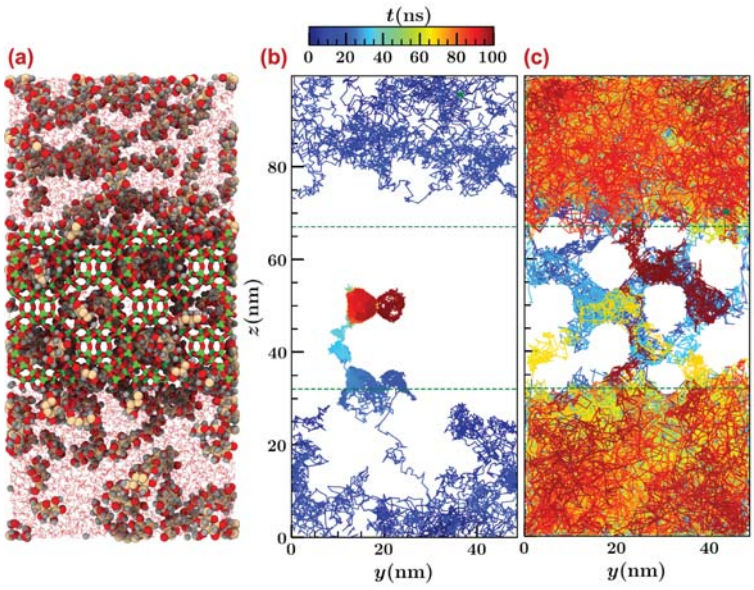

Figure 1. Snapshot of the system (a), trajectory of a glucose molecule (b), and trajectory of a water molecule (c). The middle section of the box contains zeolite while the glucose solution in present above and below the zeolite slab. The trajectories are color coded with the simulation time (color bar at the top).

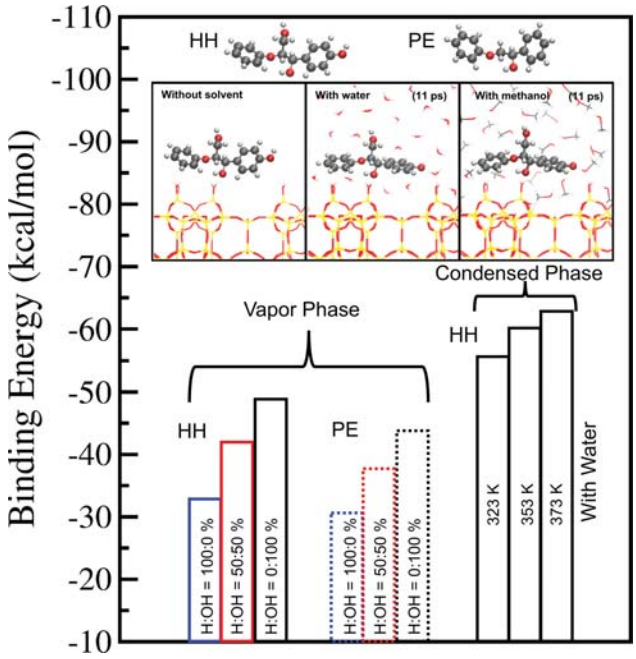

Figure 2. Binding energy of model lignin dimer compounds (1-(4-hydroxyphenyl) 2-phenoxy-1,3-propanediol (HH) and 2-phenoxy-1-phenylethanol (PE)) as a function of surface termination in the gas phase and in the presence of solvent (water). The presence of solvent enhances the interaction of the zeolite with the lignin dimer.

of collisions with the pore walls before the molecules moves to the neighboring pore. Water, on the other hand, diffuses through the pores easily. We find that Faujasite is able to accommodate up to two glucose molecules in the large cage while the Beta zeolite can accommodate only one glucose molecule due to the smaller pore size.

Effect of Solvation on Binding Modes of Lignin Model Compounds with Ether Linkage:
Electronic structure calculations were carried out to understand the binding modes of model compounds with β-O-4 linkages (1-(4-hydroxyphenyl) 2-phenoxy-1,3-propanediol (HH) and 2-phenoxy-1-phenylethanol (PE)) on MWW 2D zeolite nanosheets.[1] We have used PW91 and optB88-vdW density functionals for these calculations. The effect of different surface termination (–H vs –OH) on the binding energy is shown in Figure 2. Although the binding energies for PW91 functional are 10-15 kcal/mol smaller than the optB88-vdW functional, the qualitative trends are similar, i.e. as we increase the density of –OH group on the surface of MWW 2D nanosheet, the binding energy increases. We have also carried out *ab initio* molecular dynamics simulations in the presence of solvents. We have investigated the effect of different terminated surfaces (H:OH % = 100:0; 50:50; 0: 100 %), different temperatures (323, 353, 373 K), and different solvents (water and methanol) on the binding modes by calculating physical parameters such as bond angles and bond length. Our work shows that binding strength is enhanced by increasing number of hydroxyl groups on the surface, and binding energy varies from 10 to 15 kcal/mol in the gas phase. Also, phenolic dimer shows better binding strength than the non-phenolic dimer and the presence of solvents has significant impact on the binding configuration of both dimers. Analysis of structural changes in the presence of the solvent reveal that aromatic rings are parallel to the zeolite surface and primary interaction with zeolite is through the hydroxyl groups near the β-O-4 linkage. Furthermore, while the solvation energy decreases with increasing temperature the opposite trend is observed for the binding energy with the surface.

Effect of Molecular Structure of Phosphonium Based Ionic Liquids (ILs) on IL/Water Interface :
Phosphonium based phase-separable ionic liquids (PSILs) are promising green solvents for dissolution of

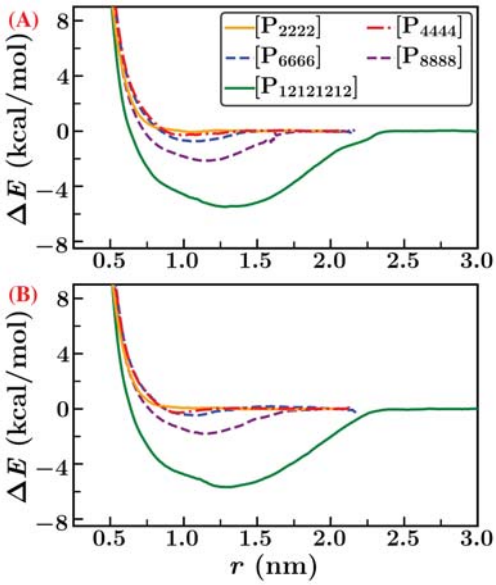

Figure 3. Snapshot at the end of 80 ns of MD simulation of phosphonium chloride (Figure A) and acetate (Figure B) IL?s and TIP3P water mixture for alkyl chain length of 2, 4, 6, 8, and 12 (for the alkyl chain length of 12, a snapshot at the end of 190 ns is shown in the figure).

cellulose and lignin, a necessary step for conversion of biomass to fuels and chemicals. The knowledge of interfacial behavior of ionic liquid/solvent systems is critical for designing efficient dissolution processes. Molecular dynamics simulations were carried out for aqueous interface of tetraalkylphosphonium ionic liquids with chloride and acetate as anions to investigate IL miscibility with water.[2] The transition zone from miscible to immiscible behavior was observed for alkyl chain lengths of 6 to 8. PMF calculations were carried out for two phosphonium ions placed in aqueous medium as a function of alkyl chain length for chloride and acetate ions. The well depth in the PMF ranges from 0 to 6 kcal/mol as we go from [P_{2222}] to [$P_{12121212}$] (see Fig. 3) The smaller cations virtually have no minimum in the potential, and these ILs are completely miscible with the aqueous phase. However, as we increase the side chain length the an attractive well depth is observed which is responsible for these ILs aggregating in small clusters leading heterogenous domains in the aqueous phase. For the IL with the largest chains there is a significant attractive interactive potential (approximately 10 times the thermal energy) and these ILs maintain a stable interface with the water phase. As PMF calculations are significantly cheaper (computationally) than complete simulation of interfacial systems, these can be used for screening potential ionic liquids for their phase behavior with specific solvents.

In order to provide the thermodynamic basis for the observed mixing behavior, we borrow concepts from the regular solution theory. Using regular solution theory one can show that when w/kT (w is the interchange energy) is 2.5 or larger both the random mixing theory and the quasi-chemical approximation predict phase separation. If we make the assumption that PMF of phosphonium ions closely mimics the interchange energy, we can use the minima in the PMF to rationalize the miscibility behavior. The calculated w/kT for [P_{2222}], [P_{4444}], [P_{6666}], [P_{8888}], and [$P_{12121212}$] for the chloride IL is 0.13, 0.48, 1.23, 3.64, and 9.26, respectively. For the acetate IL the corresponding numbers are very similar (0.07, 0.47, 0.80, 3.04, and 9.58, respectively). Based on this relatively simple analysis, we can recommend that systems with w/kT (using minimum in PMF profile as w) smaller than 2.5 would be miscible, and 2.5 to 4.0 would lead to emulsion formation, while larger than 4.0 would lead to formation of interfacial systems.

Future Plans

In the next year, we aim to complete the work on diffusion probe and solvent molecules in the nanopores of zeolite and initiate the work to look into the diffusion of macromolecules in the hierarchical zeolites. Reaction mechanism for lignin depolymerization in the presence of solvents will continue. We aim to complete implementation of selected advanced Monte Carlo algorithms in CP2K software suite.

List of Publications

1. V. Jain, W. N. Wilson, and N. Rai “Solvation Effect on Binding Modes of Model Lignin Dimer Compounds on MWW 2D-Zeolite", *J. Chem. Phys.*, **151**, 114708, 2019

2. S. Venkatesan, Md M. Huda, and N. Rai “Molecular Insights into Ionic Liquid/aqueous interface of phosphonium based phase-separable ionic liquids", *AIP Advances*, **9**, 045115, 2019

MOLECULAR STRUCTURE, BONDING AND ASSEMBLY AT NANOEMULSION AND LIPOSOME SURFACES

PI: Geraldine Richmond, 1253 University of Oregon, Eugene, OR 97403
Email: richmond@uoregon.edu

Program Scope and Definition

In recent years there has been a growing interest in emulsion particles that are in the nanoscale regime due to their unique potential for applications in drug delivery, oil recovery, and as nanoreactors for producing a range of nanomaterials including polymers and semiconductor quantum dots. Relative to micelles, little is known about the interfacial molecular processes that lead to the formation and stability of such nanoemulsions (NEs) (Fig. 1) Key to advancing the utility of these, and related nanoscale liposome systems, is to develop the needed molecular-level understanding of the structure and bonding present at the surface of these soft nanoparticles.

The objective of these studies is to advance our understanding of the molecular structure, orientation and bonding of surfactants at the surface of nanoemulsions and liposomes, and analyze the bonding characteristics of interfacial water near soft particle interfaces. Our approach involves measuring the surface vibrational spectroscopy of the surfactant coated particle surfaces in-situ using vibrational sum frequency scattering spectroscopy (VSFSS), with related complementary studies of these surfactant systems examined at the more well-defined planar oil/water interface by vibrational sum frequency spectroscopy (VSFS). Classical molecular dynamics (MD) calculations coupled with density functional theory (DFT) methods are employed to assist in spectral assignments and understanding solvation effects. Other experimental methods include dynamic light scattering (DLS), zeta potential (ZP), and surface tension (ST). Our recent publication investigating AOT stabilized nanoemulsions provides a powerful demonstration of this approach.[1]

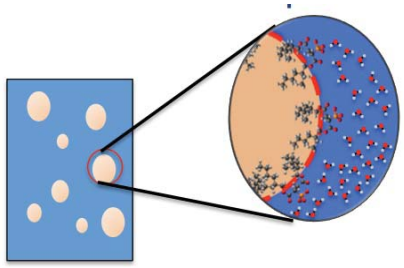

Figure 1. Cartoon of the surface of surfactant stabilized nanoemulsions.

Recent Progress:

The Formation and Surface Stabilizing Contributions to Bare NEs[2]

Although most nanoemulsions are stabilized by various surfactant mixtures, there are a few studies reporting nanoemulsions stabilized without added surfactants. Such reports beg the question as to what interfacial molecular interactions are responsible for such stabilization. Using electrophoretic mobility (EpM) measurements those studies observed the nanoemulsions possess a negative surface charge, which was invoked as the primary stabilizing factor. The source of this negative charge was concluded to be a surface enhancement of hydroxide ions. Other studies, including surface spectroscopic studies in the pioneering VSFSS work from Roke's group, of these negatively charged and presumably bare nanoemulsions with ZP values of -55 to -80 mV have suggested several molecular details responsible for droplet stabilization other than hydroxide adsorption. These include electric fields established by ordered water dipoles, charge transfer models from asymmetric hydrogen bonding environments, and the presence of trace amounts of surface-active contaminants.

In this study[2] we report the creation of bare NEs with nearly zero surface charge. These nanoemulsions produced with hexadecane as the organic solvent have a droplet size of approximately 300 nm and persist over several days. Most important is that *we find considerably different interfacial characteristics than any of the more negatively charged nanoemulsions in*

previous studies that have been assumed to be surfactant or contaminant free. These studies include EpM and VSFSS measurments of our low charge nanoemulsions (LCNEs),

Our results in particular differ from previous the VSFSS experiments seeking to measure interfacial water and hexadecane contributions. Using an appropriate mixture of D_2O and H_2O we have measured the free OD vibration by VSFSS on these LCNEs. This was not found in previous VSFSS studies of the more negatively charged, but presumably surfactant free, nanoemulsions. The frequency of this free OH (OD) indicates there is a stronger water bonding interaction with the hexadecane as compared to the planar interface, a factor we conclude contributes to droplet stabilization. These results are important for understanding water-hydrophobic interactions in general, and notably for particulates and droplets in the nano-sized regime. This free OH (OD) mode disappears in the presence of trace surfactants or impurities that also raise the NE surface charge to be in the realm of the previous VSFSS "bare" nanoemulsion studies. We conclude that the source of this higher charge is a potential contributor in the inability to observe a free OD in the previous nanoemulsion surface studies. Another VSFSS study by the Roke group of reverse nanoemulsions stabilized by 5 mM Span 80 were able to access much more of the OD stretching region of the interfacial water. No free OD mode was observed in those spectra; however enhanced water hydrogen bonding was observed for these Span coated NEs relative to Span 80 at the planar interface which showed minimal enhancement. In contrast, we conducted similar planar Span80 studies at the planar interface and found an identical water bonding enhancement as was found for their NE studies. Our contrary results draw into question as to whether there an enhanced water H-bonding network at bare nanodroplet surfaces.

On the hexadecane side, previous VSFSS studies of these highly negatively charged nanoemulsions obtained a strong spectral response from the CH modes of the surface hexadecane molecules. It was concluded the presence of some anionic surfactants failed to perturb the hydrophobic phase, and both the surfactant and hexadecane molecules oriented themselves parallel to the droplet surface. However, we find that for LCNEs with minimal contaminants that can give a negative surface charge, the signal from CH modes of hexadecane is nearly negligible, indicative of parallel orientation, until one adds trace amounts of deuterated charged surfactants at which point the CH modes appear with their dipoles largely perpendicular to the interface. We attribute this change to the influence of the hexadecane with the adsorbed surfactant. Figure 2 provides a visual for these results.

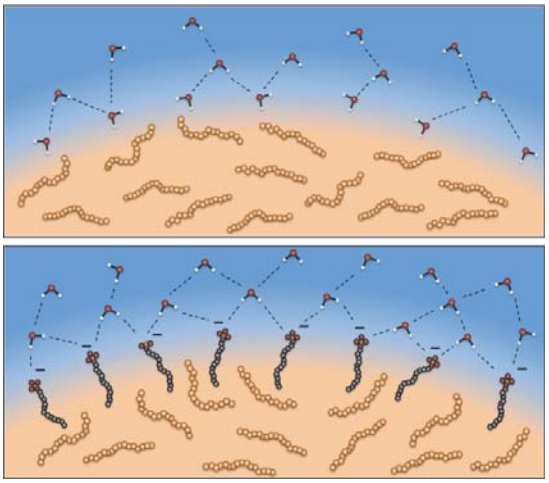

Figure 2 | Illustration of the nanoemulsion surfaces for bare (top) and surfactant covered (bottom) NEs. Hexadecane molecules lie relatively parallel to the bare droplet surface, providing room for free OD oscillators. When surfactants cover the droplet surface, a reorientation of the hexadecane occurs due to chain-chain interactions and the free OD is excluded.

Working in Tandem: Synergistic Effects in Mixed Surfactant Systems

Commercial surfactants continue to be a mainstay in products that serve a multitude of purposes in our everyday lives. Accompanying their pervasive use are environmental concerns, especially when they are used or accumulate in high concentrations. There is a growing interest

in the use of co-surfactants rather than single surfactant systems, as many of these mixtures can work synergistically to achieve the desired function with lower total surfactant concentrations. While many co-surfactant systems have proven themselves in environmental, and biological applications, the underlying forces driving their cooperative behavior is still up for debate. A deeper understanding of the molecular factors that drive these synergistic interactions at the oil-water interface will significantly accelerate their adoption and use in applications such as drug delivery or oil-remediation.

We have currently obtained very interesting and important results for several mixed surfactants systems studied at the nanoemulsion surface (sodium dodecyl sulfate (SDS) and dodecyltrimethylammonium bromide (DTAB) with linear polyethylenimine (PEI))[3] and poly(styrene sulfonate) (PSS) and polyacrylic acid (PAA) with alkyltrimethylammonium bromide surfactants (C_nTAB),[4,5] and cetyltrimethylammonium bromide (CTAB) with 1-hexanol (hexanol) at the planar oil-water interface.[6] The latter has proven to be particularly interesting with the results here.

CTAB is used in chemical, biochemical, industrial and pharmaceutical applications due to its antibacterial properties and ability to stabilize regular emulsions. As a lone surfactant, its behavior is well characterized in aqueous solutions with both its critical micelle concentration (*cmc*) and micelle structure documented. With the addition of hexanol, CTAB forms reverse emulsions, which have found applications as drug delivery vehicles, nanoscale reaction vessels, therapeutic gene delivery, protein purification, and nanoparticle templating. Solution studies of these mixed systems have shown that the addition of medium and long chain length alcohols act to lower the *cmc* of CTAB. Unknown at this point is what role interactions between the polar head group and non-polar alkyl regions of these co-surfactants play in contributing to the changes in size, shape, and surfactant packing structure at the oil-water interface where these molecules reside. The studies use VSFS, surface tensiometry, and density functional theory (DFT). Of particular emphasis and importance to the conclusions of this study is the spectroscopic characterization of the trimethylammonium head group ($N\text{-}CH_3$) modes of CTAB. Selectively deuterated CTAB isotopologues, aided by computational DFT harmonic frequency calculations, provide a more detailed view than any previous interfacial studies of the solvation and orientation of both the polar head group and hydrophobic chain of CTAB as the concentration of surfactant is varied.

When CTAB and hexanol are mixed at various concentrations a molecular dance ensues (Figure 3) that eventually results in highly synergistic adsorption and orientation of both species at the oil-water interface. Unlike CTAB alone, which shows significant interfacial molecular ordering at all concentrations, hexanol alone in the aqueous

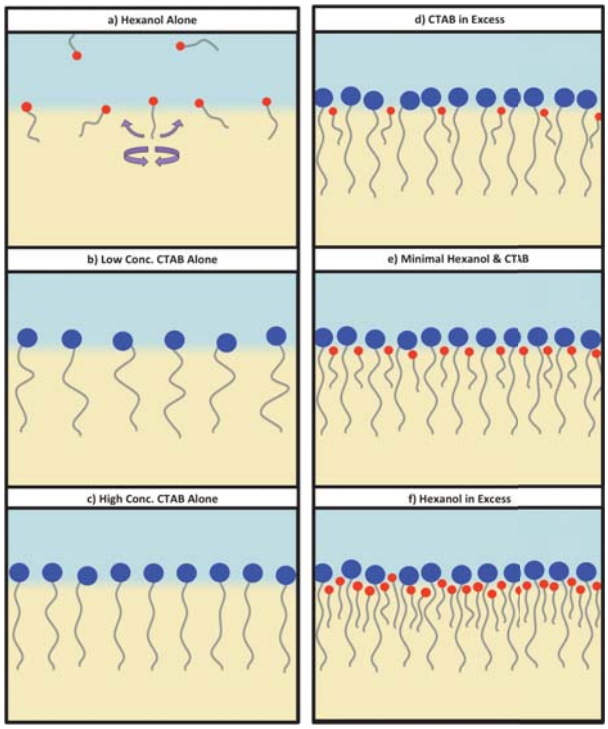

Figure 3. Cartoon of the CTAB-hexanol results.

phase does not show any interfacial ordering. However, at a specific CTAB concentration, the hexanol begins to change from its random interfacial orientation to one that mimics the chain ordering of CTAB. Increasing amounts of interfacial hexanol subsequently results in changes in the adsorptive behavior of CTAB, enhancing its adsorption. This co-surfactant behavior has implications for better understanding the molecular level interactions that give rise to tunable macroscopic configurations. For this particular system of co-adsorbates at these concentrations, it indeed takes two to tango.

Future Studies

- *Continuing fundamental studies of the molecular structure, orientation and bonding of interfacial water and oil molecules present at the surface of bare LCNEs with studies that examine the pH dependence, alkane chain variation and ionic strength.*
- *Conducting additional studies of AOT at the NE surface to understand how this branched surfactant affects the organic solvent ordering and electrostatic stabilization of these AOT NEs with varied complexing ions and ionic strength.*
- *Studying the surface interactions between polymer polyethylenimine (PEI) and surfactants sodium dodecyl sulfate (SDS) and AOT as the polymer and surfactant work synergistically to stabilize nanoemulsions.*
- *Defining the molecular factors responsible for nanoemulsion stabilization, synergistic effects and multilayering upon co-adsorption at the nanoemulsion surface of polystyrene sulfonate (PSS) and cetyltrimethylammonium bromide (CTAB).*
- *Advancing the development of a computational methodology combining classical molecular dynamics and DFT for calculating VSF spectra of large systems.*

Publications referenced above that have resulted from the studies sponsored by this grant.

[1] "Molecular Characterization of Water and Surfactant AOT at Nanoemulsion Surfaces", J.K. Hensel, A.P. Carpenter, R.K. Ciszewski, B.K. Schabes, C.T. Kittredge, F.G. Moore and G.L. Richmond, PNAS, 114, (13351-13356) 2017.

[2] "Formation and Surface-Stabilizing Contributions to Bare Nanoemulsions Created with Negligible Surface Charge", A. P. Carpenter, E. Tran, R.M. Altman and G.L. Richmond, PNAS, 116 (9214-9219) 2019.

[3] "Two's Company, Three's a Crowd: How Ions Tag Along for the Ride with SDS and PEI on a Nanoemulsion Surface", E. Tran and G. L. Richmond, in preparation.[3]

[4] "Come Together: Molecular Details into the Synergistic Effects of Polymer-Surfactant Adsorption at the Oil/Water Interface", B. Schabes, R.M. Altman, G.L. Richmond, *J. Phys. Chem. B*, **2018**, 122 (36), 8582-8590.

[5] "Helping Strands: Polyelectrolyte Assists in Surfactant Assembly below Critical Micelle Concentration, B. Schabes and G.L. Richmond, submitted to *J. Phys. Chem. B.*

[6] "Takes Two to Tango: The Choreography of the Co-Adsorption of CTAB and Hexanol at the Oil-Water Interface", R. K. Ciszewski, B. Gordon, B. Muller and G.L. Richmond, J. *Phys. Chem B*, in press. (https://doi.org/10.1021/acs.jpcb.9b05775)

Program title: **Enhancing Rare Events Sampling In Molecular Simulations**
Principal lnvestigator: Sapna Sarupria
Mailing address: 206 S Palmetto Blvd, Clemson University, Clemson, SC 29634
Email: ssarupr@g.clemson.edu

Rare events correspond to the events that occur with low frequency. These events usually have potentially widespread impact and are of considerable interest. At the molecular level, important transitions such as self-assembly and phase transitions in aqueous systems are rare events – meaning that the waiting time involved to observe even a single event is larger than the typical timescales accessible to molecular simulations. This hinders the ability to calculate the kinetics of these transitions. In our proposed research we focus on developing novel methods and the software infrastructure that implements these methods effectively on high performance computing systems to enable the studies of rare events in molecular simulations. While we motivate our work through studies of heterogeneous ice nucleation, the methods and software infrastructure developed here is applicable to any system.

Background:
The methods developed in this work are based on the forward flux sampling (FFS) method for calculations of rare events. In FFS, transitions from state A to state B are sampled through several intermediate transitions by dividing the phase space between A and B into sub-regions marked by interfaces. Several simulations are initiated at a given interface and configurations from those which reach the next interface are harvested. Then several simulations are initiated from the harvested configurations at the "new" interface to obtain configurations for the next interface. This process is continued until the final state is reached. While the process is straightforward, the application of the method to realistic systems can result in large number of simulation jobs and huge amount of data. To handle these large jobs and amounts of data effectively, we have developed SAFFIRE. SAFFIRE represents a collaboration of state-of-the-art techniques in molecular simulations with those from Big Data to enable rare event simulations at massive scales. SAFFIRE is designed to be adaptive, data-intensive, high-performance, elastic, and resilient. SAFFIRE uses Hadoop in a novel manner to handle the millions of simulations performed and files generated in FFS calculations. Through this approach we have been able to address several of the challenges related to implementing FFS.

Using SAFFIRE we have performed some of the largest scale FFS studies of ice and hydrate nucleation. We find that even with these extensive simulations, large number of successful transition pathways arise from a handful of configurations at the initial stages of the transition. This is further challenging because it cannot be predicted *a priori* whether the starting configurations will lead to successful transition pathways and therefore, it cannot be corrected for without performing the largescale simulations! This necessitates developing methods that overcome these challenges. In this project we use a multipronged approach to develop methods that address such challenges.

Program scope:
In our project, we combine state-of-the-art tools in molecular simulations, BigData and multitasking handling systems, and visualization techniques to develop a robust infrastructure for performing rare event simulations. We build FFS to develop multidimensional FFS methods

(nDFFS) that will enable us to address the issue of finding appropriate order parameters for any given transition on-the-fly. This methodology has the potential of addressing the major knowledge gap – lack of an ability to find reaction coordinates on-the-fly – in simulations of rare events. We do so by simultaneously developing novel FFS based methods, integrating them with machine learning techniques and assimilating it into SAFFIRE to test our methods beyond test cases – on more realistic systems such as ice nucleation.

Recent progress:

We have developed multiple approaches to perform nDFFS calculations and studied them using toy models. We had developed set-based sampling method and linear combination forward flux sampling. We identified that the former had more promise and continued to develop it further. Consequently, we have developed the contour forward flux sampling (cFFS) method.

Contour Forward Flux Sampling (cFFS): We extend FFS to use multiple collective variables (CVs) on-the-fly. The next interface is placed based on the sampling of the CVs obtained from trajectories propagated at any given interface. This enables us to have any "shape" of the interface. That is, the interface is identified as a nonlinear combination of the specified CVs. An example of sampling from cFFS is shown in Figure 1. As can be seen, we are able to outline the underlying potential energy surface (PES) for the non-simple toy models.

There are several advantages to cFFS:

1. Only the combination of the CVs needs to differentiate between the two basins and not each of the CV.
2. cFFS reveals the relative role of each CV – if a system does not move along a given CV, it is possible that the CV is not relevant to the transition. However, this will not impede cFFS as the transition will continue to progress along the other CV.
3. There is substantial flexibility in the CVs that can be used with cFFS.
4. We also evaluated the computational cost and sampling efficiency of cFFS. We compare the results between 1DFFS with suboptimal CV, 1DFFS with optimal CV, cFFS and standard Langevin dynamics. We find that in most cases 2DFFS gives us improved sampling for the same or slightly higher computational cost.
5. cFFS is especially powerful in cases with multiple transition tubes. This is described further below and also shown in Figure 2.

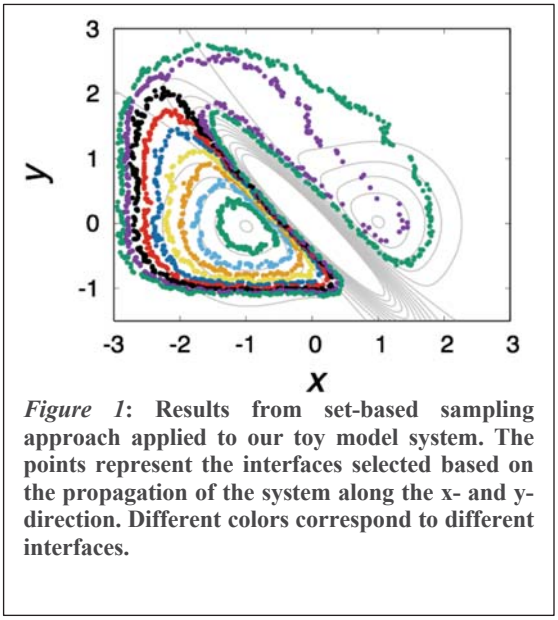

***Figure 1*: Results from set-based sampling approach applied to our toy model system. The points represent the interfaces selected based on the propagation of the system along the x- and y-direction. Different colors correspond to different interfaces.**

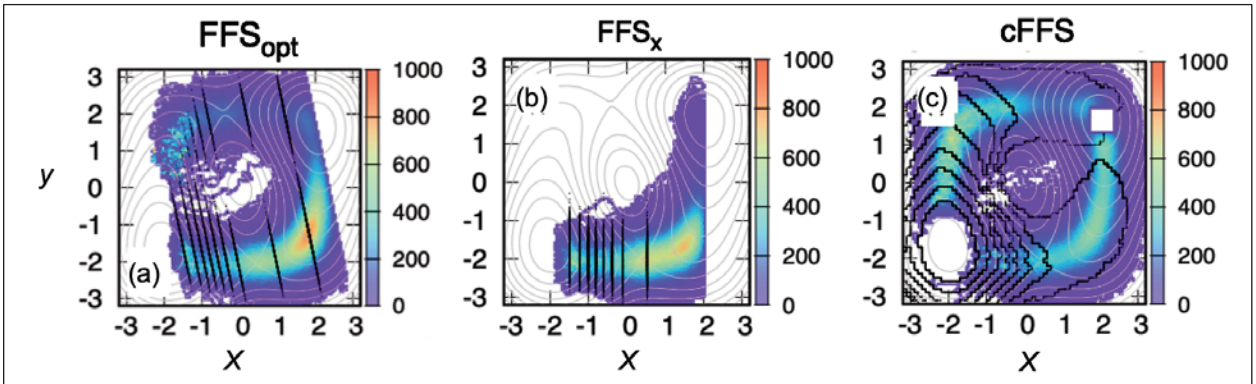

Figure 2: **Comparison of transition path sampling obtained from (a) FFS with optimal CV, (b) FFS using x as the CV and (c) cFFS using x and y as the two CVs. As can be seen, FFS even with optimal CV struggles to sample both the transition tubes. On the other hand, cFFS is able to access these. PES contours are shown as gray lines. Configurations at each interface are shown with black points. Transition path ensemble sampling is represented by the heat map.**

Multiple transition tubes with cFFS: We studied transitions in PES that included multiple transition tubes. We studied multiple systems changing the relative gradient of the PES leading to the transition tubes as well as the height of the barrier in the transition tubes. In Fig. 2 we show one case of such a PES where the barrier heights of the two tubes are similar and it is expected that both the transition tubes will be sampled equally in the transition path ensemble. The results obtained from 1DFFS with the optimal CV (in this case a combination of x and y) and from 1DFFS with x as the CV are shown in Fig. 2(a) and (b). Interestingly, neither of these are able to capture both the transition tubes. In case of the sub-optimal CV (i.e. x) one transition tube is entirely missed. The optimal CV improves the sampling some – both tubes are sampled but the sampling in the two tubes is not equal. Fig. 2(c) shows the results from cFFS simulations. Both the transition tubes are sampled, and the sampling is equal in the transition regions of both the tubes as is expected. This indicates that using the 2 CVs simultaneously, each of which by themselves are suboptimal order parameters, helps improve the sampling tremendously.

We also demonstrated cFFS in systems using velocity and position as the two CVs which can be extremely helpful in cases where momentum plays an important role in driving the transition.

Machine learning based method for structure identification:
We have developed a method based on PointNet to identify local structure in molecular simulations. A primary challenge in applying machine learning techniques to simulation is selecting the appropriate input features. This challenge is system-specific and requires significant human input and intuition. In contrast, our approach is a generic framework that requires no system-specific feature engineering and operates on the raw output of the simulations, i.e., atomic positions. In this method, the input to the PointNet neural network is the distances of the neighbors within a cut-off distance. The cut-off distance is the only parameter that is determined by the user. We demonstrated the method on crystal structure identification in the following systems:

- Lennard-Jones (four different phases): We were able to differentiate between HCP, FCC, BCC and liquid structure with 99.2% accuracy. The PointNet was able to differentiate

between the different crystal structure even in systems with mixed structures such as in a growing crystal nucleus.

- water (eight different phases): The PointNet was tested on liquid, Ih, Ic, Ice-III, Ice-V, Ice-VI, hydrate sI, and hydrate sII structures. It was able to differentiate between all these phases and the accuracy was as high as 99.1% using only the coordinates of the oxygen atoms. The accuracy was increased to 99.6% when both oxygen and hydrogen atoms were used in the network. This is, to the best of our knowledge, the only neural network that can differentiate amongst so many water phases with only one user-defined parameter and no feature engineering.
- mesophase (six different phases) systems: We further tested the system on mesophases and found that we were able to differentiate amongst liquid (liq), lamellar (lam), lxs, hexagonal (hex), gyroid (gyr), and body- centered cubic (bcc) phases.

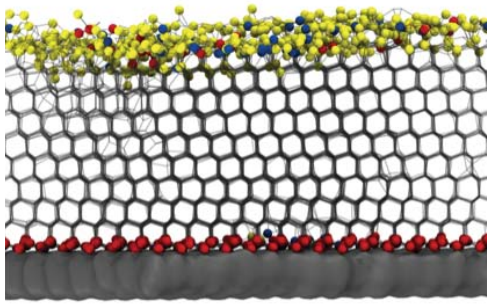

Figure 3: **Classification of atoms from PointNet for interfacial systems. The atoms that belong to an interfacial class are shown as spheres.**

The method is also applicable to heterogeneous nucleation and it can even predict the crystal phases of atoms near external interfaces (see Fig. 3). The strength of this approach worth noting is that extending the PointNet to interfacial systems did not require any additional simulations. We were able to generate the training set for interfacial systems using only the data obtained from simulations of the bulk systems.

Future Plans

- We plan to apply cFFS to more challenging problems such as hydrate nucleation.
- We will begin to apply our methods on reacting systems.
- We plan to develop methods to extract reaction coordinate information from the FFS results. This includes using some of the recently developed machine learning techniques combined with maximum likelihood methods.

Publications from DOE Sponsored research:

1. **DeFever, R.S**., Targonski, C., **Hall, S. W.**, B., Smith, M.C., Sarupria, S. "A generalized deep learning approach for local structure identification in molecular simulations", RSc Chemical Science, 10, 7503-7515 (DOI: 10.1039/c9sc02097g) (2019) Highlighted in the themed collection: 2019 Chemical Science HOT Article Collection
2. W. Hanger, **R. S. DeFever**, J. Kilgannon, A. Apon, *S. Sarupria and *L. Ngo, "Building A Scalable Forward Flux Sampling Framework using Big Data and HPC", Practice and Experience in Advanced Research Computing (PEARC19), (accepted, and presented)
3. **DeFever, Ryan S**. and *Sarupria, S., "Contour forward flux sampling: Sampling rare events along multiple collective variables", J. Chem. Phys. 150, 024103 (2019)

Grant number and Grant title:
DE-SC0015448 Enhancing Rare Events Sampling in Molecular Simulations of Complex Systems

Students: Ryan DeFever (PhD student), graduated in August 2019
Steven Hall (PhD student)

Equilibrium Structure and Dynamics of Aqueous Solutions and Interfaces

Richard Saykally (RJSaykally@lbl.gov), Musahid Ahmed (mahmed@lbl.gov), Phillip L. Geissler (plgeissler@lbl.gov), Kranthi Mandadapu (KKMandadapu@lbl.gov), and Teresa Head-Gordon (TLHead-Gordon@lbl.gov)
Lawrence Berkeley National Laboratory, Chemical Sciences Division, 1 Cyclotron Road, Berkeley, CA 94720

Program Scope:

Solvation of ions and molecules is central for governing chemical transformations in many energy technologies. Key processes include electrochemical transport, ion pair formation and crystallization, corrosion, as well as chemical reactions in solutions and at interfaces. The goal of this work is to develop predictive models of electrolyte behavior in bulk solution, at interfaces and in confined environments.

Recent Progress:

Geissler has derived and verified finite size corrections for simulations of interfacial solvation.[1] These corrections presume that dielectric continuum theory (DCT) accurately describes the polarization response of water at nanometer scales and above. Using this method to evaluate nonlinear solvent response to the charging of a solute, we find that DCT fails in important ways to describe the interfacial adsorption thermodynamics of small ions. Together, these results establish a length scale below which DCT breaks down, approximately 1-2 molecular diameters. At larger scales, DCT appears to be a realistic caricature of water even in the heterogeneous environment presented by the liquid-vapor interface. Recent extensions to asymmetric systems, which can support a net polarization between two interfaces, show similar agreement and demonstrate the robustness of water's dielectric response down to near-monolayer liquid films.

The powerful atom-selective probing of molecular interactions afforded by soft X-ray spectroscopy has been combined with the surface-selective probing capability of second harmonic generation in the first demonstration of both resonant enhancement and surface selectivity of soft X-ray SHG at the Trieste free electron laser facility, carried out by Saykally and collaborators.[2,3] The concomitant multiphoton absorption spectra of the carbon target was also quantified by both experiment and theory. These results open the door for the general study of surfaces and interfaces by these powerful new spectroscopic approaches.

As a route to further clarifying the mechanism that selectively drives ions to and away from the air/water interface, Saykally and coworkers have developed a new experiment (Broadband Deep UV Sum Frequency Generation) for measuring the complete charge transfer to solvent (CTTS) spectrum of interfacial anions, and have applied it to the prototypical cases of the iodide and thiocyanate anions.[4] Comparison with bulk solution 2-photon CTTS spectra provides a new variable for constructing general theoretical models to explain interfacial ion behavior, which are underway in the Geissler and Head Gordon groups. Our studies of molecular adsorption to solid-liquid interfaces were extended to polymer systems in a study of aqueous pollutant adsorption to the water-polystyrene interface, using SHG scattering spectroscopy of polystyrene bead solutions;[5] extensions to study ion adsorption to desalination polymer interfaces are planned, in collaboration with the Daniel Miller group.

Flexible nanoscale confinement of solvent is critical to understanding the role that bending fluctuations play on solvation processes where soft interfaces are ubiquitous.[6] Head-Gordon and coworkers showed that the phase behavior of water confined between flexible and rigid graphene sheets are remarkably different, since flexible walls introduce a very different sequence of water phases due to the possibility of phase coexistence that is impossible to observe with rigid walls.[7]

Orienting water molecules in the homogeneous liquid is challenging due to the ultrafast dissipation of rotational excitation energy through the hydrogen-bonded network. Recently the Havenith group have demonstrated the observation of strong transient anisotropy of liquid water through librational excitation using single-color pump-probe experiments at 12.3 THz, with the birefringence exceeding previously reported values by three to five orders of magnitude. Head-Gordon and co-workers have developed a theory that replaces the third order response with a material response property amenable to molecular dynamics simulation in order to explain the strong anisotropy, and the theory and molecular dynamics simulation show that the rotationally damped motion of water molecules in the librational band is resonantly driven at this frequency. By addition of salt ($MgSO_4$), the theory and experiments show that hydration water is instead dominated by the local electric field of the Mg ion, resulting in reduction of water molecules that can be dynamically perturbed by THz pulses.[8]

The Mandadapu group developed a coarse-grained lattice model, the Arrow—Potts model,[9] explaining the competition between crystallization and vitrification in glass-forming materials. Such competition manifests as a non-monotonic behavior in the time-temperature-transformation (TTT) diagrams, which is captured in this model and explained by the existence of two distinct regimes in the formation of polycrystalline materials: crystal nucleation and growth. At high temperatures, crystallization is dominated by the nucleation and growth of compact and fluctuating crystal grains. At low temperatures, crystal growth is influenced by glassy dynamics, and proceeds through dynamically heterogeneous and hierarchical relaxation pathways that produce fractal patterns and ramified crystals. These phenomena are explained by combining the Kolmogorov-Johnson-Mehl-Avrami theory with the field theory of nucleation, a random walk theory for crystal growth, and the dynamical facilitation theory for glassy dynamics. This unified theory yields an "analytical formula" relating the crystallization timescale to the nucleation and growth rate through universal exponents governing glassy dynamics of the model, which accurately predicts the non-monotonic TTT diagrams. Both the model and theory explain ordering in various glassy systems, including organic molecules, crystallization of nano-crystallites, bulk metallic glass alloys and colloidal suspensions. This work could also be in broader synergy with the Bruce Kay group from PNNL and the analytical formula should be applicable to study the heterogeneous dynamics in amorphous/supercooled water, and nucleation and crystallization kinetics of ice.

Ahmed, in collaboration with Oleg Kostko (scientist@LBNL), seeks to understand nucleation and crystallization from solutions where non-equilibrium pathways for molecular growth may exist. X-ray spectroscopy provides a local probe of a sample's electronic structure with elemental and site-specificity and is thus ideally suited for understanding the molecular mechanisms underlying phase separation and the formation of initial solid particles in an aqueous solution, and chemical reactions in aerosols. Soft X-ray velocity map imaging (VMI) photoelectron spectroscopy has been used to probe inelastic and elastic scattering in the condensed phase, represented by the liquid branched hydrocarbon squalene. The VMI spectra collected above the C 1s edge from the unsupported nanoparticles of squalene provided information on the photoelectron signal intensity as well as angular distribution and on secondary electrons. These data allowed for the extraction of electron inelastic and elastic scattering cross-sections. The technique developed here holds promise for characterization of electron transport parameters in the condensed phase and chemical reactivity.[10] In collaboration with Kevin Wilson, we have examined the formation and evolution of chemical gradients at aerosol interfaces. The heterogeneous reaction of hydroxyl radicals (OH) on ~200 nm particles of pure squalane (a

branched, liquid hydrocarbon) and octacosane (a linear, solid hydrocarbon) and binary mixtures of the two are used to understand how diffusion limitations and phase separation impact the particle reactivity.[11]

Future Plans:

Geissler's work on aqueous interfaces will continue in two directions. One focuses on the intrinsic orientational structure of water layers near the air-water interface. Response to external electric fields reveals an intriguing robustness of lateral hydrogen bonding at the liquid's periphery. To examine the origin of this highly stable structural motif, we are extending a mean field theory developed by Adam Willard and coworkers. We are specifically adding self-consistent response to this formulation, as well as a necessary asymmetry between hydrogen bond donation and acceptance. A second future direction explores the impact of microscopic density fluctuations on amphiphilic membranes. The understanding of hydrophobicity chemists have gained in the last decade centers on such solvent density fluctuations, but the stability of amphiphilic mesostructures has not been considered from this perspective. We anticipate that lipid rearrangements due to extreme water density fluctuations can clarify how membrane proteins facilitate the reorganization of phospholipid bilayers.

The Broadband DUV-SHG experimental approach will be used by Saykally and coworkers to measure CTTS spectra of other surface-enhanced ions, emphasizing the study of counterion effects on the spectra. The long-term goal is to develop a complete model of ion adsorption to aqueous interfaces with the Geissler group. Studies of ion adsorption will be extended beyond air-water and graphene-water to interfaces with both hydrophilic and hydrophobic polymers, and ultimately, to water-metal systems, seeking to quantify entropy and enthalpy effects. The use of the Trieste FERMI soft X-ray free electron laser facility will be extended to the study of liquid interfaces with atom-selective and surface-selective nonlinear spectroscopy, using the liquid microjet technology developed by this group. The carbonate system previously investigated by X-ray absorption spectroscopy will be the first target.

Pump-probe THz spectroscopy from experiment and theory for water and simple salt solution holds the promise to manipulate and/or map hydration dynamics by the presence of strong AC and DC electric fields. The Head-Gordon proposes to probe or even control solvation behavior in more complicated environments, e.g. at interfaces and to induce chemical transformations in water by using simulated THz fields as guidance and to work with Havenith, Saykally, and Ahmed in future studies of these same systems.

Mandadapu and co-workers discovered the orderphobic effect in interfaces of lipid bilayers: a long-range physical force mediated primarily by the in-plane order–disorder phase transitions, which assembles solutes together. Mandadapu group now plans to study the interplay between orderphobic effect and the other existing forces, in particular forces arising from elastic bending of interfaces and interfacial tension. The orderphobic effect by itself leads to large domains of solutes. Using novel modeling techniques for deformations of liquid interfaces based on mathematical tools of differential geometry, and advanced sampling tools, Mandadapu group aims to study the aspect of local bending of the bilayers in the presence of nano-domains, and how it provides repelling forces between such domains of solutes. If this hypothesis is true, then there could be a limiting size of such nano-domains, which can further lead to droplets of lipid bilayers. Studying these effects should also have synergistic aspects towards Kevin Wilson’s work on droplet formation from surfactant interfaces. Mandadapu group also plans to study the aspects of crystallization and vitrification in atomistic systems of glass formers, with specific examples of water and metallic alloys. Specific properties that will be probed are self-diffusion coefficients of

molecules and the role of dynamic heterogeneity in understanding the diffusion coefficients relevant for crystallization kinetics. Lastly, Mandadapu aims to validate the Arrow-Potts model rigorously with experiments. To this end, Mandadapu group is working with various experimental groups to obtain crystallization kinetics data for wide variety of glass forming systems. If validated against available experimental data, then the Arrow-Potts model provides universal mechanisms illustrating the competitions between crystallization and vitrification, with implications to wide varieties of interfacial and bulk systems.

To probe the early stages of nanoparticle nucleation processes in solution (a liquid to solid transition), Ahmed proposes a multimodal strategy of interrogating free nanoparticles in space using X-ray spectroscopies coupled to Raman, IR and Terahertz spectroscopy. These spectroscopies are very sensitive to water phase change and will allow for determination of experimental conditions when aqueous aerosols exist either in liquid or in the solid phase. We will explore how the interface changes upon increase of the salt concentration and decrease of amount of water in the nanoparticle. We will utilize the quantitative ability of the recently developed VMI XPS/NEXAFS techniques to measure relative amounts of different chemical elements coupled with the depth profiling to characterize the aerosol interface. We plan to perform depth profiling of free nanoparticles in various stages of nucleation. This will allow for the detection of early stages of salt nucleation on the surface of aerosol nanoparticles. Another system of interest for X-Ray interrogation, arginine-oleic acid solutions, provide a rich environment to generate micelles, vesicles and sponges, dependent on concentration, pH and temperature. We seek to provide data that would be amenable to interrogation by Mandadapu's and Head-Gordon's theoretical program, to probe dynamics at the liquid-liquid and liquid-solid interfaces.

Publications Acknowledging DOE support (2018-present):

[1] Cox, S. J. and Geissler, P.L. "Interfacial Ion Solvation: Obtaining the Thermodynamic Limit from Molecular Simulations" *J. Chem. Phys.* 2018,148, 222823. DOI: 10.1063/1.5020563

[2] Lam, R. K., et al. "Two-photon absorption of soft X-ray free electron laser radiation by graphite near the carbon K-absorption edge" *Chem. Phys. Lett.*, 703, pp 112-116 (2018).

[3] Lam, R. K., et al. "Soft X-Ray Second Harmonic Generation as an Interfacial Probe " *Phys. Rev. Lett.*, 120, 023901 (2018)

[4] Mizuno, H., Rizzuto, A. M., Saykally, R. J. "Charge-Transfer-to-Solvent Spectrum of Thiocyanate at the Air/Water Interface Measured by Broadband Deep Ultraviolet Electronic Sum Frequency Generation Spectroscopy" *J. Phys. Chem. Lett.,* 9, 4753-4757 (2018)

[5] Cole, W. T. S., Wei, H., Nguyen, S. C., Harris, C. B., Miller, D. J., Saykally, R. J. "Dynamics of Micropollutant Adsorption to Polystyrene Surfaces Probed by Angle-Resolved Second Harmonic Scattering" *J. Phys. Chem. C*, 123 (23), 14362-14369 , (2019)

[6] E. Jurrus, et al. (2018). Improvements to the APBS biomolecular solvation software suite. *Protein Sci 27 (1), 112-128.*

[7] L. Ruiz Pestana, L. E. Felberg, T. Head-Gordon (2018). Coexistence of multilayered phases of nanoconfined water: the importance of flexible confining surfaces. *ACS Nano, 2 (1), 448–454.*

[8] Novelli, F.; Pestana, L.R.; Bennett, K. C.; Dessmann, N.; Sebastiani, F; Adams, E. M.; Ilkhchy, K. S. ; Stavrias, N.; Eless, V.; Ockelmann, T.; Colchero, A.; Hoberg, C.; Schwaab, G.; Van Der Meer, L.A.F.G.; Head-Gordon, T.; Havenith, M. (2019). Strong anisotropy in liquid water upon librational excitation using terahertz laser fields. *Nature Comm., final revisions.*

[9] Hasyim, M., and Mandadapu, K. K., (Preprint available on request).

[10] O. Kostko, M. I. Jacobs, B. Xu, K. R. Wilson, M. Ahmed. Velocity map imaging of inelastic and elastic low energy electron scattering in organic nanoparticles, Arxiv (2019)

[11] Jacobs, M. I.; Xu, B.; Kostko, O.; Wiegel, A. A.; Houle, F. A.; Ahmed, M.; Wilson, K. R. Using Nanoparticle X-ray Spectroscopy to Probe the Formation of Reactive Chemical Gradients in Diffusion-Limited Aerosols. *J Phys Chem A* 2019, *123* (28), 6034.

Molecular Theory and Modeling

Gregory K. Schenter
Physical Sciences Division
Pacific Northwest National Laboratory
902 Battelle Blvd, Mail Stop K1-83
Richland, WA 99352
greg.schenter@pnnl.gov

The overarching goals of the Molecular Theory & Modeling Program are: 1) development of a fundamental comprehension of the driving forces, processes and phenomena, such as solvation, nucleation, assembly, transport, and reaction, in complex condensed-phase, heterogeneous and interfacial molecular environments, and 2) development of theoretical and computational methods required to accelerate scientific advances in condensed-phase and interfacial molecular science. In current efforts, we focus on the balance between descriptions of molecular interaction and statistical mechanical sampling. We find that the water exchange process can control chemical reaction and transport phenomena. It is necessary to find the proper balance between the ion-water and water-water interaction. In our studies, we search for the appropriate amount of explicit treatment of electronic structure that allows for efficient sampling of a statistical mechanical ensemble of a system of interest. We are still assessing the most effective representation of molecular interaction, finding a balance between efficiency and accuracy required to generate statistical mechanical ensembles for the prediction of properties and response that drive collective phenomena. In addition, we are learning about the proper balance between short-range treatment of molecular interaction and long-range interaction. We are influenced by the work of Paesani where the balance between explicit many-body treatment of short-range interaction and long-range described by multipole-Coulomb interaction is systematically explored.[4] In our studies we consider both descriptions that rely on a systematic many-body expansion as well as direct Density Functional Theory simulations using the recent meta-GGA SCAN functional of Perdew.[2] In both studies, we take ensembles generated by models of molecular interaction, predict an EXAFS spectrum and compare to measured signals. We are learning that simpler models are not robust enough to recover the balance between ion-water distances and the stiffness of the interaction in the condensed phase. (Debye-Waller factor or effective vibrational frequency) See Figures 1 and 2.

We continue to identify the distinguishing features of the disruption of the water network in response to the presence of ions, exploring the robustness of some empirical potentials and density functional theory for describing this interaction. We are examining the relation between continuum and molecular descriptions of electrolytes, extending what we have learned to concentrated electrolytes and solid/electrolyte interfaces. We are also interested in characterizing the driving forces of collective phenomena. A critical task is to identify and characterize collective coordinates and effective reaction coordinates.[5][6][7] We characterize the mean field thermodynamic landscape, the potential of mean force, as well as dynamical corrections to motion, the effective friction. In doing so, we are moving beyond geometrical order parameters, such as interatomic distance, and are exploring such collective descriptions such as coordination, electric fields, and local vibrational frequencies. Throughout, we construct effective Hamiltonian and General Langevin Equation descriptions of motion and find consistency with Transition State Theory characterization of rare event processes. This approach has been applied to ion-pairing at

interfaces, solvent exchange and the associated spectroscopic signatures, as well as a Marcus-like description of ion-pairing.

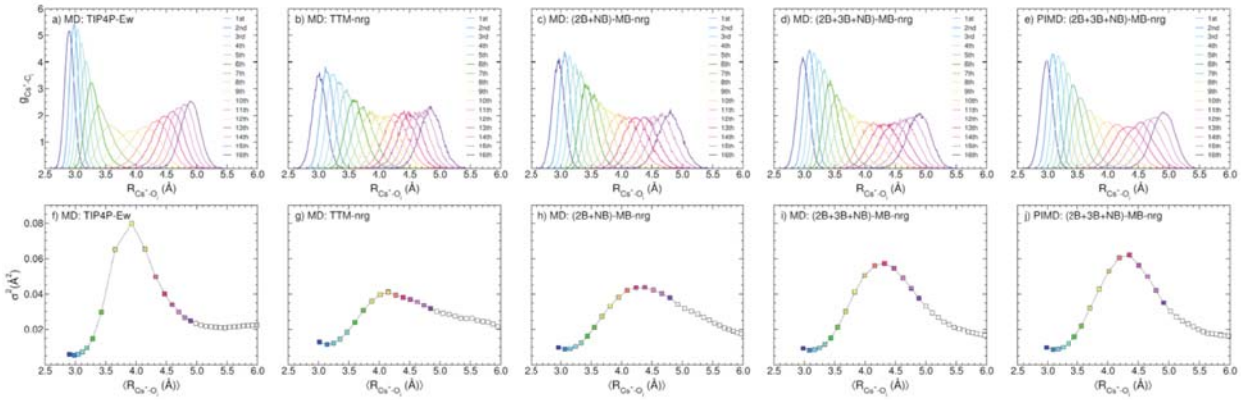

Figure 1. Top: Incremental radial distribution functions corresponding to Classical MD, TIP4P-Ew, TTM-nrg, (2B+NB)-MB-nrg, (2B+3B+NB)-MB-nrg, and Path Integral MD (2B+3B+NB)-MB-nrg descriptions of molecular interaction and the ensemble. This sequence represents the inclusion of more detail. Below: corresponding variance vs. average distance. These curves are a strong indicator of the resulting EXAFS spectra. Details are in Ref [4].

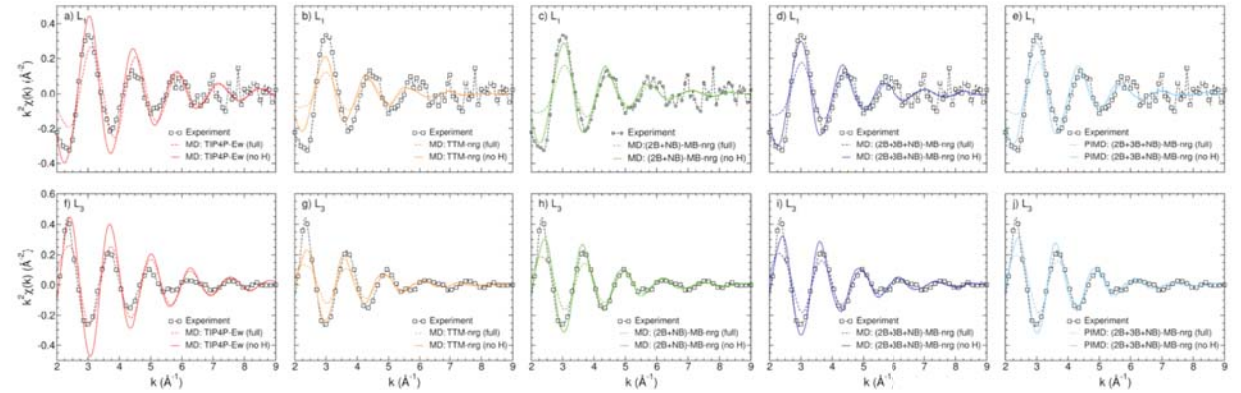

Figure 2. The resulting EXAFS spectra corresponding to the sequence defined in Figure 1. Top: L1-edge, Bottom: L3-edge. We find that increased detail gives improved agreement between simulation and measurement. Details are in Ref. [4]

Acknowledgements.

Molecular Theory and Modeling FWP 16249 Postdoc: Evgenii O. Fetisov
The Molecular Theory and Modeling FWP 16249 is co-managed by CTC and CPIMS programs of the U.S Department of Energy, Office of Science, Office of Basic Energy Sciences, Division of Chemical Sciences, Geosciences, and Biosciences. This work was influenced by members of the group including, Shawn M. Kathmann, Chris J. Mundy, Sotiris S. Xantheas, and Marat Valiev. This work was performed with Evgenii Fetisov (PNNL), Mirza Galib (PNNL), Santanu Roy (PNNL), Tim Duignan (PNNL), and John Fulton (PNNL). We also acknowledge computer resources from NERSC. Battelle operates Pacific Northwest National Laboratory for the US

Department of Energy. The Molecular Theory and Modeling FWP 16249 is co-managed by CTC and CPIMS programs of DOE Office of Basic Energy Sciences Division of Chemical Sciences, Geosciences, and Biosciences.

Publications with BES support (2018-present):

1. Evgenii O. Fetisov, Marcel D. Baer, J. Ilja Siepmann, Gregory K. Schenter, Shawn M. Kathmann, and Christopher J. Mundy, "The Statistical Mechanics of Solution-phase Nucleation: CaCO3 Revisited," FOMMS 2018 volume of "Molecular Modeling and Simulation: Applications and Perspectives" edited by Ed Maginn.
2. Timothy Duignan, Gregory K. Schenter, Mirza Galib, Marcel D. Baer, Jan Wilhelm, Jürg Hutter, Mauro Del Ben, Xiu Song Zhao, and Christopher J. Mundy, "Hydration Structure of Sodium and Potassium Ions with DFT-MD," doi.org/10.26434/chemrxiv.7466426.v1
3. A. I. Kolesnikov, L. M. Anovitz, F. C. Hawthorne, A. Podlesnyak, and G. K. Schenter, "Effect of fine-tuning pore structures on the dynamics of confined water," J. Chem. Phys. 150, 204706 (2019).
4. Debbie Zhuang, Marc Riera, Gregory K. Schenter, John L. Fulton and Francesco Paesani, "Many-Body Effects Determine the Local Hydration Structure of Cs+ in Solution," Journal of Physical Chemistry Letters 10(3): 406-412 (2019).
5. M. Galib, G. K. Schenter, C. J. Mundy, N. Govind, and J. L. Fulton, "Unraveling the spectral signatures of solvent ordering in K-edge XANES of aqueous Na+," J. Chem. Phys. 149, 124503 (2018).
6. Liem Dang and Gregory K. Schenter, "Rate theory of ion pairing at the water liquid-vapor interface: A case of sodium iodide," Journal of Chemical Physics 148(22): 7, (2018).
7. Santanu Roy, Mirza Galib, Gregory K. Schenter, and Christopher J. Mundy, "On the relation between Marcus theory and ultrafast spectroscopy of solvation kinetics," Chemical Physics Letters 692, 407-415 (2018).
8. Richard C. Remsing, Timothy T. Duignan, Marcel D. Baer, Gregory K. Schenter, Christopher J. Mundy, and John D. Weeks, "Water Lone Pair Delocalization in Classical and Quantum Descriptions of the Hydration of Model Ions," The journal of physical chemistry. B 122 (13), 3519-3527 (2018).
9. Katja Henzler, Evgenii O. Fetisov, Mirza Galib, Marcel D. Baer, Benjamin A. Legg, Camelia Borca, Jacinta M. Xto, Sonia Pin, John L. Fulton, Gregory K. Schenter, Niranjan Govind, J. Ilja Siepmann, Christopher J. Mundy, Thomas Huthwelker, and James J. De Yoreo, "Supersaturated calcium carbonate solutions are classical," Science Advances 4 (1) (2018).

Program Title: Understanding Chemical Bond Dynamics in Liquids Using Mixed Quantum/Classical Molecular Dynamics Simulation

Principal Investigator Info: Professor Benjamin J. Schwartz
Department of Chemistry and Biochemistry
University of California, Los Angeles
Los Angeles, CA 90095-1569 USA
Voice: 310-206-4113; Fax: 310-206-4038
E-mail: schwartz@chem.ucla.edu

Program Scope: One of the central themes of modern physical chemistry is elucidating the elementary steps associated with chemical reactions. In the gas phase, our understanding is largely complete. In principle, knowledge of the potential energy surfaces and the initial reactant trajectories is sufficient to predict the details of the reaction mechanism. In condensed phases, however, changes in reactant charge distribution or size during a reaction are strongly coupled to motions of the solvent molecules: solvent dynamics can stabilize (or destabilize) the energy of the transition state, controlling not only the effective barrier for a reaction but also how long that barrier persists. In addition, 'caging' by the solvent can promote recombination of recently-broken chemical bonds. All of these solvent effects, which play a crucial role in determining the rate or possibly even the products of chemical reactions, take place on ps or sub-ps time scales.

This program presents a description of both short- and longer-ranged studies designed to attack the frontiers of chemical reaction dynamics in the condensed phase. The goal of this projects will elucidate the molecular basis for solvation, non-adiabatic relaxation, and multi-electron quantum mechanical effects in solution-phase chemical reactivity, with emphasis on the critical realms of equilibrium chemical bond dynamics and bond breaking/bond formation.

Recent Progress: We chose to begin our study by focusing on the Na_2 molecule because it can be well described in mixed quantum/classical simulations; the molecule can be thought of as two classical Na^+ cores that are held together by two quantum mechanical valence bonding electrons. In our simulations, we treat the two quantum mechanical bonding electrons using configuration-interaction-with-singles-and-doubles (CISD),[1] which is equivalent to full CI since only two explicit electrons are involved. The interactions between the bonding electrons and the Na^+ cores[2] and the THF[3] or Ar[4] solvent molecules are described using previously-developed pseudopotentials. In this way, we can accurately calculate how immersion of Na_2 in solvents like liquid Ar or THF affects the molecular electronic and vibrational structure of this relatively simple solute.

Because there is relatively little exchange and correlation between the bonding electrons and those in the Na^+ core, our MQC description of the Na_2 molecule in the gas phase gives good agreement with high-level quantum chemistry calculations. Fig. 1a shows that the gas-phase Na_2 valence electron density forms a symmetric ovoid around the Na_2 center of mass, as expected from the ideas of molecular-orbital theory. When we insert the Na_2 molecule into solution, however, interactions

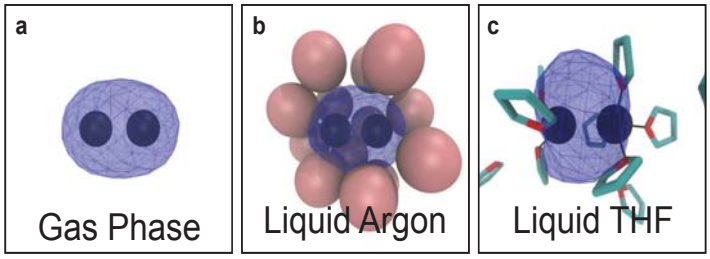

Figure 1: Representative snapshots of Na_2 reveal deformation of the bonding electronic density in the condensed phase.

with the solvent molecules produce a valence electron density that is deformed relative to that in the gas phase. Fig. 1b shows that when Na_2 is placed in liquid Ar, Pauli repulsion interactions from the surrounding cage of Ar atoms, on average, compress the solute's bonding electronic density leading to a stiffer, tighter chemical bond.[5]

We also inserted the Na_2 molecule into liquid THF, and when we did, we got a surprise.[6] THF molecules are known to chelate Na^+ in solution, with THF oxygen sites forming metal-oxygen dative bonds with a strength similar to that of a hydrogen bond, about 5 kcal/mol. Figure 1c shows that local interactions with the solvent displace the solute valence electron density to expose part of each Na^+ core for chelation by the THF oxygen sites. The net effect of these dative interactions with the solvent is to cause the solute valence electron density to spill out away from the bond axis, leading to instantaneous dipole moments that are much larger than in liquid Ar. Also in contrast to the bond compression seen in liquid Ar, the THF—Na^+ interactions lead to a large increase in the Na–Na bond length. These distortions result from the fact that different numbers of THF molecules can chelate (i.e. make weak dative bonds) with the Na atom cores. We find that in THF solution, the system has three distinct coordination states: 3 THFs on each Na, 2 on one and 4 on the other, and 3 on one and 4 on the other. Even though each Na^+–THF dative bond has a strength that is similar only to that of a hydrogen bond, the collective interaction of the solute with the solvent produces a variety of new chemical species that are in equilibrium, each of which is distinguished only by the involvement of the solvent.

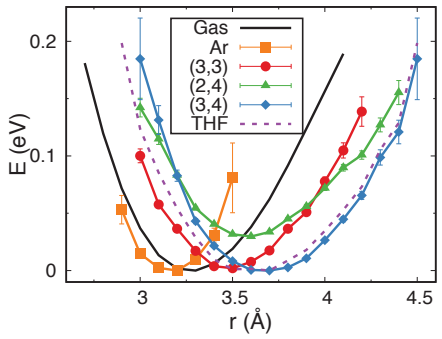

Figure 2: Potentials of mean force of the different stable coordination states of Na_2 in liquid THF.

How unique are the Na_2 chemical species that differ only in their local coordination with the solvent? In Fig. 2 we compare the potential energy of the gas-phase Na_2 molecule (black curve) to the potentials of mean force (PMFs) for the molecule in liquid Ar (orange curve), in liquid THF on average (purple dotted curve), and for each of the stable THF-solvated coordination states (red, green and blue curves) as a function of the Na–Na bond distance; these are the potential energy surfaces that govern how the two Na atoms move in each of the respective environments. The figure shows clearly that the overall PMF for the sodium dimer in liquid THF is not smooth; there are wiggles at the bottom of the well that result from the presence of the different (and distinct) solvent coordination states. Thus, it makes much more sense to think of the Na_2/THF system as three different molecules in equilibrium: as summarized in Table 1, each THF-coordination state has a different Na–Na bond length (the position of the minimum in the PMF) and a different vibrational frequency (the curvature of the PMF around the minimum), verifying that each is a unique chemical species. Indeed, the calculated UV-Vis and IR spectra for the three coordination states are quite distinct, so that it should be possible to observe them experimentally.[6]

To see how the effects of being in a solvent affect photodissociation dynamics, we have recently completed a study of the sodium dimer cation molecule (Na_2^+) in liquid Ar and THF. We chose the cation because its lowest exited state potential energy surface in the gas phase is dissociative (unlike the Na_2 neutral molecule, where the lowest several singlet excited states are bound); moreover, the lowest excited state of the cation is well described at the CISD level of theory. We repeated the analysis above for Na_2^+, and found similar behavior, but with exaggerated effects since the solvent is better able to distort the single bonding electron. For

example, the induced dipole moment in liquid Ar is much larger for the cation than the neutral, and in THF, we find coordination states of (5,5) and (4,5) predominate.

When we promote the cation molecule to its lowest excited state in the gas phase, the molecule dissociates with the bonding electron wavefunction split equally between the two departing Na^+ cores, indicating that with nothing to break the symmetry, it is equally likely for the electron to end up with one Na^+ or the other (i.e., to make dissociation products $Na^+ + Na$). However, we get several surprises in solution. First, when exciting the molecule in liquid Ar, we find that after a few hundred femtoseconds on average, the wavefunction localizes onto one of the two Na^+'s and leaves the other one bare. In other words, interactions with the solvent break the local symmetry and effectively make a measurement on the excited-state wavefunction, causing collapse on to one of the two atoms. The amount of time this measurement process takes varies from on trajectory to the next, and we are still exploring the possibilities of identifying a particular solvent coordinate that is responsible for this quantum decoherence event.

When we promote the cation to its lowest excited state in liquid THF, the resulting dynamics are even more interesting. After Franck-Condon excitation, the node of the excited-state wavefunction lies *parallel* to the Na–Na bond axis, so that there is no driving force for dissociation. Interestingly, over the first few hundred femtoseconds, the primary excited state dynamics serve to rotate the node until it lies roughly perpendicular to the bond axis, leading to a situation roughly similar to that in Ar. Thus, even though the molecule has a vastly different ground-state electronic structure in liquid THF than in the gas phase, the excited-state electronic structure in THF prefers to be similar to the gas phase, for reasons we do not yet entirely understand. The excited wavefunction produces a large Hellman-Feynman force on the datively-bonded THF angles, causing them to push together to make room for the electronic wavefunction to stick out the ends of the molecule so that the node can rotate. The dynamics of this process also varies from trajectory to trajectory, and we are currently exploring the reasons why the dynamics in THF behave this way.

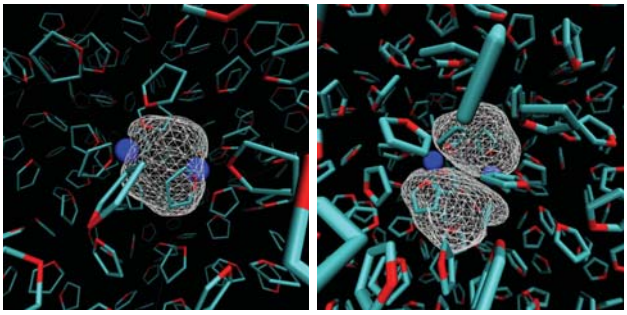

Figure 3: Left: Ground state snapshot of Na_2^+ in liquid THF; clearly the wavefunction is distorted to expose the Na^+ cores to make 4 or 5 dative bonds with the oxygens on the solvent. Right: Franck-Condon excited state for the same configuration. Note that the node in the wave-function lies parallel to the bond axis, explaining the vastly different electron structure of the solvent complex compared to the gas-phase molecule. After excitation, the node rotates to lie perpendicular to the bond, leading to photodissociation and eventual electron localization.

Future Plans: For the immediate future, we plan on continuing our exploration of how local specific solvent interactions can alter molecular identity with regard to excited-state dynamics. The fact that the dative bond interactions responsible for changing identity here are comparable to the strengths of H-bonds means that the idea of the solvent playing an explicit role in molecular identity is general to any chemical system with local specific interactions of about this strength.

Over the longer term, we plan to address how the solvent alters molecular identity for intrinsically asymmetric molecules such as Na-K, which can be treated with the same level of theory but where the two halves of the molecule have different electron affinities and different sizes, and thus different potentials for chelation.

Publications:

1) D. Widmer and B. J. Schwartz, "Solvents can control solute molecular identity," *Nature Chem.* **S41557-018-066z**, 1-7 (2018). DOI: 10.1038/s41557-018-066-z.

2) C.-C. Zho, V. Vlcek, D. Neuhauser and B. J. Schwartz, "Thermal Equilibration Controls H-Bonding and the Vertical Detachment Energy of Water Cluster Anions," *J. Phys. Chem. Lett.* **9**, 5173-8 (2018). DOI: 10.1021/acs.jpclett.8b02152.

References:

[1] Glover, W. J., Larsen, R. E. & Schwartz, B. J. First principles multi-electron mixed quantum/classical simulations in the condensed phase. I. An efficient Fourier-grid method for solving the many-electron problem. *J. Chem. Phys.* **132**, 144101 (2010).

[2] Glover, W. J., Larsen, R. E. & Schwartz, B. J. The roles of electronic exchange and correlation in charge-transfer-to-solvent dynamics: many-electron non-adiabatic mixed quantum/classical simulations of photoexcited sodium anions in the condensed phase. *J. Chem. Phys.* **129**, 1–20 (2008).

[3] Smallwood, C. J., Mejia, C. N., Glover, W. R., Larsen, R. E. & Schwartz, B. J. A computationally-efficient exact pseudopotential method. 2. Application to the molecular pseudopotential of an excess electron interacting with tetrahydrofuran (THF). *J. Chem. Phys.* **125**, 9681–9691 (2006).

[4] Gervais, B. et al. Simple DFT model of clusters embedded in rare gas matrix: trapping sites and spectroscopic properties of Na embedded in Ar. *J. Chem. Phys.* **121**, 8466–8480 (2004).

[5] Glover, W. J., Larsen, R. E. & Schwartz, B. J. How does a solvent affect chemical bonds? Mixed quantum/classical simulations with a full CI treatment of the bonding electrons. *J. Phys. Chem. Lett.* **1**, 165–169 (2010).

[6] D. Widmer and B. J. Schwartz, "Solvents can control solute molecular identity," *Nature Chem.* **S41557-018-066z**, 1-7 (2018).

DE-SC0007347 **Princeton University**

Understanding Surfaces and Interfaces of Photocatalytic Oxide Materials with First Principles Theory and Simulations

Annabella Selloni,
Department of Chemistry, Princeton University
phone (609) 258-3837; Email: aselloni@princeton.edu

Program Scope

This theoretical research project continues and extends previous DOE-funded work on the surfaces and aqueous interfaces of titanium dioxide (TiO_2) and related (photo-)catalytically active metal oxides. TiO_2 is a widely used photocatalyst and functionally versatile material with a large variety of applications, as well as an important model system for fundamental studies of metal oxide surfaces and interfaces. The overall goal of this project is to obtain a comprehensive understanding of the properties and structure-function relationships on the surfaces and aqueous interfaces of TiO_2, as this knowledge can ultimately contribute to an improvement of the performance of this material and provide useful insights into the behavior of other oxide materials as well.

Recent Progress

Period Covered: from 09/01/2018 to 09/27/2019.

Structure, Polarization, and Sum Frequency Generation Spectrum of Interfacial Water on Anatase TiO_2. The interface of water with the majority anatase TiO_2 (101) surface was investigated using ab initio molecular dynamics (AIMD) with the strongly constrained and appropriately normed (SCAN) density functional that was recently shown to provide an excellent description of the properties of bulk liquid water. Our simulations predict that water forms a stable bilayer of intact molecules with ice-like dynamics and enhanced dipole moment and polarizability on the anatase surface. The orientational order and H-bond environment of water in the bilayer are reflected in the computed sum frequency generation (SFG) spectrum, which is found to agree well with recent experimental measurements in the OH stretching frequency range (3000-3600 cm-1), indicating that water dissociation is not essential to describe the spectrum of the hydrophilic anatase surface. Additional AIMD simulations for a model interface with a 66% fraction of dissociated water in the contact layer show that surface hydroxyls disrupt the order in the bilayer and lead to a much faster orientational dynamics of interfacial water in comparison to the non-hydroxylated surface. Nonetheless, the computed SFG spectrum for the hydroxylated surface is also in agreement with experiment, suggesting that SFG measurements in a wider frequency range would be necessary to unambiguously identify the character of interfacial water on anatase.

***Structural evolution of titanium dioxide during reduction in high pressure hydrogen*.** The excellent photocatalytic properties of TiO_2 under UV light have long motivated the search for doping strategies capable of extending its photoactivity to the visible. One promising approach is high-pressure hydrogenation, which results in reduced "black TiO_2" nanoparticles (NPs) with a crystalline core and a disordered shell that absorb the whole spectrum of visible light. We have elucidated the formation mechanism and relevant structural features of black TiO_2 using first-

principles-validated reactive force field molecular dynamics simulations of anatase TiO_2 surfaces and nanoparticles (NPs) in high-temperature, high-pressure hydrogen atmosphere. Simulations reveal that surface oxygen vacancies (V_OS) created upon reaction of H_2 with surface O atoms. tend to diffuse toward the bulk but encounter a high barrier for subsurface migration on {001} facets, which initiates the disordering of NP's surface. Besides supporting the key role of the hydrogenated amorphous shell in the photoactivity of black TiO_2, our results provide insight into the properties of the disordered surface layer that is observed to form on anatase nanocrystals under reaction conditions relevant to photocatalytic water splitting.

Surface structure and chemistry of perovskite tantalates. First-principles calculations were carried out to investigate the structure, energetics and electronic properties of the majority (001) surfaces of $NaTaO_3$ (NTO), a perovskite oxide with excellent photocatalytic properties, and $KTaO_3$ (KTO), a closely related but somewhat less active compound. Being polar, NTO(001) and KTO (001) require charge compensation to be stabilized. We examined a number of possible structural models for these surfaces by comparing their formation energies to those of the pure NaO/KO and TaO_2 terminations. Our results show that a "cation-exchange" reconstruction is energetically most favorable for NTO(001) under vacuum conditions, whereas for KTO(001) this reconstruction competes with a "striped" phase with equally-exposed KO and TaO_2 terraces actually observed in recent experiments. NTO is found to exhibit enhanced structural flexibility and more effective charge compensation in comparison to KTO, which is attributed to the significantly smaller size of Na^+ relative to K^+. Upon exposure to water, a (2×1) hydroxylated structure is by far most favorable for both NTO and KTO. This structure can thus provide a basis for the mechanistic understanding of photocatalytic processes on NTO and KTO surfaces.

Adsorption and reactions on anatase TiO_2(101). In collaboration with Cristiana Di Valentin (U. Milano-Bicocca) and the experimental group of Ulrike Diebold [TU Wien], we have investigated the surface chemistry and photochemistry of the anatase TiO2(101) surface through a combination of scanning tunneling microscopy (STM), temperature-programmed desorption (TPD), X-ray photoemission spectroscopy (XPS) and density functional theory (DFT). One of the investigated reactions was the adsorption of methanol on anatase (101) and its interaction with UV light. Isolated methanol molecules did not show any changes even after high exposures of UV irradiation. Two ways of methanol activation were identified: either via reaction with coadsorbed oxygen or terminal OH− groups, or via dosing higher methanol coverages, above ≈0.5 ML. In the first case, the photoreaction results in the production of formaldehyde and water (Figure B.4). In the latter case, methyl formate is produced; however small amounts of water are also observed, suggesting that additional pathways may be present. In both scenarios, the key step for methanol photoactivation is its partial dissociation, i.e., methoxy formation. This is either obtained by transferring a proton to coadsorbed OH or O_2, or it becomes feasible at higher methanol coverages where the kinetics of methanol dissociation is more favorable thanks to a "shuttled" proton transfer mechanism.

FUTURE PLANS

Free Energy of Water Dissociation at the Water – Anatase TiO2 Interface from Ab Initio Deep Potential Molecular Dynamics. One of the most fundamental and controversial issues in the study of the anatase-water interface (and of many other metal oxide-water interfaces as well) concerns the nature, molecular versus dissociated, of water adsorption on the oxide surface. The presence

of dissociated water on TiO_2 is often assumed to explain the mechanism of photochemical water splitting, the wetting transition and the functionalization of TiO_2 surfaces. However, the equilibrium coverage of dissociated water on TiO_2 in contact with liquid water is unknown both theoretically and experimentally, limiting our understanding of the surface chemistry of aqueous TiO_2 interfaces. We will address this question using ab-initio based neural network (NN) interatomic potentials to represent the potential energy surface of the anatase-water interface. This will allow us to carry out molecular dynamics simulations of tens of nanoseconds on systems of thousands of atoms and use enhanced sampling techniques to obtain converged free energy surfaces of proton transfer at the aqueous anatase interface as a function of suitable reaction coordinates.

Understanding the competing interactions of Carboxylic Acids and Water on TiO_2 Surfaces under Ambient Conditions. Among the most intriguing properties of TiO_2 is its switch from hydrophobic to hydrophilic character upon irradiation with UV light. One of the mechanisms proposed to explain this behavior involves the photo-oxidation of hydrophobic hydrocarbons typically present on TiO_2 under ambient conditions. Strong support for this mechanism has recently emerged from several studies. In particular, experiments under controlled conditions have shown that a rutile TiO_2 (110) surface in contact with air or ambient water selectively adsorbs atmospheric formic and acetic acid, resulting in the formation of a hydrophobic carboxylate monolayer that can be removed by UV irradiation. To understand the detailed mechanisms of these processes, we will initially focus on formic/acetic acid on dry surfaces, in particular on anatase (101), for which experimental studies have recently been carried out by Z. Dohnalek and collaborators at PNNL. Next, model systems in humid/aqueous environment will be investigated starting from surfaces with a few co-adsorbed carboxylates and water molecules and finally considering full carboxylate monolayers on TiO_2 surfaces immersed in water. Ab initio Molecular Dynamics simulations will be carried out to compare the behaviors of rutile and anatase TiO_2 surfaces. These simulations will be further used to train NN potentials which will allow us to carry out studies on larger models and longer time scales.

List of publications

Period Covered: from 09/01/2017 to 09/27/2019.

Funded by DE-SC0007347 (this project)

1. Xunhua Zhao, A. Selloni, Structure and Stability of $NaTaO_3$(001) and $KTaO_3$(001) Surfaces, *Phys. Rev. Materials* **2019**, 3, 015801.
2. Giulia Righi, Rita Magri, Annabella Selloni, H_2 dissociation on noble metal single atom catalysts adsorbed on and doped into CeO_2(111), *J. Phys. Chem*. C **2019**, *123*, 9875-9883.
3. Sencer Selçuk, Xunhua Zhao, Annabella Selloni, Structural Evolution of Titanium Dioxide during reduction in high pressure hydrogen, *Nature Materials*, **2018,** 17, 923.
4. Marcos F Calegari Andrade, Hsin-Yu Ko, Roberto Car, A. Selloni, Structure, Polarization, and Sum Frequency Generation Spectrum of Interfacial Water on Anatase TiO_2, *J. Phys. Chem. Letters,* **2018,** 9, 6716-6721**.**
5. Xunhua Zhao, Sencer Selçuk, Annabella Selloni, Formation and stability of reduced TiOx layers on anatase TiO_2(101): identification of a novel Ti_2O_3 phase, *Phys. Rev. Materials* **2018**, 2, 015801.

6. Annabella Selloni, Titania and Its Outstanding Properties: Insights from First Principles Calculations, Handbook of Materials Modeling: Applications: Current and Emerging Materials, Springer International Publishing, **2018**

Funded by DE-SC0007347 (this project) with co-funding from other sources:

1. Bo Wen, Wen-Jin Yin, Annabella Selloni, Li-Min Liu, Defects, Adsorbates and Photoactivity of Rutile TiO_2 (110): Insight by First-Principles Calculations, *J. Phys. Chem. Letters***, 2018,** 9, 5281-5287.
2. Yue Lu, Wen-Jin Yin, Kai-Lin Peng, Kwan Wang, Qi Hu, Annabella Selloni, Fu-Rong Chen, Li-Min Liu, Man-Ling Sui, Self-hydrogenated shell promoting photocatalytic H_2 evolution on anatase TiO_2. *Nature Communications*, **2018**, 9, 2752.
3. Immad M Nadeem, Jon PW Treacy, Sencer Selcuk, Xavier Torrelles, Hadeel Hussain, Axel Wilson, David C Grinter, Gregory Cabailh, Oier Bikondoa, Chris Nicklin, Annabella Selloni, Jörg Zegenhagen, Robert Lindsay, Geoff Thornton, Water Dissociates at the Aqueous Interface with Reduced Anatase TiO_2(101), *J. Phys. Chem. Letters*, **2018**, *9*, 3131-3136
4. Bo Wen, Qunqing Hao, Wen-Jin Yin, Le Zhang, Zhiqiang Wang, Tianjun Wang, Chuanyao Zhou, Annabella Selloni, Xueming Yang, Li-Min Liu, Electronic Structure and Photoabsorption of Ti^{3+} Ions in reduced Anatase and Rutile TiO_2, *Phys. Chem. Chem. Phys.* **2018**, 20, 17658-17665.
5. Xiao Shi, Steven L. Bernasek, and Annabella Selloni, Mechanism and Activity of CO Oxidation on (001) and (110) Surfaces of Spinel Co_3O_4, $NiCo_2O_4$ and $NiFe_2O_4$: a DFT+U study, *Surf. Sci.* **2018**, 677, 278-283.
6. Wen-Jin Yin, Bo Wen, Chuanyao Zhou, Annabella Selloni, Li-Min Liu, Excess Electrons in Reduced Anatase and Rutile TiO_2, *Surf. Sci. Reports* **2018**, 73, 58-82.
7. Moritz Müller, Daniel Sánchez-Portal, He Lin, Gian Paolo Brivio, Annabella Selloni, Guido Fratesi, Effect of Structural Fluctuations on Elastic Lifetimes of Adsorbate States: Isonicotinic Acid on Rutile (110), *J. Phys. Chem. C,* **2018**, 122, 7575-7585
8. Jan Balajka, Ulrich Aschauer, Stijn Mertens, Annabella Selloni, Michael Schmid, and Ulrike Diebold, Surface Structure of TiO_2 Rutile (011) Exposed to Liquid Water, *J. Phys. Chem. C*, **2017**, 121, 26424-26431.
9. M. Setvin, X. Shi, J. Hulva, T. Simschitz, G. S. Parkinson, M. Schmid, C. Di Valentin, A. Selloni, U. Diebold, Methanol on anatase TiO_2 (101): Mechanistic insights into photocatalysis, *ACS Catalysis*, **2017**, 7, 7081.

Development of Metal-Free Photocatalysts

Kevin L. Shuford
Department of Chemistry, Baylor University, One Bear Place #97348, Waco, TX 76798
(254) 710-2576, kevin_shuford@baylor.edu

Program Scope

Solar fuels show great promise as clean, sustainable energy sources; however, established technologies are still plagued by high price, toxicity concerns, or low efficiencies. There is a critical need for inexpensive, benign materials that can effectively harness the sun's energy. The overarching objective of this project is to evaluate the compatibility of novel material combinations for use as metal-free, heterojunction photocatalysts. Our central hypothesis is that by tuning the electronic structure of individual components in hybrid composites, via selective chemical modifications and physical stimuli to the interface, we can improve the photocatalytic properties of the overall assembly. We will determine factors that affect energy band gaps and band edge positions in isolated photocatalyst systems as well as explore routes to modulate heterojunction band alignments in composite assemblies. Our results will predict accessible pathways for charge carriers in new composite photocatalysts, facilitating access to more of the solar spectrum via inexpensive, environmentally-friendly material combinations.

Recent Progress

As a first step toward understanding the surface chemistry of doped carbon 2D materials, we examined a set of molecular analogues to glean insight into the bonding network upon varying dopant type and connectivity. A compendium of pnictogen and chalcogen substituted boron heterocycles were assessed for their aromatic character by first principles density functional theory. Group-15 and Group-16

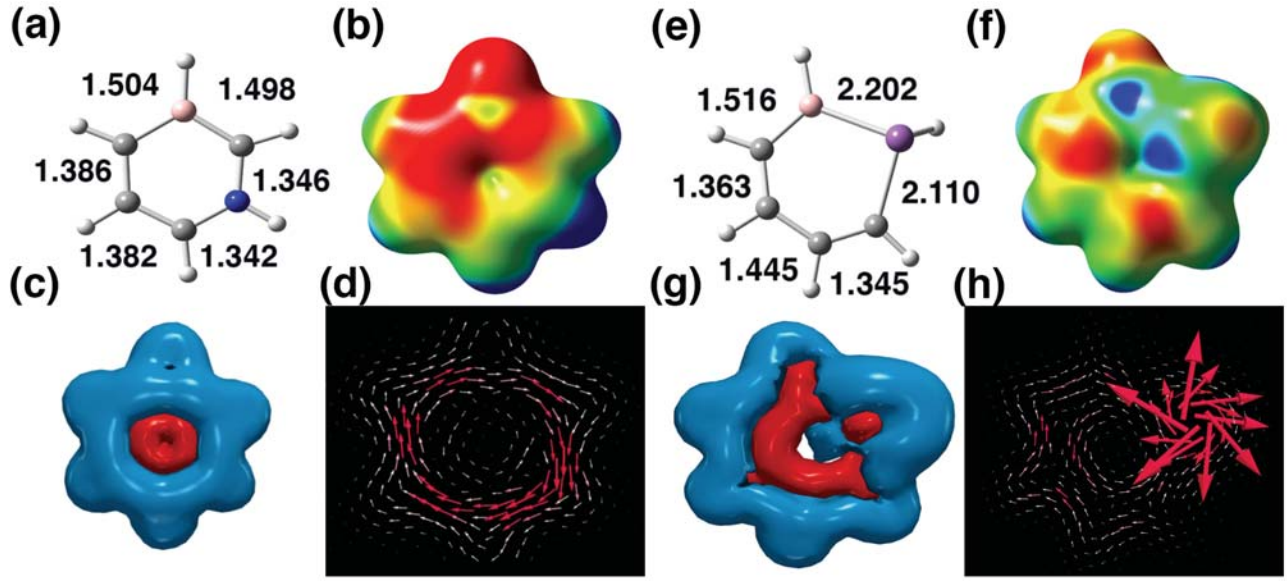

Figure 1: Optimized pnictaborines and aromaticity metrics for (a)-(d) 1,3-azaborine (most aromatic) and (e)-(h) 1,2-stibaborine (least aromatic). (a)/(e) optimized ground state geometry and equilibrium bond lengths (Ang.), (b)/(f) electrostatic potential maps, (c)/(g) signed modulus of the current density displaying the location of diatropic (blue) and paratropic (red) current, and (d)/(h) current maps 1 Angstrom above the molecular plane. The electrostatic potentials are projected onto the ground state electron density to identify regions of charge inhomogeneity. Isosurface values range from $-1.0 \times 10^{-4} - 1.0 \times 10^{-1}$ a.u. (blue to red). The signed modulus of the current is given in ± 0.01 nAT^{-1}.

elements were placed at the ortho-, meta-, and para-positions of six-membered rings relative to boron to assess their impact on the aromaticity of the unsaturated heterocycles (results summarized in Figs. 1 and 2 respectively). Aromaticity was analyzed by a multidimensional approach using nuclear independent chemical shifts, gauge-including magnetically induced current, as well as natural bond orbital and natural resonance theory analyses. Based on these methods, we observe a general decline of aromaticity in heavier pnictaborines while the chalcogen analogues maintain relatively strong aromatic character. These general trends result from complementary π-π^* natural bond order interactions that sustain resonance within the ring of each heterocycle establishing a pattern of cyclic delocalization. Consequently, natural resonance theory displays strong resonance, which is corroborated with the signed modulus of ring current, toroidal vortices of current maps, and elevated average induced current throughout the ring. The 1,3-configurations for pnictaborines and chalcogenaborines are generally more aromatic compared to the 1,2- and 1,4-isomers, which contain π-holes that limit diatropism within the heterocycles. However, an energetic trend favors the 1,2-heterocycles in both groups, with a few exceptions driven in large-part by π-donation of the lone pair on the heteroatom to the p_z orbital on the adjacent boron resulting in stabilization. The importance of planarity for high aromaticity is demonstrated, especially in the pnictaborine isomers where pyramidalization at the pnictogen is favored, while bond regularity seems a less important criterion.

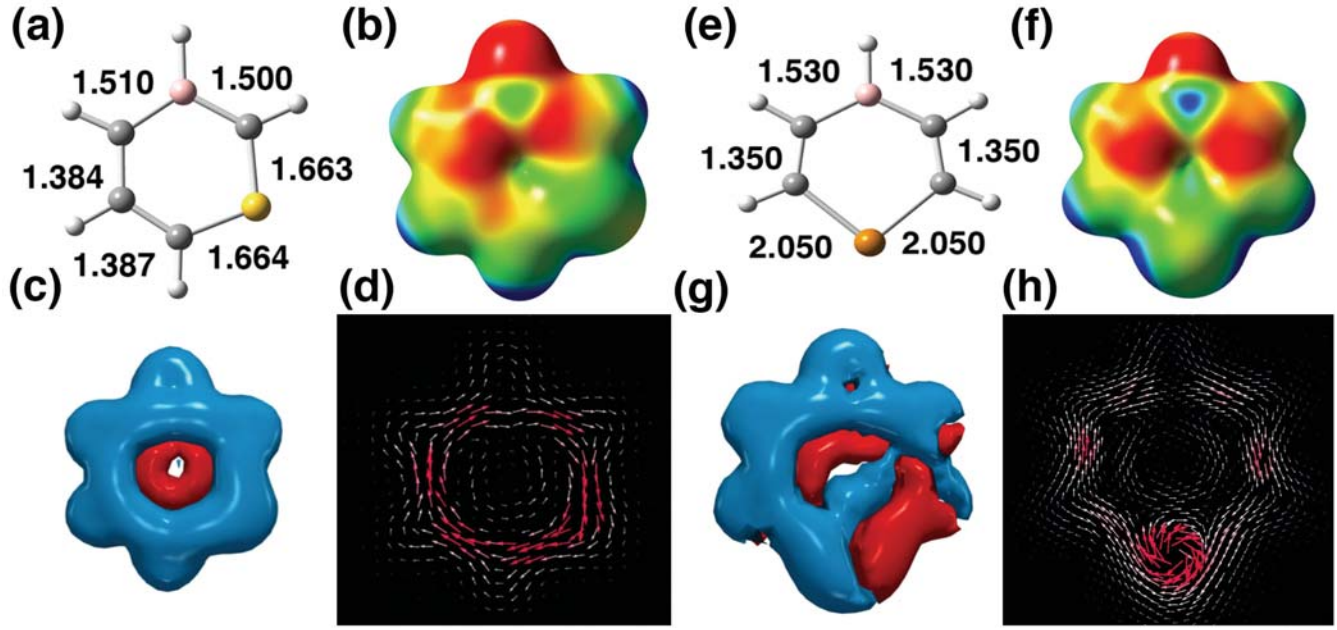

Figure 2: Optimized chalcogenaborines and aromaticity metrics for (a)-(d) 1,3-thiaborine (most aromatic) and (e)-(h) 1,4-telluraborine (least aromatic). (a)/(e) optimized ground state geometry and equilibrium bond lengths (Ang.), (b)/(f) electrostatic potential maps, (c)/(g) signed modulus of the current density displaying the location of diatropic (blue) and paratropic (red) current, and (d)/(h) current maps 1 Angstrom above the molecular plane. The electrostatic potentials are projected onto the ground state electron density to identify regions of charge inhomogeneity. Isosurface values range from $-1.0 \times 10^{-4} - 1.0 \times 10^{-1}$ a.u. (blue to red). The signed modulus of the current is given in ± 0.01 nAT^{-1}.

Future Plans

Our recent work demonstrates how chemical dopants, surface adsorbates, and mechanical strain can create and modulate band gaps. By controlling these surface perturbations, the electronic properties of the material can be tuned with selectivity. One can imagine extrapolating these concepts to controlling both energetics in individual materials and band alignments in assemblies to enhance relevant

photocatalytic processes that occur at material interfaces. We will use a combination of molecular quantum chemistry and periodic system approaches to determine the fundamental chemical and photophysical properties of emerging photocatalytic materials. Our near-term plans are to focus on the 2D material graphitic carbon nitride. Specifically, we will determine the effects of chemical doping and size-dependent quantum confinement on the electronic structure and optical properties of graphitic carbon nitride. Elemental dopants will be added to graphitic carbon nitride via lattice substitutions and interstitial sites to ascertain changes to electronic structure. Quantum confinement effects in these systems will be gauged by examining absorption properties of zero-dimensional quantum dots up to the bulk material. These studies are underway currently. Later phases of the project will combine graphitic carbon nitride with other materials to form metal-free composites for photocatalysis.

Publications Acknowledging this Grant (start date September 2018)

- Paul A. Brown, Caleb D. Martin, and Kevin L. Shuford, "Aromaticity of Unsaturated BEC_4 Heterocycles (E = N, P, As, Sb, O, S, Se, Te)," Phys. Chem. Chem. Phys. **21**, 18458-18466 (2019).
- O. Tara Liyanage, Matthew R. Brantley, Emvia I. Calixte, Touradj Solouki, Kevin L. Shuford, and Elyssia Gallagher, "Characterization of Electrospray Ionization (ESI) Parameters for In-ESI Hydrogen/Deuterium Exchange of Carbohydrate-Metal Ion Adducts," J. Amer. Soc. Mass Spectrom. **30**, 235-247 (2019).

Ultra-nano, Single-Atom Catalysts Applied to Energy-Related Challenges

Mary Jane Shultz
Pearson Laboratory, Chemistry Department
Tufts University, 62 Talbot Ave., Medford, MA 02155
Mary.Shultz@Tufts.edu

Program Scope: The overarching theme of our program is to understand and ultimately control chemistry and dynamics at complex, oxide interfaces. Within this larger scope, this project focuses on three transformations:

- Removing CO from fuels to prevent poisoning the catalysts (most frequently Pt).
- Transforming CO_2 into high-value products, targeting the first step: H-atom transfer (ideally from water).
- Leveraging stability of a $Li_{0.55}TiO_{2.27}$ phase with ultra-nano TiO_2 particles to extend the life of Li-ion batteries; use TiO_2 ultra-nano particle chemistry to remove the solid-electrolyte interphase to reduce resistence.

The basic substrate consists of anatase TiO_2 ultra-nano particles; these are defined as particles less than 2 nm. This small size is chosen to avoid one of the banes of nanoscience: reproducible substrate generation. A 1 nm particle contains only 96 formula units; the size and shape are determined by surface energy minimization. Doping these small particles with a single Fe atom results in Fe in the (001) face since the surface energy of iron oxide is intermediate between that of the (101) and (001) bounding faces. The single Fe atom serves as an engineered defect. Upon irradiation, the photo generated electron is captured at the Fe site, lowering the electron energy, quenching the hydrogen generation reaction, and making the electron available for selected transformations. Thus, the basic substrate for the targeted transformations is single-iron doped, ultra-nano anatase, denoted Fe·TiUNP.

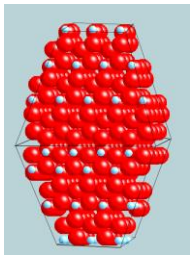

Ball-and-stick model of a 1 nm, anatase TiO_2 particle with ideal

Recent Progress: Just prior to the start of this work, we leveraged electron capture by Fe to deposit single-atom Pt on these particles, denoted as Pt-Fe·TiUNP. Successful single-atom capture is detected via CO-DRIFTS. Extended photosynthesis times produce Pt clusters, evidenced via the bridge-bonded resonances. Within the project, XAFS is used to detect Pt binding, coordination, and oxidation state in both single-atom and cluster samples. Preliminary analysis of this data will be reported.

Future Plans: This project has just begun (September 2019). The first phase consists of characterizing CO, CO_2, H_2O, CH_3OH, and H_2CO binding to both Fe·TiUNP and Pt-Fe·TiUNP. Characterization will use the Shultz-lab invented nonlinear interferometer (NLI) and sum frequency generation (SFG) with immobilized particles. The NLI is uniquely capable of detecting the complex, thus linear, spectrum at an interface. The neat binding experiments will be followed by competitive binding, adding H_2 to the mixture. CO, CO_2, and H_2O interacting with the particles constitutes a complex mixture.

An Atomic-scale Approach for Understanding and Controlling Chemical Reactivity and Selectivity on Metal Alloys

E. Charles H. Sykes (charles.sykes@tufts.edu)
Department of Chemistry, Tufts University, 62 Talbot Ave, Medford, MA 02155

Program Scope:

Catalytic hydrogenations and dehydrogenations are critical steps in many industries including agricultural, chemicals, foods and pharmaceuticals. In the petroleum refining industry, for instance, catalytic hydrogenations are performed to produce light, hydrogen rich products like gasoline. Hydrogen activation, uptake, and reaction are also important phenomena in fuel cells, hydrogen storage devices, materials processing, and sensing. Typical heterogeneous catalysts involve nanoparticles composed of expensive noble metals or alloys based on metals like Pt, Pd, and Rh. Our goal is to alloy these reactive metals, at the single atom limit, with more inert and often much cheaper hosts and to understand how the local atomic geometry affects reactivity.

The CPIMS program has supported Sykes lab work in developing a new class of model alloy catalysts that we have termed *Single-Atom Alloys* (SAAs) and understanding their ability to activate H_2 and enable spillover of species like hydrogen atoms or alkoxy groups to the support where ultra-selective reactions can occur. Spurred by our fundamental studies, many research groups around the world have now shown that our SAA concept is valid in real catalysts working under ambient conditions. For example, selective hydrogenation of acetylene, butadiene, and acrolein, as well as Uhlmann coupling have been demonstrated. Our goal is to now push this work beyond hydrogenation chemistry and study the ability of SAAs to perform C-H activation chemistry and dehydrogenation reactions, as well as probing the effect of surface structure on reactivity, and combining two different SAAs in one surface to enable trifunctional chemistry. Mostly recently we have spectroscopically and microscopically characterized a promising new SAA (RhCu) and understood the gating of H_2 evolution by CO on the PtCu SAA, the so-called leaky cork effect.

Recent Progress A: Combining STM, RAIRS and TPD to Decipher the Dispersion and Interactions Between Active Sites in RhCu Single-Atom Alloys

This study examined the atomic-scale structure of a new SAA (RhCu) which is predicted by theory to have even lower C-H activation barriers than PtCu (*Nature Chemistry* 2018, 10, 325). Our results reveal that Rh primarily alloys into Cu in the regions at step edges, and at low coverages, Rh exists as individual, isolated atoms primarily in Rh rich brims as seen in Figure 1. In these experiments we examined the alloying of Rh with a Cu(111) Surface Structure Spread Single Crystal (S^4C) crystal. Due to the domed shape of the S^4C crystal, we are able to examine regions of different local step density by moving from the flat (111) orientated center of the crystal to the more stepped exterior regions. Figure 1A shows a clean Cu surface free from defects. After deposition of small amounts of Rh at 380 K, we see the appearance of isolated Rh atoms (depressions) in the Cu surface as shown in Figure 1B. A majority of the Rh atoms appear in brims along step edges, while some appear scattered throughout the terraces. This suggests that there are two alloying mechanisms present; a major pathway where the Rh diffuses on the terrace and place exchanges into the upper terrace at a step edge, and a minor pathway where the Rh directly place exchanges in the terrace. As seen in Figure 1C, we tend to find denser brims above larger terraces, indicating that the terraces act like a catchment area for incoming Rh atoms which

diffuse to ascending step edges before alloying into the upper terraces. The inset in Figure 1C shows that each depression is indeed identical in size and shape.

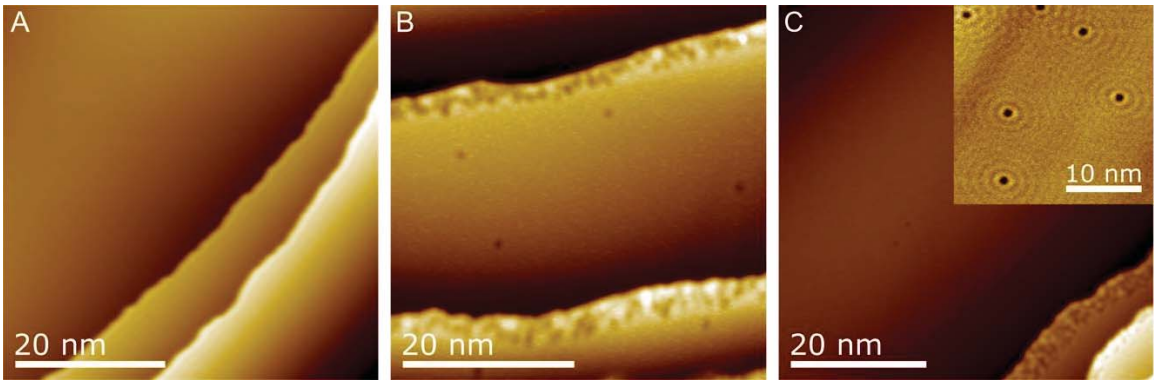

Figure 1: LT-STM images showing formation of a RhCu(111) SAA. (A) Clean Cu surface with large defect free regions and monatomic step edges. (B) RhCu alloy where Rh sites image as depressions showing isolated Rh atoms in brims along step edges as well as in terraces. (C) Dense brims of isolated Rh sites above a large lower terrace demonstrating how underlying terraces act as catchment areas for incoming Rh which place exchange at step edges into the upper terrace. Inset shows atomic resolution of Rh sites.

Using CO as a probe molecule in RAIRS, we examine how surface step density leads to changes in the vibrational frequency due to local crowding of Rh atom sites during alloying. We preformed isotope experiments to deconvolute frequency shifts due to chemical and dipolar interactions, showing that CO on isolated Rh sites interact *via* dipole-dipole coupling and not chemical interactions. As seen in Figure 2, we observe a lower wavenumber peak corresponding to $^{13}C^{16}O$ around 1950 cm^{-1} and a high wavenumber peak for $^{12}C^{16}O$ around 2000 cm^{-1}. Note that the size of the RAIRS peaks is difficult to relate to absolute coverage of surface sites, as it is well known minority species can display deceptively large features. The fact that we see 2 features in these spectra verifies our earlier assumption that there is indeed 1 CO per Rh and not 2 CO per Rh in a dicarbonyl configuration which is known to exhibit 3 peaks in isotopically labeled experiments due to the presence of distinct $^{16}O^{13}C$-Rh-$^{13}C^{16}O$, $^{16}O^{13}C$-Rh-$^{12}C^{16}O$, and $^{16}O^{12}C$-Rh-$^{12}C^{16}O$ symmetric stretching modes.

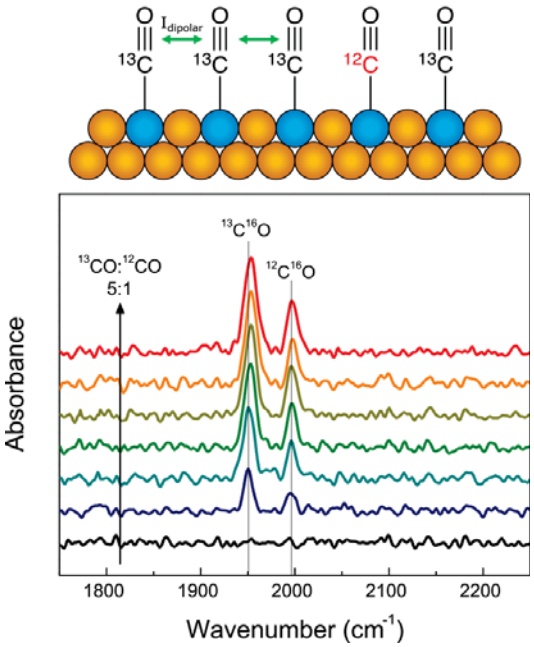

Figure 2: RAIRS spectra as the coverage of CO is increased on a stepped 1% RhCu(111) alloy held at 250 K. The CO is a 5:1 mixture of $^{13}C^{16}O$:$^{12}C^{16}O$, used to decouple the effects of dipole-dipole coupling and chemical shifts.

Finally, CO TPD experiments demonstrated that single Rh atoms bind CO rather strongly, in agreement with previous theoretical work. Together, these experiments provide a detailed picture of the atomic-scale structure of this new SAA and provide important signatures of the SAA such as CO desorption temperature and CO vibrational structure. These data should serve as benchmarks for the catalysis community in the characterization of RhCu SAAs which recent theory work has predicted to be highly active for C-H activation and selective dehydrogenation reactions.

Recent Progress B: CO Mediated H_2 Release from PtCu Single-Atom Alloys: The "Leaky" Molecular Cork Effect

Hydrogen activation, uptake and reaction are important phenomena in heterogeneous catalysis, fuel cells, hydrogen storage devices, materials processing, and sensing. The traditional view of these processes involves molecules adsorbing somewhat uniformly over a surface, migrating to preferred/active sites, followed by reaction or desorption. We report a second system in which the uptake and release of hydrogen from a copper surface occurs solely through 1% of the surface sites which are individual, isolated, catalytically active Pt atoms. We show that the surface can either be kept free of hydrogen by pre-adsorption of carbon monoxide or that hydrogen can be trapped on the surface by post-adsorption. In this way the coverage of the surface as a whole can be controlled by the addition of a single molecule to a minority atomic-scale site which we first discovered in 2013 and termed the *Molecular Cork* effect (Nature Materials 2013, 12, 523).

However, unlike the original Pd/Cu Molecular Cork system, we observe experimentally with Pt/Cu that CO does not desorb prior to H-H recombination. Using high-resolution STM experiments and DFT calculations we show that CO adsorption is specific to single Pt atoms rather than pure Cu(111). Moreover, using KMC (Stamatakis, UCL) we determine that CO is a site blocker for H_2 desorption via single Pt atoms at temperatures up to 55 K beyond the desorption temperature of H_2 in the absence of CO. Analyzing the KMC reaction statistics reveals that some H_2 leaks slowly from surface Cu sites whilst CO molecules are blocking the Pt active sites. However, and most significantly, the majority of H_2 is evolved via recombination at isolated Pt atoms after desorption of the first CO molecule, which explains the experimental results whereby significant H_2 desorption occurs before any CO is detected.

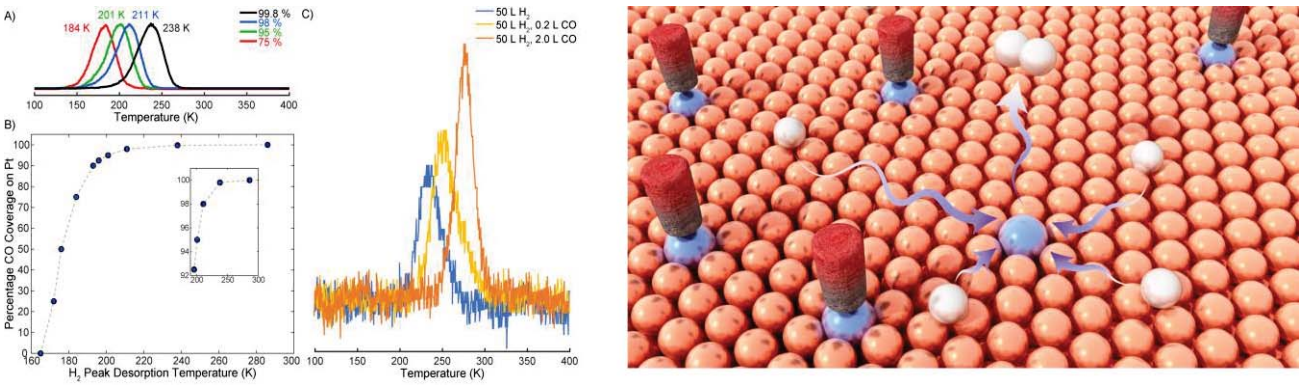

Figure 3. A and B show KMC data for the H_2 desorption peak temperature as a function of CO coverage. C shows corresponding experimental H_2 desorption data. As Pt-CO coverages approach unity the H_2 desorption peaks shift to much higher temperature. Schematic illustrates this leaky cork effect in that desorption of just one CO molecule leads to fast recombination and desorption of multiple H_2 molecules.

This new system constitutes a *"Leaky" Molecular Cork* effect for H_2 evolution from single-atom alloys and demonstrates that a combination of experiment and theory are required to fully understand the interaction of H and CO and their competition for active sites. These important phenomena must be taken into consideration in order for reaction mechanisms on alloy catalysts to be understood.

Future Plans: Despite the many heterogenous catalysis groups that have taken up Single-Atom Alloys we, with the exception of the Trenary group at UIC doing RAIRS, are the only group performing UHV

surface science work on SAAs. Our approach offers the opportunity to study the atomic-scale composition and structure of active sites and relate this information to their ability to activate, spillover and react industrially relevant small molecules. We continue to work closely with theorists (Stamatakis and Michaelides at UCL) enabling us to predict and test new SAA combinations in well defined environments and guide the heterogenous catalysis community. Our future work is aimed at:

1) Studying chemistry on RhCu single-atom alloys which are predicted by DFT to have even lower C-H activation barriers than PtCu.

2) Make and test trimetallic SAA model catalysts to investigate if the bifunctional nature we have demonstrated for 2 component SAAs can be extended to "3 site" model catalysts.

3) Examining the structure sensitivity (or lack thereof) on SAA surface chemistry by extending the surface science studies to (100) and (110) facets as well as stepped crystals.

DOE-Sponsored Research Publications in the Last Two Years:

1) "Carbon Monoxide Mediated Hydrogen Release from PtCu Single-Atom Alloys: The Punctured Molecular Cork Effect" M. T. Darby, F. R. Lucci, M. D. Marcinkowski, Andrew J. Therrien, A. Michaelides, M. Stamatakis, E. C. H. Sykes ***The Journal of Physical Chemistry C*** 2019, 123 10419-10428. The Sykes lab contribution to this manuscript was funded solely by CPIMS.
2) "Pt/Cu Single-atom Alloys as Coke-resistant Catalysts for Efficient C-H Activation" M. D. Marcinkowski, M. T. Darby, J. Liu, J. M. Wimble, F. R. Lucci, S. Lee, A. Michaelides, M. Flytzani-Stephanopoulos, M. Stamatakis, E. C. H. Sykes ***Nature Chemistry*** 2018, 10 325 (The surface science part of this project (Sykes) was solely funded by CPIMS – collaborator MFS was funded by DOE DE-FG02-05ER15730 for the catalysis side of the project)
3) "Single-Atom Alloys as a Reductionist Approach to the Rational Design of Heterogeneous Catalysts" G. Giannakakis, M. Flytzani-Stephanopoulos, E. C. H. Sykes ***Accounts of Chemical Research*** 2018, 52 237-247 The Sykes lab contribution to this manuscript was funded solely by CPIMS.
4) "Lonely Atoms with Special Gifts: Breaking Linear Scaling Relationships in Heterogeneous Catalysis with Single-Atom Alloys" M. Darby, M. Stamatakis, A. Michaelides, E. C. H. Sykes ***The Journal of Physical Chemistry Letters*** 2018, 9, 5636 [featured cover] (The Sykes lab contribution to this manuscript was funded solely by CPIMS, computational investigations by collaborators at UCL were supported by IMASC EFRC DE-SC0012573)
5) "Elucidating the Stability and Reactivity of Surface Intermediates on Single Atom Alloy Catalysts" M. T. Darby, R. Reocreux, E. C. H. Sykes, A. Michaelides, M. Stamatakis ***ACS Catalysis*** 2018, 8 5038 (computational investigations of this work were supported by IMASC EFRC DE-SC0012573)
6) Carbon Monoxide Poisoning Resistance and Structural Stability of Single Atom Alloys" M. T. Darby, E. C. H. Sykes, A. Michaelides, M. Stamatakis ***Topics in Catalysis*** 2018, 61 428 (The Sykes lab contribution to this manuscript was funded solely by CPIMS, DFT collaborators had European funding)
7) "Controlling Selectivity in the Ullmann Reaction on Cu(111)" E. A. Lewis, M. D. Marcinkowski, C. J. Murphy, M. L. Liriano, A. J. Therrien, A. Pronschinske, and E. C. H. Sykes ***Chemical Communications*** 2017, 53 7816-7819 CPIMS only

Excitons in Low-Dimensional Perovskites

William A. Tisdale
Department of Chemical Engineering
Massachusetts Institute of Technology, Cambridge, MA 02139
tisdale@mit.edu

Program Scope

The goal of this research effort is to obtain a deeper understanding of strongly bound excitonic states in low-dimensional halide perovskites. We will study how excitons in these quantum-confined materials move, how they interact with the polar lattice, and how their behavior can be manipulated through chemical or structural modification.

Recent Progress – Sep 2019

Synthesis and Structural Characterization of 2D Halide Perovskite Quantum Wells

Layered perovskites are hybrid 2D materials, formed through the self-assembly of inorganic lead halide networks separated by organic ammonium cation layers. In these natural quantum-well structures, quantum and dielectric confinement lead to strongly bound excitonic states that depend sensitively on the material composition. We have synthesized layered two-dimensional lead halide perovskite crystals with controllable inorganic quantum-well thickness (n = 1, 2, 3, 4), organic spacer chain length (butyl-, pentyl-, hexylammonium), A-site cation (methylammonium, formamidinium), and halide anion (iodide, bromide). Using single-crystal X-ray diffraction, we refined crystal structures for the iodide family as a function of these compositional parameters and across their temperature dependent phase transitions (Fig. 1). Most intriguing, we observe a reversible first-order phase transition corresponding to a partial melting transition of the alkylammonium chains separating the inorganic perovskite layers. The observed behavior is analogous to melting transitions identified in other 2D molecular systems, including alkanethiol monolayers self-assembled on gold surfaces and Langmuir-Blodgett films at liquid interfaces.

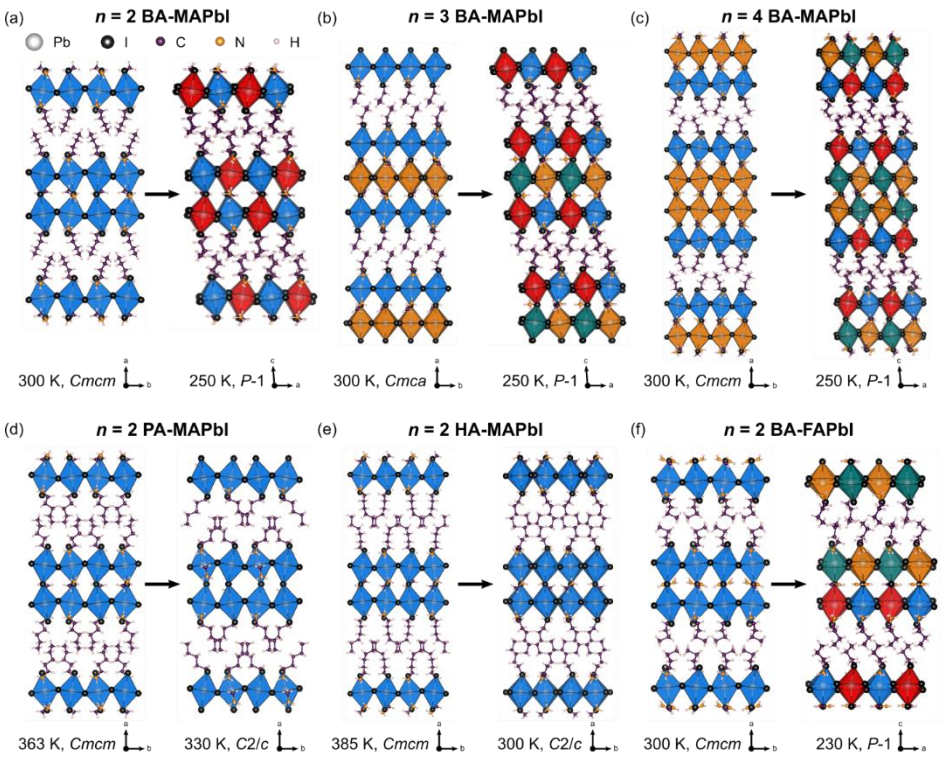

Figure 1. Near-room-temperature structural phase transitions in 2D alkylammonium lead iodide perovskite quantum wells with varying inorganic well thickness (n=2, 3, 4) and alkylammonium chain length (butyl-, pentyl-, hexylammonium). From Paritmongkol *et al., Chem. Mater.* 31, 5592-5607 (2019).

Exciton-Lattice Interactions in 2D Halide Perovskite Quantum Wells

Using a combination of excited state resonant impulsive stimulated Raman scattering (RISRS), low-frequency Raman scattering, density functional theory (DFT), and temperature-dependent photoluminescence, we investigated the effect of alkylammonium organic cation length on exciton-phonon coupling in the series of 2D lead iodide perovskites $(C_xH_{2x+1}NH_3)_2PbI_4$ with chain lengths ranging from four to nine carbons (C_4–C_9). We found that motion of the inorganic Pb-I cages comprises the majority of relevant phonon modes, whose frequencies are unchanged despite more than a doubling of the organic cation length. Accompanying motion of the alkylammonium organic cations is mechanically driven by displacement of the heavy iodide ions through Coulombic attraction and hydrogen-bonding, but coherence of the organic cation motion with the inorganic cage does not extend past the fourth carbon in the chain. The remarkable consistency in exciton-phonon coupling across this series of 2D lead iodide perovskites suggests that the exciton is highly confined along the stacking axis of these layered structures, and the similarity in electronic dynamics is consistent with previously reported polaronic effects dominated by inorganic cage motion, with minimal contributions from the organic cation.

Biexcitons in Colloidal $CsPbBr_3$ Perovskite Nanocrystals

Exciton-exciton interaction energies in semiconductor nanocrystals are difficult to characterize because the strength of the interaction is usually smaller than the spectral width of exciton transitions in optical absorption spectra. Furthermore, fitting transient absorption (TA) spectra of inorganic nanomaterials where the component spectra of different excited states are nearly or completely overlapped is particularly problematic. To enable robust spectral deconvolution, we developed a target analysis model for extracting excited state spectra and dynamics from TA data using a Markov chain Monte Carlo (MCMC) sampler to visualize and understand uncertainty in the model fits. We demonstrated the utility of this approach by extracting the overlapping component spectra and dynamics of single- and biexciton states in $CsPbBr_3$ nanocrystals. Significantly, refinement of the component spectra was accomplished by fitting the entire fluence-dependent series of ensemble TA data using the Poisson statistics of photon absorption, providing multiple checks for internal consistency. Moreover, we used this analysis to determine that previous estimates of the biexciton binding energy are universally too high, and that the biexciton interaction may even become repulsive in the smallest perovskite nanocrystals at room temperature.

Future Plans

A key focus for the coming year is visualization of exciton and charge carrier transport in 2D and 3D halide perovskites. Using funds from this award we have purchased a Montana Instruments Cryostation Microscope, which enables high stability optical microscopy at cryogenic temperatures. Using spatially resolved transient photoluminescence, we will study exciton and carrier diffusivity in single crystal and thin film (polycrystalline) perovskite materials as a function of temperature. A key goal is to probe the mechanism of transport and assess the potential interplay between polaron formation and exciton diffusivity.

Publications citing CPIMS support (since 2018)

1. "Setting an Upper Bound to the Exciton Binding Energy in $CsPbBr_3$ Perovskite Nanocrystals"
K.E. Shulenberger, M.N. Ashner, S.K. Ha, F. Krieg, M.V. Kovalenko, W.A. Tisdale,* M.G. Bawendi;*
J. Phys. Chem. Lett. 10, 5680-5686 (2019).

2. "Synthetic Variation and Structural Trends in Layered Two-Dimensional Alkylammonium Lead Halide Perovskites"
W. Paritmongkol, N.S. Dahod, A. Stollmann, N. Mao, C. Settens, S.-L. Zheng, W.A. Tisdale;
Chem. Mater. 31, 5592-5607 (2019).

3. "Epitaxial Dimers and Auger-Assisted Detrapping in PbS Quantum Dot Solids"
R.H. Gilmore, Y. Liu, W. Shcherbakov-Wu, N.S. Dahod, E.M.Y. Lee, M.C. Weidman, H. Li, J. Jean, V. Bulović, A.P. Willard, J.C. Grossman, W.A. Tisdale;
Matter 1, 250-265 (2019).

4. "Excitons in 2D Organic-Inorganic Halide Perovskites"
C.M Mauck & W.A. Tisdale;
Trends in Chemistry 1, 380-393 (2019).

5. "Melting Transitions of the Organic Subphase in Layered Two-Dimensional Halide Perovskites"
N.S. Dahod, W. Paritmongkol, A. Stollmann, C. Settens, S.-L. Zheng, W.A. Tisdale;
J. Phys. Chem. Lett. 10, 2924-2930 (2019).

6. "Markov Chain Monte Carlo Sampling for Target Analysis of Transient Absorption Spectra"
M.N. Ashner, S.W. Winslow, J.W. Swan, W.A. Tisdale;
J. Phys. Chem. A 123, 3893-3902 (2019).

7. "Towards Stable Deep-Blue Luminescent Colloidal Lead Halide Perovskite Nanoplatelets: Systematic Photostability Investigation"
S.K. Ha, C.M. Mauck, W.A. Tisdale;
Chem. Mater. 31, 2486-2496 (2019).

8. "Synthetic Lateral Metal-Semiconductor Heterostructures of Transition Metal Disulfides,"
W.S. Leong, Q. Ji, N. Mao, Y. Han, H. Wang, A. Goodman, A. Vignon, C. Su, Y. Guo, P.-C. Shen, Z. Gao, D. Muller, W.A. Tisdale, J. Kong;
J. Am. Chem. Soc. 140, 12354-12358 (2018).

9. "Ideal Bandgap in a Ruddlesden-Popper Chalcogenide for Single-Junction Solar Cells,"
S. Niu, D. Sarkar, K. Williams, Y. Zhou, Y. Li, E. Bianco, H. Huyan, S.B. Cronin, M. McConney, R. Haiges, R. Jaramillo, D.J. Singh, W.A. Tisdale, R. Kapadia, J. Ravichandran;
Chem. Mater. 30, 4882-4886 (2018).

10. "Inverse Temperature Dependence of Charge Carrier Hopping in Quantum Dot Solids,"
R.H. Gilmore, S.W. Winslow, E.M.Y. Lee, M.N. Ashner, K.G. Yager, A.P. Willard, W.A. Tisdale;
ACS Nano 12, 7741-7749 (2018).

11. "Ultrafast Charge Transfer at a Quantum Dot/2D Materials Interface Probed by Second Harmonic Generation,"
A.J. Goodman, N.S. Dahod, W.A. Tisdale;
J. Phys. Chem. Lett. 9, 4227-4232 (2018).

12. "Phase-Modulated Degenerate Parametric Amplification Microscopy,"
Y. Gao, A.J. Goodman, P.C. Shen, J. Kong, W.A. Tisdale;
Nano Lett. 18, 5001-5006 (2018).

Structural Dynamics in Complex Liquids Studied with Multidimensional Vibrational Spectroscopy

Andrei Tokmakoff

Department of Chemistry, James Franck Institute, and Institute for Biophysical Dynamics
The University of Chicago, Chicago, IL 60637
E-mail: tokmakoff@uchicago.edu

Water's rich hydrogen bonding (H-bonding) dynamics allow ionic species, particularly the proton, to integrate and transport rapidly along the H-bond network. These properties make aqueous systems ideal for alternative energy sources such as fuel cells, water oxidation catalysis, and aqueous battery technology. The aim of our research program is to study the molecular details of H-bond reorganization mechanisms in water and how these processes impact the solvation and transport of ions in the aqueous phase.

In the past year, our research has focused on interrogating solvation structure and dynamics in acidic aqueous solutions with ultrafast infrared spectroscopy. Simultaneous collection of parallel and perpendicular polarization geometries has enabled direct observation of ion interactions and proton transfer with two-dimensional infrared (2D IR) and transient absorption spectroscopy. High-level anharmonic vibrational calculations from the Bowman group (Emory University) have provided crucial insight for understanding the infrared spectrum of aqueous acids, and continuing work is underway to assign and interpret the vibrational excited states probed in the 2D IR spectrum. Finally, we are developing a broadband infrared excitation light source which produces 100-fs, multi-microjoule pulses spanning the entire mid-IR (1000–4000 cm^{-1}). This will enable us to faithfully measure the broad continuous absorption with nonlinear spectroscopy.

One of the distinctive characteristics of the aqueous excess proton is its extremely high polarizability, which results to a significant extent from the large degree of structural reorganization possible in its solvation structure. An important question when studying the structure of the $H^+(aq)$ complex is the specific role of the counter anions in solution, how they affect the excess proton. If the anion is in close proximity to the excess proton, or if perhaps it is in direct contact, in the form of an ion pair, it might play a significant role in reshaping the solvation structure of the excess proton, and perhaps change its nature entirely. To study this effect, we have performed a series of 2D IR measurements on nitric acid solutions as a function of concentration. At very high concentrations, higher than approximately 4M, we observe a distinct intermolecular cross peak between the asymmetric stretch mode of the nitrate ion and the acid bending mode, indicative of the formation of a significant population of contracted ion pairs. These ion pairs are structurally distinct from undissociated nitric acid molecules, but have a similar concentration dependence. Furthermore, this intermolecular cross peak appears on the high-frequency side of the acid bending band, around 1800 cm^{-1} rather than 1750 cm^{-1}, suggesting that the proximity of the nitrate ion results in the excess proton taking on a more hydronium-like structure as opposed to the more symmetrically shared Zundel-like structure observed when the excess proton is not participating in an ion pair. This demonstrates the structural adaptability of the solvation complex of the excess proton in water.

Previous work in our group demonstrated that picosecond proton transfer kinetics can be directly observed through polarization anisotropy decay experiments. By exciting the bend modes of the aqueous proton and detecting the polarization-sensitive transient absorption, we observe

reorientation kinetics that persist on a 2.5 ps timescale. Given that the aqueous proton bend dipole is parallel to the O-O axis and the 2.5 ps timescale is consistent with aqueous H-bond reorganization, we concluded that the reorientation of the hydrated proton bend reports on irreversible proton transfer kinetics.

We have expanded the above experiment to multiple temperatures ranging from 5–55 °C, concentrations of 1M–4M, and in solutions with different counterions to learn about the energetic barriers associated with the proton transfer process. We find that protonated bend reorientation follows Arrhenius kinetics, with barriers ranging from 2.4 kcal/mol in 1M and 2M HCl to 1.3 kcal/mol in 4M HCl. We also find that the barrier is more strongly determined by anion identity and concentration than proton concentration. The 1M HCl reorientation barrier agrees with values of the proton diffusion barrier determined from NMR relaxation experiments (2.4 kcal/mol) and MS-EVB simulations (2.7 kcal/mol), reinforcing the notion that proton bend reorientation reports on proton transfer. The proton transfer barrier is more than 1 kcal/mol less than the barrier for H-bond reorganization in neat water (3.8 kcal/mol), which is counterintuitive given the relatively strong H-bonding around the excess proton. This observation along with the dependence on counterion indicate that collective H-bond dynamics of the aqueous solution drive the proton transfer process. Surprisingly, we find a counterintuitive trend that proton transfer slows down in solutions with lowered barrier, increasing from τ_{or} = 1.9 ps in 1M HCl to τ_{or} = 2.3 ps in 4M HCl at 35 °C. Within an Eyring equation framework, we find that the timescale increases due to reductions in activation entropy $\Delta S^{\ddagger}$, whereas the barrier decreases due to reduced activation enthalpy $\Delta H^{\ddagger}$. The enthalpy decrease arises due to the increased fraction of relatively weaker H-bonds to halide anions, and the diminished entropy indicates that the counterions reduce configurational entropy by crowding and can even obstruct potential proton transfer pathways.

To conduct a detailed investigation of the highly anharmonic proton stretching band at 1200 cm^{-1}, we have been collaborating with Joel Bowman's group at Emory University to calculate the IR spectra of 800 independent aqueous proton configurations with high-level vibrational self-consistent field/ virtual configuration interaction (VSCF/VCI) calculations. Because the nuclear motions of the aqueous proton are confined in a highly anharmonic and multi-dimensional potential energy well, VSCF/VCI calculations are more adept to model the IR spectrum than conventional harmonic frequency calculations. The aggregate spectrum from the 800 $H^+(H_2O)_6$ configurations shows much improved agreement with the experimental IR spectrum of the aqueous proton compared to the harmonic IR spectrum, even without dynamical contributions to the lineshape. Decomposition of the spectrum by atomistic geometric parameters demonstrate contributions from a broad distribution of geometries ranging from distorted Eigen-like to asymmetric Zundel-like spectral characteristics. We also find trends in the proton stretch vibrational frequency with structural parameters, with the strongest correlation of this frequency with $\langle R_{OH} \rangle$, the quantum expectation value of the distance between the excess proton and its nearest oxygen. These analyses provide clarity on the role of anharmonicity in the linear IR spectrum of the aqueous proton for interpretation in future experiments and simulations.

We are currently continuing our collaboration with the Bowman group to use the anharmonic calculations for interpreting the 2D IR spectrum of the aqueous proton. VSCF/VCI calculations include excited-state energy levels and combination bands, which are directly interrogated in a 2D spectrum and provide rich information on the nature of anharmonic coupling between the nuclear motions of the aqueous proton complex. We are particularly interested in the proton stretching vibration and its coupled modes as a highly anharmonic system. For Zundel-like configurations, we find an ω_{21} energy gap that is larger than the fundamental ω_{10} transition, which

agrees with 2D IR experiments. To understand these results in detail, we have generated two-dimensional potential energy slices of the proton stretch potential to investigate coupling with modes that are expected to be strongly coupled with the proton stretch, in particular the O-O stretching and the concerted bending modes of the two waters flanking the excess proton. Analysis of the anharmonic contributions to these potentials for various configurations will help explain frequency position, heterogeneous contributions to lineshape broadening, and anharmonic coupling of various modes to the proton stretching vibration.

We are continuing to develop new light sources for use in ultrafast IR spectroscopy. This work is driven by the particularly broad spectral features and sub-100 fs dynamics in aqueous acid systems, which push the boundaries of current state-of-the-art methods for IR pulse generation. Our group previously developed a broadband IR probe source using filamentation in N_2 to produce 50-fs, 10 nanojoule pulses spanning the mid-IR. While this source has enabled broadband detection, excitation in the IR requires microjoule-levels of pulse energy. To this end, we build a GaSe-based optical parametric amplifier (OPA), which produces 10 microjoule, 100 fs pulses spanning 1000–4000 cm^{-1}. The OPA is seeded by broadband pulses generated from filamentation and pumped by 100 microjoule, 2 micron pulses from the idler of a commercial TOPAS OPA. Several parameters of the OPA—crystal length, phase-matching angle, beam spot sizes, focusing optics, and pump wavelength—were tuned to adjust the spectrum and power of the amplified light, yielding a 10% conversion of pump power in the amplification process. While the spectrum and intensity of the resulting pulses are suitable for use as a broadband excitation source, ongoing work is aimed at improving pulse compression towards the Fourier-transform limit of 8 fs. Care has been taken to minimize the material in the beam path, as any material will add chirp to such a broad pulse. Frequency-resolved optical gating will be used to analyze the full temporal profile of the pulse, providing insight for the how to approach compression. Second-order dispersion can be compensated with material with oppositely signed dispersion. If there is significant third-order dispersion, then a compressor will be necessary. Possible designs include a Si prism compressor or a deformable mirror-based compressor. The intense, broad pulses produced in this OPA will enable the characterization of the 2D IR lineshapes of broad aqueous acid features, which hold valuable information about the structural dynamics in these systems.

DOE Supported Publications 2018–2019

1. "Broadband 2D IR spectroscopy reveals dominant asymmetric $H_5O_2^+$ proton hydration structures in acid solutions," Joseph A. Fournier, William B. Carpenter, Nicholas H.C. Lewis, and Andrei Tokmakoff, *Nature Chemistry*, **10** (2018) 932–937. DOI: 10.1038/s41557-018-0091-y
2. "Direct Observation of Ion Pairing in Aqueous Nitric Acid Using 2D Infrared Spectroscopy," Nicholas H.C. Lewis, Joseph A. Fournier, William B. Carpenter, and Andrei Tokmakoff, *Journal of Physical Chemistry B*, **123** (2019), 225–238. DOI: 10.1021/acs.jpcb.8b10019
3. "Entropic Barriers in the Kinetics of Aqueous Proton Transfer," William B. Carpenter, Nicholas H.C. Lewis, Joseph A. Fournier, and Andrei Tokmakoff, *Journal of Chemical Physics,* **151** (2019) 034501. DOI: 10.1063/1.5108907
4. "High-Level VSCF/VCI Calculations Decode the Vibrational Spectrum of the Aqueous Proton," Qi Yu, William B. Carpenter, Nicholas H. C. Lewis, Andrei Tokmakoff, Joel M. Bowman, *Journal of Physical Chemistry B*, **123** (2019), 7214-7224. DOI: 10.1021/acs.jpcb.9b05723

Molecular based analysis of solvation processes – from clusters to bulk

Marat Valiev

Environmental Molecular Sciences Laboratory, Pacific Northwest National Laboratory, P. O. Box 999, Richland, Washington 993521

Abstract

The focus of our project is on building molecular level understanding of aqueous solutions, targeting a wide range of systems. The approach is based on development and application of advanced simulation methods that include various levels of quantum and classical descriptions.

Solute-specific effects play an important role in determining the overall behavior of an aqueous solution including molecular shape, charge distribution, and hydrogen bonding. These effects are amplified in solvated clusters, providing a window into understanding the corresponding behavior at the bulk level. Our investigation in this area is done in collaboration with photoelectron spectroscopy of size-selected negatively charged clusters performed by Xue-Bin Wang (PNNL). The key experimental observable is the electron binding energy (EBE), which is sensitive to cluster structure and chemical composition, allowing identification of the experimentally observed clusters. Simulations play an important role in this process by providing the link between cluster structure and the EBE. Our recent work in this area involved analysis of solvated dicarboxylate species ($^{-}O_2C(CH_2)_2CO_2^{-}$) in complex with Na^+ and K^+ metal cations. Our results have shown that evolution of aqueous solvation shell emphasizes coordination of the negatively charged carboxylate groups accompanied by simultaneous interaction with metal cation. In the solvation range investigated experimentally (up to 6 waters), Na+ retains direct contact with the dicarboxylate species, i.e. contact ion-pair (CIP) complex. Further modeling studies show the evidence of alternative solvent separated ion-pair complex once the solvation range approaches 8 waters, however its energy still remains above (~7-8 kcal/mol) the CIP complex. At higher number of waters, experimental spectra also show development of a weak low energy band. Our calculations suggest that the signal may be attributed to the quaternary complex consisting of Na+, H_2O, OH^- and singly protonated dicarboxylate anion. Such complex appears to be stabilized at the solvation range corresponding to the appearance of the low EBE band, however its energy is fairly high compared to the ternary structure. Further work in this area will involve analysis of bifunctional carboxylate species (e.g. amino acids) and tri-carboxylate compounds (e.g. citrate).

We also continue our efforts in developing fundamental statistical mechanics theory of molecular liquids based on classical density functional theory (cDFT) framework. Our ultimate goal is to develop a systematic approach to generate reduced statistical mechanics models for molecular liquids based on classical or ab-initio derived potentials. Current cDFT implementations such as three-dimensional reference interaction site mode (3D-RISM) have significant problems treating of chemical bonding interactions. This issue is addressed in our decent reformulation of cDFT. The preliminary results for inhomogeneous diatomic liquids show that this new approach provides a significant improvement over 3D-RISM eliminating unphysical density build up in the forbidden region near the solute.

Project Publications:

T. Pirojsirikul, M. Valiev, A. W. Götz, J. Weare, R. Walker, K. Kowalski, Combined Quantum-Mechanical Molecular Mechanics Calculations with NWChem and AMBER: Excited State Properties of Green Fluorescent Protein Chromophore Analogue in Aqueous Solution. J. Comp. Chem., **2017**, 38(18), 1631-1639

Hou, G.-L., Zhang, J., Valiev, M., Wang, X.-B., Structures and energetics of hydrated deprotonated cis-pinonic acid anion clusters and their atmospheric relevance Phys. Chem. Chem. Phys., **2017**, 19, 10676 -10684

Hou, G.-L., Wang, X.-B., and Marat Valiev, Formation of (HCOO–)(H2SO4) Anion Clusters: Violation of Gas-Phase Acidity Predictions, J. Am. Chem. Soc. **2017** 139 (33), 11321-11324

M. Valiev, G. Chuev, Site density models of inhomogeneous classical molecular liquids. J. Stat. Mech.: Theory and Experiment. 2018. 093201. 10.1088/1742-5468/aad6bf.

Li R., S. Deng, G. Hou, M. Valiev, and X. Wang. 2018. "Photoelectron spectroscopy of solvated dicarboxylate and alkali metal ion clusters, M+[O2C(CH2)2CO2]2- [H2O]n (M = Na, K, n = 1-6)." *Physical Chemistry Chemical Physics. PCCP* 20, no. 46:29051-29060, doi:10.1039/c8cp03896a

Hou G., M. Valiev, and X. Wang. 2019. "Sulfuric acid and aromatic carboxylate clusters H_2SO_4•$ArCOO^-$: structures, properties, and their relevance to the initial aerosol nucleation." *International Journal of Mass Spectrometry* 439, doi:10.1016/j.ijms.2019.02.001

Catalysis Driven by Confined Hot Carriers at the Liquid/Metal/Zeolite Interface

Bin Wang
School of Chemical, Biological and Materials Engineering
University of Oklahoma, 100 E. Boyd St. Norman, OK 73019
e-mail: wang_cbme@ou.edu

Program Scope: In chemical industry controlling the activity and selectivity of a chemical conversion process is of immense importance. Traditionally, dissipation of thermal energy drives transformation of reactants, which may lead to formation of a variety of products; it remains a key challenge to design a process that dissociation and formation of specific chemical bonds can be triggered to form desirable products with very high selectivity, preferably at low temperatures and pressures. Introduction of light-sensitive solid materials into catalysis provides a powerful, alternate strategy for this purpose.

In this light-driven process, positive and negative charges, which are generated through photoexcitation of coinage metal nanoparticles, stimulate the dynamics of chemical bonds in the reactants adsorbed on the metal. The objective of this research is to provide fundamental understanding of this light-driven bond dynamics at the molecular level and to develop a low-temperature, all optical catalysis process that is driven by plasmonic hot carriers confined in microporous structures. We plan to, using first-principles computational simulations, explore the following concepts:

a. Interfacial charge transfer between metal and adsorbed molecules on crystalline metal surfaces and supported metal nanoparticles.
b. Mechanism of surface-plasmon-assisted bond formation on metal surfaces such as formation of O-H and C-H bond in hydrogenation reactions.
c. Effects of confinement on the structural dynamics and optical properties of metal nanoparticles in microporous materials with varied pore sizes/shapes.
d. Interaction between the confined non-equilibrium charges and the acid sites in microporous materials with different confinement and acid strength.
e. Mechanism of electron- and hole-driven reactions in microporous materials.

Recent Progress and Future Plans: The dynamic and non-equilibrium nature of plasmonic catalysis necessitates first-principles simulations at both the ground state and the excited states. We will employ ab initio molecular dynamics simulations to track the atomic dynamics of the nanoclusters, density functional theory calculations to reveal the interfacial charge transfer and band alignment, nudged elastic band and dimer methods for calculations of the activation barriers, and the delta self-consistent field method to investigate the bond dynamics at the excited states. As the start of this project, the current efforts have been focused on the hydrogenation of the N=O bond in nitrophenol and the C≡C triple bond in phenylacetylene, both of which have shown enhanced activity and/or selectivity in plasmonic catalysis as compared to the conventional thermal reactions. We find very recently that, in the delta self-consistent field calculations, the activation barrier can be significantly reduced when specific empty states are partially occupied. The same approach will be applied to study reactions in confined spaces where metal nanoparticles are embedded in the microporous cavities offered by zeolite.

A major outcome of this DOE grant would be a paradigm by which one can understand the bond dynamics (vibration, formation and dissociation) perturbed by the hot carriers that are either injected or directly excited in the molecules. Based on this fundamental understanding, we may tune the photon energy, the particle size/shape, and the interfacial chemistry to target specific bond dynamics and drive a desirable reaction while other competing reactions are suppressed.

CPIMS-sponsored publications during the past two years – There are no publications to report because this is a new award, with a start date of September 1, 2019.

Chemical Kinetics and Dynamics at Interfaces

Cluster Model Investigation of Ion Solvation and Reactivity

Xue-Bin Wang

Physical Sciences Division, Pacific Northwest National Laboratory, P.O. Box 999, MS K8-88, Richland, WA 99352. E-mail: xuebin.wang@pnnl.gov

Collaborators include: J Warneke, WT Borden, SH Strauss, OV Boltalina, CC Cummins, J M. Goicoechea, E Aprà, N Govind, SS Xantheas, M Valiev

Program Scope

We aim at obtaining the fundamental interactions of aqueous electrolyte solutions, the solvation of complex anions, ion-pairing of polyatomic anion with cations, and chemical reactivity under a variety of condensed phase environments using gaseous clusters as model systems. Clusters occupy an intermediate region between gas phase molecules and the condensed states of matter and play an important role in heterogeneous catalysis, aerosol chemistry, and biological processes. We use electrospray ionization (ESI) to generate various molecular and ionic clusters to simulate key species involved in the condensed phase reactions and transformations, and characterize them using cryogenic negative ion photoelectron spectroscopy (NIPES) and high-resolution velocity-map imaging (VMI) photoelectron spectroscopy. Inter- and intra-molecular interactions and their variation as function of size and composition, important to understand complex chemical reactions and nucleation processes in condensed and interfacial phases can be directly obtained. Experiments and *ab initio* calculations are synergistically combined to

- Obtain a molecular-level understanding of the solvation and stabilization of Hofmeister anions, ion specific effects in hydrated anion and neutral clusters, and stepwise salt dissolution processes;
- Study temperature-dependent conformation changes and isomer populations of complex clusters;
- Explore new concepts and chemistries unique to the cluster domain and distinctly different from isolated molecules and bulk;
- Investigate intrinsic electronic structures of environmentally and catalytically important species and reactive diradicals;
- Quantify thermodynamic driving forces resulting from hydrogen-bonded networks formed in aerosol nucleation processes and enzymatic catalytic reactions

The central goal of this research program is obtaining a fundamental understanding of environmental materials and solution chemistry important to many primary DOE missions, and enhancing scientific synergies between experimental and theoretical studies towards achieving such goals.

Recent Progress

Photoelectron spectroscopy of solvated dicarboxylate dianion and alkali metal cation clusters, $M^+[O_2C(CH_2)_2CO_2]^{2-}$ $[H_2O]_n$ (M=Na, K; n=1-6): We carried out combined experimental photoelectron spectroscopy and theoretical modeling studies of solvated succinate dianion ($^-O_2C(CH_2)_2CO_2^-$) in complex with Na^+ and K^+ metal cations. These ternary clusters serve as simple models for investigation of aqueous ion/solute specific effects that play an important role in biological systems. The experimental characterization of these systems was performed in the presence of up to six solvating waters. For both Na^+ and K^+, we observe one major broad band that gradually shifts to higher electron binding energy (EBE) with increasing number of waters. For Na^+, further detailed analysis of the experimental spectra was performed using *ab-initio* calculations. In particular, we have identified structures of the lowest energy clusters whose EBE

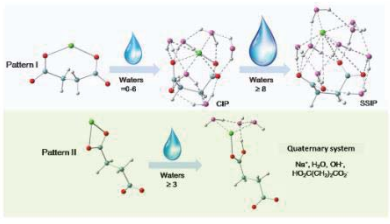

values match the experimental spectra. Our results show that evolution of the aqueous solvation shell emphasizes coordination of the negatively charged carboxylate groups accompanied by simultaneous interaction with the metal cation. Calculations also indicate that in the solvation range investigated experimentally (up to 6 waters), Na^+ retains direct contact with the dicarboxylate species, i.e. a contact ion-pair (CIP) complex. Preliminary modeling studies show evidence of a solvent separated ion-pair (SSIP) complex once the solvation range approaches 8 waters. At higher number of waters ($n \geq 3$ for Na^+ and $n \geq 5$ for K^+), the experimental spectra exhibit emergence of a weak low energy band. Our calculations for Na^+ indicate the existence of a quaternary complex consisting of Na^+, H_2O, OH^- and a singly-protonated dicarboxylate anion ($HO_2C(CH)_2CO_2^-$). This complex appears to be stabilized at the solvation range corresponding to the appearance of the low EBE band and does match its peak, even though the energy of such complex is fairly high compared to the ternary structure (*Phys. Chem. Chem. Phys.* **2018**, *20*, 29051).

Direct Observation of Hierarchic Molecular Interactions Critical to Biogenic Aerosol Formation: Small clusters consisting of sulfuric acid/bisulfate and oxidized organics have been identified in both aerosol field measurements and laboratory experiments, and their formation is suggested to be rate-limiting steps in new particle formation processes. However, the underlying molecular mechanism of these clusters formation is still largely unclear. We have shown through an integrated negative ion photoelectron spectroscopy and quantum chemical study on a series of (HSO_4^-)(organic molecule) surrogate binary clusters that the functional groups are more important in determining the extent of the enhanced role of the organics in aerosol formation process than the average carbon oxidation states or O/C ratios. Such extent has been quantified explicitly for specific functional groups, revealing highly hierarchic intermolecular interactions critical to aerosol formation. Born-Oppenheimer molecular dynamics simulations have been employed to probe the water binding abilities of these clusters under ambient conditions, and their statistical hydrogen bonding networks. (*Communications Chemistry* **2018**, *1*, 37).

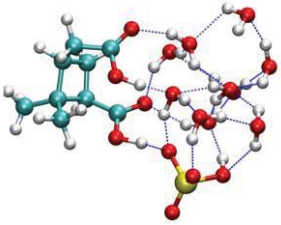

Photoelectron spectroscopic and computational study of [EDTA•*M*(III)]$^-$ complexes (*M* = H_3, Al, Sc, V−Co): Metal-EDTA complexes are common biological redox reagents. We have generated a series of such complexes, [EDTA•*M*(III)]$^-$ (*M* = Al, Sc, V-Co), via electrospray ionization and characterized them by cryogenic mass-selected negative ion photoelectron spectroscopy (NIPES) and quantum chemical computations. Experiments clearly reveal one more spectral band at low electron binding energy for transition metal complexes with d electrons (*M* = V-Co) than those without d electrons (*M* = Al and Sc). Quantum chemical calculations suggest that all of the metal-complexes possess hexacoordinated metal-ligand binding motifs, with the calculated adiabatic/vertical detachment energy (ADE/VDE) and band gaps in good agreement with the experimental values. Direct spectrum and electronic structure analyses indicted that [EDTA•V(III)]$^-$ can be easily oxidized to [EDTA•V(IV)] with the smallest ADE/VDE of 3.95/4.40 eV among these metal-complexes, but further oxidation is hindered by the existence of a 2.30 eV band gap, a fact that accords with the special redox behavior of vanadium-containing species in biological cells. Spin density and molecular orbital analyses reveal that [EDTA•V(III)]$^-$ is overwhelmingly detached from vanadium atom, in stark contrast to [EDTA•Sc(III)/Al(III)]$^-$ where the detachment occurs from the EDTA ligand. For all other metal complex anions, from *M* = Cr to Co, the detachment process is derived from contributions from both the metal and ligand. The intrinsic electronic and geometric structures of these complexes, obtained in this work, provide a molecular foundation to better understand their redox chemistries and specific metal bindings in condensed phases and biological cells. (*Phys. Chem. Chem. Phys*. **2018**, *20*, 19458).

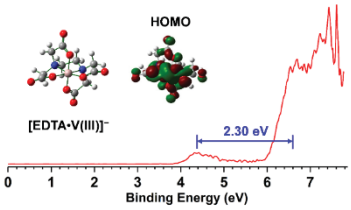

Deviation from the *trans*-Effect in Ligand-Exchange Reactions of Zeise's Ions $PtCl_3(C_2H_4)^-$ with Heavier Halides (Br^-, I^-): Four new Zeise's family ions with mixed halide ligands, i.e., $PtCl_nX_{3-n}(C_2H_4)^-$ (X = Br, I; n = 1, 2), were synthesized via ligand-exchange reactions of KX salts with $KPtCl_3(C_2H_4)$ in aqueous solutions, and were detected in vacuum via electrospray ionization mass spectrometry. Their photoelectron spectra reveal a series of well-resolved spectral peaks with their electron binding energies (EBEs) decreasing with increasing halide size, with I having a much stronger effect than Br, i.e., 4.57 ($-Cl_3$) > 4.56 ($-Cl_2Br$) > 4.53 ($-ClBr_2$) > 4.34 ($-Cl_2I$) > 4.30 eV ($-ClI_2$). *Ab initio* electronic structure calculations including spin-orbit coupling (SOC) predict that the *cis*- and *trans*-isomers are nearly isoenergetic with the *cis*- for $-Cl_2X$, and the *trans*- for $-ClX_2$ slightly favored, respectively. Excited-state spectra calculated with time-dependent density functional theory (TDDFT), and their comparison with experiment suggest that for each species, both the *cis*- and *trans*- configurations coexist and contribute to the observed spectra, a fact that clearly deviates from the prediction from the widely accepted *trans*-effect, which suggests that only one isomer would have formed. (*J. Phys. Chem. A.* **2018**, *122*, 1209).

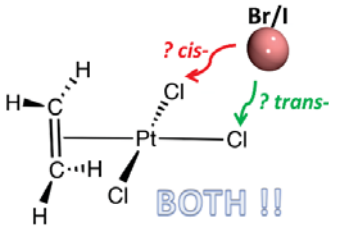

Future Directions

The main thrust of our BES program will continue to be on cluster model studies of condensed phase phenomena in the gas phase. The experimental capabilities that we have developed give us the opportunity to attack a broad range of fundamental chemical physics problems pertinent to ionic solvation, solution chemistry, homogeneous / heterogeneous catalysis, aerosol chemistry, biological processes, and material synthesis. The ability to cool and control ion temperature, when combined with wavenumber energy resolution VMI will enable us to study different isomer populations and conformation changes of environmentally important hydrated clusters. Another major direction will employ gaseous clusters to model ion-specific interactions in solutions, ion transport, inert compound activation, ion-receptor interactions in biological systems, and the initial stages of nucleation processes relevant to atmospheric aerosol formation.

References to Publications of DOE CPIMS Sponsored Research (during the past two years)

1. Jonas Warneke, Gao-Lei Hou, Edoardo Aprà, Carsten Jenne, Zheng Yang, Zhengbo Qin, Karol Kowalski, Xue-Bin Wang, and Sotiris S. Xantheas, "Electronic Structure and Stability of $[B_{12}X_{12}]^{2-}$ (X=F−At): A Combined Photoelectron Spectroscopic and Theoretical Study", *J. Am. Chem. Soc*. **2017**, *139*, 14749-14756.
2. Gao-Lei Hou, Xue-Bin Wang, Anne B. McCoy, and Weston Thatcher Borden, "Experimental and Theoretical Studies of the $F^\bullet$ + H-F Transition-State Region by Photodetachment of $[F{-}H{-}F]^-$", *J. Phys. Chem. A.* **2017**, *121*, 7895-7902.
3. Long K. San, Sarah N. Spisak, Cristina Dubceac, Shihu H. M. Deng, Igor V. Kuvychko, Marina A. Petrukhina, Xue-Bin Wang, Alexey A. Popov, Steven H. Strauss, and Olga V. Boltalina, "Experimental and DFT Studies of the Electron-Withdrawing Ability of Perfluoroalkyl (R_F) Groups: Electron Affinities of $PAH(R_F)_n$ Increase Significantly with Increasing RF Chain Length", *Chem. Eur. J.* **2018**, *24*, 1441-1447.
4. Gao-Lei Hou, Niranjan Govind, Sotiris S. Xantheas, Xue-Bin Wang, "Deviation from the *trans*-Effect in Ligand-Exchange Reactions of Zeise's Ions $PtCl_3(C_2H_4)^-$ with Heavier Halides (Br^-, I^-)", *J. Phys. Chem. A.* **2018**, *122*, 1209-1214.
5. David A. Hrovat, Xue-Bin Wang, and Weston Thatcher Borden, "Calculations of the Relative Energies of the Low-lying Electronic States of 2,7-Naphthoquinodimethane and 2,7-Naphthoquinone. Substitution of Oxygen for CH_2 Is Predicted to Increase the Singlet-Triplet Energy Difference (ΔE_{ST})", *J. Phys. Org. Chem.* **2018**, e3824.
6. Zheng Yang, David A. Hrovat, Gao-Lei Hou, Weston Thatcher Borden, and Xue-Bin Wang, "Negative Ion Photoelectron Spectroscopy Confirms the Prediction of the Relative Energies of the Low-Lying Electronic States of 2,7- Napthoquinone", *J. Phys. Chem. A.* **2018,** *122*, 4838-4844.

7. Qinqin Yuan, Zheng Yang, Renzhong Li, Wesley J. Transue, Zhipeng Li, Ling Jiang, Niranjan Govind, Christopher C. Cummins, and Xue-Bin Wang, "Magnetic-bottle and velocity-map imaging photoelectron spectroscopy of **A**PS$^-$ (**A** = $C_{14}H_{10}$ or anthracene): electron structure, spin-orbit coupling of **A**PS$^•$, and dipole-bound state of **A**PS$^-$", *Chin. J. Chem. Phys*. **2018**, *31*, 463-470.
8. Gao-Lei Hou, Wei Lin, Xue-Bin Wang, "Direct Observation of Hierarchic Molecular Interactions Critical to Biogenic Aerosol Formation" , *Communications Chemistry*, **2018**, *1*, 37.
9. Qinqin Yuan, Xiang-Tao Kong, Gao-Lei Hou, Ling Jiang, and Xue-Bin Wang, "Photoelectron spectroscopic and computational study of [EDTA•*M*(III)]$^-$ complexes (*M* = H_3, Al, Sc, V−Co)" *Phys. Chem. Chem. Phys*. **2018**, *20*, 19458-19469.
10. David Hrovat, Xue-Bin Wang, Weston T. Borden, "Calculations on 1,8-Naphthoquinone Predict that the Ground State of this Diradical Is a Singlet" *J. Comput. Chem.* **2019,** *40*, 119-126
11. Ren-Zhong Li, Shihu H. M. Deng, Gao-Lei Hou, Marat Valiev and Xue-Bin Wang, "Photoelectron spectroscopy of solvated dicarboxylate and alkali metal ion clusters, $M^+[O_2C(CH_2)_2CO_2]^{2-}$ $[H_2O]_n$ (M=Na, K; n = 1-6)" *Phys. Chem. Chem. Phys.* **2018**, *20*, 29051-29060.
12. Jonas Warneke, Markus Rohdenburg, Judy Kuan-Yu Liu, Erynn Johnson, Xin Ma, Rashmi Kumar, Pei Su, Edoardo Aprà, Xuebin Wang, Carsten Jenne, Maik Finze, Hilkka I. Kenttämaa, Julia Laskin, "Gas phase fragmentation of adducts between dioxygen and *closo*-borate radical anions" *Int. J. mass Spectrum*. **2019**, *436*, 71-78.
13. Jonas Warneke, Szymon Z. Konieczka, Gao-Lei Hou, Edoardo Aprà, Christoph Kerpen, Fabian Keppner, Thomas C. Schäfer, Michael Deckert, Zheng Yang, Eric J. Bylaska, Grant E. Johnson, Julia Laskin, Sotiris S. Xantheas, Xue-Bin Wang, Maik Finze, "Properties of perhalogenated {*closo*-B_{10}} and {*closo*-B_{11}} multiply charged anions and a critical comparison with {*closo*-B_{12}} in the gas and the condensed Phase" *Phys. Chem. Chem. Phys.* **2019**, *21*, 5903 – 5915.
14. Qinqin Yuan, Xiang-Tao Kong, Gao-Lei Hou, Ling Jiang, and Xue-Bin Wang, "electrospray ionization photoelectron spectroscopy of cryogenic [EDTA•*M*(II)]$^{2-}$ complexes (*M* = Ca, V−Zn): electronic structures and intrinsic redox properties" *Faraday Discussions*, **2019**, *217*, 383-395.
15. Gao-Lei Hou, Marat Valiev, and Xue-Bin Wang, "Sulfuric acid and aromatic carboxylate clusters H_2SO_4•$ArCOO^-$: Structures, properties, and their relevance to the initial aerosol nucleation". *Int. J. Mass. Spectro*. **2019**, *439*, 27-33.
16. Zheng Yang, David A. Hrovat, Gao-Lei Hou, Weston Thatcher Borden, and Xue-Bin Wang, **"**Negative Ion Photoelectron Spectroscopy Confirms the Prediction of a Singlet Ground State for the 1,8-Naphthoquinone Diradical". *J. Phys. Chem. A* **2019**, *123*, 3142-3148.
17. Issaka Seidu, Prateek Goel, Xiao-Gang Wang, Bo Chen, Xue-Bin Wang, and Tao Zeng, "Vibronic interaction in CO_3^- photo-detachment: Jahn-Teller effects beyond structural distortion and general formalisms for vibronic hamiltonians in trigonal symmetries". *Phys. Chem. Chem. Phys.* **2019**, *21*, 8679-8690.
18. Martin Mayer, Valentin van Lessen, Markus Rohdenburg, Gao-Lei Hou, Zheng Yang, Rüdiger M. Exner, Edoardo Apra, Vladimir A. Azov, Simon Grabowsky, Sotiris S. Xantheas, Knut R. Asmis, Xue-Bin Wang, Carsten Jenne and Jonas Warneke, "Rational design of an argon-binding superelectrophilic anion", *Proc. Natl. Acad. Sci.* **2019**, *116*, 8167-8172.
19. Edoardo Aprà, Jonas Warneke, Sotiris S. Xantheas, Xue-Bin Wang, "A benchmark photoelectron spectroscopic and theoretical study of the electronic stability of $[B_{12}H_{12}]^{2-}$", *J. Chem. Phys.* **2019**,*150*, 164306-1-8.
20. Zhipeng Li, Zhubin Hu, Yanrong Jiang, Qinqin Yuan, Haitao Sun, Xue-Bin Wang, and Zhenrong Sun, "Electronic Structures and Binding Motifs of Sodium Polysulfide Clusters $NaSn^-$ (n = 5–9): A joint negative ion photoelectron spectroscopy and computational investigation", *J. Chem. Phys.* **2019**, *150*, 244305-1-9.
21. Jian Luo, Jun Zhu, De-Hui Tuo, Qinqin Yuan, Lei Wang, Xue-Bin Wang, Yu-Fei Ao, Qi-Qiang Wang, De-Xian Wang, "Macrocycle-Directed Construction of Tetrahedral Anion-π Receptors for Nesting Anions with Complementary Geometry", Chemistry–a European Journal, **2019** (DOI: 10.1002/chem.201903272)
22. Qinqin Yuan, Frank Tambornino, Alexander Hinz, Weston Thatcher Borden, Jose M. Goicoechea, Bo Chen, Xue-Bin Wang, "Photoelectron Spectroscopy and Theoretical Studies of $PCSe^-$, $AsCS^-$, $AsCSe^-$, and $NCSe^-$: Insights into the Electronic Structures of the Whole Family of ECX^- (*E* = N, P, and As; *X* = O, S, and Se) anions" *Angew. Chem. Int. Ed*. **2019**, (DOI: 10.1002/anie.201906904).

Nonequilibrium Properties of Driven Electrochemical Interfaces

PI: Adam P. Willard
Massachusetts Institute of Technology, Department of Chemistry
77 Massachusetts Ave., Cambridge, MA 02139
awillard@mit.edu

Program Scope:
The influence of nanoscale disorder on individual electrochemical processes is an important problem that is yet to be fully understood. Disorder due to variations in local electrolyte composition or irregular interfacial geometries can influence chemical dynamics and thereby lead to heterogeneous chemical reactivity. It is difficult to asses the importance of this heterogeneity using traditional theoretical approaches (such as those based on the developments of Gouy, Chapman, and Stern) because these approaches are primarily based on mean field approximations, and thus omit the explicit effects of molecular/nanoscale disorder. The development of theoretical techniques that are capable of modeling these effects and quantifying their influence on chemical processes thus have the potential to provide important new physical insight.

Reactive electrochemical systems are inherently out of equilibrium. Active processes, such as interfacial electron transfer, influence both the static and dynamic properties of the interfacial environment, and ultimately drive the flux of reactive species across the electrochemical interface. Understanding and characterizing the nonequilibrium response of the interfacial environment is thus essential for predicting and quantifying these effects. The primary goal of this program is to investigate the static and dynamic properties of electrochemical interfaces driven out of equilibrium, and to determine how these nonequilibrium systems are affected by the presence of nanoscale disorder.

Our approach utilizes all-atom molecular simulation and coarse grained modeling to explore the properties of electrolytes under changing conditions of the electrostatic environment. We utilize general phenomenological models that provide the capability to explicitly evaluate the theoretical assumptions that underlie traditional electrochemical theories. Unlike traditional theoretical frameworks our models do not rely on the assumption that the electrochemical environment is a rapidly relaxing homogeneous continuum. Instead, our models explicitly treat the spatial fluctuations of charged species that drive individual electrochemical processes.

Our simulations also include a stochastic model of interfacial charge transfer to simulate active model electrochemistry. This allows us to explicitly evaluate the interplay between charge mobility within the electrolyte and charge creation/annihilation at the electrochemical interface. By exploring this interplay, and how it is affected by nanoscale disorder at the interface, we aim to reveal fundamental physical insight into the microscopic processes that drive reactivity at driven electrochemical interfaces.

Recent Progress:
Over the last year, we have made progress on two scientific fronts. The first is the development of a model for including constant potential boundary conditions that are capable of electron transfer in classical molecular dynamics simulations. The second is a theoretical study of the influence of image charges on the microscopic electrostatic potential fluctuations near an electrode surface. Both of these developments are described in more detail below.

Modeling constant potential electrochemically active boundary conditions in molecular simulation: In classical molecular dynamics, traditional force fields lack the functionality to model constant potential electrodes or to simulate chemical reactivity. Over the past 20 years, numerous methodological advances have targeted this lack of functionality. This includes the development of methods for simulating constant potential electrodes, reactive force fields for simulating bond making/breaking, and stochastic approaches to modeling interfacial electron transfer events. Despite these separate advances, there have been no MD-

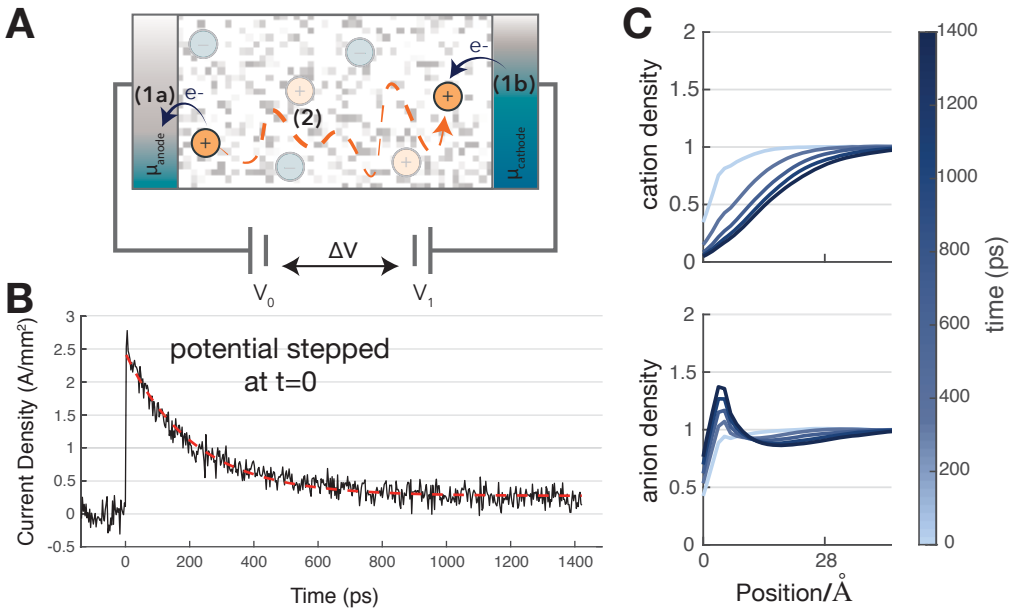

Figure 1. Simulating nonequilibrium double-layer formation in a model electrochemical cell. (A) Schematic illustration of our simulation method, which includes constant potential electrochemically active electrodes with independently tunable potentials. (B) Simulation data of the model current generated after a step change in the electrode potential difference. (C) The buildup of the double layer structure at the left-hand electrode following the potential change.

based models that combine both tunable constant potential electrodes and the capability for interfacial electron transfer that is sensitive to fluctuations in the electrolyte system.

Recently, we have developed a model for electrochemically active and electrostatically consistent electrodes held under constant potential conditions that is fully compatible with standard classical molecular dynamics. This model (1) treats the constant potential boundaries in a computationally efficient manner, (2) allows for outer-sphere oxidation and reduction at both electrodes, and (3) can include the effect of ion intercalation into the electrode, so that both the total charge and number of redox-active particles in the electrolyte can fluctuate throughout the course of the simulation. The functionality provided by our model enables a computationally efficient simulation of the microscopic dynamics of the electrolyte-electrolyte interface under operating conditions. We use this framework to simulate nonequilibrium processes, such as the interplay between current flow and double-layer formation following a step change in applied electrode potential, as illustrated in Fig. 1.

One of the primary challenges in modeling an electrochemical cell is efficiently handling the electrostatic interactions between the electrodes and the electrolyte. To capture the correct electrostatic behavior, proper treatment of the simulation cell boundary conditions and electrode polarizability are essential. Because of the long-range nature of Coulomb interactions, distance-based cutoff methods give the incorrect asymptotic behavior and the periodicity of the system needs to be considered carefully. Our model focuses

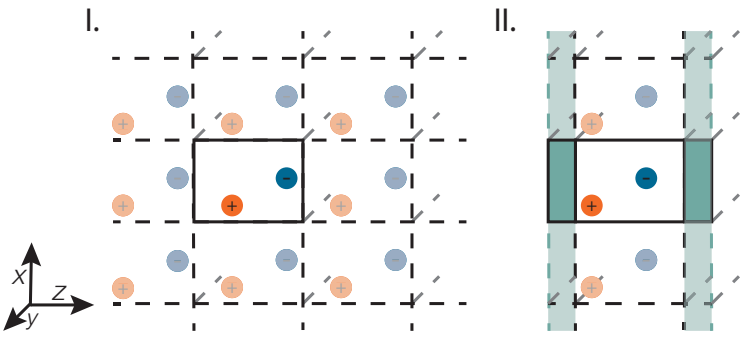

Figure 2. A schematic comparison of I. a fully three-dimensional periodic system and II. a slab system with finite width in the *z* direction. Both systems are illustrated in two-dimensions for convenience.

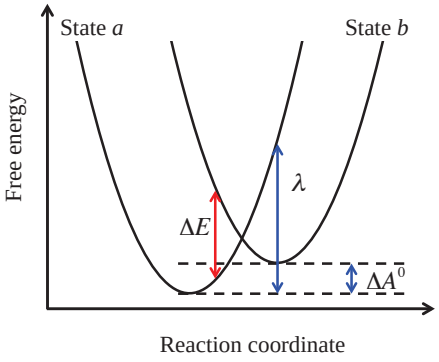

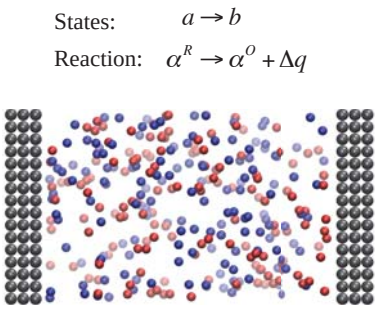

Figure 3 (Left) Marcus curves for diabatic energy surfaces of a redox reaction, with states a and b representing the different location of the transferred charge. (Right) For a redox reaction in an electrochemical cell, a double-electrode setup is employed, and the charge is transferred between the redox species (blue and red spheres) and the polarizable electrodes (gray spheres).

specifically on simulation cells with parallel planar electrodes positioned at the boundaries of the z directions and periodically replicated in the other x and y directions. Figure 2 shows the difference in long range symmetry between a bulk system periodically replicated in all directions and a two-dimensional slab system appropriate for modeling an interfacial system. Summation techniques for the calculation of electrostatic forces and energies in a two-dimensional slab system exist, but are more computationally expensive and less numerically robust than a standard three-dimensional calculation.

The effect of image charges on nanoscale potential fluctuations at the electrochemical interface: The interface between an electrode and an electrolyte solution can support the presence of strong electric fields due to charge buildup on the electrode surface. These fields can be tuned, by varying the electrode potential to promote chemical reactivity charge separation, and charge transfer. On average, these fields have smoothly varying profiles that are appropriately described by simple continuum models, however, over molecular time and length scales they are expected to be rugged and irregular due to the effects of microscopic thermal fluctuations. These fluctuations are not apparent in standard electrochemical measurements, yet they are known to play a fundamental role in driving solution-phase electron transfer reactions, for example as described by Marcus theory (see Fig. 3). Much remains to be understood about how these fluctuations are modified in the vicinity of an electrode interface.

One of the fundamental physical properties of a conducting electrode is that it can polarize in response to potential fluctuations in the electrolyte. At a planar electrode, this polarization response is conveniently conceptualized in terms of image charges. One implication of the image charge picture is that the electrode's contribution to potential fluctuations within the electrolyte has statistics that are analogous to that of the electrolyte. However, the image plane imposes a constraint on these fluctuations - that they are equal and opposite - that can has general and predictable physical consequences near the electrode.

We have recently developed a theory for quantifying these consequences and evaluating their influence on simple outer-sphere type interfacial electron transfer processes. Our approach applies continuum electrostatics to develop a coarse-grained statistical field theory with mirror-plane boundary conditions that effectively capture image charge effects. We start with the one-dimensional electrostatic potential profile, $\phi(z)$, resolved in the direction perpendicular to a pair of opposing infinite planar electrodes located at positions $z = 0$ and $z = 1$. We express this potential in a basis of sine functions,

$$\psi_q(z) = \sin(qz),$$

where $q \equiv n\pi$. This basis of odd functions encodes the mirror symmetry of the image plane and ensures boundary conditions of $\phi(0) = \phi(1) = 0$. In this basis, the corresponding electrostatic potential is given in terms of the Fourier components of the charge density field,

By using this basis and assuming a Gaussian charge density field we have shown that the variance of the real-space electrostatic potential is position dependent and given by,

$$\mathrm{Var}\left[\phi(z)\right] = \frac{16\sigma_\rho^2}{\pi^2}\sum_{n=1}^{\infty}\frac{\sin^2(n\pi z)}{\left(n^2+4\kappa^2/\pi\right)^2},$$

where σ_ρ^2 is the variance of the Gaussian charge density fluctuations and κ is the inverse of the Debye screening length. This relationship predicts a decrease in the variance of the electrostatic fluctuations near the electrode surface relative to that within the bulk liquid. To validate this theory we have carried out numerical simulations of an electrolyte in implicit solvent confined between two constant potential electrodes, as shown in Fig. 3a. We find that simulated variance, as reflected in the Madelung potential distribution, agrees qualitatively with theoretical predictions. Figure 4 also highlights the implications of this position dependent variance for Marcus-like outer-sphere electron transfer.

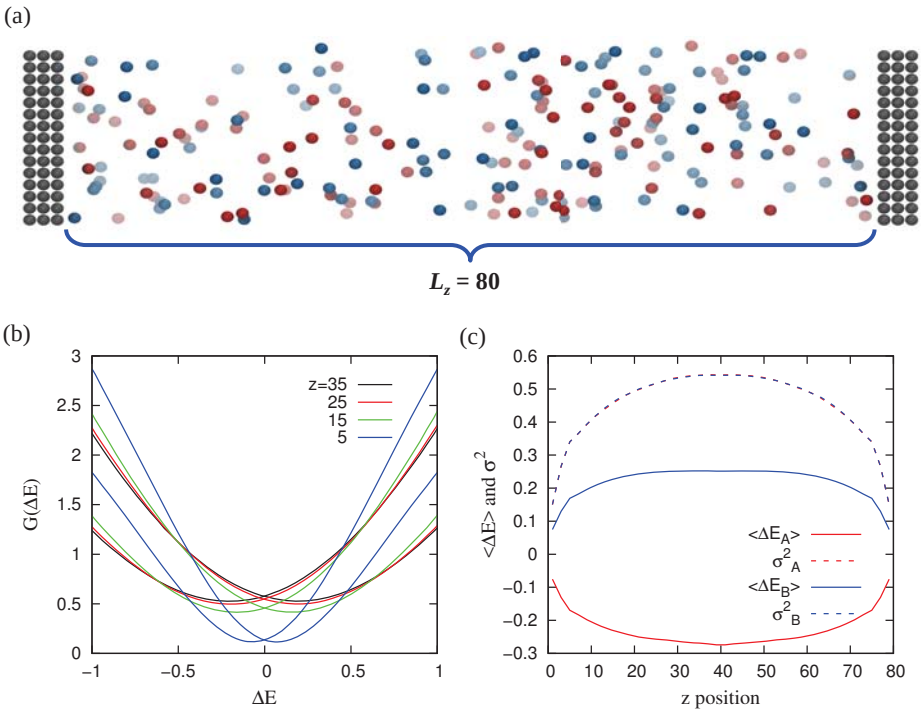

Figure 4. (a) Scheme of the double-electrode setup, mimicking an electrochemical cell. The inter-electrode distance is 80 in reduced unit. (b) Marcus parabolas for the states A ($\langle \Delta E \rangle > 0$) and B ($\langle \Delta E \rangle < 0$) at different z_α values, where$z_\alpha = 35$ is near the center of the cell, while $z_\alpha = 5$ is near the electrode interface. (c) The position dependent profile of the mean and variance of ΔE. Note that $\sigma^2[\Delta E^\alpha]$ (red triangles) overlays $\sigma^2[\Delta E^b]$ (blue dashed line).

Future Plans:

Future plans for this program will combine our newly developed simulation tools and coarse grained model to explore the properties of driven electrochemical systems. Specifically, we will focus on investigating the structural and dynamical properties of the electrochemical double layer, and how these properties vary when systems are driven out of equilibrium by interfacial electrochemical. We will apply our newly developed simulation tools and coarse grained models to study the screening response of electrolytes systems, such as that illustrate in Fig. 4, that are forced out of equilibrium by some external bias.

Publications:

K. A. Dwelle and A. P. Willard, "Constant potential, electrochemically active boundary conditions for electrochemical simulation", *J. Phys. Chem. C*, 123, 39, 24095-24103, (2019)

Real-Time Dynamics in Density Functional Tight Binding (DFTB): Towards Accurate Quantum Simulations for Large Chemical Systems

Bryan M. Wong
Department of Chemical & Environmental Engineering, Materials Science & Engineering Program, and Department of Physics & Astronomy
University of California-Riverside, Riverside, CA 92521
E-mail: bryan.wong@ucr.edu, Web: http://www.bmwong-group.com

1. Program Scope

This project is comprised of two complementary (but parallel) thrusts: (1) implementing massively-parallelized computing hardware (with new computational hardware that may replace GPUs) in the density functional tight binding (DFTB) approach and (2) developing new capabilities in DFTB to calculate the electronic structure and dynamics of large chemical systems. While classical molecular dynamics can handle hundreds of thousands of atoms, it cannot provide a first-principles based description of chemical systems at the quantum level. At the other extreme, conventional Kohn-Sham DFT methods can probe the true quantum mechanical nature of chemical systems; however, these methods cannot tackle the large sizes and length scales relevant to dynamics simulations of realistic systems. The DFTB formalism utilized in this project provides a viable approach for probing these large systems at a quantum mechanical level of detail. However, to utilize the DFTB approach for accurate calculations of electronic properties, it is crucial to incorporate *quantum-based corrections* in DFTB since exchange-correlation effects can still remain very strong in these large systems. At the same time, enhancing the computational efficiency of DFTB is also essential since optimal computational performance is required for addressing the large size scales associated with realistic chemical systems. As such, the new non-empirical corrections and computing hardware enhancements implemented in this project will enable accurate *and* computationally efficient approaches to directly probe electronic properties in these large, complex systems.

2. Recent Progress

During the past year we have devoted half of our initial efforts to massive parallelization (discussed briefly in Section 3. Future Plans) of the DFTB electron dynamics code and the other half of our focus to an in-depth assessment of the accuracy of density functional theory (DFT) and DFTB itself. Our progress on two of the topics related to DFT/DFTB performance is briefly highlighted below.

Recently, several studies on charge-localization effects in the *N*,*N*'-dimethylpiperazine (DMP^+) diamine cation have emerged as prototypical examples for testing the accuracy of density functional theory (DFT) methods. Within these studies, various DFT methods were examined and conclusions were made that "all DFT functionals commonly used today, including hybrid functionals with exact exchange, fail to predict a stable charge-localized state." This surprising conclusion is based on prior usage of a self-interaction correction (namely, complex-valued Perdew-Zunger Self-Interaction Correction (PZ-SIC)) to DFT, which appears to give excellent agreement with experiment and other wavefunction-based benchmarks. Since the publication of these prior studies, the same DMP^+ molecule has been cited in numerous subsequent studies as a prototypical example of the importance of self-interaction corrections for accurately calculating other chemical systems. This past year, we carried out new high-level CCSD(T) analyses on the

DMP^+ cation to show that DFT actually performs quite well for this system (in contrast to prior conclusions that all DFT functionals fail), whereas the PZ-SIC approach is the outlier that is inconsistent with the high-level CCSD(T) (coupled-cluster with single and double excitations and perturbative triples) calculations.

In **Figure 1**, we re-plot the PZ-SIC and M06-HF (Minnesota '06 with 100% Hartree Fock exchange) potential energy curves overlaid on top of our new MP2 (Møller-Plesset 2nd order perturbation theory), CCSD (coupled-cluster with single and double excitations), and CCSD(T) calculations. The charge-delocalized dimelthylpiperazine ($DMP\text{-}D^+$) structure occupies the global minimum on the potential energy curve and is characterized by a positive charge that is delocalized over the two equivalent nitrogen atoms. In contrast, the charge-localized dimelthylpiperazine ($DMP\text{-}L^+$) structure occupies a local minimum on the potential energy curve and has a positive charge that is localized on only one of the nitrogen atoms. The CCSD_CCSD(T)-SP and MP2_CCSD(T)-SP legend labels in **Figure 1** denote single-point (SP) energy calculations that were carried out with the CCSD(T) method using geometry-optimized structures obtained with CCSD and MP2, respectively. To maintain a consistent comparison with previous studies, the same basis sets from prior studies were used throughout this work (all optimizations were carried out with the aug-cc-pVDZ (augmented correlation-consistent polarized valence double-zeta) basis set, and single-point energy CCSD(T) calculations utilized the cc-pVTZ (correlation-consistent polarized valence triple-zeta) basis). It is worth noting that previous studies did not examine any details of the transition state structure using high-level wavefunction-based calculations, which we reported for the first time in *Nature Communications* (see Ref. 9 in Publications acknowledging DOE grant). Upon examination of **Figure 1**, we observe several clear trends. First, all three wavefunction-based approaches (CCSD, CCSD_CCSD(T)-SP, and MP2_CCSD(T)-SP) are in agreement by producing a potential energy curve with an extremely small energy barrier (< 0.01 eV), which is in stark contrast to the much larger 0.2 eV barrier obtained from the PZ-SIC approach. Most interestingly, a single-point CCSD(T) energy calculation on top of the CCSD- and MP2-optimized geometries further lowers the barrier to the point where it more closely resembles the M06-HF potential energy curve. While we take the CCSD_CCSD(T)-SP curve in **Figure 1** to be the most accurate calculation among all the methods studied, it is interesting to note that the MP2_CCSD(T)-SP curve still closely resembles both the CCSD_CCSD(T)-SP and M06-HF curves. In addition to the

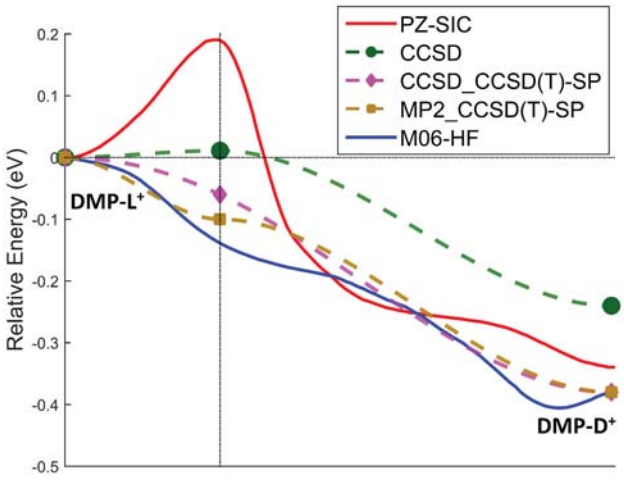

Figure 1. Calculated potential energy curve between the localized and delocalized state of the dimelthylpiperazine cation. The CCSD_CCSD(T)-SP and MP2_CCSD(T)-SP legend labels denote single-point energy calculations that were carried out with the CCSD(T) method using geometry-optimized structures obtained with CCSD and MP2, respectively. All three wavefunction-based approaches (CCSD, CCSD_CCSD(T)-SP, and MP2_CCSD(T)-SP) are in agreement by producing an extremely small energy barrier (< 0.01 eV), with the CCSD_CCSD(T)-SP and MP2_CCSD(T)-SP curves, in close agreement with the M06-HF DFT calculations.

barrier height, the CCSD(T) single-point calculations alter the relative energy difference between the DMP-D^+ and DMP-L^+ structures such that CCSD_CCSD(T)-SP and MP2_CCSD(T)-SP curves are even closer in agreement with the M06-HF DFT calculations. Taken together, both the small barrier heights and the DMP-D^+/DMP-L^+ relative energy differences obtained from the high-level CCSD(T) calculations show good agreement with DFT, and it is actually the PZ-SIC calculation that is the outlier and inconsistent with the highly-accurate CCSD(T) benchmarks. Our findings have important ramifications for improving DFT/DFTB for large systems since these calculations demonstrate that caution should be taken in applying self-interaction corrections as these can lead to incorrect results in certain chemical systems.

In our second assessment of DFT/DFTB performance on predicting electronic properties of complex systems, we examined the linear polarizability (α) and second hyperpolarizability (γ) in a series of cyanine-type molecules, as predicted with various range-separated functionals and CCSD(T)-based methods. Cyanine dyes comprise a subset of π-conjugated organic systems that exhibit remarkably strong linear and nonlinear optical (NLO) response electronic properties. In the past 50 years, these NLO properties have been harnessed in a variety of advanced materials and technologies such as electro-optic waveguide devices, memory devices, three-dimensional fluorescence microscopy, and nanofabrication. As such, predictive computational methods, particularly quantum chemical methods, offer a rational approach for guiding future experimental efforts to obtain tailored NLO properties in these functional π-conjugated systems. Contrary to previous work on these systems, we found that the lowest energy electronic states for large streptocyanine oligomers are not closed-shell singlets, and improved accuracy can be obtained with certain DFT methods by allowing the system to relax to a lower-energy broken-symmetry solution. Our extensive analyses were complemented by new large-scale CCSD(T) and explicitly correlated CCSD(T)-F12 calculations that comprise the most complete and accurate benchmarks of α and γ for the streptocyanine systems to date. Taken together, our CCSD(T) and broken-symmetry DFT calculations (1) show that the MP2 benchmarks used in previous studies still exhibit significant errors (~ 25% for α and ~100% for γ) and, therefore, the MP2 calculations should not be used as reliable benchmarks for polarizabilities or hyperpolarizabilities, and (2) emphasize the importance of testing for a lower-energy open-shell configuration when calculating nonlinear optical properties for these systems. This work was prominently featured as a front cover (cf. **Figure 2**) of the *Journal of Computational Chemistry* (see Ref. 8 in Publications acknowledging DOE grant)

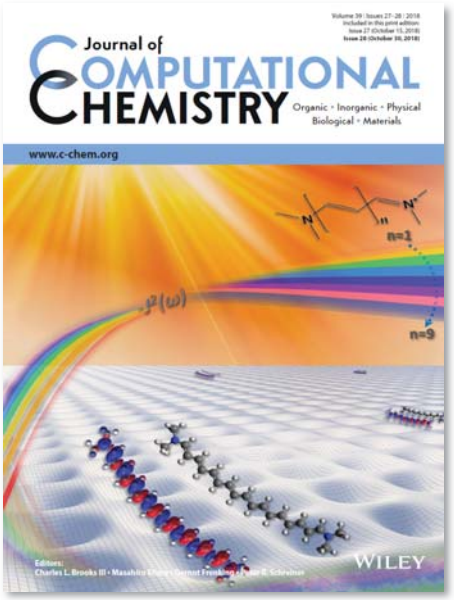

Figure 2. Cover article on nonlinear optical response properties of streptocyanine molecules.

3. Future Plans

To enhance the computational efficiency of the DFTB approach, we intend to continue our implementation of massively-parallelized computing hardware to accelerate real-time DFTB electron dynamics. Specifically, we have already made immense progress in developing customized hardware for calculating the time propagation of the DFTB density matrix to

understand the electronic properties of large chemical systems. **Figure 3** depicts a high-level view of the blocked matrix multiplication engine that we have nearly completed for these specific calculations. In short, this hardware engine is composed of six modules including the *Scheduler*, *Reader*, *Read A Controller*, *Read B Controller*, *Multiply-and-accumulate*, and the *Writer*. Together, these computational hardware modules allow the seamless multiplication of large, sparse, complex-valued matrices to yield the electronic absorption spectrum of large chemical systems. In addition, preliminary tests in our group have shown that this computational scheme is competitive with the speedup associated with modern Graphical Processing Units (GPUs). Further tests and publication of these exciting results is anticipated in the future plans of this grant. This DOE Grant has partially supported 3 Postdoctoral Associates, 3 PhD students, and 2 MS students.

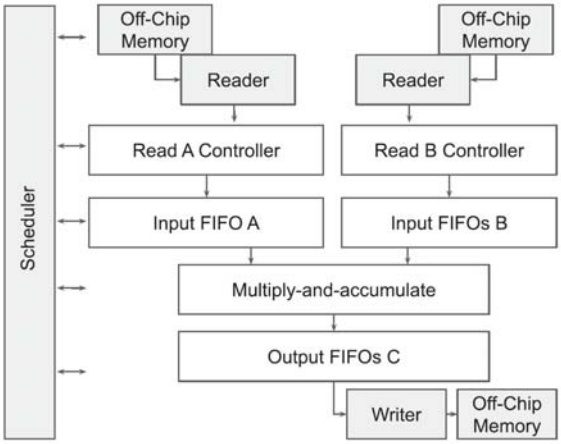

Figure 3. High-level view of the matrix multiplication hardware engine developed in the Wong lab for matrix multiplication of large, sparse, complex-values matrices in real-time DFTB dynamics.

Grant Number and Title: DE-SC0016269: **"**Non-Empirical and Self-Interaction Corrections for DFTB: Towards Accurate Quantum Simulations for Large Mesoscale Systems**"**

Publications acknowledging DOE grant DE-SC0016269 in the last two years:

1. A. A. Barragan, N. V. Ilawe, L. Zhong, B. M. Wong, and L. Mangolini, *"A Non-Thermal Plasma Route to Plasmonic TiN Nanoparticles."* Journal of Physical Chemistry C, **121**, 2316 (2017).
2. S. Pari, I. A. Wang, H. Liu, and B. M. Wong, *"Sulfate Radical Oxidation of Aromatic Contaminants: A Detailed Assessment of Density Functional Theory and High-Level Quantum Chemical Methods."* Environmental Science: Processes & Impacts, **19**, 395 (2017). **(Cover Article & Invited Paper)**
3. L. N. Anderson, M. B. Oviedo, and B. M. Wong, *"Accurate Electron Affinities and Orbital Energies of Anions from a Non-Empirically Tuned Range-Separated Density Functional Theory Approach."* Journal of Chemical Theory and Computation, **13**, 1656 (2017).
4. N. V. Ilawe, M. B. Oviedo, and B. M. Wong, *"Real-Time Quantum Dynamics of Long-Range Electronic Excitation Transfer in Plasmonic Nanoantennas."* Journal of Chemical Theory and Computation, **13**, 3442 (2017).
5. L. N. Anderson, F. W. Aquino, A. E. Raeber, X. Chen, and B. M. Wong, *"Halogen Bonding Interactions: Revised Benchmarks and a New Assessment of Exchange vs Dispersion."* Journal of Chemical Theory and Computation, **14**, 180 (2018).
6. N. V. Ilawe, M. B. Oviedo, and B. M. Wong, *"Effect of Quantum Tunneling on the Efficiency of Excitation Energy Transfer in Plasmonic Nanoparticle Chain Waveguides."* Journal of Materials Chemistry C, **6**, 5857 (2018). **(Cover Article)**
7. F. W. Aquino and B. M. Wong, *"Additional Insights between Fermi-Löwdin Orbital SIC and the Localization Equation Constraints in SIC-DFT"* Journal of Physical Chemistry Letters, **9**, 6456 (2018).
8. L. Xu, A. Kumar, and B. M. Wong, *"Linear Polarizabilities and Second Hyperpolarizabilities of Streptocyanines: Results from Broken-Symmetry DFT and New CCSD(T) Benchmarks"* Journal of Computational Chemistry, **39**, 2350 (2018). **(Cover Article)**
9. Z. A. Ali, F. W. Aquino, and B. M. Wong, *"The Diamine Cation is Not a Chemical Example where Density Functional Theory Fails"* Nature Communications, **9**, 4733 (2018).

Intermolecular Interactions in the Gas and the Condensed Phase

Sotiris S. Xantheas
Advanced Computing, Mathematics & Data Division,
Pacific Northwest National Laboratory, PO Box 999, MS K1-83, Richland WA 99352
sotiris.xantheas@pnnl.gov
Department of Chemistry, University of Washington, Seattle, WA 98195
xantheas@uw.edu

Program Scope: The overarching themes of this research component of the Molecular Theory & Modeling Program are:

- establish accurate benchmarks for archetypal intermolecular interactions, aqueous clusters and guest – host interactions relevant to energy applications,
- incorporate the appropriate physics into models (classical or quantum) that explicitly account for the desired behavior,
- elucidate the molecular level factors that control complex behavior,
- understand the interplay between the molecular level information and the macroscopic properties of complex aqueous environments.

The ultimate goal of the program is *to develop accurate descriptions of intermolecular interactions for complex environments that include molecular level detail*.

Recent Progress: In recent work, we have relied on the application of the fragmentation method to decompose the total energy, gradient, and second derivatives of a cluster based on overlapping fragments; in particular, we used the Molecular Tailoring Approach (MTA) of Gadre and coworkers to obtain a new global minimum for (H2O)25 in conjunction with a Monte Carlo (MC) sampling method where all fragments were computed at the MP2 level of theory. We have also tested the MTA approach for clusters with as many as 100 molecules and obtained the total energy within a fraction of a milli-Hartree of the full MP2 calculation of the whole cluster. Finally, we are currently developing a new database of ~5M networks that correspond to local minima in water clusters with up to n = 30 molecules and that lie within the range of 0–5 kcal/mol from the putative minimum. This database is being assembled using a MC advanced sampling technique with the TTM2.1-F interaction potential and the resulting low-energy networks are being subsequently refined at the MP2/aug-cc-pVTZ level of theory.

In addition, we have revisited the many-body expansion for water, looking at the convergence of the individual terms in the MB expansion with the level of electronic structure theory. In particular, we have computed these terms with basis sets up to the Complete Basis Set (CBS) limit and found an unexpected result: the MB expansion seems to "oscillate" around zero with the smaller (aug-cc-pVDZ) basis set, giving the incorrect impression that a cancellation of the positive and negative energy terms is responsible for the overall accepted truncation of the series at the 3- or 4-body term. However, the use of much larger basis sets up to aug-cc-pV5Z render a completely different picture: all terms up to the 4-body converge to a well-defined limit, with the larger terms being zero. Quite surprisingly, this behavior is accurately reproduced when the

Basis Set Superposition Error (BSSE) is included (i.e., the BSSE-corrected 5- and higher-body terms are zero). One of the main thrusts of the proposed research (vide infra) relies on the combination of variants of the previously described methods and results to arrive at a truly ab initio description of complex aqueous cluster and condensed-phase environments.

Future Work: We propose relying on a fragmentation approach based on the appropriate truncation of the MB expansion with the relevant terms computed either fully ab initio (for the 1-, 2-, and possibly the 3-body terms) or from a purely electrostatic description (for the 3- and 4-body terms). This approach is trivially parallelizable and can make efficient use of recent and forthcoming LCC (LCF) architectures within the DOE national laboratory system. Our previous results necessitate using either a very large (aug-cc-pV5Z) basis set or the inclusion of BSSE corrections in the individual MB terms, a fact that is computationally prohibitive in the sampling of the system's dynamics. While the former is feasible, albeit requiring a large amount of computer resources via a brute-force approach (i.e., computing all fragments up to the MB truncation with a very large basis set), we will opt for the latter and use a smaller (aug-cc-pVDZ) basis set with a simultaneous estimate of BSSE corrections. This is because the full calculation of BSSE corrections using the traditional (Boys-Bernardi) approach is a drawback that defeats the purpose of breaking the whole system into pieces, as the full calculation for the system will be required. Our approach would be to draw from the group's expertise to define descriptors of the relative energetics of the various MB terms based on geometry and connectivity and derive a classical description of the higher terms (3- and 4-body) based on electrostatics. We have already assembled a large database of BSSE-corrected 3- and 4-body terms from water $(H_2O)_n$ and ion–water $M^+(H_2O)_n$ (M=Li, Na, K, Rb, Cs) cluster calculations, with n up to 21 and k (order of the MB expansion) up to 4, that will be used as the initial training set. We will consider adding configurations from liquid water simulations with the TTM2.1-F potential that encompass fully solvated molecules that include the first and second solvation shells in the database. We will draw on PNNL's expertise in machine (supervised and/or unsupervised) learning and neural network development to establish a neural network for liquid water as well as descriptors related to the BSSE-corrected 3- and 4-body terms based on local geometry and network connectivity. We will particularly rely on these data science approaches to obtain descriptors of BSSE corrections based on the first and second nearest-neighbor connectivity and structure. Due to the nature of the nearest-neighbor 2-B term, we expect that the BSSE correction for that term will vary according to the nearest-neighbor O-O distance, which can be used as a descriptor. We will further seek descriptors of the higher MB terms ($n > 3$) based on supervised learning or the training of neural networks based on the local (nearest neighbor) and immediately extended (next nearest neighbor, donor or acceptor connectivity) environments. To this end, we will start from recent ideas regarding MB descriptors and extend them to include system-specific quantities such as hydrogen-bonded network connectivity, fragment distance, etc. We will finally consider the use of graph theory to represent the local connectivity and relate it to the sign and magnitude of these higher-order interactions.

Within the fragmentation approach based on the ab initio evaluation of the 1- and 2-body terms and the possible estimate of the 3- and 4-body terms from the developed descriptors, it would be possible to perform classical and nuclear quantum simulations for large clusters and ultimately the condensed phase. For this purpose, we propose to develop a socket linking i-PI (setting up the molecular dynamics simulations) with the NWChem and SPEC libraries (providing the ab initio energies and gradients). We will implement capabilities for obtaining first and second derivatives of the energy of the system from its fragments as previously shown for the $(H_2O)_{25}$

cluster, thus allowing for minimizations, dynamics, and a direct path to the spectroscopic features of these systems.

The results based on fragmentation schemes will be validated using the full calculations that will be performed for clathrate hydrate-like structures of $M^+(H_2O)_{20}$ and $X@(H_2O)_{20}$ clusters. Gas hydrates are guest–host scaffolds that have been considered as a source for low-carbon or alternative fuels or as depositories to store carbon dioxide; however, little is known about their chemical structure or about processes occurring at the molecular level. Given the very weak interaction between the host's hollow water cages and the guest molecules, higher levels of theory such as CCSD(T) are needed to obtain accurate energetics. These can serve as guides in the parametrization of interaction potentials or in choosing lower levels of electronic structure theory (i.e., DFT) to subsequently probe their dynamical properties. We propose performing CCSD(T) electronic structure calculations with large, correlation-consistent basis sets (up to aug-cc-pVQZ) to obtain accurate energetics for the accommodation of several H_2 molecules in the hollow $(H_2O)_{20}$ and $(H_2O)_{24}$ water cages, which are the building blocks of the structure I (sI) clathrate hydrate lattice. We will extend those calculations to the CH_4 and CO_2 guest molecules as well as explore the MB effect arising from the occupation of two adjacent cages by guest molecules in the lattice. We will also investigate the barrier and molecular mechanisms that correspond to the diffusion of the guest species from one cage to the neighboring one.

Publications Acknowledging this Grant in the last 2 years

1. G. E. Douberly, R. E. Miller and S. S. Xantheas, "Formation of Exotic Networks of Water Clusters in Liquid Helium Droplets Facilitated by the Presence of Neon Atoms", *Journal of the American Chemical Society* **139**, 4152 (2017). Included in *Science* **355**, 1388 (2017) under *Research in Other Journals*
2. S. Yoo Willow and S. S. Xantheas, "A Molecular Level Insight of the Effect of Hofmeister Anions on the Interfacial Surface Tension of a Model Protein", *Journal of Physical Chemistry Letters* **8**, 1574 (2017)
3. S. Yoo and S. S. Xantheas, "Structures, Energetics and Spectroscopic Fingerprints of Water Clusters *n*=2-24" in *Handbook of Computational Chemistry,* J. Leszczynski (editor), 2nd Edition, Springer International Publishing Switzerland, ISBN 978-3-319-27281-8, Chapter 26, pp. 1139 –1175 (2017)
4. T. B. Ward, E. Miliordos, P. D. Carnegie, S. S. Xantheas, M. A. Duncan, "Ortho-Para Interconversion in Cation-Water Complexes: The Case of $V^+(H_2O)$ and $Nb^+(H_2O)$ Clusters", *Journal of Chemical Physics* **146**, 224305 (2017)
5. P. Hamm, G. S. Fanourgakis, S. S. Xantheas, "A surprisingly simple correlation between the classical and quantum structural networks in liquid water", *Journal of Chemical Physics*, **147**, 064506 (2017)
6. G.-L. Hou, N. Govind, S. S. Xantheas, X.-B. Wang, "Deviation from the *trans*-Effect in Ligand-Exchange Reactions of Zeise's Ions $PtCl_3(C_2H_4)^-$ with Heavier Halides (Br^-, I^-)", *Journal of Physical Chemistry A* **122**, 1209 (2018)

7. A. Mukhopadhyay, S. S. Xantheas, R. J. Saykally, "The Water Dimer II: Theoretical Investigations", Frontiers Article (invited), *Chemical Physics Letters* **700**, 163 (2018). Journal Cover

8. J. P. Heindel, Q. Yu, J. M. Bowman, S. S. Xantheas, "Benchmark electronic structure calculations for the $H_3O^+(H_2O)_n$, n=0–5, clusters and tests of an existing 1,2,3-body potential energy surface with a new 4-body correction", *Journal of Chemical Theory and Computation* **14**, 4553 (2018)

9. M. A. Boyer, O. Marsalek, J. P. Heindel, T. E. Markland, A. B. McCoy, and S. S. Xantheas, "Beyond Badger's Rule: The Origins and Generality of the Structure-Spectra Relationship of Aqueous Hydrogen Bonds", *Journal of Physical Chemistry Letters* **10**, 918 (2019)

10. S.-I. Ishiuchi, H. Wako, S. S. Xantheas and M. Fujii, "Probing the selectivity of Li^+ and Na^+ cations on noradrenaline at the molecular level", invited article for special issue on "*Advances in ion spectroscopy - from astrophysics to biology*" *Faraday Discussions* **217**, 396 (2019)

11. M. Ahmed, K. Asmis, I. Avdonin, M. K. Beyer, E. Bieske, S. Bougueroua, C.-W. Chou, S. Daly, O. Dopfer, L. Ellis-Gibbings, V. Gabelica, M.-P. Gaigeot, M. Gatchell, B. Gerber, C. Johnson, M. Johnson, K. Jordan, A. Krylov, M. Mayer, L. McCaslin, A. B. McCoy, D. Neumark, M. Oncak, J. Oomens, A. Rijs, T. Rizzo, J. Roithova, P. Sarre, S. Schlemmer, J. Simons, M. Stockett, A. Trevitt, J. Verlet, X.-B. Wang, R. Wester, S. Willitsch and S. Xantheas, "Controlling internal degrees: general Discussion" in special issue on "*Advances in ion spectroscopy - from astrophysics to biology*" *Faraday Discussions* in press **217**, 138 (2019)

12. J. Simons, M. Johnson, K. Asmis, A. B. McCoy, S. Daly, R. Wester, A. Rijs, P. Sarre, M.-P. Gaigeot, R. Mabbs, K. Jordan, C. Dessent, D. Neumark, C.-W. Chou, B. Gerber, O. Dopfer, J. Oomens, A. Krylov, S. Schlemmer, S. Willitsch, J. Verlet, R. Wild, M. Gatchell, M. Stockett, J. Roithova, M. K. Beyer, S. Xantheas, J. Gibbard and P. Dohnal, "Pushing resolution in frequency and time: general discussion", in special issue on "*Advances in ion spectroscopy - from astrophysics to biology*" *Faraday Discussions* **217**, 290 (2019)

13. M. Ahmed, S. Daly, C. Dessent, O. Dopfer, V. Gabelica, M.-P. Gaigeot, M. Gatchell, B. Gerber, J. Gibbard, C. Johnson, M. Johnson, K. Jordan, A. Krylov, K. Lovelock, M. Mayer, L. McCaslin, A. B. McCoy, D. Neumark, S. Brøndsted Nielsen, J. Oomens, A. Rijs, T. Rizzo, J. Roithova, J. Simons, M. Stockett, A. Trevitt, J. Verlet, X.-B. Wang, R. Wester and S. Xantheas, "Going large(r): general discussion", in special issue on "*Advances in ion spectroscopy - from astrophysics to biology*" *Faraday Discussions* **217**, 476 (2019)

The emergent photophysics and photochemistry of molecular polaritons: a theoretical and computational investigation

DE-SC0019188

Joel Yuen-Zhou

Department of Chemistry and Biochemistry,

University of California San Diego,

9500 Gilman Dr MC 0340, La Jolla, 92093-0314, USA

joelyuen@ucsd.edu

Program scope. This project started in September 2018 and aims to develop a comprehensive theoretical and computational framework to address a new class of emergent room-temperature photophysical and photochemical processes afforded by molecular polaritons (MPs), namely, hybrid states arising from the strong coupling of organic dye electronic/vibronic excitations and confined electromagnetic modes (Fig. 1). Recent experimental progress on MPs prompts for the development of robust theoretical tools that can describe the novel phenomenology afforded by these systems under realistic dissipative conditions. Our project aims to fill this gap. The molecular or photonic components of MPs can be tuned to rationally modify the physicochemical properties of molecular matter. In this work, we will first pioneer formalisms based on open-quantum systems theory to address the low-energy dynamics of MPs in the presence of room-temperature realistic conditions such as in the presence of static and dynamic molecular disorder as well as absorptive losses in the electromagnetic environment. This framework will allow us to harness MPs to design control strategies of great interest to the missions of DOE-BES such harvesting of dark molecular populations (work in progress) or even exotic paradigms for the remote control of chemical reactions (Fig. 2) in condensed phases. Given the emergent many-body flavor of the problems of interest where many electrons, vibrations, and photons interact with one another, our approach

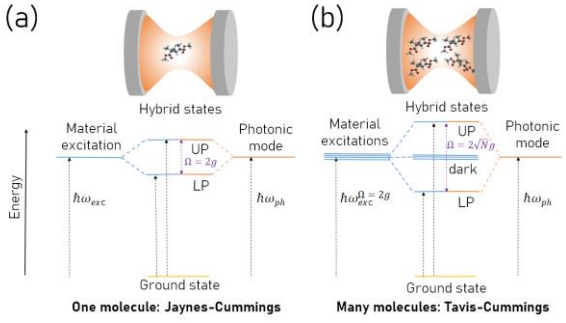

Fig. 1. The various flavors of strong light-matter coupling. A tightly confined electromagnetic mode can couple to a (a) single ($N = 1$) or (b) many ($N \gg 1$) molecular transitions. In both cases, hybrid light-matter states called upper and lower polaritons (UP, LP) are formed, which are separated in energy by a collectively enhanced Rabi splitting $\Omega = 2\sqrt{N}g$. Having $N \gg 1$ yields a large number ($N - 1$) of dark states which do not couple to light and which are crucial in the description of incoherent dynamics of molecular polaritons. Most experiments at present belong to the (b) case. Adapted from [1].

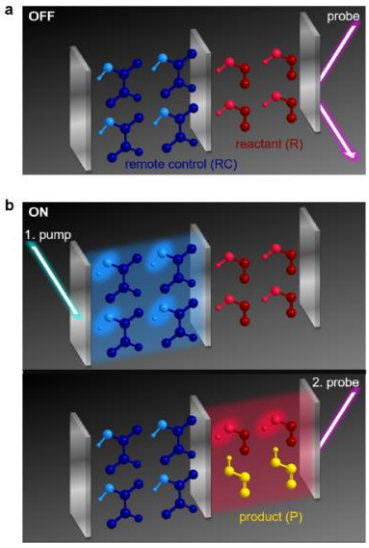

Fig. 2. Schematic of remote control of infrared-induced conformational isomerization of HONO. a, Without excitation of 'remote catalyst' (RC, blue) Tc-glyoxylic acid, the 'probe' laser pulse impinging on the mirror of the cavity containing reactant (R, red) *cis*-HONO is reflected; the reaction does not occur. **b**, First, a pump laser pulse impinging on the mirror of the RC cavity excites a polariton whose character is predominantly this cavity and the strongly coupled OH (light blue) stretch of RC. Within <100 ps, coupling between this vibration and solvent modes induces relaxation from the eigenstate to optically uncoupled (dark) RC states. Next, the 'probe' pulse efficiently excites a polariton whose character is predominantly the impinged cavity and the strongly coupled OH (light red) stretch of R; R is subsequently converted into the product (P, gold) *trans*-HONO. Adapted from [2]

will construct effective Hamiltonian theories that can capture the essential dynamical features of the problems in question. To ensure relevance to experiments, we will routinely supplement our models with parameters obtained from computational quantum chemistry and from spectroscopic data in the literature or from our experimental collaborators.

Recent progress. This year, we published an invited perspective on the subject of polariton chemistry [1] as well as a theory demonstrating that it is in fact possible to control chemical reactions remotely [2]: by saturating the molecular transitions in one cavity, one can control the chemical reactivity of molecules in another cavity (see Fig. 2). The latter seems to be a universal phenomenon of molecular polaritons and introduces new paradigms of "quantum-optically-mediated" chemical processes, where the light-harvester locally stores energy and via communication through the delocalized electromagnetic mode affects the properties of molecules that are a few wavelengths apart.

Future plans. We are currently considering explicit generalizations of the remote-control idea to the electronic excitation domain. We aim to manipulate an electron transfer or isomerization process remotely and develop a phase diagram of the photonic and molecular parameters that optimize such process. We are also theoretically exploring the various regimes of dark-state population harvesting via polaritons in terms of vibronic coupling, transition dipole density, photonic modes, and molecular density.

List of publications.

[1] J. Yuen-Zhou and V. M. Menon, Polariton chemistry: thinking inside the (photon) box, Proc. Nat. Acad. Sci., 116 (12) 5214 (2019).

[2] M. Du, R. F. Ribeiro, L. A. Martínez-Martínez, and J. Yuen-Zhou, Remote control of chemistry in optical cavities, Chem 5, 5, 1167 (2019).

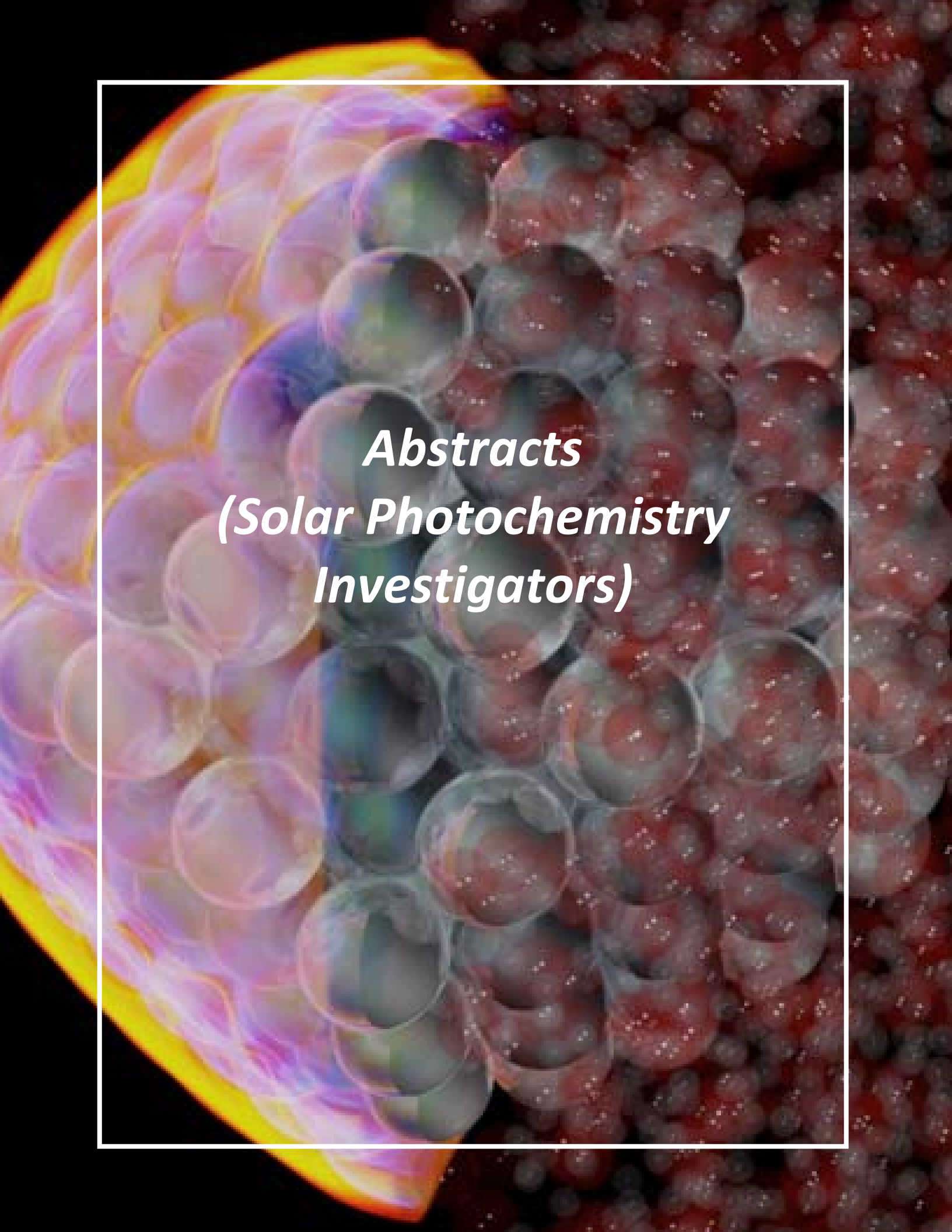

Abstracts (Solar Photochemistry Investigators)

Fundamental advances in radiation chemistry
2. Probing Radical Structure and Kinetics

Principal Investigators

DM Bartels (bartels.5@nd.edu), I Carmichael, I Janik, A Lisovskaya

Notre Dame Radiation Laboratory, University of Notre Dame, Notre Dame, IN 46556

Program SCOPE

The action of ionizing radiation almost universally produces charge and spin separation, thus it is not surprising that a major focus of the NDRL is the structure and reactivity of free radicals. In the present subtask we consider free radical structure and reactivity at a fundamental level, and develop and use theoretical techniques to elucidate the observed behaviors. Issues addressed in this subtask will find strong overlap with other scientific disciplines. Challenges being addressed include the experimental and theoretical investigation of solvated electron reaction rates, determination of the redox potentials of hyper-reduced transition metal ions, resonance Raman study of radical ion hydration shells, quantitative measurement and modeling of time-resolved EPR (CIDEP) of the H atom in water, and radiolytic oxidation of aqueous halide ions.

Recent PROGRESS AND FUTURE PLANS

In 2010 the widely accepted "cavity" structure of the hydrated electron was challenged on the basis of a new and "improved" pseudopotential of Larson, Glover and Schwartz (LGS), that reproduced numerous properties of the electron with a non-cavity structure whereby the electron exists mainly in-between water molecules in a densified region of solution. It was pointed out that the partial molar volume would be negative for this structure, so we set out to measure this property to settle the cavity vs. non-cavity issue. The partial molar volume of the hydrated electron was investigated with pulse radiolysis and transient absorption at 25°C and at 200°C by measuring the pressure-dependence of the equilibrium constant for $(e^-)_{aq} + NH_4^+ \Leftrightarrow H + NH_3$. In the presence of 0.1M NH_3/NH_4^+, initial excess of $(e^-)_{aq}$ produced with a short radiolysis pulse is observed to approach an equilibrium on a hundred-microsecond timescale. At 2kbar pressure the equilibrium constant decreases by only 6%. Using tabulated molar volumes for ammonia and ammonium, we have the result $\overline{V}(e^-_{aq}) - \overline{V}(H) = 11.3$ cc/mole, confirming that $\overline{V}(e^-_{aq})$ is positive and even larger than the hydrophobic H atom. Assuming on the basis of recent molecular

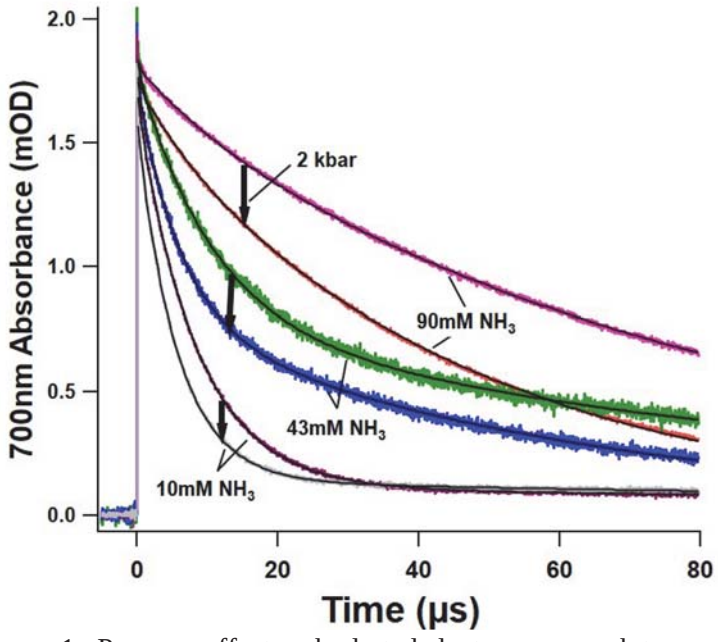

Figure 1. Pressure effect on hydrated electron approach to equilibrium $(e^-)_{aq} + NH_4^+ \Leftrightarrow H + NH_3$. Effect is small at 2kbar, proving that molar volume of $(e^-)_{aq}$ is positive.

dynamics simulations the molar volume of H atom is somewhat less than that of H_2, we estimate $\overline{V}(e^-)_{aq}$ = 26±6 cc/mole. Less reliable data collected at 200°C and 1250 bar suggests $\overline{V}(e^-_{aq}) - \overline{V}(H)$ = 18.5 cc/mole at this temperature, and allows us to establish with certainty $\overline{V}(e^-_{aq}) - \overline{V}(H) > 0.0$ cc/mole. At both temperatures, the positive molar volume is consistent with an electron that exists largely in a solvent void (cavity), ruling out the LGS non-cavity structure. Further investigation of solvated electrons in water and alcohols will be carried out in the coming year by recording the resonance Raman spectra vs. temperature.

In a recent study of hydrated electron reaction rates, we found that the redox potentials for aqueous transition metal couples, $M^{2+/+}$ (M = Zn, Mn, Fe, Co, Ni) are not known. The problem is that the hexa-aquo starting complexes lose water molecules in the reduction, meaning that reorganization is large, and the electron transfer reactions are slow. We are studying the redox potentials of $M^{2+/+}$ couples using pulsed radiolysis and their reactions with a number of reference compounds of known reduction potentials. These measurements have substantially reduced the range of uncertainty for several of the couples, but uncertainty is still very large. It was found that Mn^+ can reduce $Co(sep)^{3+}$, setting the upper limit for the $Mn^{2+/+}$ couple E^0 to be -0.30V vs. NHE. The reaction of Co^+ and Ni^+ with $Ru(bpy)_3^{2+}$ has been observed giving E^0 = -1.3V for the upper limit of the $M^{2+/+}$ couples. The experiments with $Zn^{2+/+}$ have confirmed that the redox potential for this couple must be the most negative among those of the ions investigated, with $E^0 < -1.9$ V vs. NHE. In the coming year we hope to conclude the study by effectively measuring against all the available standards. The radiation chemistry of these hyper-reduced transition metal ions dissolved in the cooling water of nuclear reactors (corrosion products) can substantially affect transport of radioactivity and exposure of workers.

Room temperature ionic liquids (RTILs) have been suggested for use in nuclear fuel reprocessing, so their radiation stability and free radical chemistry have been investigated in a number of studies. We carried out EPR spin trapping experiments on a series of representative irradiated RTILs several years ago, and the analysis was finally completed in the last year. The radiolytic stability of ionic liquids composed of bis(trifluoromethylsulfonyl)imide anion (Tf_2N^-) and triethylammonium, 1-butyl-1-methylpyrrolidinium, trihexyl(tetradecyl)phosphonium, 1-hexyl-3-methylpyridinium and 1-hexyl-3-methylimidazolium ($hmim^+$) cations was studied using the spin trap α-(4-Pyridyl-1-oxide)-*N*-tert-butylnitrone (POBN). Total trapped radical yields were measured as a function of POBN concentration and as a function of radiation dose by double integration of the broad unresolved lines. Well-resolved motionally narrowed EPR spectra for the trapped radicals were obtained by dilution of the ILs with CH_2Cl_2 after irradiation. The trapped radicals were identified

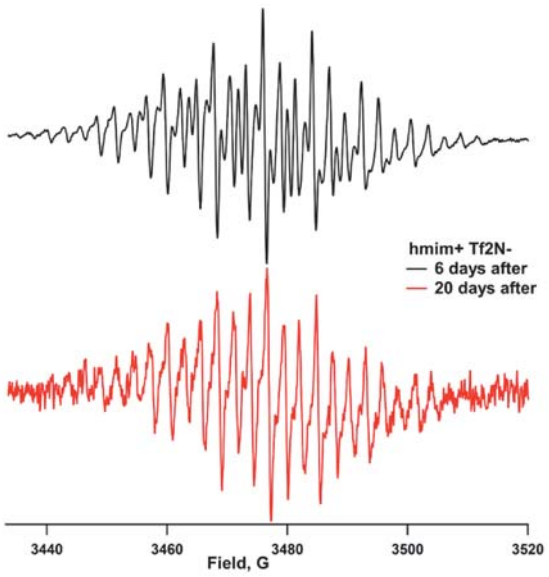

Figure 2. Narrow-line EPR spectra of persistent radicals in $hmim^+Tf_2N^-$ ionic liquid 6 days and 20 days following gamma irradiation. Change of the spectrum suggests at least two stable forms.

as mainly carbon-centered alkyl and $\cdot CF_3$ and their ratio varies greatly across the series of ILs. Expected nitrogen-centered radicals derived from Tf_2N^- were not observed. In general the spin-trapping technique was disappointing because the newly created radicals tended to destroy the POBN-adducts too quickly. The $hmim^+$ liquid proved most interesting because a large part of the trapped radical yield (entirely carbon-centered) grew in over several hours after irradiation. We also discovered a complicated narrow-line stable radical signal in this neat ionic liquid with no spin trap added, which grows in over several hours after irradiation, and decays over several weeks (Figure 2.). We propose that these delayed signals result from trapping of electrons in a weakly bound EPR-silent "dimer of dimer cations", which slowly releases radical species. In the coming year we hope to identify the stable radical with *ab initio* calculations and deuterium substitution experiments to close out the project.

Recent transient Raman studies of the CO_2^- radical in water have led to the vibrational properties of this important radical intermediate. More importantly the evidence of the electron being shared between the bent CO_2 and its hydration shell at an energy of about ~ 0.28 eV above the ground electronic state was obtained. The corresponding electronic state has a life-time of several femtoseconds, consistent with the theoretically predicted value. No evidence of non-equivalence of the two CO bonds was found, which suggested that the partially detached electron is symmetrically situated between CO_2 and the water molecule. Because of the electron not being localized on CO_2, the Raman scattered photon does not terminate into a vibrational state corresponding to the CO_2^- overtones above 0.28+/-0.03 eV or higher. Now in a follow up study, we have examined its sulfur analogue CS_2^-. We have prepared the radical anion in water by pulse radiolysis with Raman detection up to 4000 cm^{-1} to monitor its vibrational fingerprints. The Raman spectrum, excited in the resonance with the 270 nm (λ_{max}) absorption of CS_2^- is dominated by a very strong band at 666 cm^{-1}, associated with the symmetric C-S stretching vibration, its overtones, and combinations with SCS bending vibration of 330 cm^{-1}. Solvation shell bending and stretching modes are also enhanced, suggesting contribution to the excited state of the radical anion analogous to CO_2^-. From the progression of overtones, and the first order anharmonicity of 2.57cm^{-1}, we estimate a continuum of vibrational states at an energy of roughly 5.4 eV. Unlike CO_2^-, CS_2^- did not show any evidence

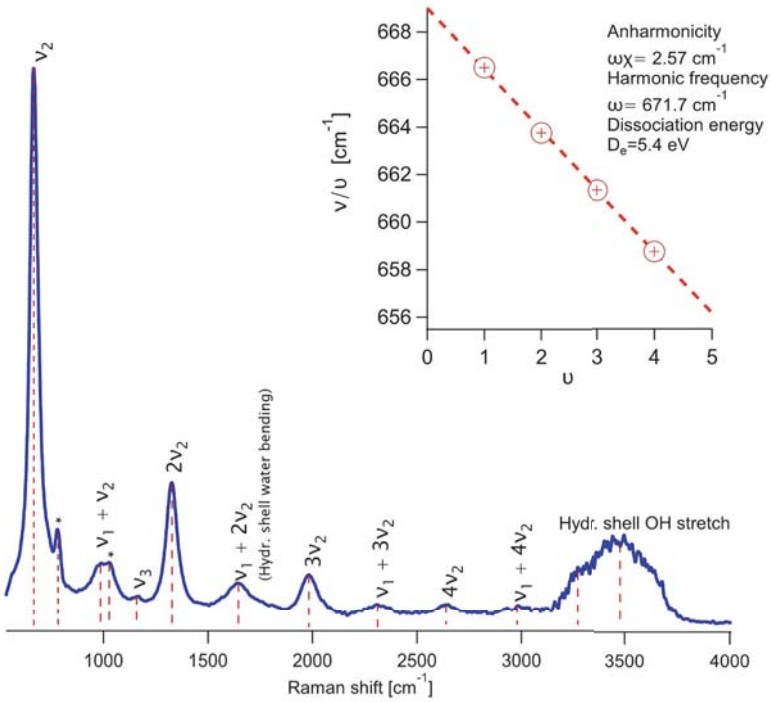

Figure 3. Resonance Raman spectrum of CS_2^- radical anion probed at 270 nm in water.
Inset: Plot of vibrational frequency vs. vibrational quantum number [spectroscopic parameters of CS_2^-].

of electron detachment up to the energies of ~0.5eV. DFT calculations reproduced experimental frequencies fairly well predicting a molecular geometry of CS_2^- with CS bond lengths of 1.638A and CSC angle of 143.3^o.

The selenocyanate dimer radical anion $(SeCN)_2^{\bullet-}$, prepared by electron pulse irradiation of selenocyanate anion $(SeCN)^-$ in water, has been examined by transient absorption, time-resolved Raman and range-separated hybrid (RSH) density functional (ωB97x and LC-ωPBE) theory. In transient absorption studies no OH-adduct formation ($SeCNOH^-$) has been apparent even at pH as high as 14 contrasting findings of analogous studies of OH induced oxidation of SCN^-. The Raman spectrum of $(SeCN)_2^{\bullet-}$, excited in resonance with the 450 nm (λ_{max}) absorption of the radical, is dominated by a very strong band at 140.5 cm^{-1}, associated with the Se-Se stretching vibration, its overtones and combinations. A striking feature of the $(SeCN)_2^{\bullet-}$ Raman spectrum is the relative sharpness of the 140.5 cm^{-1} band compared to the S-S band at 220 cm^{-1} in thiocyanate radical anion $(SCN)_2^{\bullet-}$. The difference of which is explained in terms of a time-averaged site effect. Calculations, which reproduce experimental frequencies fairly well, predict a molecular geometry with the SeSe bond length of 2.917 ($\pm$0.04) Å, the SeC bond length of 1.819 ($\pm$0.004) Å and the CN bond length of 1.155 ($\pm$0.002) Å. An anharmonicity of 0.44 cm^{-1} has been determined for the 140.5 cm^{-1} Se-Se vibration which led to a dissociation energy of ~1.4 eV for the SeSe bond, using the Morse potential in a diatomic approximation. This value, estimated for the radical confined in a solvent cage, compares well with the calculated gas-phase energy, 1.32±0.04 eV, required for the radical to dissociate into $(SeCN)^{\bullet}$ and $(SeCN)^-$ fragments. The enthalpy of dissociation in water has been measured (0.36 eV) and compared with the value estimated by accounting for the solvent dielectric effects in structural calculations.

Publications with BES support (2017-2019)

Janik I., Carmichael I., Tripathi G.N.R., *J. Chem. Phys.*, **2017**, *146*, 214305. Transient Raman spectra, structure and thermochemistry of the thiocyanate dimer radical anion in water.

Sargent, L., Sterniczuk, M., Bartels, D.M., *Radiat. Phys. Chem.* **2017**, *135*, 18-22. Reaction rate of H atoms with N_2O in hot water.

Janik I., Tripathi G.N.R., *J. Chem. Phys.* **2019**, *150*, 094304. The selenocyanate dimer radical anion in water: Transient Raman spectra, structure, and reaction dynamics.

Janik, I., Lisovskaya, A., Bartels, D.M., *J Phys. Chem. Lett.* **2019,** 10, 2220. Partial Molar Volume of the Hydrated Electron.

Tarabek, P., Lisovskaya, A., Bartels, D.M., *J. Phys. Chem. B* **2019**, submitted. γ-Radiolysis of Room Temperature Ionic Liquids. An EPR Spin-Trapping Study.

Bartels, D.M., *J Phys. Chem. Lett.* **2019,** 10, 4910. Is the Hydrated Electron Vertical Detachment Genuinely Bimodal?

Fundamental advances in radiation chemistry
1. From energy deposition to medium decomposition

Principal Investigators

I. Carmichael (carmichael.1@nd.edu), D.M. Bartels, I. Janik, J.A. LaVerne, S. Ptasińska
Notre Dame Radiation Laboratory, University of Notre Dame, Notre Dame, IN 46556

Program scope

Ionizing radiation, in the form of γ-rays or high-energy electrons, when impinging on a condensed phase, deposits energy (on the order of tens of eVs) in a series of widely separated (on the order of tens of nanometers) clusters of ionization and excitation events (spurs) along a twisting and potentially branching track. Along the length of this track the overall energy dissipation, the linear energy transfer (LET), is less than one eV per nanometer. In contrast, heavy ions such as α-particles forge a dense columnar path of ionizations and excitations as spurs overlap with much larger values of LET. These disparate environments result in different chemical outcomes.

In addition to its many significant achievements in experimental radiation chemistry, the NDRL has a deep history in the successful modeling of such tracks, particularly in room-temperature aqueous media. This work presses forward the fundamental science underpinning the observed chemical outcomes and the continued development of models applicable to the wide range of extreme environments present across the DOE complex.

We consider the optical response of the medium, then probe primary events searching for a comprehensive understanding of the mechanisms behind low-energy-electron-induced fragmentations and the observed sharp differences between radiolytic yields in aromatics and aliphatics. How this chemistry impacts key modern structural characterization techniques, transmission electron microscopy and macromolecular crystallography is interrogated next and track structure models are extended to account for extreme environments of temperature, pressure, and radiation dose and dose rate now likely to be encountered. Some non-traditional radiation sources, atmospheric pressure plasma jets and plasma/liquid surface electrodes are also explored.

Recent Progress and Future Plans

Vacuum ultraviolet (VUV) spectroscopy was used to explore the density dependence of the supercritical carbon dioxide electronic absorption spectra over the wavelength range 1455-2000 Å at 34.5 °C. Pressures were varied from 19 to 137 bar, giving a corresponding density range of 0.036-0.767 g cm^{-3}. The vibronic structure inherent in the spectrum is apparent at the lowest densities, but gradually diminishes in magnitude with increasing density. At a density of 0.595 g cm^{-3} the structure is no longer apparent. This loss of detail cannot be explained by collisional broadening or dimerization, and we suggest gradual perturbation of the monomer electronic and vibrational structure with increasing density, similar to that observed in our recent studies of supercritical water.

In collaboration with Resonance Ltd. we finished designs and construction of an in-house apparatus for studies of VUV absorption in sub- and supercritical fluids. A VUV light source based on customized VM200 VUV double grating monochromator coupled to a high-power (150W) deuterium lamp assembly has been constructed and is currently under control software testing and debugging.

Optical emission (OE) spectra of shielding-gas-controlled helium atmospheric pressure plasma jets (APPJ) in contact with a conductive (phosphate-buffered saline, PBS) and nonconductive (DI water) liquid surfaces were detected. The shielding gases used were dry and wet gases (i.e., with a relative humidity of above 95%) of nitrogen, breathing air, and oxygen. The OE measurements showed that the plasma jet, when in contact with PBS, develops a structure resembling a glow discharge. Moreover, we recorded two-dimensional (2D) OE intensity maps of excited plasma species directly above the liquid. We made the first measurements of this type for shielding gases, in which the O_2 content varied from 0% to 100%. We observed that in spite of overall decrease in emission brightness, the atomic oxygen emission in the plasma core increase as the O_2 content in the shielding gas increased ($N_2 \rightarrow$ Air $\rightarrow O_2$). Interestingly, excited plasma species produced were significantly different than those in free APPJs with no target.

Furthermore, the 2D reactive oxygen species (ROS) distribution at the liquid surface was strongly dependent on both the shielding gas composition and the liquid conductivity. The 2D ROS distributions were visualized by using a potassium iodide-starch reagent. As the O_2 content in the shielding gas increased, there was a strong increase in the measured ROS concentration near the plasma jet, as well as a far-reaching ROS concentration. Therefore, the increase in atomic oxygen emission in the plasma core was tentatively correlated with an increase in ROS measured at distances far from the plasma jet. The observation of long-distance ROS led us to a suggestion that the presence of O_2 in the shielding gas likely leads to the production of O_3. Such long-distance ROS were not detected when using pure N_2 shielding gas. In the case of wet shielding gas, we observed a decrease in the ROS produced outside of the APPJ. Our results indicate that using a shielding gas with varying amounts of O_2 or H_2O can provide a control over the spatial distribution and concentration of the produced ROS at the APPJ/liquid interface. In the next step, we will continue to systematically investigate other plasma factors and use machine learning tools to indicate what are the factors or synergies between them to manipulate ROS production for a better control of plasma desired effects.

We have now extended our DEA studies on heterocyclic compounds, mainly five-membered rings: isoxazole, imidazole, pyrazole, pyrrole, 1-methyl-, and 2-methylimidazole. In addition to DEA spectroscopy, we have employed, in collaborations with other groups, electron transmission spectroscopy to probe resonances formed at low energies for these molecules. The observed resonance structures were assigned based on quantum chemical calculations including both molecular orbital and density functional theory (DFT) - based approaches. Furthermore, multichannel effective range theory (ERT) calculations, which include both dipolar and polarization interactions were also performed to reproduce experimental low-energy resonances. These calculations allowed us to associate formation of temporary anionic states bound by long-range electron-molecule interactions. Among many of findings in these studies, we confirmed positions of the lowest π^* vertical attachment energy states, values for which we previously reported in the literature. However, the lowest π^* shape resonance matches the position of the DEA peak caused by the dehydrogenation of the parent molecule; therefore, it is still unclear to provide possible contributions from mechanisms other than vibronic π^*/σ^* mixing. Sharp and narrow resonances (so-called “cusps”) were observed in the electron transmission spectra close to 0.5 eV for all compounds with an N-H bond. In many cases, DEA-induced loss of multiple hydrogen atoms from the heterocyclic compounds was

observed. This multiple H loss was most likely accompanied by ring opening and formation of H radicals and H_2 molecules as neutral counterparts. Interestingly, ring opening can also occur when the two heteroatoms occupy adjacent positions in the ring. In general, our studies showed that the mechanisms of H atom stripping are complex, potentially involving intramolecular rearrangements, dissociation and formation of several covalent bonds, and also depend on the type and position of heteroatoms in the ring. Current experimental and theoretical work is aimed at providing a comprehensive dissociation mechanism of other substituted aromatics (e.g., benzaldehyde), and heterocyclic compounds.

Radiation damage, inflicted during data collection, continues to impede successful macromolecular structure determination by techniques employing ionizing radiation to obtain scattering (EM) or diffraction (MX) patterns. Systematic X-ray investigations into this phenomenon have identified two separate indicators of damage as a function of dose: global and specific. The former, global damage, results in a loss of the measured reflection intensities, particularly those at high resolution, due mainly to physical processes such as unit-cell expansion leading to increasing crystal non-isomorphism[40]. On the other hand, specific damage is typically observed by reconstructing changes in electron density maps as dose increases. Damage to particular amino acid residues is observed to occur in a reproducible order with increasing dose across a wide range of proteins. First redox active metal centers are affected, next disulfide bridges exhibit density loss, then glutamates and aspartates are decarboxylated, tyrosine residues incur damage around their hydroxyl group, and subsequently the carbon-sulfur bonds in methionine residues are apparently cleaved. Importantly, this specific damage often occurs at doses well below those at which there is any obvious degradation of the diffraction pattern.

Radiation chemical experience might suggest, and we and others have shown, that at least some of the damage agents can be intercepted by the introduction of appropriate scavengers. However, the occurrence of an extensive and diverse radiation chemistry in the various crystallization screens and buffers used in sample preparation can lead to confusing results.

Similar effects no doubt complicate attempts to assign mechanisms in related techniques such as protein footprinting, small-angle X-ray scattering and in the damage observed during electron microscopy. Indeed, with the introduction of much improved electron detectors, there has been a distinct shift in emphasis towards recovering macromolecular structural data from electron diffraction images. Here too we might expect the effects of radiation damage to be widespread.

Radiation chemical insight into the redox properties of the tyrosyl radical argues strongly against the putative finding of OH loss from tyrosine residues during data collection from myrosinase crystals. For each residue in the protein, we have introduced the concept of a damage signature plot that contains the observed electron density loss for all atoms of that residue at a specific dose. Since the doses absorbed may differ in each damage series, we have normalized against changes around the backbone carbon atoms to account for any underlying global damage. No significant difference was observed in the corresponding plots for tyrosine and phenylalanine residues. No loss of phenolic OH is thus implied.

Again focusing on specific damage, we have probed radiation effects in nucleoprotein complexes. Reliable quantitative analysis of radiation damage sites from such complex series of macromolecular diffraction data mandated the development of a computational tool generally applicable to the field, the RIDL (Radiation-Induced Density Loss) pipeline. RIDL identifies an atom-centered search radius to quantify the electron density loss, enabling the unambiguous characterization of the influence of features such as solvent accessibility, packing density, and neighboring groups on radiation sensitivity

We continue to strive to fully understanding the radiation chemistry involved in damage creation, developing metrics to reliably reveal its presence and suggesting possible mitigation strategies

Publications with BES support (2017-2019)

E. de la Mora, N. Coquelle, C.S. Bury, M. Rosenthal, E.F. Garman, I. Carmichael, M. Burghammer, J.-P. Colletier, M. Weik. **2019,** *submitted*. Radiation damage and dose limits in serial synchrotron crystallography at cryo- and room temperatures.

T. Marin, I. Janik, D.M. Bartels, *Phys. Chem. Chem. Phys.* **2019**, *accepted*. Ultraviolet charge-transfer-to-solvent spectroscopy of halide and hydroxide ions in subcritical and supercritical water.

V. Bugris, V. Harmat, G. Ferenc, S. Brockhauser, I. Carmichael and E. F. Garman, *J. Synchrotron Radiat.* **2019** *26*, 998-1009. Radiation-damage investigation of a DNA 16-mer.

J. Kapaldo, X. Han, S. Ptasinska. 2019 *Plasma Processes and Polymers* **2019** 1800169. Shielding-gas-controlled atmospheric pressure plasma jets: Optical emission, reactive oxygen species, and the effect on cancer cells.

Z. Li, M. Ryszka, M. M. Dawley, I. Carmichael, K. Bravaya and S. Ptasińska *Phys. Rev. Lett.* **2019** *122*, 073002 Dipole-supported electronic resonances mediate electron induced amide bond cleavage.

S.A. Pshenichnyuk, I.I. Fabrikant, A. Modelli, S. Ptasińska, A.S. Komolov. *Phys. Rev. A* **2019** *100* 012708. Resonance electron interaction with five-membered heterocyclic compounds: Vibrational Feshbach resonances and hydrogen atom stripping.

E.R. Adhikari, V. Samara, S. Ptasińska. *Biolog. Chem.*, **2018**, *400*, 93-100. Total yield of reactive species originating from an atmospheric pressure plasma jet in real time.

E.R. Adhikari, V. Samara, S. Ptasińska. *J. Phys. D*, **2018**, *51* 185202. Influence of O_2 or H_2O in a plasma jet and its environment on plasma electrical and biochemical performances.

V. Samara, S. Ptasińska. *J. Vac. Sci. Technol. A*, **2018**, *36*, 04F402. Interferometry of plasma bursts in helium atmospheric-pressure plasma jets.

Z. Li, I. Carmichael, S. Ptasińska *Phys. Chem. Chem. Phys.* **2018**, *20*, 18271-8. Dissociative electron attachment induced ring opening in five-membered heterocyclic compounds.

C. Bury, I. Carmichael and E. F. Garman. *J. Synchrotron Radiat.* **2017** *24*, 7-18. OH cleavage from tyrosine: debunking a myth.

J. Gorfinkiel, S. Ptasińska. *J, Phys. B*, **2017**, *50*, 182001. Electron scattering from molecules and molecular aggregates of biological relevance.

Z. Li, A.R. Milosavljević, I. Carmichael, S. Ptasińska. *Phys. Rev. Lett*. **2017**, *119*, 053402. Direct observation and characterization of neutral radicals from a dissociative electron attachment process.

S. Ptasińska, M.A. Śmiałek, A.R. Milosavljević, B. Sivaraman *Eur. Phys. J. D*, **2017**, *71*, 264. Low-energy interactions related to atmospheric and extreme conditions.

A. Ribar, K. Fink, Z. Li, S. Ptasińska, I. Carmichael, L. Feketeová, S. Denifl. *Phys. Chem. Chem. Phys.* **2017**, *19*, 6406-15. Stripping off hydrogens in imidazole triggered by the attachment of a single electron.

M. Ryszka, E. Alizadeh, Z. Li, S. Ptasińska. *J. Chem. Phys.* **2017**, *147*, 094303. Low-energy electron-induced dissociation in gas-phase nicotine, pyridine, and methyl-pyrrolidine.

Basic Radiation Chemistry Impacting Nuclear Power Generation

Principal Investigators

Jay A. LaVerne (laverne.1@nd.edu), David M. Bartels, Irek Janik, and Aliaksandra Lisovskaya
Notre Dame Radiation Laboratory, University of Notre Dame, Notre Dame, IN 46556

Program Scope

Advances in the development of nuclear power and in the maintenance of our present fleet of reactors requires fundamental radiation chemistry studies on complex systems containing water, organics, and interfaces. This program is an extension of studies on fundamental radiation chemical effects in homogeneous media that have been and continue to be a major effort at the NDRL. The extensive knowledge obtained for water, aqueous solutions, and organic liquids is being expanded to more directly address specific needs in the nuclear power industry. The program probes reactor water chemistry at operating conditions of BWR and PWR reactors, as well as the radiation chemistry at the molecular level occurring at interfaces. Development of newer separation systems that are more efficient and economic are being aided by fundamental studies on the organic separation media as well as the aqueous phases containing the high concentration of salts commonly associated with these systems. Track modeling calculations are aiding in the design of experiments and understanding the underlying mechanisms.

Recent Progress and Future Plans

The main stable oxidizing species produced in water radiolysis of concern to reactor water systems is H_2O_2. This species has long been known to be formed almost exclusively through the combination reactions of OH radicals. Added solvents, interfaces or even impurities in the water can scavenge OH radicals or react directly with H_2O_2 to decrease is yield. For instance, it is common to add H_2 to reactor water to scavenge OH radicals. Halides are also very good scavengers of OH radicals. There is a renewed interest in the radiolysis of aqueous solutions of highly concentrated chlorides and bromides due to the possible use of seawater as a coolant in emergency conditions. Simple addition of halogens to aqueous solutions of H_2O_2 leads to its decomposition due to a thermal reaction that may well be acid catalyzed. Initial efforts to examine the radiation dependence of H_2O_2 production on bromide concentration found unexpected behavior. The radiolysis of dilute bromide solutions has been extensively studied, but little information is available on concentrated solutions. The initial radiolytic formation of bromine atoms in concentrated bromide solutions quickly leads to transient Br_2^-species that disproportionate to give the stable Br_3^-. The latter species is easily measured spectroscopically. Variation of Br_3^- with dose was found to be strongly dependent on the bromide vendor and sample purification. The conclusion is that high concentrations of bromide also contain sufficient concentrations of an impurity (most likely another halide) to make these measurements inconsistent. Pulse radiolysis studies confirmed that it is the disproportionation reaction of Br_2^- that is causing the discrepancies. At high bromide concentrations, the formation of the transient Br_2^-species is too fast for interference by impurities. Future studies will examine the radiation chemistry of chloride solutions with the hope that impurities are not as prevalent.

Minor concentrations of CO_2 impurity in the cooling water of nuclear reactors can affect the radiation redox chemistry in the reactor core. Reactions of the hydrated electron are expected to be the most dominant decay mode. The rate of CO_2 reduction by hydrated electrons has been

measured at various temperatures up to 350ºC using pulse radiolysis with transient absorption detection (Fig. 1). The Arrhenius plot for the reaction of a hydrated electron with CO_2 is linear up to 200ºC, and then a slope appears, giving a drop at a temperature above 300ºC. This drop indicates that the reaction of e^-_{aq} with CO_2 at higher temperatures is not diffusion-limited. Activation energy of the reaction at a temperature of from 5 to 200°C was equal to 15.9 kJ/mol. Similar Arrhenius plots and activation energies were obtained in previous work for the reaction between hydrated electrons and N_2O, which is isoelectronic with CO_2. The obtained data of temperature-dependent reaction rate constants should be useful for studying radiation chemistry in nuclear reactors.

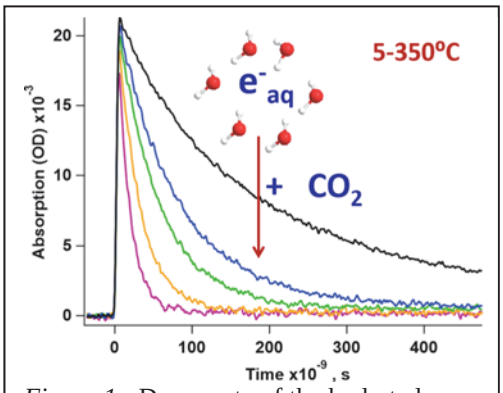

Figure 1 - Decay rate of the hydrated electron reaction with CO_2 with increasing temperature.

A major part of our understanding of the underlying mechanisms involved in radiolysis comes from modeling efforts. The Notre Dame Radiation Laboratory was one of the major participants in the modern era of Monte Carlo based track structure calculations. These calculations are based on a collision-by-collision approach of the incident radiation and all secondary electrons down to thermal energies. An Independent Reaction Times (IRT) methodology is then used to follow the subsequent chemistry for comparison with experiments. Considerable effort was made in the last period to reestablish access to the Monte Carlo track codes. Accomplishments in the fundamental research of track structure simulations falls under three thrusts, the implementation of the track-structure code, the creation and deployment of supporting analysis/management scripts, and the data collected. For the first, the setup and testing of the high energy, high LET track structure code took a significant amount of time to implement correctly. This complex set of FORTRAN 77 programs are interlaced with a variety of highly specialized input, transition and output files, as well as a convoluted set of experimental data files. Major accomplishments of launching this code includes: having a highly specialized directory structure that allows for simulation of gamma, and high LET particles with accuracy and precision on a computer cluster; the launch of a version control tracking for all future changes made to the code for forwards and backwards compatibility; and the generation of a vast new set of complex input files for simulation of carbon and alpha particles that can be used with any aqueous system.

The second set of achievements lies in the management and analysis scripts generated that allow for speed and readability of the large number of simulations and their corresponding output files. The first in this set of accomplishments is the implementation of a simple and reproducible directory structure that is linked to sorting and data analysis scripts. This implementation will allow for long-term storage and logical access to previous data in addition to the reproducible analysis of yields into a format that can be easily visualized. The second accomplishment lies within the data management scripts of the program that have been updated to run correctly on the Notre Dame Centre for Research Computing cluster. They have also been updated to run entire data sets of high LET particles, iterating over particle energy and scavenger concentration in a single submission script without overwriting results.

Finally, the last set of achievements is centered on the data collected. Two systems in particular were studied, glycylglycine and formate. Glycylglycine was used to check the backwards compatibility of the code as there had been a number of changes made to the source code and files since the last publication. This exercise resulted in corrections to charge cycling approximations used for alpha particles as well as incorporating a variety of charge cycling approximations for high LET particles that previously had not functioned properly. We successfully simulated the previous glycylglycine data and are currently working on improving this set of simulations. The formate simulations are the first of their kind and data was run for protons, alpha particles and carbon ions across four orders of magnitude of formate concentration. These predicted results were compared with experimental yields of CO_2 and the data matches reasonably well for protons and alpha particles. The simulations led to the discovery that using a Gaussian distribution for the radical distribution of reactive species at high LET breaks down, and a broader distribution for pre-solvated electrons and/or OH radicals may be more realistic.

Publications with BES support (2017-2019)

A. Lisovskaya and D. M. Bartels (2019) “Reduction of CO_2 by Hydrated Electrons in High Temperature Water”, **Radiation Physics and Chemistry,** *158*, 61-63.

J. Schofield, J. A. La Verne, D. Robertson, P. Collon and S. M. Pimblott **(2019)** "Material Dependence on the Mean Charge State of Light Ions in Titanium, Zirconium and copper", **Physical Chemistry Chemical Physics**. In press.

M. T. Postek, D. L. Poster, A. E. Vladar, M. S. Driscoll, J. A. LaVerne, Z. Tsinas and M. I. Al-Sheikhly **(2018)** "Ionizing radiation processing and its potential in advancing biorefining and nanocellulose composite materials manufacturing", **Radiation Physics and Chemistry** *143*, 47-52.

J. A. La Verne, N. A. I. Tratnik and A. Sasgen **(2018)** "Gas Production in the Radiolysis of Poly(dimethylsiloxanes)", **Radiation Physics and Chemistry** *142*, 50-53.

K. Iwamatsu, S. Sundin and J. A. LaVerne **(2018)** "Hydrogen Peroxide Kinetics in Water Radiolysis", **Radiation Physics and Chemistry** *145*, 207-212.

S. C. Reiff and J. A. LaVerne **(2017)** "Radiolysis of water with aluminum oxide surfaces", **Radiation Physics and Chemistry** *131*, 46-50.

J. A. LaVerne and S. R. Kleemola **(2017)** "Hydrogen Production in the Radiolysis of Dodecane and Hexane", **Solvent Extraction and Ion Exchange** *35*, 210-220.

G. P. Horne, S. M. Pimblott and J. A. LaVerne **(2017)** "Inhibition of Radiolytic Molecular Hydrogen Formation by Quenching of Excited State Water", **Journal of Physical Chemistry B** *121*, 5385-5390.

S. Feister, D. R. Austin, J. T. Morrison, K. D. Frische, C. Orban, G. Ngirmang, A. Handler, J. A. La Verne, E. A. Chowdhury and W. M. Roquemore **(2017)** "Relativistic Electron Acceleration by mJ-class kHz Lasers Normally Incident on Liquid Targets", **Optics Express** *25*, 18736-18750.

Pulse Radiolysis Used to Study the Effects of a Massive Structural Change on Charge Transfer

Principal Investigators: Andrew R. Cook and John R. Miller
Chemistry Division, Brookhaven National Laboratory, Upton, NY, 11973 USA
acook@bnl.gov, jrmiller@bnl.gov

Program Scope:

This program applies both photoexcitation and ionization by short pulses of fast electrons to investigate fundamental chemical problems relevant to the production and efficient use of energy and thus obtain unique insights not attainable with other techniques. These studies may play an important role in the development of safer, more effective, and environmentally beneficial processes for the chemical conversion of solar energy. Picosecond pulse radiolysis at the Laser Electron Accelerator Facility (LEAF) is employed to generate and study reactive chemical intermediates or other non-equilibrium states of matter in ways that are complementary to photolysis and electrochemistry and often uniquely accessible by radiolysis. This program also develops new tools for such investigations, applies them to chemical questions, and makes them available to the research community. Advanced experimental capabilities, such as Optical Fiber Single-Shot detection system (OFSS), allow us to work on fascinating systems with ~10 ps time-resolution that were previously prohibitive for technical reasons.

Recent Progress:

The Impact of Huge Structural Changes on Electron Transfer and Measurement of Redox

Potentials: Reduction of ortho-12-Carborane.

A massive structural change accompanies electron capture by the 1,2-dicarba-*closo*-dodecaborane (**I**) cage molecule indicated by the C-C bond-length change from 1.62 Å in the neutral to 2.39 Å in the radical anion. This change is seen in the figure below, where the left structure is the neutral geometry, and the center one is the radical anion. It is also possible to make a dianion at the electrode leading to an even larger structural change. Focusing on one-electron reduction to form the anion we can ask: What effect does this structural change have on 1) measurement of the redox potential 2) Rate constants for electron transfer?

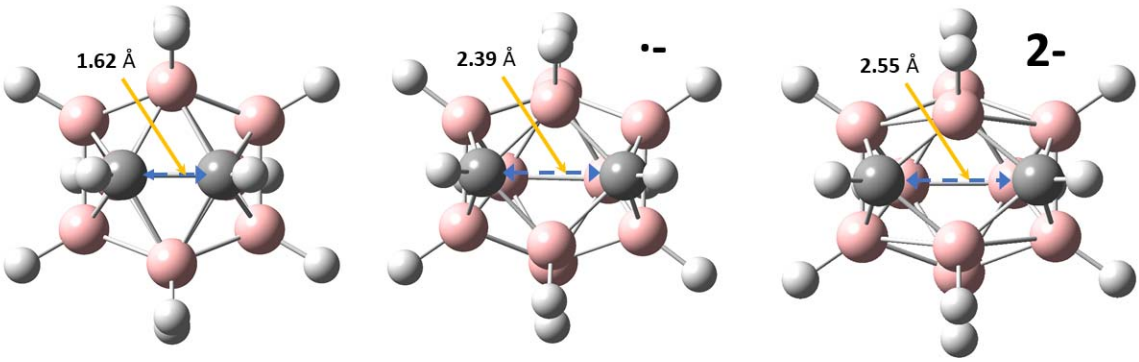

The mystery of the redox potential Bimolecular electron transfer (ET) by pulse radiolysis found a reduction potential of E^0= -1.92 V vs. $Fc^{+/0}$ for **1** and rate constants that slowed greatly for ET to or from **1** when the redox partner had a potential near this E^0 (see Figure at right). The determination of redox potential in the pulse radiolysis experiments in THF solution utilized measured, reversible potentials for the partners. One such partner, diacetylbenzene (Ac2Bz) has a potential almost identical to that of **1**, but in similar experiments its reactions with other partners are all near the diffusion-controlled limit (upper panel), with little variation with thermodynamics of the reaction, in contrast to reactions of **1**, for which rate constants vary by a factor of 10^5.

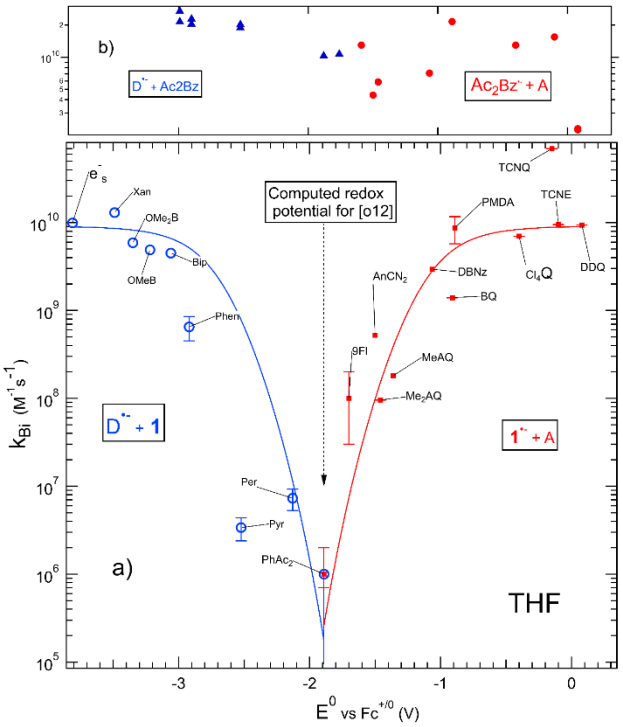

Two electrochemical techniques could detect no current at potentials near E^0, finding instead peaks or polarographic waves near -3.1 V, which is 1.2 V more negative than E^0. These peaks were irreversible so they might not provide accurate redox potentials. So which redox potential is correct: that from electrochemistry or that from electron transfer reactions by pulse radiolysis?

Additional evidence comes from anion photoelectron spectroscopy by Zhang and Bowen (Zhang, X. X.; Bowen, K. "A Photoelectron Spectroscopic and Computational Study of the o-Dicarbadodecaborane Parent Anion", *J. Chem. Phys.*, **2016**, *144)*. They obtained an estimate of the redox potential in the gas phase that is inexact, but close to the value of -1.92 V vs. Fc determined in the pulse radiolysis experiments, and definitely incompatible with a potential near -

3.1 V. Another electrochemical technique, electrochemical catalysis, which utilizes a mixture of two molecules, also supported the correctness of the -1.92 V redox potential. The conclusion seems clear that electrochemistry can not obtain a reliable potential due to the large structural change, but pulse radiolysis can.

The Mystery of Electron Transfer Rate Constants A second mystery concerns the electron transfer rate constants determined by electrochemistry and measured near -3.1 V, compared with those measured by pulse radiolysis. A large structural change can greatly slow electron transfer rate constants and shift the positions of CV waves. Electrochemistry simulations made using DigiSim can explain the shifted peaks at -3.1 V, but require electrochemical rate constants near $1x10^{-10}$ cm/s at E^0, a factor of 10^{-10} relative to molecules undergoing facile ET. This factor of 10^{-10} compared to ~10^{-5} for bimolecular ET presents a puzzle. We can understand this five-decade discrepancy as a manifestation of one of the “Frumkin Effects” in which only part of the applied voltage is available to drive ET at the electrode to provide a resolution to this puzzle.

Publications of DOE sponsored research that have appeared in the last 2 years:

1-4

1. Bird, M. J.; Iyoda, T.; Bonura, N.; Bakalis, J.; Ledbetter, A. J.; Miller, J. R. "Effects of electrolytes on redox potentials through ion pairing", *Journal of Electroanalytical Chemistry,* **2017**, *804*, 107-115.
2. Chen, H. C.; Cook, A. R.; Asaoka, S.; Boschen, J. S.; Windus, T. L.; Miller, J. R. "Escape of anions from geminate recombination in THF due to charge delocalization (vol 19, pg 32272, 2017)", *Physical Chemistry Chemical Physics,* **2018**, *20*, 3841-3842.
3. Cook, A. R.; Asaoka, S.; Li, X.; Miller, J. R. "Electron Transport with Mobility, mu > 86 cm(2)/(V s), in a 74 nm Long Polyfluorene", *Journal of Physical Chemistry Letters,* **2019**, *10*, 171-175.
4. Cook, A. R.; Valasek, M.; Funston, A. M.; Poliakov, P.; Michl, J.; Miller, J. R. "p-Carborane Conjugation in Radical Anions of Cage-Cage and Cage-Phenyl Compounds", *Journal of Physical Chemistry A,* **2018**, *122*, 798-810.

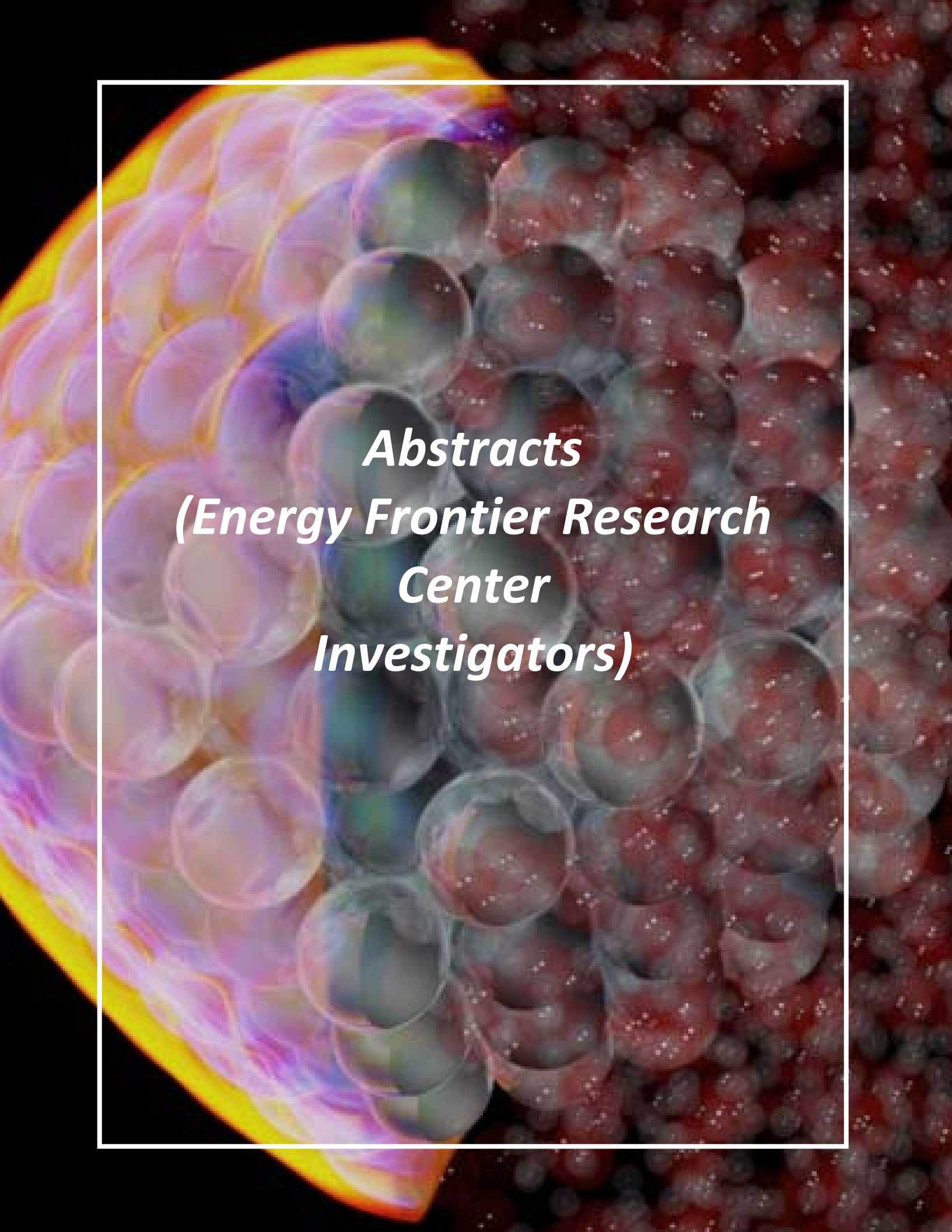

Abstracts (Energy Frontier Research Center Investigators)

The Molten Salts in Extreme Environments Energy Frontier Research Center (MSEE)

James Wishart, Director
Lead Institution: Brookhaven National Laboratory

MSEE's Mission*: To provide a fundamental understanding of molten salt bulk and interfacial chemistry that will underpin molten salt reactor technology.*

Molten Salt Reactors (MSRs) are a potentially game-changing technology that could enable cost-competitive, safe, and more sustainable commercial nuclear power generation. Proposed designs employ molten salts in the temperature range of 500 – 900 ˚C acting as coolants for solid-fueled reactors or in other cases where the nuclear fuel dissolved in the molten salt as combined coolant and fuel. Consequently, the development of reliable MSRs requires a comprehensive understanding of the physical properties and chemistry of molten salts and of their interfacial interactions with reactor materials.

The Energy Frontier Research Center for Molten Salts in Extreme Environments (MSEE) is providing fundamental and predictive understanding of the bulk and interfacial chemistry of molten salts in the operating environments expected for MSRs. MSEE addresses this challenge through a coordinated experimental and theoretical effort to elucidate the atomic and molecular basis of molten salt behavior, including interactions with solutes (dissolved materials such as nuclear fuel and fission products) and interfaces, under the coupled extremes of temperature and radiation.

The research of MSEE is organized into two interrelated thrusts. The first is *Molten Salt Properties and Reactivity*, which aims to understand how molecular-scale interactions, structure and dynamics lead to macroscale properties. A key focus is to learn how the interactions between molten salts and solutes affect physical properties and control solubility and reactivity. The second thrust, *Interfacial and Corrosion Processes in Molten Salt Environments*, aims to understand the atomic-scale structure and dynamics at interfaces and related mechanisms of interfacial and corrosion processes between molten salts and materials, including the effects of extreme environments such as radiation and high temperature.

Thrust 1: Molten Salt Properties and Reactivity

Aim 1: Determine the structure and dynamics of molten salt solutions across scales of length and temperature. Powerful X-ray, neutron-scattering and optical spectroscopy techniques are employed and coupled with computational approaches to interpret observations and validate predictions in order to assemble a dynamic model of molten salt structure.

Aim 2: Elucidate the principles that control metal ion solvation, speciation and solubility in molten salts. The same methods are used to understand changes in solution structure, dynamics and thermal properties when solutes, including actinides and fission products, are dissolved in molten salts.

Aim 3: Understand how radiation affects salt solution chemistry and solute speciation. Radiation chemistry techniques are used to examine the radiation-driven reactions of molten salts and materials dissolved in them.

Thrust 2: Interfacial and Corrosion Processes in Molten Salt Environments

Aim 1: Measure and predict the structures and dynamics of molten salts at interfaces. X-ray and neutron reflectivity measurements are integrated with new modeling approaches to provide fundamental new information on surface ordering and dynamics of molten salts and to elucidate how these structures determine energy and charge transfer across the interface.

Aim 2: Kinetics of interfacial reactions leading to corrosion. *In-situ* experimental techniques, enabled by advances in characterization capabilities, will provide unprecedented temporal and spatial resolution for quantifying interfacial reactions and help us understand and predict non-equilibrium, metastable states formed during the reactions at interfaces.

A deeper knowledge on molten salt structure and properties, and the behavior of the actinides, fission products and corrosion products in molten salt solution under radiolytic conditions, will strengthen the scientific foundation for the practical implementation of MSRs. A stronger understanding of redox chemistry and solvation of solutes such as fuel metal ions and fission products will contribute to better predictions of precipitation, participation in corrosion reactions, gas generation and failure to behave as desired in fission product separations. Improved molecular knowledge of the corrosive interactions of molten salts will suggest ways to mitigate challenges to the performance of nuclear reactor materials, and also in solar thermal collectors. MSEE will focus on filling those knowledge gaps to enable safer, higher performing and more reliable MSR systems, as well as to extend our scientific understanding of the general fundamental chemical processes in molten salts.

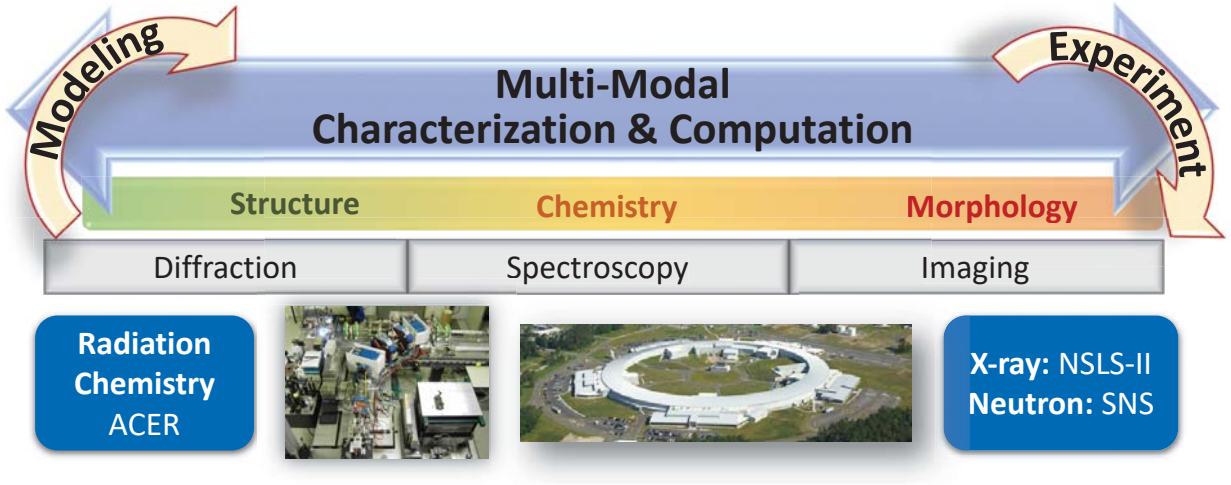

Molten Salts in Extreme Environments (MSEE)	
Brookhaven National Laboratory	James Wishart (Director), Eric Dooryhee, Simerjeet Gill, Anatoly Frenkel, Benjamin Ocko, Kotaro Sasaki
Idaho National Laboratory	Simon Pimblott (Deputy Director and Interim Thrust 2 Leader), Ruchi Gakhar, Gregory Horne Lingfeng He
Oak Ridge National Laboratory	Shannon Mahurin (Thrust 1 Leader), Vyacheslav Bryantsev, Sheng Dai, Xiao-Guang Sun
University of Iowa	Claudio Margulis
University of Notre Dame	Jay LaVerne, Edward Maginn
Stony Brook University	Yu-Chen Karen Chen-Wiegart

Contact: James Wishart, Director, wishart@bnl.gov
631-344-4327, https://www.bnl.gov/moltensalts/